RESPONSE PROPERTIES OF INPUTS TO DURATION-TUNED NEURONS

INFERRED RESPONSE PROPERTIES OF THE SYNAPTIC INPUTS UNDERLYING DURATION-TUNED NEURONS IN THE BIG BROWN BAT

By ROBERTO VALDIZÓN-RODRÍGUEZ, B.Sc.

A Thesis submitted to the School of Graduate Studies in Partial Fulfilment of the Requirements for the Degree Doctor of Philosophy

McMaster University DOCTOR OF PHILOSOPHY (2019) Hamilton, Ontario

Department of Psychology, Neuroscience & Behaviour

TITLE: Inferred Response Properties of the Synaptic Inputs Underlying Duration-Tuned Neurons in the Big Brown Bat

AUTHOR: Roberto Valdizón-Rodríguez, B.Sc. (McMaster University)
SUPERVISOR: Dr. Paul A. Faure
NUMBER OF PAGES: xvii, 287

Abstract

Duration tuning in the mammalian inferior colliculus (IC) is created by the interaction of excitatory and inhibitory synaptic inputs. We used extracellular recording and paired-tone stimulation to measure the strength and time-course of the contralateral inhibition and offset-evoked excitation underlying duration-tuned neurons (DTNs) in the IC of the awake bat. The onset time of a short, best duration (BD), excitatory probe tone was varied relative to the onset of a longer-duration, non-excitatory (NE) suppressor tone. Spikes evoked by the roving BD tone were suppressed or facilitated when the stationary NE tone was varied in frequency or amplitude. When the NE tone frequency was presented away from the cell's best excitatory frequency (BEF) or at lower SPLs, the onset of inhibition was relatively constant whereas the offset and duration of inhibition decreased. Excitatory and inhibitory frequency response areas were measured and best inhibitory frequencies matched best excitatory frequencies; however, inhibitory bandwidths were broader than excitatory bandwidths. Excitatory rate-level and inhibitory suppression-level functions were also measured and the dynamic ranges and inflection points were similar, which is hypothesized to play a role in the level tolerance of responses measured from DTNs. We compared the latency of offset-locked facilitation to the onset or offset of inhibition as a function of frequency and amplitude; we found that the facilitation was more related to the onset of inhibition. Moreover, facilitation typically preceded the offset of inhibition – suggesting that it is a separate excitatory input to DTNs and not a rebound from inhibition. We conclude that DTNs receive inputs that generate and preserve temporal selectivity.

This dissertation is dedicated to my mother, Elizabeth Valdizón-Rodríguez.

Your strength, dedication, kindness, and tireless love inspire me every day.

Nunca dejes de soñar. Te quiero mucho Mamí.

Acknowledgements

When I was very young, I would gaze intently as the wind blew over the grass while my mother held me – this is probably the earliest evidence for my curiosity, and desire to observe the world – or so I'm told. From that point onwards, I developed a fascination for science and for learning by doing experiments. The journey to this point has been both joyful and challenging and I want to dedicate this section to all of those people who made it possible.

My undergraduate degree was in chemistry but I became passionate about auditory neuroscience through my electives which were focused on biology and biochemistry. In my final year, I took a course called "Audition" which introduced me to the fascinating world of hearing. I loved the course so much that when it was over, I talked to the instructor about joining their research lab: The McMaster Batlab. Eventually, I was able to join the lab and embark on the greatest adventure I could ever have imagined. For this and so much more I am inexpressibly grateful to Dr. Paul A. Faure for taking me into his lab. Paul challenged me to be the best I could be – he helped me through the overwhelming task of data collection/analysis and writing, took care of me when I was sick on conferences, discovered new breakfast/taco spots with me in California, and taught me to love the diverse, beautiful, and awesome world of bats. Paul, thank you for pushing me to become the scientist I am today; this dissertation would not be possible without all of your support.

I am also grateful to my committee members, Ian Bruce, Patrick Bennett, and Deda Gillespie for their support and guidance over these past years. Each of you has challenged me to be a better scientist and showed me to think about my work in a unique way.

I would like to thank Riziq Sayegh for introducing me the electrophysiological techniques necessary to perform single-unit extracellular neurophysiology.

I would like to extend a huge thank you to past and present graduate student and post-doc lab mates: Brandon Aubie, Larissa Bueno, Taylor Byron, Alejandra Ceballos-Vasquez, Daniel Dubovan, Lucas Greville, Thomas Groulx, Zeeshan Haqqee, Rob Mastroieni, Doreen Möckel, James Morrison, and Riziq Sayegh. All of you have been so encouraging to work with and have played a role in this thesis. We talked about science but we also did life together. Your friendship has been invaluable throughout this time.

I have also had the great honour of mentoring and/or training some of the members in the lab: Taylor Byron, Daniel Dubovan, Zeeshan Haqqee, Imtiaz Karamat, Nabeel Khaja, Dominika Kovaleva, Rob Mastroieni, Doreen Möckel, James Morrison, and Haichao Zhang. Thank you for bearing with me and learning what I had to show you. I hope that I was able to transmit not only the knowledge to complete your projects but a passion for auditory neurophysiology.

I would like to thank some past and present members of the office: Blake Anderson, Carling Baxter, Dan Case, Liu Cheng, Alan Cooper, Zac Durisko, David Filice, Shane Golden, Xiaomeng Guo, Joshua Hinds, Joseph Mentlik, Sam Molot-Toker, Andrew Scott, Isvarya Venu, and Hugo Wang. I would also like to add some members of the department:

Arnav Bharadwaj, Arjun Kathir, Siyi Ma, Shane Simon, and Donna Waxman. The office/department was a place where I could find friendship and camaraderie. All of you encouraged me beyond what you can know.

I am very grateful to the ladies in the Psychology office who kept the department running: Milica Pavlica, Sally Presutti, Nancy Riddell, and Wendy Selbie. If it weren't for you, I don't know where I would be. You genuinely care about students and take care of far more than just the administrative running of the department.

I would like to extend a huge thank you to my best friend Daniel Manickam. We finished chemistry together and we have been friends ever since. You have been a source of encouragement to me throughout this PhD. Not only that but I appreciated when we were able to hang out and take a breather from the lab. Thanks for being there for me up to now – I appreciate your friendship.

I would like to thank my (*adoptive*) family: Aimee, Brandon, and Isabelle Cousins, Joyceson Canagaratnam, Maria Irudayaraj, and Elijah Joyceson, Deepika Manickam, Marie Manickam, and Prince Manickam. You guys always kept me in your plans. Thanks for so many family dinners/adventures and everything in between. Most importantly, thank you for finding room for me in the family.

I would like to thank my brother, René Valdizón-Rodríguez, for being so supportive throughout all of my schooling. You always believed in me. You were also thoughtful about my health and wellness while I was in school – sometimes I needed to be reminded.

Not only that, but you were an inspiration to me in the early years of my scientific career when I saw how dedicated you were to learning.

I am grateful to my sister, Sophia Valdizón-Rodríguez, who always gave me advice and listened to me when I had something to say. I appreciate who you are and I am excited about who you will become! Keep working hard and don't ever stop being the smart, creative, problem solver that you have always been. Also, never forget how profound what you have accomplished is – be encouraged and look towards the future!

Thank you to Ueli Reichen for all the ways you've helped me throughout my PhD. You moved me to Hamilton (several times) and supported me and my family in so many ways. Thanks for cooking meals for me when I came over, it is probably the best food I will ever have in my life. Your example of hard work, perseverance, and passion is something that I hope to emulate every day.

There are no words to express my gratitude for my Mom, Elizabeth Valdizón-Rodríguez. Throughout my doctorate you gave me guidance, brought me food, helped me do laundry, helped me move, and so much more. I appreciate your kindness, your hard work, and your desire to create a better future for everyone around you. Most importantly I am thankful for your unconditional love, which I know will always be there for me regardless of what happens. This thesis is dedicated to you for all you do. *Te quiero*.

Finally, to my nephew, Tiago Roberto Valdizón-Rodríguez, thank you for coming into our lives. You are a joy to us all. Know that my love for you is deeper than the oceans, stretches higher than the skies, and cannot be destroyed by anything in between. I want you

to discover who you are, knowing that you are safe and loved. Experience the world around you and find your passion. When you do find it, work hard at it and let nothing get in your way – except family – always make time for family. Remember: be the best person you can be, and greatness will follow.

Table of Contents

List of Figures

List of Tables

Declaration of Academic Achievement

Chapter 1 - Introduction

Author: Roberto Valdizón-Rodríguez

Chapter 2 - Frequency tuning of synaptic inhibition underlying duration-tuned neurons in the mammalian inferior colliculus

Authors: Roberto Valdizón-Rodríguez and Paul A. Faure

Publication: Journal of Neurophysiology (2017) 117: 1636–1656

Comments: R.V.-R. performed experiments; R.V.-R. and P.A.F. analyzed data; R.V.-R. and P.A.F. interpreted results of experiments; R.V.-R. and P.A.F. prepared figures; R.V.-R. and P.A.F. drafted manuscript; R.V.-R. and P.A.F. edited and revised manuscript; P.A.F. conceived and designed research.

Chapter 3 - Effect of Sound Pressure Level on Contralateral Inhibition Underlying Duration-Tuned Neurons in the Mammalian Inferior Colliculus

Authors: Roberto Valdizón-Rodríguez, Dominika Kovaleva, and Paul A. Faure

Publication: Journal of Neurophysiology (2019) 122: 184–202

Comments: R.V.-R. and P.A.F. performed experiments; R.V.-R., D.K., and P.A.F. analyzed data; R.V.-R., D.K., and P.A.F. interpreted results of experiments; R.V.-R., D.K., and P.A.F. prepared figures; R.V.-R., D.K., and P.A.F. drafted manuscript; R.V.-R., D.K., and P.A.F. edited and revised manuscript; P.A.F. conceived and designed research.

Chapter 4 - Response Properties of Offset Facilitation in Duration-Tuned Neurons

Authors: Roberto Valdizón-Rodríguez, Haichao Zhang, and Paul A. Faure

Publication: In preparation

Comments: R.V.-R. and P.A.F. performed experiments; R.V.-R., H.Z., and P.A.F. analyzed data; R.V.-R., H.Z., and P.A.F. interpreted results of experiments; R.V.-R., H.Z., and P.A.F. prepared figures; R.V.-R., H.Z., and P.A.F. drafted manuscript; R.V.-R., H.Z., and P.A.F. edited and revised manuscript; P.A.F. conceived and designed research.

Chapter 5 - Discussion

Author: Roberto Valdizón-Rodríguez

Chapter 1 – Introduction

Frequency, amplitude and how they vary over time are the three most elementary physical attributes of sound and represent biologically important structural properties of sound. When these properties are within the bioacoustic range of hearing, they can be used by the central auditory system to make inferences about acoustic stimuli in the environment. To do this, the auditory nervous system uses filters to represent particular physical properties of sounds and relay the information to neural circuits and pathways that affect attention, govern motor responses and eventually play a role in behaviour (Ehrlich et al. 1997). Thus, an understanding of the brain circuits that form a representation of these elementary characteristics is an important question in auditory neurophysiology research.

Temporal features of sound are important in forming the structure of several acoustic features including frequency modulations, amplitude modulations, stimulus ordering, sound onset/offset, gap duration, and stimulus duration. Of these features, stimulus duration is perhaps the simplest and is a very distinct and salient characteristic of acoustic signals found across biologically important sounds. Stimulus duration is important in human speech (Denes 1955; Shannon et al. 1995), in identifying conspecific mating calls (Pollack and Hoy 1979) and social calls (Narins and Capranica 1978), in predator-prey behaviour/interactions (Faure et al. 1990; Manser 2001; Chan et al. 2010), and for more specialized acoustic behaviour such as echolocation in bats (Simmons 1971; Suga and O'Neill 1979; O'Neill and Suga 1982). Hence, encoding and recognizing stimulus duration is necessary for a normal sense of hearing in most vertebrates.

One class of cells that are characterized by their neurophysiological selectivity to stimulus duration are called duration-tuned neurons (DTNs). The spiking responses of DTNs have been found to encode sound durations on the order of milliseconds. These cells have been found across several vertebrate species at different levels of the central auditory pathway, including the torus semi-circularis of anurans (homologue of the mammalian inferior colliculus) where they were originally discovered (Potter 1965; Gooler and Feng 1992; Leary et al. 2008) and the inferior colliculus of bats (Jen and Schlegel 1982; Pinheiro et al. 1991; Casseday et al. 1994; Ehrlich et al. 1997; Fuzessery and Hall 1999; Faure et al. 2003; Mora and Kössl 2004; Luo et al. 2008), guinea pigs (Wang et al. 2006), chinchillas (Chen 1998), mice (Brand et al. 2000; Xia et al. 2000; Tan and Borst 2007), and rats (Pérez-González et al. 2006). They have also been recorded from the auditory thalamus in guinea pigs (He 2002), and the auditory cortex of cats (He et al. 1997) and bats (Galazyuk and Feng 1997). Moreover, neurons with duration selectivity have been found in many non-auditory neural pathways such as the visual cortex of cats (Duysens et al. 1996), in vibration-sensitive ganglia of southern green stinkbugs (Zorović 2011) and in the knollenorgans (electrosensory receptors) of mormyrid electric fish (Lyons-Warren et al. 2012). In each case, the range of encoded durations is within the bounds of the behaviourally-relevant range of signal/vocalization durations for each species (Sayegh et al. 2011). This indicates that DTNs are important across different taxa and sensory modalities and suggests that neural tuning to signal duration is a highly conserved function of the nervous system.

Previous studies on DTNs indicate the existence of at least three distinct response classes determined by the relative number of spikes evoked across all stimulus durations at or near the cell's best excitatory frequency (BEF) (Jen and Zhou 1999; Faure et al. 2003; Sayegh et al. 2011). (1) Short-pass DTNs have spike counts that reach a maximum at a specific duration, called the best duration (BD), and drop to <50% of the maximum response at signal durations longer than BD but not shorter. (2) Band pass cells also have a BD but show a decrease in spiking to <50% of the maximum response when stimulated with signals both shorter and longer than the cell's BD. (3) Finally, long pass DTNs show little to no spiking at signal durations shorter than some minimum duration, but at longer durations they respond typically with sustained spiking that lasts as long or longer than the duration of the stimulus. Some evidence for the existence of band-reject DTNs has been found in the velvety free tailed bat, *Molossus molossus* (Mora and Kössl 2004). This fourth category of duration tuning is characterized by strong spiking at multiple stimulus durations and a decrease to <50% of the maximum response at a range of signal durations in between.

Mechanistically, duration tuning in the auditory midbrain is thought to be created *de novo* from the temporal interaction of neural excitation and inhibition as evidenced by electrophysiological (Casseday et al. 1994; Ehrlich et al. 1997; Faure et al. 2003), neuropharmacological (Casseday et al. 1994, 2000; Jen and Feng 1999; Jen and Wu 2005) and computational data (Aubie et al. 2009, 2012). This body of research has generated hypothetical conceptual models of duration selectivity that require a few synaptic inputs whose relative strength and timing shapes the basic response properties of DTNs (Sayegh et al. 2011; Alluri et al. 2016). These models can explain various intracellular and

extracellular observations of DTNs, and are supported by computational studies that can reproduce spiking patterns of DTNs recorded *in vivo* across several vertebrate species (Aubie et al. 2009, 2012).

Most of the proposed mechanisms of duration-tuning can be summarized as variations of two mechanisms: (1) the coincidence detection mechanism, and (2) the anti-coincidence detection mechanism. In the coincidence detection mechanism of duration tuning, duration selectivity is created through the temporal interaction of three putative synaptic inputs: (1) a fast, onset-evoked sustained inhibitory input (SUS_I); (2) a transient, onset-evoked excitatory input (ON_E) that is subthreshold by itself; and (3) a transient, offset-evoked excitatory input (OFF_E) that is subthreshold by itself and is sometimes hypothesized to result from post-inhibitory rebound excitation following the hyperpolarization from the OFF_E component (Narins and Capranica 1980; Casseday et al. 1994; Covey et al. 1996; Faure et al. 2003; Aubie et al. 2009; Sayegh et al. 2011). The postsynaptic potential of the DTN only becomes suprathreshold when the ON_E and OFF_E events coincide. Conversely, spiking will not occur in the DTN when the OFF_E event precedes or follows the ON_E event. By altering the latency of either the ON_E or OFF_E events in the circuit, it is possible to generate the different duration filter response classes observed (e.g. short-pass or bandpass DTNs; Aubie et al. 2009, 2012; Sayegh et al. 2011). For example, if the ON_E and OFF_E events have similar latencies at the shortest integration time for the inputs, then the cell will exhibit short-pass duration tuning. Alternatively, bandpass duration tuning can result when the OFF_E event precedes the ON_E event in response to short stimulus durations and thus the two synaptic inputs can only coincide at intermediate

stimulus durations; at longer durations, the OFF_E follows the ON_E event and thus fails to produce spiking. The SUS_I event appears to sharpen duration selectivity so that the ON_E and OFF_E events remain subthreshold at stimulus durations outside of the temporal bandwidth of duration tuning. The SUS_I event also modulates temporal response properties of the DTN such as its first spike latency (FSL), BD, and duration filter response class (Casseday et al. 1994, 2000; Jen and Feng 1999; Faure et al. 2003; Jen and Wu 2005; Sayegh et al. 2014). Because the latency of the OFF_E event increases with the duration of the stimulus, one prediction of the coincidence detection mechanism of duration tuning is that the FSL of a DTN will be time-locked to stimulus offset (Sayegh et al., 2011). In support of this prediction, *in vivo* recordings from echolocating bats reveal that DTNs have FSLs time-locked to stimulus offset (Fuzessery and Hall 1999; Faure et al. 2003).

The anti-coincidence mechanism of duration tuning proposes the temporal interaction of two synaptic inputs: (1) a slow, transient, onset-evoked excitatory input (ON_E) that is suprathreshold by itself; and (2) a fast, onset-evoked, sustained inhibition (SUS_I) (Fuzessery and Hall 1999; Leary et al. 2008; Alluri et al. 2016). In this model, spiking is suppressed when the SUS_I event temporally overlaps with the ON_E event. At the shortest integration times for the synaptic inputs, the latency of the ON_E event is longer than the latency of the SUS_I event so suprathreshold excitation does not overlap with the sustained inhibition. At longer stimulus durations spiking becomes suppressed because SUS_I temporally overlaps with the ON_E. The anti-coincidence mechanism naturally results in short-pass duration selectivity but can also create different duration filter response

classes. For example, bandpass duration tuning occurs when the ON_E input requires a sufficiently long duration to elicit excitation (Leary et al. 2008; Alluri et al. 2016).

Both the coincidence detection and anti-coincidence mechanisms of duration tuning rely on the presence of sustained inhibition to produce duration selectivity. Several experiments have revealed the importance of inhibition in creating DTNs. For example, application of pharmacological antagonists that block inhibitory neurotransmitters has shown that duration selectivity broadens or is eliminated when inhibition is absent (Casseday et al. 1994, 2000; Fuzessery and Hall 1999; Jen and Feng 1999; Jen and Wu 2005; Yin et al. 2008). Furthermore, evidence from extracellular single-unit and intracellular whole-cell patch-clamp recordings has shown that short-pass and/or bandpass DTNs receive an onset evoked, inhibitory input that precedes excitatory inputs to cell, and that inhibition is sustained for as long or longer than the duration of the stimulus (Casseday et al. 1994, 2000; Covey et al. 1996; Ehrlich et al. 1997; Faure et al. 2003; Leary et al. 2008). These data demonstrate that duration selectivity is created, in part, by inhibitory control of excitatory responses.

The exact role DTNs play in normal hearing remains unknown. In echolocating bats, duration tuning is thought to play a role in echolocation and foraging behaviour. This view is supported by the fact that the distribution of neural BDs corresponds to the range of echolocation pulse durations that are emitted in different phases of hunting in the big brown bat (Ehrlich et al. 1997), pallid bat (Fuzessery 1994), velvety free-tailed bat (Mora and Kössl 2004), and mustached bat (Macias et al. 2013). If duration tuning is involved in echolocation, then DTNs would likely require unique variations in the inputs creating

duration tuning to facilitate the processing of echolocation calls and echoes. These variations might be used to create neurons with different temporal tuning profiles and response specificity that can cope with the variety and complexity of calls used in echolocation. To illustrate this, consider how insectivorous bats forage. Many bats that fly in open spaces emit loud, narrowband search signals of long duration and low frequency because these signal features are adapted for long range detection. Once a bat has detected a prey item it closes in to capture it. In the approach phase of hunting, signal duration, amplitude, and inter-pulse-interval are reduced but signal bandwidth is initially increased by emitting a broadband downward frequency modulated sweep. During the capture phase of hunting, signal bandwidth is reduced along with duration, amplitude, and interpulse interval culminating in a terminal buzz (Schnitzler and Kalko 2001). To form an accurate image of their prey and surroundings, the bat's neural circuits and pathways need to compare signal features of faint, returning echoes to their outgoing calls. Because echolocating bats emit a wide variety of species- and foraging-specific signal types that differ in amplitude, frequency, and duration it seems likely that populations of DTNs could play a role in mediating a variety of auditory functions and behaviours.

The aim of this thesis is to explore the response properties of the synaptic inputs to DTNs to understand their role in creating temporal selectivity and normal hearing. In Chapter 2, I used single-unit recording and paired-tone stimulation to measure the spectral tuning of the inhibitory inputs to DTNs. I found that the onset of inhibition was independent of stimulus frequency, whereas the offset and duration of inhibition systematically decreased as the stimulus frequency departed from the cell's best excitatory frequency.

Typically, a cell's best inhibitory frequency matched its best excitatory frequency; however, inhibitory bandwidths were more broadly tuned than excitatory bandwidths. The chapter concludes by examining the role and potential sources of the neural inhibition acting on DTNs.

In Chapter 3, I measured the strength and time course of neural inhibition to changes in sound level using single-unit extracellular recording and paired tone stimulation. The onset or latency of the inhibition acting on DTNs decreased while the offset/duration of inhibition lengthened as the stimulus level increased from 0 to +10 dB above threshold; however, no further changes in the timing of inhibition were observed when stimulus amplitude was increased to +20 dB re: threshold. I also measured excitatory rate-level and inhibitory suppression-level response functions from DTNs and found that the shapes of both functions were related. Importantly, the results from this chapter suggest a possible mechanism for level tolerance in the responses of auditory DTNs.

In Chapter 4, I describe the response properties of an offset-evoked, excitatory input in DTNS that is observed as a transient facilitation in spiking during paired tone stimulation. Spike facilitation typically occurred before the offset of inhibition and was more related to the onset of inhibition than the offset of inhibition when stimulus frequency or amplitude was varied. The data indicate that the mechanism of spike facilitation was a separate excitatory synaptic input and was not caused by post-inhibitory rebound excitation following the offset of inhibition.

Chapter 2 – Frequency Tuning of Synaptic Inhibition Underlying Duration-Tuned Neurons in the Mammalian Inferior Colliculus

2.1 – Abstract

Inhibition plays an important role in creating the temporal response properties of duration-tuned neurons (DTNs) in the mammalian inferior colliculus (IC). Neurophysiological and computational studies indicate that duration selectivity in the IC is created through the convergence of excitatory and inhibitory synaptic inputs offset in time. We used paired-tone stimulation and extracellular recording to measure the frequency tuning of the inhibition acting on DTNs in the IC of the big brown bat (*Eptesicus fuscus*). We stimulated DTNs with pairs of tones differing in duration, onset time, and frequency. The onset time of a short, best-duration (BD), probe tone set to the best excitatory frequency (BEF) was varied relative to the onset of a longer-duration, nonexcitatory (NE) tone whose frequency was varied. When the NE tone frequency was near or within the cell's excitatory bandwidth (eBW), BD tone-evoked spikes were suppressed by an onset-evoked inhibition. The onset of the spike suppression was independent of stimulus frequency, but both the offset and duration of the suppression decreased as the NE tone frequency departed from the BEF. We measured the inhibitory frequency response area, best inhibitory frequency (BIF), and inhibitory bandwidth (iBW) of each cell. We found that the BIF closely matched the BEF, but the iBW was broader and usually overlapped the eBW measured from the same cell. These data suggest that temporal selectivity of midbrain DTNs is created and preserved by having cells receive an onset-evoked, constant-latency, broadband inhibition that largely overlaps the cell's excitatory receptive field. We conclude by discussing possible neural sources of the inhibition.

2.2 – Introduction

Temporal features of bioacoustic stimuli are critical for conveying information regarding signal meaning. Examples of temporal features include the rate and direction of frequency modulation, the rate and depth of amplitude modulation, the sequence of acoustic elements in a complex signal, and signal duration. Within the central nervous system there exists a class of auditory cells with spiking responses selective for signal duration called duration-tuned neurons (DTNs). These cells provide a potential neural mechanism for duration discrimination on the order of milliseconds such as observed in human speech (Shannon et al. 1995), amphibian mating calls (Narins and Capranica 1980), and the vocalizations of echolocating bats (Schnitzler and Kalko 2001). Moreover, DTNs have been reported from multiple sensory modalities (Duysens et al. 1996) and vertebrate species (Brand et al. 2000; He et al. 1997; Leary et al. 2008; Pérez-González et al. 2006; Wang et al. 2006), and in each case neuronal best durations correlate with species-specific stimulus durations. Thus duration selectivity is hypothesized to be a general feature of sensory processing that has been adapted to the biological constraints of an organism (Sayegh et al. 2011).

The spectral tuning of auditory DTNs is of particular interest given that spectral and temporal features of biological sounds are often comodulated (Heil et al. 1992; Suga 1984). Recent studies have shown that DTNs in the mammalian inferior colliculus (IC) show a trade-off in their spectro-temporal response resolutions in a manner analogous to resonant electrical filters (Morrison et al. 2014). Moreover, the frequency selectivity of a DTN can change when it is stimulated with sound pulses that are varied in duration (Wu

and Jen 2008a). These findings demonstrate that the temporal features of an acoustic stimulus can modify the frequency tuning of the inputs to DTNs; however, it is unknown how the inhibitory inputs underlying the temporally selective responses of DTNs are modified by stimulus frequency. These data are important because they may provide information about the anatomical origin and function(s) of the inhibitory synaptic inputs to midbrain DTNs.

The present study used a modified version of paired-tone stimulation (Faure et al. 2003) to characterize the spectral tuning of the inhibitory inputs acting on DTNs in the IC. The paradigm involves stimulating a DTN with a pair of pure tone pulses: a short-duration, excitatory probe tone set to the cell's best duration (BD) and best excitatory frequency (BEF) and a longer-duration, nonexcitatory (NE) tone that was varied in frequency. The strength and time course of the inhibition evoked by the NE tone were quantified by varying the interstimulus interval (ISI) of the tone pair and measuring the range of ISIs over which BD tone-evoked responses were suppressed by the NE tone. We found that the onset of inhibition acting on DTNs had a constant latency when the NE tone frequency was near or within the cell's excitatory bandwidth (eBW); however, the duration of the spike suppression systematically decreased as the frequency of the NE tone moved away from its BEF. We used this response feature to measure the best inhibitory frequency (BIF) and inhibitory bandwidth (iBW) of each cell. Our results show that BIFs of DTNs matched their BEFs; however, the iBW was more broadly tuned and largely overlapped the eBW of the same cell. We conclude that this wideband inhibition, which is responsible for creating

the physiological property of duration selectivity, helps to preserve the temporal specificity of auditory DTNs in the mammalian IC.

2.3 – Materials and Methods

2.3.1 – Surgical preparation

Electrophysiological recordings were obtained from the IC of 19 big brown bats (*Eptesicus fuscus*) of both sexes (5 male, 14 female). Before recording, each bat underwent a preparatory surgery in which a small stainless steel post was glued to the dorsal surface of the skull. The head post prevented movement of the bat's head during recording and precisely replicated the head position between sessions in the stereotaxic apparatus (David Kopf Instruments model 1900). Before surgery, bats were administered buprenorphine (Temgesic) (~0.03 ml sc; 0.025 mg/kg) and placed in an anesthesia induction chamber (12 × 10 × 10 cm, length × width × height), where they inhaled a 1–5% isoflurane-oxygen mixture (flow rate = 1 l/min). The anesthetized bat was then placed in a foam-lined body restraint, which held the bat firmly but comfortably while still allowing access to the bat's head. The bat's mouth was placed in a custom bite bar designed to keep the head stable during surgery and fitted with a custom gas mask for continuous anesthetic inhalation. The hair overlying the skull was shaved, and the skin was disinfected with a povidone-iodine surgical scrub (Betadine). A local anesthetic (~0.2 ml bupivacaine sc; 5 mg/ml) was administered before a midline incision was made in the scalp. The temporal muscles were reflected to reveal the dorsal surface of the skull, which was then scraped clean and swabbed with 70–100% ethanol. After drying, a metal head post was glued to the skull overlying the cortex with cyanoacrylate superglue cured with liquid hardener (Pacer Zip Kicker). One end of a chlorided silver wire attached to the head post was placed under the temporal musculature and served as the reference electrode. The wound was then covered

with a piece of Gelfoam coated with Polysporin to prevent infection. After surgery, bats were allowed to recover individually in a stainless steel holding cage (¼-in. mesh) located in a temperature- and humidity-controlled room and were provided food and water ad libitum. All procedures were approved by the McMaster University Animal Research Ethics Board and were in accordance with guidelines for the care and use of experimental animals published by the Canadian Council on Animal Care.

2.3.2 – Electrophysiological recordings

Recordings began 1–2 days after surgery. Each bat was used in one to eight recording sessions lasting 4–8 h each and conducted on separate days. Neural recordings were terminated if the bat showed any signs of discomfort. Between sessions, the electrode penetration site was covered with a piece of contact lens and Gelfoam coated in Polysporin. Recordings were conducted inside a double-walled sound attenuation booth with electrical shielding (Industrial Acoustics). Before recording, bats were administered a neuroleptic [0.3 ml; 1:1 (vol/vol) mixture of 0.025 mg/ml fentanyl citrate and 1.25 mg/ml Inapsine (droperidol); 19.1 mg/kg]. Once this took effect, bats were placed in a foam-lined body restraint that was suspended by springs within a small-animal stereotaxic frame customized for bats (ASI Instruments). The entire apparatus was set atop an air vibration table (TMC Micro-G). The bat's head was immobilized by securing the head post to a stainless steel rod attached to a manual micromanipulator (ASI Instruments) mounted on the stereotaxic frame (David Kopf Instruments). A craniotomy was performed with a scalpel blade, and the dura mater over the dorsal portion of the IC was removed with a sharp pin for the insertion of recording electrodes. The IC can be visually identified as two white ellipses

below the translucent skull. Single-unit extracellular recordings were obtained with thin-walled borosilicate glass microelectrodes (outside diameter = 1.2 mm; A-M Systems) filled with 1.5 M NaCl. Typical electrode resistances ranged between 15 and 30 MΩ. Electrodes were positioned over the exposed IC with manual micromanipulators (ASI Instruments) and advanced into the brain with a stepping hydraulic micropositioner (Kopf model 2650). Extracellular action potentials were recorded with a neuroprobe amplifier (A-M Systems model 1600) whose 10× output was band-pass filtered and further amplified (500–1,000×) by a Tucker Davis Technologies spike preconditioner (TDT PC1; low-pass f_c = 7 kHz, high-pass f_c = 300 Hz). Spike times were logged onto a computer by passing the TDT PC1 output to a spike discriminator (TDT SD1) and then an event timer (TDT ET1) synchronized to a timing generator (TDT TG6).

2.3.3 – Stimulus generation and data collection

Stimulus generation and online data collection were controlled with custom software that shows spike times as dot raster displays ordered by the acoustic parameter that was varied. Sound stimuli were digitally generated with a two-channel array processor (TDT Apos II; 357 kHz sampling rate) optically interfaced to two digital-to-analog converters (TDT DA3-2) whose individual outputs were fed to a low-pass antialiasing filter (TDT FT6-2; f_c = 120 kHz), a programmable attenuator (TDT PA5), and two signal mixers (TDT SM5) with equal weighting. The output of each mixer was then fed to a manual attenuator (Leader LAT-45) before final amplification (Krohn-Hite model 7500). Stimuli were presented monaurally with a Brüel & Kjær (B&K) ¼-in. condenser microphone (type 4939; protective grid on), modified for use as a loudspeaker with a transmitting adaptor

(B&K type UA-9020) to correct for nonlinearities in the transfer function. The loudspeaker was positioned ~1 mm in front of the external auditory meatus. The output of the speaker, measured with a B&K type 4138 ⅛-in. condenser microphone (90° incidence; grid off) connected to a measuring amplifier (B&K type 2606) and a band-pass filter (Krone-Hite model 3500), was quantified with a sound calibrator (B&K type 4231) and is expressed in decibels sound pressure level (dB SPL re 20 µPa) equivalent to the peak amplitude of continuous tones of the same frequency. The loudspeaker transfer function was flat ± 6 dB from 28 to 118 kHz, and there was at least 30-dB attenuation at the ear opposite the source (Ehrlich et al. 1997). At sound frequencies <15 kHz the transducers generate harmonic distortions. To compensate for the distortions, we excluded data points collected with frequencies <15 kHz. All stimuli had rise/fall times of 0.4 ms, shaped with a squared cosine function, and were presented at a rate of 3 Hz.

Search stimuli consisted of two pure tones that differed in duration (typically 1 and 4 ms, ISI ≥ 110 ms) and were presented monaurally to the ear contralateral to the IC recorded. Upon isolating a unit we determined its BEF (0.1- to 1-kHz resolution), BD (1-ms resolution), and duration filter response class at the BEF (Sayegh et al. 2011). Our study focused specifically on DTNs, so we did not record responses from other types of IC neurons.

Previous studies have categorized DTNs into three duration filter response classes depending on the relative number of spikes evoked across all stimulus durations tested. Our study focused exclusively on band-pass and short-pass DTNs. Band-pass DTNs respond

maximally at the BD and drop to ≤50% of the peak spike count in response to stimulus durations both shorter and longer than the BD. Short-pass DTNs also respond maximally at the BD and drop to ≤50% of the peak spike count in response to stimulus durations that are longer, but not shorter, than the BD. Example duration raster plots and duration filter functions for a band-pass and a short-pass DTN are shown in Fig. 2.1.

Using BEF and BD stimuli, we then measured the cell's rate-level function and minimum acoustic response threshold (5-dB resolution). With this information, a cell's excitatory frequency response area (eFRA) was measured at +10 dB re threshold to determine its excitatory spectral bandwidth (eBW), defined as the lowest and highest frequencies where the spike count was ≥50% of the maximum. We used the eBW of each cell to calculate a quality (Q) factor that describes the sharpness of frequency tuning, defined as $Q_{10\,dB}$ = BEF/eBW.

2.3.4 – Paired tone stimulation with BEF and non-BEF NE tones

We used paired-tone stimulation to measure the strength and time course of the inhibition evoked by a longer-duration NE tone that was varied in frequency. The paradigm consisted of stimulating a cell with a pair of pure tone pulses that differed in duration and ISI (Faure et al. 2003). The BD tone was set to the cell's BD and BEF to evoke maximal excitation. The NE tone was set to a nonexcitatory duration that was typically 10 times the duration of the BD tone. We did this to ensure that the NE tone would be nonexcitatory and so that there would be a constant energy relationship between the two signals, regardless of each cell's actual BD. The onset time of the NE tone was fixed between stimulus presentations, while the onset time of the BD tone was randomly varied in 2- to

4-ms steps so that it preceded, overlapped with, and followed the NE tone. The two tones were electronically mixed and presented to the contralateral ear at an amplitude of +10 dB re BD tone threshold. The BD and NE tones were matched in starting phase and could constructively or destructively interfere when they overlapped. When the BD and NE tones were matched in frequency the two signals always constructively interfered, resulting in a composite signal with an amplitude pedestal of +6 dB for the duration of overlap. When the BD and NE tone frequencies were not matched, the resultant signal contained an amplitude pedestal that was sinusoidally amplitude modulated with a modulation index = 1.

To quantify the spectral properties of the inhibition acting on DTNs, we first collected responses with the BD and NE tones matched to the cell's BEF. We then collected responses from the same cell with the BD tone set to the BEF and the NE tone mismatched in frequency. We tested all DTNs with five NE tone frequencies standardized to the eBW of each cell (Fig. 2.2). To obtain these frequencies, the eBW was first divided into lower (L_{eBW}) and higher (H_{eBW}) spectral partitions (re BEF). The five standardized NE tone frequencies were selected as *1*) 1.5 times the span of the L_{eBW} below the BEF ($1.5L_{eBW}$), *2*) the midpoint of the L_{eBW}($0.5L_{eBW}$), *3*) the BEF, *4*) the midpoint of the H_{eBW} ($0.5H_{eBW}$), and *5*) 1.5 times the span of the H_{eBW} above the BEF ($1.5H_{eBW}$). Thus each cell was tested with at least three NE tone frequencies within its 50% eBW (BEF, $0.5L_{eBW}$, $0.5H_{eBW}$) and two NE tone frequencies outside its 50% eBW ($1.5L_{eBW}$, $1.5H_{eBW}$). Whenever possible, additional NE tone frequencies were also tested.

This version of the paired-tone stimulation paradigm is analogous to the classic two-tone stimulation paradigm used for measuring the inhibitory frequency tuning

properties of auditory neurons (Fuzessery and Feng 1982; Sutter et al. 1999). In two-tone stimulation cells are presented with a pair of pure tones, with the probe tone fixed to the cell's BEF (analogous to our BD tone) and a test tone that is varied in frequency (analogous to our NE tone). Unlike classic two-tone stimulation, our paired-tone stimulation paradigm used two signals of unequal duration. The NE tone was 10 times the duration of the BD tone and, critically, was varied in ISI to measure the time course of the inhibition evoked by the NE tone.

2.3.5 – Measuring the onset and offset of inhibition with spike counts and latencies

We measured the duration and latency of the inhibition evoked by the NE tone by observing the time points when the BD tone-evoked spike count became suppressed and/or altered in latency, using the same criteria as Sayegh et al. (2014). To measure the time course of the inhibition evoked by the NE tone, we first quantified the cell's baseline responses evoked by the BD tone at the 10 longest ISIs when the BD tone preceded the NE tone (see baseline data points in Fig. 2.3). This baseline reflects responses evoked by the BD tone in the absence of inhibition evoked by the NE tone. For each cell, we calculated the mean ± SD baseline spike count, first spike latency (FSL), and last spike latency (LSL). For the example short-pass DTN in Fig. 2.3A, baseline spiking was measured from responses falling within the parallelogram. The baseline spike count was 1.76 ± 0.80 spikes per stimulus, whereas the baseline FSL was 21.66 ± 2.06 ms and the baseline LSL was 25.25 ± 2.93 ms. Using three criteria, we compared baseline responses with those obtained at each ISI to determine when spike counts or latencies were altered by NE tone-evoked inhibition.

As in our previous studies with paired-tone stimulation, we used a combination of detection criteria to measure the time course of inhibition evoked by the NE tone (Faure et al. 2003; Sayegh et al. 2012, 2014). We used a 50% change in the evoked spike count as the initial criterion to delineate the time points for the onset and offset of spike suppression. Whenever possible, we also used a 1 SD change in spike latency to further refine and extend those estimates because we have found spike latency changes to be a more sensitive indicator for the presence of inhibition than changes in spike counts.

With a spike count criterion, spiking was said to be suppressed when the mean spikes per stimulus decreased to ≤50% of baseline. The use of this criterion is depicted in Fig. 2.3*B*; data points below the dashed line, which represents 50% of the baseline spike count, were defined as suppressed. With a FSL criterion, spiking was said to be altered when the mean FSL deviated by >1 SD from baseline. The use of this criterion is depicted in Fig. 2.3*C*; data points falling above or below the two dashed lines, which represent ±1 SD of the baseline FSL, were defined as altered. Finally, with a LSL criterion, spiking was said to be altered when the mean LSL deviated by >1 SD from baseline. The use of this criterion is depicted in Fig. 2.3*D*; data points falling above or below the dashed lines representing ±1 SD of the baseline LSL were defined as altered.

Each criterion yielded a set of ISIs when the BD tone-evoked spikes were suppressed and/or altered in latency. Two time points were obtained from the three sets of ISIs recorded: the onset of spike suppression (T_1) and the offset of spike suppression (T_2). The value of T_1 was defined as the shortest ISI, starting from when the BD tone preceded the NE tone and moving toward larger positive ISIs, when the spike count and/or latency

became altered and the next two consecutive ISIs also deviated for a given criterion. The value of T_2 was defined as the shortest ISI, following T_1, when the spike count and/or latency remained altered and the next two consecutive ISIs had returned to within baseline values for a given criterion. Ideally, three values of T_1 and T_2 were obtained from the changes in spike count, FSL, and LSL for each cell. For the example cell in Fig. 2.3, the values of T_1 and T_2 were −1 ms and 39 ms with only a spike count criterion, 1 ms and 39 ms with only a FSL criterion, and −3 ms and 1 ms with only a LSL criterion.

The final values of T_1 and T_2 were chosen to be those that were most sensitive in capturing the time course of the suppressed response evoked by the NE tone with a spike count and/or spike latency criterion. The use of spike counts or spike latencies (or both) to quantify changes in a neuron's responsiveness has previously been validated (Faure et al. 2003; Sayegh et al. 2012, 2014). In cases in which cells responded with only a single spike per stimulus [i.e., baseline first spike latency (L_{first}) = baseline last spike latency (L_{last})], a change in spike count was typically used for selecting T_1 and T_2 because this criterion was more accurate in reflecting the time course of the evoked inhibition. For cells that responded with more than one spike per stimulus (i.e., $L_{first} < L_{last}$) or in cases where the spike count of the cell had recovered to within 50% of baseline even though L_{first} or L_{last} (or both) was still clearly deviated by >1 SD from baseline, a change in spike latency was typically used for selecting T_1 and T_2 because this criterion was more sensitive in reflecting the time course of the evoked inhibition. In cases in which the mean spike count or latency had not returned to within 50% or 1 SD of baseline, respectively, over the range of ISIs presented, T_2 was conservatively estimated as the longest ISI tested. For the example cell

shown in Fig. 2.3, the final value of T_1 was −3 ms and was obtained with a LSL criterion, whereas the final value of T_2 was 39 ms and could be obtained with either a spike count or FSL criterion.

We conducted a separate analysis to determine whether the choice of criterion to detect a response change (i.e., a 50% change or 1 SD change) interacted with the measured neural parameter (spike count or latency). For the 38 cells tested with five standardized frequency conditions ($38 \times 5 = 190$ observations), we compared the final values of T_1 and T_2 that were selected with a *1*) 50% spike count criterion, *2*) 50% spike latency criterion, *3*) 1 SD spike count criterion, and *4*) 1 SD spike latency criterion. The results of this analysis (not shown) revealed that a 50% criterion worked best for detecting deviations in spike count (but not spike latency) data and a 1 SD criterion worked best for detecting deviations in spike latency (but not spike count) data. There were two reasons for this conclusion. *1*) The use of a single criterion did not perform well and was too conservative. For example, there were cases where the spike count of a cell had returned to within 50% of baseline even though its FSL and/or LSL were still clearly deviated by >1 SD from baseline (see, e.g., Fig. 2.7). There were also cases in which spike counts had decreased by 50% (but not by 1 SD) from baseline even though spike latencies from the same cell were deviated by 1 SD (but not by 50%) from baseline. In these instances, we used the criterion that most sensitively and accurately captured the time course of the cell's altered response. *2*) It was impossible to apply the same numerical criterion—a 50% change or 1 SD deviation—to both spike count and latency data. For example, a 50% change in spike count was able to detect the onset/offset of inhibition in 188 of 190 observations (98.9%),

whereas a 50% change in spike latency was able to detect the onset/offset of inhibition in only 52 of 190 observations (27.4%). This demonstrates that a 50% spike latency change was less useful as a detection criterion, likely because most cells were incapable of exhibiting large latency deviations. Similarly, a 1 SD change in spike count detected the onset/offset of inhibition in 146 of 190 observations (76.8%), whereas a 1 SD change in spike latency detected the onset/offset of inhibition in 164 of 190 observations (86.3%). This demonstrates that a 1 SD latency criterion more frequently detected altered responses compared with a 50% latency criterion. Finally, 41 of 190 observations (21.6%) had spike counts with a SD that was larger than the mean, and in these cases inhibition could never be detected with a 1 SD change in spike count because a cell cannot have a spike count below 0. This demonstrates the limitation of this measure with respect to spike counts.

In summary, and as in previous studies (Faure et al. 2003; Sayegh et al. 2012, 2014), we used a mixture of criteria—either a 50% change in spike count or a 1 SD change in spike latency—to detect deviations and demark the onset/offset of altered responses in midbrain DTNs because this was the most sensitive and accurate method for measuring the time course of NE tone-evoked inhibition during paired-tone stimulation. In all instances, the final choice of criterion was confirmed by visual inspection.

2.3.6 – Determining the latency and duration of NE tone evoked inhibition

The final values T_1 and T_2 were used to calculate the effective (observable) start time (T_{start}), end time (T_{end}), and duration of inhibition (D_{IHB}) evoked by the NE tone as:

$$T_{start} = T_1 + L_{last} - D_{BD}, \quad (1)$$

$$T_{end} = T_2 + L_{first} - D_{BD}, \text{ and,} \quad (2)$$

$$D_{IHB} = T_{end} - T_{start}, \quad (3)$$

Where L_{first} was the baseline FSL, L_{last} was the baseline LSL, and D_{BD} was the duration of the BD tone. The onset (T_1) and offset (T_2) of changes in a cell's evoked responses were detected at ISIs where the BD tone-evoked spike count and/or latency deviated (see *Measuring onset and offset of inhibition with spike counts and latencies*). Because the paired-tone stimulation paradigm uses a roving BD tone and a stationary NE tone, changes to a cell's evoked response will depend on the relative timing of the two signals. When the BD tone leads (follows) the NE tone, it is the last (first) spikes in the BD tone-evoked response that initially (finally) become altered (recovered) in number and/or latency owing to the onset (offset) of inhibition evoked by the NE tone. Thus, in the equation for T_{start} (T_{end}), the baseline LSL (FSL) is added to T_1 (T_2) because spikes would have occurred at this location in time were they not suppressed by inhibition evoked by the NE tone. Because T_1 (T_2) was measured with respect to BD tone offset whereas the baseline LSL (FSL) was measured with respect to BD tone onset, subtracting the duration of the BD tone from T_1 + LSL (T_2 + FSL) aligns both time axes with respect to NE tone onset.

A DTN was said to have leading inhibition when the onset of inhibition evoked by the NE tone occurred before the FSL (i.e., $T_{start} < L_{first}$) but was said to have lagging inhibition when the onset of NE tone-evoked inhibition occurred after the FSL (i.e., $T_{start} > L_{first}$). A DTN was said to have persistent inhibition when D_{IHB} was longer than the NE tone duration (D_{NE}) evoking the suppression (i.e., $D_{IHB} > D_{NE}$).

For the example cell shown in Fig. 2.3, $T_{start} = 19.25$ ms, $T_{end} = 57.66$ ms, and $D_{IHB} = 38.41$ ms. The cell showed leading inhibition because the latency of inhibition evoked by the NE tone occurred 2.41 ms before the 21.66-ms FSL ($L_{first} - T_{start} = 2.41$ ms). The cell also showed persistent inhibition because the duration of inhibition evoked by the NE tone was 8.41 ms longer than the duration of the 30-ms NE tone ($D_{IHB} - D_{NE} = 8.41$ ms). After stimulation, the cell's FSL and LSL returned to baseline; however, the mean spike count over the 10 longest positive ISIs when the BD tone followed the NE tone (1.16 ± 0.83 spikes/stimulus) was still significantly lower [$t(15.7) = 5.6$, $P \ll 0.001$] than the cell's baseline spike count (1.76 ± 0.80 spikes/stimulus). This suggests that persistent inhibition may have extended well beyond stimulus offset. Long-lasting persistent inhibition in DTNs has been reported previously during both extracellular and whole cell recordings (Covey et al., 1996; Faure et al., 2003; Leary et al., 2008; Alluri et al., 2016).

2.3.7 – Measuring the iFRA, BIF, and iBW

We obtained a normalized isolevel inhibitory frequency response area (iFRA) and used it to measure the BIF and iBW of each DTN at +10 dB above the excitatory threshold (Fig. 2.4). A normalized iFRA was calculated by dividing the duration of inhibition evoked at each NE tone frequency by the duration of inhibition evoked at the BEF, denoted as D_{IHB}/D_{IHB}(BEF) and plotted as a function of NE tone frequency in octaves (re BEF). The frequency with the largest value was defined as the BIF. To estimate the iBW, we calculated separate linear regressions to measure the low ($Slope_{Low}$) and high ($Slope_{High}$) slopes of the isolevel iFRA tuning (re BIF) and defined the two cutoff frequencies by interpolating the regression to 50% of the value at the BIF (e.g., Fig. 2.4). Not every NE

tone frequency was included in the linear regression calculations; the highest (or lowest) frequency included was the first normalized data point ≤ 0.1, starting from the BIF and moving higher (or lower) in frequency. A cell was said to have a multipeaked iFRA if data points outside of the iBW returned to ≥50% of the normalized value at the BEF. Cells with fewer than three data points to measure an iFRA slope were excluded from statistical analyses (n = 4).

2.3.8 – Data analysis

Spike count data are displayed as means ± SD, except in Fig. 2.1, Fig. 2.3, Fig. 2.6, and Fig. 2.7, where these data are plotted as means ± SE to assist in visual interpretation. All data were tested for normality and homogeneity of variances with Shapiro-Wilk and Bartlett tests, respectively. We used parametric statistics when data were normally distributed with equal variances; otherwise, equivalent nonparametric statistical tests were used and data are reported as medians and interquartile ranges (IQRs).

We obtained neural recordings and measured basic response properties from 43 DTNs in the IC of *E. fuscus*. In some experiments it was not possible to obtain data from the same cell under all conditions (e.g., the cell was lost), and when this occurred our sample size decreased. Not every DTN showed evidence of inhibition during paired-tone stimulation at each of the five standardized NE tone frequencies, and when this occurred data from these cells were excluded from repeated-measures statistical analyses (n = 5); otherwise, the data were included in summary statistics, figures, and/or tables.

Linear regression was used to evaluate the relationship between electrode depth and a cell's BEF. A Kruskal-Wallis test was used to compare excitatory FSLs as a function of SPL re threshold. Cochran's Q-test was used to compare the proportion of cells showing leading/lagging or persistent inhibition at the five standardized NE tone frequencies. Welch's *t*-test (unequal variances) was used to detect elevated/depressed spike counts (re baseline) in the 10 longest positive ISIs when the BD tone followed the NE tone. The duration of leading/lagging or persistent inhibition measured at the five standardized NE tone frequencies was compared with a Friedman test followed by Nemenyi post hoc tests for all pairwise comparisons; cells for which inhibition could not be measured ($n = 5$) were not included in this repeated-measures analysis. A Mann-Whitney *U*-test was used to compare the duration of leading/lagging inhibition in band-pass cells and short-pass DTNs and the difference between the BEF and BIF. Linear regressions were used to evaluate the relationship between the duration of leading/lagging inhibition and BD or FSL at the five standardized NE tone frequencies and to measure the low ($Slope_{Low}$)- and high ($Slope_{High}$)-frequency tuning slopes of the iFRA for each cell. A Wilcoxon signed-rank test was used to compare the eBW and iBW sizes, excitatory $Q_{10\ dB}$ and inhibitory Q factors, and the $Slope_{Low}$ and $Slope_{High}$values measured from each cell's iFRA. All statistical tests were performed in SPSS or R and used a test-wise type I error rate of $\alpha = 0.05$.

2.4 – Results

2.4.1 – Tonotopic organization of DTNs in the IC

Tonotopic organization is a general property that is created at the basilar membrane and maintained throughout the nuclei of the central auditory nervous system. In *E. fuscus*, tonotopic organization has also been well documented (Covey and Casseday 1991; Grothe et al. 2001; Haplea et al. 1994). We examined the spatial distribution of neural BEFs in our population of 43 DTNs and found a strong positive correlation between recording electrode depth and BEF (Fig. 2.5*A*; $R^2 = 0.639$, $P \ll 0.001$). This finding demonstrates that DTNs are also tonotopically organized, thus replicating previous findings about duration tuning in the IC (Haplea et al. 1994; Jen and Wu 2006; Morrison et al. 2014; Pinheiro et al. 1991; Sayegh et al. 2012). Most of the DTNs in our sample (97.6%) had BEFs that fell between 20 and 70 kHz. This frequency range encompasses most of the bandwidth of echolocation calls emitted by *E. fuscus*(Casseday and Covey 1992) and also matches its most sensitive hearing range (Koay et al. 1997).

2.4.2 – Effect of SPL on FSL

Across the population of DTNs we examined how FSL changed as a function of stimulus level and found that excitatory response latencies remained more or less constant and were independent of the SPL above threshold [Fig. 2.5*B*; $\chi^2(4) = 2.67$, $P = 0.614$]. These data demonstrate that the excitatory FSLs of DTNs are time locked to stimulus onset and do not vary with changes in stimulus amplitude. This result contrasts with most other types of auditory neurons, where the FSL systematically decreases with increasing stimulus level (e.g., Heil 2004; Mörchen et al. 1978; Rose et al. 1963; Tan et al. 2008).

Some auditory neurons show paradoxical latency shift (PLS), in which the cell's FSL increases with increasing stimulus amplitude. Neurons with PLS have been described from both the auditory cortex (Hechavarría and Kössl 2014; Sullivan 1982a, 1982b) and IC (Covey et al. 1996; Galazyuk et al. 2005; Galazyuk and Feng 2001; Hechavarría et al. 2011; Klug et al. 2000; Macías et al. 2016). We did not find evidence of PLS in the population of DTNs in our sample. Mechanistically, two conditions must be satisfied for a cell to exhibit PLS: *1*) the onset of inhibition must lead or begin simultaneously with the onset of excitation, and *2*) the strength of inhibition must increase more quickly than the strength of excitation with increasing stimulus level. The leading inhibition that is important for creating duration selectivity satisfies the first condition (Casseday et al. 1994, 2000; Covey et al. 1996; Faure et al. 2003; Sayegh et al. 2014), but the amplitude tolerance of the spiking responses of auditory DTNs does not satisfy the second condition (Fremouw et al. 2005; Zhou and Jen 2001).

2.4.3 – Inhibition evoked at the BEF and at non-BEFs

Responses evoked from a band-pass DTN during paired-tone stimulation with the NE tone set to the cell's BEF and to a non-BEF within the cell's 50% eBW are shown in Fig. 2.6. The dot raster display and duration filter function for this cell are shown in Fig. 2.1*A*. When stimulated at +10 dB re threshold, the BEF of the cell was 17.5 kHz and its eBW ranged from 16.3 to 20.0 kHz (note: the BEF was 17.0 kHz when stimulated at +20 dB re threshold; Fig. 2.1*A*). When the BD and NE tones were matched and set to the cell's BEF (Fig. 2.6*A*), a large reduction in the spike count (Fig. 2.6*B*) and significant deviations in both the FSL and LSL were observed when the 2-ms BD tone and 20-ms NE tone were

sufficiently close in time (Fig. 2.6, *C* and *D*). This included ISIs when the BD tone immediately preceded, was simultaneous with, and immediately followed the NE tone. The final value for T_1 was −2 ms, and this value concurred across all three criteria. The final value for T_2 was 42 ms and was derived from changes to the cell's FSL. The effective duration of spike suppression was 41.63 ms. This neuron showed leading inhibition because $L_{first} = 11.59$ ms and $T_{start} = 9.96$ ms; hence the onset of inhibition preceded the cell's FSL by 1.63 ms. The cell also showed evidence of persistent inhibition because the effective duration of the altered response lasted 21.63 ms beyond the offset of the 20-ms NE tone. After the offset of inhibition, there was no difference between the baseline spike count (1.78 ± 1.51 spikes/stimulus) and the spike count evoked at the 10 longest positive ISIs when the BD tone followed the NE [1.53 ± 1.35 spikes/stimulus; $t(17.47) = 1.1$, $P = 0.287$]. Note the transient increase in the evoked spike count (and latencies) near the offset of the NE tone at ISIs between 18 and 20 ms (Fig. 2.6, *A* and *B*). This offset facilitation has been reported in previous in vivo studies of DTNs that have used paired-tone stimulation (Faure et al. 2003) and may reflect an offset-evoked excitatory event that is a component of conceptual and computational models of duration tuning (Aubie et al. 2009).

Response suppression was also observed when the roving BD tone was presented at the BEF (17.5 kHz) and the stationary NE tone was presented at a non-BEF (18.75 kHz) within the cell's 50% eBW (Fig. 2.6*E*). When the NE tone was set to a non-BEF the onset of spike suppression occurred at the same time as when the NE tone was set to the cell's BEF (compare Fig. 2.6, *B* and *F*); however, the duration of spike suppression was noticeably shorter, as evidenced by changes in the cell's evoked spike count (Fig. 2.6*F*)

but not by deviations in the evoked FSL (Fig. 2.6*G*) or LSL (Fig. 2.6*H*). The final value for T_1 was −2 ms and was derived from changes in spike count and/or LSL. The final value for T_2 decreased to 18 ms and was derived from changes in the evoked spike count. The effective duration of inhibition was 18.14 ms, which was shorter than the duration of inhibition when the NE tone was set to the BEF. Leading inhibition was observed in the non-BEF condition because $L_{first} = 11.33$ ms and $T_{start} = 9.19$ ms; hence the onset of inhibition preceded the cell's FSL by 2.14 ms. The cell did not show persistent inhibition because the effective duration of inhibition was −1.86 ms shorter than the duration of the 20-ms NE tone. After the offset of inhibition, there was no difference between the baseline spike count (1.46 ± 1.28 spikes/stimulus) and the counts evoked at the 10 longest positive ISIs when the BD tone followed the NE tone [1.52 ± 1.21 spikes/stimulus; $t(18.00) = 0.3$, $P = 0.736$].

Comparing across the two conditions, the onset of inhibition was similar regardless of whether the NE tone was set to the cell's BEF or to a non-BEF within its eBW. A sustained inhibition was evoked when the NE tone was set to the BEF, but its duration was shorter when the NE tone was set to a non-BEF within the cell's eBW. Persistent inhibition was only observed when the NE tone was set to the BEF, indicating that the inhibition evoked at non-BEFs was weaker in strength and/or shorter in duration compared with the BEF condition.

Responses evoked from a short-pass DTN during paired-tone stimulation with the NE tone set to the cell's BEF and to a non-BEF outside of the cell's 50% eBW are shown in Fig. 2.7. The dot raster display and duration filter function for this cell are shown in Fig.

2.1*B*. The BEF of the cell was 42.0 kHz, and its eBW ranged from 41.0 to 44.0 kHz at +10 dB above threshold. When the BD and NE tones were matched and set to the cell's BEF (Fig. 2.7*A*), there was a large reduction in the spike count (Fig. 2.7*B*) and significant deviations in both the FSL and LSL (Fig. 2.7, *C* and *D*) when the 1-ms BD tone and 10-ms NE tone were sufficiently close in time. This included ISIs when the BD tone immediately preceded, was simultaneous with, and immediately followed the NE tone. The final value for T_1 was −7 ms and was derived from a change in spike count. The final value for T_2 was 57 ms and could be derived from a change in either FSL or LSL. The effective duration of spike suppression was 61.57 ms. This neuron showed leading inhibition because $L_{first} = 22.95$ ms and $T_{start} = 17.38$ ms; hence the onset of inhibition preceded the cell's FSL by 5.57 ms. The cell also had persistent inhibition because the effective duration of spike suppression lasted 51.57 ms beyond the offset of the 10-ms NE tone. Compared with the baseline value (1.41 ± 0.65 spikes/stimulus), spike counts evoked at the 10 longest positive ISIs when the BD tone followed the NE tone were slightly higher [1.84 ± 0.64 spikes/stimulus; $t(16.2) = 5.5$, $P < 0.001$]. The 10 data points averaged to calculate the baseline response are shown as white circles with an X in Fig. 2.7. In this cell two or three data points included in the baseline spike count appear to be decreasing owing to inhibition evoked by the NE tone. The net effect of including these values in the cell's baseline response calculation was a slightly more stringent (conservative) criterion for detecting changes in the evoked spike count, with the overall effect resulting in an underestimation of the time course of inhibition evoked by the NE tone.

Response suppression was again observed when the roving BD tone was presented at the cell's BEF (42.0 kHz) and the stationary NE tone was presented at a non-BEF (38.0 kHz) located outside of the cell's 50% eBW; however, the duration of suppression was noticeably smaller (Fig. 2.7*E*). Further analyses showed a reduction in the spike count (Fig. 2.7*F*) and deviations in both the FSL (Fig. 2.7*G*) and LSL (Fig. 2.7*H*) of the cell. As in the BEF condition, the final value for T_1 was −7 ms and was derived from a change in spike count. The final value for T_2 decreased to 45 ms and was derived from a change in LSL. This resulted in an effective duration of inhibition of 50.30 ms, which was shorter than the duration of inhibition in the BEF condition. The cell showed leading inhibition in the non-BEF condition because $L_{first} = 23.38$ ms and $T_{start} = 17.08$ ms; hence the onset of inhibition preceded the cell's FSL by 6.30 ms. The cell also showed persistent inhibition because the effective duration of inhibition was 40.30 ms longer than the duration of the 10-ms NE tone. Compared with the baseline count (1.16 ± 0.56 spikes/stimulus), spike counts evoked at the 10 longest positive ISIs when the BD tone followed the NE tone (1.66 ± 0.70 spikes/stimulus) were higher [$t(17.2) = 4.7$, $P < 0.001$].

Across the two frequency conditions, the onset of inhibition was similar regardless of whether the NE tone was set to the cell's BEF (17.38 ms) or to a non-BEF (17.08 ms). A long-lasting, sustained inhibition was also evoked when the NE tone was either matched or unmatched to the BEF. Because persistent inhibition was longer when the NE tone was set to the cell's BEF, this suggests that the inhibition evoked at non-BEFs was either weaker and/or shorter lasting. Another feature apparent in this cell was increased spike counts (compared with baseline) following the presentation of the NE tone in both the matched

and unmatched frequency conditions (Fig. 2.7, *B* and *F*). Because the increase in spiking was long lasting and not time locked to the stimulus, it is difficult to attribute the elevated response to a specific mechanism—such as postinhibitory rebound excitation or a separate offset-evoked excitatory synaptic input—that is responsible for creating the short-pass duration selectivity of the cell. We know that postinhibitory rebound excitations can last from a few milliseconds to several seconds (Barrio et al. 1994; Chandler et al. 1994; Hodgkin and Huxley 1952; Koch and Grothe 2003; Owen et al. 1984; Tell and Bradley 1994). Given the cell's long FSL (~23.0 ms) and strong leading inhibition (5.6 ms), we speculate that there would have been no difference between baseline and recovery spike counts if the cell's baseline responses had been estimated with a slightly longer gap between the leading BD tone and lagging NE tone. In the last part of this section we report on the consistency of depressed/elevated spike counts (re baseline) in DTNs following the presentation of the NE tone during paired-tone stimulation.

We tested 43 DTNs using paired-tone stimulation with the NE tone set to five standardized frequencies relative to each cell's eBW (Fig. 2.2): three frequencies within the 50% eBW (BEF, $0.5L_{eBW}$, $0.5H_{eBW}$) and two frequencies outside the 50% eBW ($1.5L_{eBW}$, $1.5H_{eBW}$). Spiking was suppressed in all 43 cells (100%) when the NE tone was presented in the $1.5L_{eBW}$, $0.5L_{eBW}$, BEF, and $0.5H_{eBW}$ frequency conditions; however, only 38 cells (88.4%) showed measurable inhibition when the NE tone was set to the $1.5H_{eBW}$ high-frequency condition. These data indicate that the strength of the NE tone-evoked inhibition varies with sound frequency.

Leading inhibition was observed in 55% (104/190) of the observations on 38 DTNs that were tested with the five standardized NE tone frequencies, and the proportion of cells with leading inhibition did not differ across the frequencies [$\chi^2(4) = 1.70$, $P = 0.79$, $n = 38$]. Additionally, the amount of leading/lagging inhibition (i.e. the relative timing of the onset of inhibition and excitation) did not differ across the five NE tone frequencies [$\chi^2(4) = 4.82$, $P = 0.31$, $n = 38$], with the mean value remaining relatively constant between 0 and 2 ms (Fig. 2.8*A*, black boxes). These results demonstrate that the latency of the inhibition evoked during paired-tone stimulation was more or less constant across NE tone frequencies within or near the cell's 50% eBW.

In contrast, the proportion of cells with persistent inhibition differed across the five NE tone frequencies. Additionally, the duration of this persistent inhibition differed across the five standardized NE tone frequencies (Table 2.1). The longest average duration of persistent inhibition occurred when the NE tone was set to the cell's BEF but decreased as the NE tone frequency was increased or decreased, forming an inverted V shape centered at the BEF (Fig. 2.8*B*, black boxes). The shape of this inverted V was asymmetric, with higher NE tone frequencies evoking shorter effective durations of persistent inhibition compared with lower NE tone frequencies. In contrast to the results for the onset of inhibition, these results demonstrate that the offset of NE tone-evoked inhibition systematically decreased as the NE frequency moved away from the BEF.

With regard to the consistency of poststimulatory effects (i.e., elevated or depressed spike counts compared with baseline), we reanalyzed our entire data set of 38 cells tested with five standardized NE tone frequencies (190 observations) and compared baseline

spikes counts to those measured in the 10 longest positive ISIs when the BD tone followed the NE tone. There were 38 observations when the BD and NE tones were matched in frequency; 15 (39.5%) showed no difference, and 8 (21%) had elevated and 15 (39.5%) depressed spike counts (re baseline) following the presentation of the NE tone. For the remaining 152 observations when the BD and NE tone were mismatched in frequency, 82 (53.9%) showed no difference and 14 (9.2%) had elevated and 56 (36.8%) depressed spike counts (re baseline) following the presentation of the NE tone. With regard to the number of neurons, there were 12 cells with elevated spike counts: 6 at one frequency condition, 3 at two conditions, 2 at three conditions, 1 at four conditions, and 0 in all five frequency conditions. The number of cells with elevated spike counts was smallest at the most extreme NE tone frequencies, with the distribution being $1.5L_{eBW} = 6$ cells, $0.5L_{eBW} = 3$ cells, BEF = 8 cells, $0.5H_{eBW} = 1$ cell, and $1.5H_{eBW} = 4$ cells. There were 29 cells with depressed spike counts: 11 at one frequency condition, 6 at two conditions, 4 at three conditions, 6 at four conditions, and 2 in all five frequency conditions. The number of cells with depressed spike counts was also smallest at the most extreme NE tone frequencies, with the distribution being $1.5L_{eBW} = 13$ cells, $0.5L_{eBW} = 16$ cells, BEF = 15 cells, $0.5H_{eBW} = 16$ cells, and $1.5H_{eBW} = 11$ cells. This latter result is consistent with the shortening of the offset of inhibition as the frequency of the NE tone was moved further away from the BEF (see Fig. 2.8*B*). Overall, these data demonstrate that most DTNs did not show consistent poststimulatory effects (i.e., spike count facilitation or spike count depression) during paired-tone stimulation. When they occurred, poststimulatory effects were most frequent when the NE tone was set to the cell's BEF. One interesting possibility

is that cells with poststimulatory elevated spike counts could be displaying a weak form of delay tuning (Macías et al. 2012; Portfors and Wenstrup 1999, 2001) and/or interval tuning (Leary et al. 2008), and such responses may help *E. fuscus* process ecologically relevant combinations of long- and short-duration sounds separated in time (e.g., during mother-pup social interactions; Mayberry and Faure 2014; Monroy et al. 2011). Future studies should continue to explore any relationship that exists between duration tuning and delay tuning.

2.4.4 – Relation of leading/lagging inhibition to BD, FSL, and duration filter class

Leading inhibition is an important feature of many auditory neurons and plays a role in binaural hearing (Carney and Yin 1989), temporal processing (Galazyuk et al. 2005), and encoding frequency modulated sweeps (Razak and Fuzessery 2006; Fuzessery et al. 2011). Because leading inhibition has been observed in several types of IC neurons, regardless of whether or not they are duration-tuned (e.g. Faingold et al. 1991; Covey et al. 1996; Kuwada et al. 1997; Faure et al. 2003; Voytenko and Galazyuk 2008), this suggests that it is a general property of central auditory processing. Conceptual and computational models of DTNs combined with evidence from electrophysiological recordings indicate that a cell's BD and duration filter response class depend, in part, on the amount of leading inhibition (Aubie et al. 2009, 2012; Casseday et al. 1994, 2000; Ehrlich et al. 1997; Faure et al. 2003; Fremouw et al. 2005; Fuzessery and Hall, 1999). Previous studies have also reported a positive relation between the duration of leading inhibition and BD and/or FSL (Faure et al. 2003; Sayegh et al. 2014).

We evaluated our data for similar relations at the five standardized NE tone frequencies and found a positive correlation between the duration of leading inhibition and BD in all conditions (Fig. 2.9*A*). The correlation was strongest when the NE tone matched the BD tone and both were set to the cell's BEF but systematically decreased as the NE tone departed from the BEF (Table 2.2). It is important to note that when we removed the 8-ms BD putative outlier point and reanalyzed our data, the results were nearly identical: four of the five standardized frequency conditions ($0.5L_{eBW}$, BEF, $0.5H_{eBW}$, and $1.5H_{eBW}$) maintained a positive correlation between BD and the duration of leading inhibition (i.e. duration of inhibitory advance re excitation) (Fig. 2.9*A*). Many studies in *E. fuscus* have reported DTNs with BDs ≥ 8 ms (e.g., Faure et al. 2003; Ma and Suga 2001; Morrison et al. 2014; Pinheiro et al. 1991), including the original report in bats (Jen and Schlegel 1982). Because the BD and duration of leading inhibition of this cell were not atypical, we conclude that this data point was not an outlier.

There was also a positive correlation between the duration of leading inhibition and FSL for the standardized NE tone frequencies except the $1.5H_{eBW}$ condition (Fig. 2.9*B*). The relationship was strongest when the NE tone matched the BD tone and was set to the cell's BEF and decreased as the NE tone frequency moved away from the BEF (Table 2.2). The strength of the relationship decreased more quickly for NE tone frequencies higher than the BEF, revealing an asymmetry in the correlation with changes in sound frequency. Altogether, these results demonstrate that DTNs with short BDs and FSLs have shorter durations of leading inhibition than cells with longer BDs and FSLs regardless of the frequency used to evoked the inhibition.

Previous paired-tone stimulation studies have also found that the duration of leading inhibition relates to the duration filter class of a DTN, with short-pass cells having shorter durations of leading inhibition than band-pass DTNs when the BD and NE tones were matched in frequency (Faure et al. 2003; Sayegh et al. 2014). We compared the duration of leading inhibition evoked in short-pass and band-pass DTNs in each NE tone frequency condition (Table 2.3). The duration of leading inhibition differed between short-pass and band-pass DTNs when the BD and NE tones were matched at the cell's BEF and when the NE tone was unmatched and higher in frequency than the BD tone in the 0.5 H_{eBW} condition. Although there was a trend, the duration of leading inhibition between short-pass and band-pass DTNs was not significant in the 1.5L_{eBW}, 0.5L_{eBW}, and 1.5H_{eBW} NE tone frequency conditions. In addition to replicating previous in vivo observations, our results expand the findings to other NE tone frequencies by demonstrating that the onset of inhibition to DTNs is broadly tuned and largely frequency invariant.

2.4.5 – Comparing excitatory and inhibitory BFs, FRAs, BWs, and Q factors

We used single BD tone pulses at different frequencies to construct each cell's eFRA and measure its BEF and eBW. We then collected paired-tone stimulation responses from the same DTN at different NE tone frequencies to construct each cell's iFRA and measure its BIF and iBW. Figure 2.10*A* shows an example eFRA measured from a DTN with a BEF of 51.0 kHz and an eBW of 4 kHz (ranging between 49.0 and 53.0 kHz). Excitation in the cell was narrowly tuned, and its excitatory $Q_{10\ dB}$ was 12.75. Figure 2.10*B* shows the cell's iFRA with a BIF of 51.0 kHz. In this cell, the BEF exactly matched the BIF. For reference, the five standardized NE tone frequencies used to the test the cell

are also illustrated (Fig. 2.10*B*; open circles). In contrast, the cell's iBW was 16.12 kHz (ranging between 40.07 and 56.19 kHz) and its inhibitory Q was 3.16. The data demonstrate that inhibition was more broadly tuned than excitation in this DTN. Because the cell's eBW was completely (100%) overlapped by the iBW (compare overlap of gray boxes in Fig. 2.10, *A* and *B*), this suggests that the strength of inhibition was maintained over a broad range of frequencies. The low- and high-frequency slopes of the normalized iFRA were $\text{Slope}_{\text{Low}} = 1.27$ and $\text{Slope}_{\text{High}} = -3.06$, respectively. This asymmetry in the normalized duration of inhibition indicates that the strength of inhibition decreased more quickly at high vs. low frequencies.

An example DTN where the BEF did not match the BIF is shown in Fig. 2.10, *C* and *D*. The BEF of the cell was 28.6 kHz and its eBW was 2 kHz (ranging from 27.8 to 29.8 kHz), resulting in an excitatory $Q_{10\ \text{dB}}$ of 14.3 (Fig. 2.10*C*). The cell's iFRA revealed a BIF of 27.8 kHz, which was slightly mismatched (−0.04 octaves below) to the BEF. The iBW of the cell was 6.20 kHz (ranging between 23.15 and 29.35 kHz), and its inhibitory Q was 4.48 (Fig. 2.10*D*). Again, excitation in this DTN was more narrowly tuned than inhibition. The cell's eBW was nearly encapsulated by the iBW, resulting in 77.3% spectral overlap. The low- and high-frequency slopes of the normalized iFRA were $\text{Slope}_{\text{Low}} = 1.94$ and $\text{Slope}_{\text{High}} = -7.95$, respectively.

An example of a DTN with a multipeaked isolevel eFRA and iFRA is shown in Fig. 2.10, *E* and *F*. The BEF of the cell was 32.0 kHz and its eBW was 8.0 kHz (ranging from 27.0 to 35.0 kHz), resulting in an excitatory $Q_{10\ \text{dB}}$ of 4.0 (Fig. 2.10*E*). The cell also had a narrowband secondary peak of excitation (ranging from ~38.0 to 41.0 kHz; 0.25–0.36

octaves re BEF). The iFRA had a BIF of 33.5 kHz, which was 0.07 octaves higher than the BEF, and its iBW was 16.38 kHz (ranging between 18.53 and 34.91 kHz) (Fig. 2.10*F*), resulting in an inhibitory Q of 2.05. Inhibitory spectral tuning in this cell was again much broader than excitatory spectral tuning, and there was 98.9% overlap between the eBW and iBW. The slopes of the normalized iFRA were $\text{Slope}_{\text{Low}} = 0.63$ and $\text{Slope}_{\text{High}} = -8.32$, demonstrating that the cell had extremely asymmetric tuning flanks. The cell also had two small secondary inhibitory tuning peaks between 41.0 and 45.0 kHz (0.36–0.49 octaves re BEF) and between 51.0 and 56.0 kHz (0.67–0.81 octaves re BEF).

Across the population of DTNs tested we computed $\log_2(\text{BIF}) - \log_2(\text{BEF})$ and found that the difference did not differ from zero (median difference = 0.00 octaves, IQR = −0.04 to 0.00 octaves, $V = 85.0$, $P = 0.06$, $n = 39$). There were 15 cells (38.5%) where the BIF exactly matched the BEF and another 14 cells (35.9%) where BIF differed by only ±0.05 octaves from the BEF (Fig. 2.11*A*). This demonstrates that there was a close correspondence in the sound frequencies evoking maximal synaptic excitation and inhibition in DTNs. Cells with multipeaked iFRAs were observed in only 5 of 39 DTNs (12.8%).

To further examine the correspondence in spectral tuning between neural excitation and inhibition, we compared the size and amount of spectral overlap between the eBW and iBW in the same cell. The absolute size of the eBW (median = 4.0 kHz, IQR = 3.0–8.0 kHz) was smaller than the absolute size of the iBW (median = 11.76 kHz; IQR = 6.6–18.0 kHz), and the difference was highly significant ($Z = -4.91$, $P < 0.001$, $n = 39$). In 35 of 39 cells (89.7%), the lowest cutoff frequency of the eBW was higher than the lowest cutoff

frequency of the iBW. In 25 of 39 cells (64.1%), the highest cutoff frequency of the eBW was lower than the highest cutoff frequency of the iBW. In 23 of 39 cells (58.9%), the iBW completely overlapped the eBW. Across the population of DTNs tested, spectral overlap between the eBW and iBW averaged 91.7% (Fig. 2.11*B*).

To examine the sharpness of excitatory and inhibitory tuning, we compared excitatory $Q_{10\ dB}$ and inhibitory Q factors from the same neuron. There was a highly significant difference in the distribution of excitatory $Q_{10\ dB}$ (median = 9.25) and inhibitory Q factors (median = 4.16) across the population of DTNs tested (Fig. 2.12; $Z = -5.01$, $P < 0.001$, $n = 39$). Only 4 cells (10.3%) had excitatory $Q_{10\ dB}$ factors smaller than their inhibitory Q factors. This demonstrates that inhibitory inputs to DTNs were more broadly tuned in frequency than excitatory inputs. Broad inhibitory tuning has also been seen in whole cell patch-clamp recordings of awake bats, where the frequency tuning curves of most IC neurons were dominated by inhibition (Xie et al. 2007). The inhibitory Q factors of the DTNs we studied fell into a very narrow range (IQR = 2.85–5.10), whereas excitatory $Q_{10\ dB}$ factors were widely distributed (IQR = 4.86–14.30) and were similar to excitatory $Q_{10\ dB}$ factors of DTNs from a previous study (Morrison et al. 2014).

Finally, we examined the symmetry of the low- and high-frequency flanks of the isolevel iFRA by comparing the slope of the low-frequency slope ($Slope_{Low}$) to the absolute value of the slope of the high-frequency slope ($|Slope_{High}|$). Differences between the slope values reflect changes in the normalized duration of inhibition as a function of NE tone frequency. Across the population of DTNs tested, $Slope_{Low}$ values (median = 2.11, IQR = 1.27–3.69) were smaller than $|Slope_{High}|$ values (median = 4.46, IQR = 2.53–

5.98; $Z = -4.36$, $P < 0.001$, $n = 39$). Only 6 cells (15.4%) had a $Slope_{Low}$ steeper than $|Slope_{High}|$ (Fig. 2.13). These results demonstrate that inhibition was strongest for sound frequencies at and below the BIF.

2.5 – Discussion

2.5.1 – Inhibitory inputs to DTNs are onset evoked and broadly tuned in frequency

Duration tuning is an emergent electrophysiological response property that appears to be created de novo in the auditory midbrain (Ehrlich et al. 1997; Sayegh et al. 2011). Previous work has shown that duration tuning arises through the interaction of sound-evoked excitatory and inhibitory synaptic inputs that are offset in time (Casseday et al. 2000; Covey et al. 1996; Faure et al. 2003; Fuzessery and Hall 1999; Leary et al. 2008). It should be noted that, technically, neural inhibition is not required to create a duration-selective neural circuit. For example, in the coincidence mechanism of duration tuning two subthreshold excitatory components must coincide in time to cause the membrane potential of the DTN to become suprathreshold: *1*) an onset-evoked subthreshold excitatory input and *2*) an offset-evoked subthreshold excitatory input (see Aubie et al. 2009; Sayegh et al. 2011). However, application of pharmacological antagonists that block inhibitory neurotransmitters has shown that duration selectivity broadens or is eliminated when inhibition is absent (Casseday et al. 1994, 2000; Fuzessery and Hall 1999; Jen and Feng 1999; Jen and Wu 2005; Yin et al. 2008). Furthermore, evidence from extracellular single-unit and intracellular whole cell patch-clamp recordings has shown that short-pass and/or band-pass DTNs receive an onset-evoked inhibitory input that precedes its onset-evoked excitatory input and that inhibition is sustained for as long or longer than the duration of the stimulus (Casseday et al. 1994, 2000; Covey et al. 1996; Ehrlich et al. 1997; Faure et al. 2003; Leary et al. 2008). These data demonstrate that duration selectivity is created, in part, by the inhibitory control of excitatory responses.

In this study we found that neural inhibition to DTNs was broadly tuned, with an onset latency that remained constant across a wide range of sound frequencies both within and outside the 50% eBW of the cell (Fig. 2.8*A* and Fig. 2.12). In contrast, many auditory neurons show substantial changes in FSL with changes in stimulus amplitude and/or frequency (Heil 2004; Tan et al. 2008). We propose the columnar division of the ventral nucleus of the lateral lemniscus (VNLLc) as a potential location where inhibitory inputs to midbrain DTNs may originate. The VNLLc consists of a three-dimensional matrix of neurons in which projections from the anteroventral cochlear nucleus converge onto sheets of cells innervated by calyceal endings (Covey and Casseday 1986). This anatomical arrangement makes the VNLLc ideally suited for temporal processing because a large number of anteroventral cochlear nucleus inputs, all tuned to different frequencies, converge onto a small network of VNLLc neurons. This arrangement would result in VNLLc having low spectral selectivity but high temporal precision.

Several lines of evidence support the hypothesis that the VNLLc is a suitable candidate nucleus to provide inhibition to DTNs in the IC. First, the VNLLc projects primarily to the IC (Covey and Casseday 1986). Second, cells in the VNLLc have a short response latency (Covey and Casseday 1991), which is a feature of the leading inhibition to DTNs (Fig. 2.8*A* and Fig. 2.9). Third, VNLLc neurons are broadly tuned in frequency and their threshold tuning curves are asymmetric, with high-frequency flanks steeper than low-frequency flanks (Covey and Casseday 1991). The former feature matches the spectral tuning of the neural inhibition acting on DTNs (Fig. 2.10 and Fig. 2.12), while the latter matches the asymmetric steepness in the slopes of DTN iFRAs (Fig. 2.13). Third, the

responses of VNLLc neurons are primarily monaural (Covey and Casseday 1991), and a recent study using binaural paired-tone stimulation found that the responses of DTNs in the IC of *E. fuscus* were primarily created with monaural circuits (Sayegh et al. 2014). Finally, VNLL neurons with glycinergic inhibition project directly to the IC. These inputs are known to participate in the spectro-temporal processing of combination-sensitive neurons. Combination-sensitive neurons are cells whose excitatory response to one sound element is facilitated by the presentation of another sound element (Portfors and Wenstrup 1999; Yavuzoglu et al. 2011). Given that some midbrain DTNs also have combination-sensitive response selectivity for the delay between two sounds (Macías et al. 2013), this leaves open the possibility that DTNs and delay-tuned neurons may receive the same (or similar) source(s) of neural inhibition.

Despite these similarities, a majority of VNLLc neurons show phasic spiking responses, whereas the inhibition acting on DTNs is sustained, suggesting some type of tonic input. One possibility is that the small proportion of VNLLc neurons with tonic responses provide inhibitory inputs to DTNs. This seems less likely when one considers that up to a third of cells are reported to be duration selective in the IC of *E. fuscus*(Ehrlich et al. 1997) yet only 5% of VNLLc neurons had tonic responses (Covey and Casseday 1991). Another possibility is that VNLLc neurons with phasic responses provide the source of the broadly tuned, constant-latency, onset-evoked inhibition to DTNs and that other cells with tonic responses provide sustained inhibition to DTNs. In the present study, we found that the leading inhibition acting on DTNs was more broadly tuned than the later sustained inhibition (Fig. 2.8). That two components of the neural inhibition acting on DTNs had

different spectral tuning suggests they may have arisen from different sources. A previous study found that the inhibition acting on DTNs was strongest at its onset (Faure et al. 2003), suggesting that the early portion of the onset-evoked sustained inhibition had a strength and time course different from the later portion. Other studies have shown that midbrain DTNs have both γ-aminobutyric acid (GABA)ergic and glycinergic inputs (Casseday et al. 1994, 2000), raising the intriguing possibility that phasic and tonic inhibitory inputs to DTNs could be using different neurotransmitters. If true, then this may help to explain why the application of one neuropharmacological antagonist (e.g., GABA or glycine) sometimes broadened duration selectivity, whereas application of two antagonists (e.g., GABA and glycine) completely abolished it (Casseday et al. 2000; Yin et al. 2008).

2.5.2 – Mechanism of spike suppression during paired tone stimulation

Previous studies using paired-tone stimulation on DTNs have assumed that spike suppression was caused by synaptic inhibition (e.g., Faure et al. 2003; Sayegh et al. 2014). Intracellular recordings have shown that DTNs receive prominent synaptic inhibition (Covey et al. 1996; Leary et al. 2008). Moreover, iontophoresis of inhibitory neurotransmitter antagonists has demonstrated that synaptic inhibition is necessary for the electrophysiological response property of duration tuning (Casseday et al. 1994, 2000; Fuzessery and Hall 1999; Jen and Feng 1999; Jen and Wu 2005; Yin et al. 2008). An alternative is that spike suppression was caused by postsynaptic mechanisms, such as intrinsic membrane properties of a cell triggered by synaptically mediated excitation, instead of synaptic inhibition. For example, the biophysical properties of the family of small-conductance calcium-activated potassium (SK_{Ca}) channels can cause spike

suppression after a cell receives a depolarizing (excitatory) event due to an increase in intracellular calcium (Hu and Mooney 2005; Sah 1996; Sah and Faber 2002). Activation of the SK_{Ca} channel following an action potential causes an afterhyperpolarization that suppresses spiking from milliseconds to seconds. If intrinsic membrane properties caused spike suppression in DTNs during paired-tone stimulation, then the strength and time course of the suppression should correlate to the excitatory response. Our data demonstrate that suppression was unrelated to the presence or strength of suprathreshold excitation. Spike suppression occurred in DTNs stimulated with NE tone frequencies falling both within and outside the eFRA (e.g., Fig. 2.10). Additionally, the evoked suppression was more broadly tuned than the evoked excitation in the same cell (Figs. 2.8, 2.10, and 2.12), and in most DTNs stimulated with long-duration BEF tones there was no spiking event to activate an intrinsic mechanism. Finally, although intrinsic membrane properties may account for the persistent inhibition of DTNs during paired-tone stimulation (Figs. 2.3, 2.6, 2.7, and 2.8*B*), they do not explain leading inhibition.

2.5.3 – Response properties of DTNs are stable across the eBW

The neural inhibition acting on DTNs displays four properties that may help to ensure that a cell's BD, duration filter class, and basic response properties remain stable with changes in sound frequency: *1*) the onset of inhibition was frequency tolerant (Fig. 2.8*A*); *2*) sustained inhibition lasted nearly as long or longer than the duration of the stimulus evoking the inhibition (Fig. 2.8*B*); *3*) the BIF matched the BEF (Fig. 2.11*A*); and *4*) inhibition was as broad as (Fig. 2.11*B*) or more broadly tuned than (Fig. 2.8and Fig. 2.10) excitation.

That the latency of inhibition to DTNs was tolerant to changes in stimulus frequency suggests that the onset of inhibition plays an important role in shaping the BD, duration filter class (i.e., short-pass or band-pass), temporal bandwidth of duration tuning, and FSL because these response properties are created, in part, by the difference in latency between inhibition and excitation (Aubie et al. 2009, 2012; Casseday et al. 1994, 2000; Covey et al. 1996; Faure et al. 2003; Fuzessery and Hall 1999; Sayegh et al. 2014). Our study replicated and extended this finding by demonstrating that the duration of leading inhibition remained constant across a broad range of NE tone frequencies (Fig. 2.8*A*). Moreover, the correlation between leading inhibition and BD (or FSL or duration filter class) was also roughly maintained across the cell's eFRA (Fig. 2.9; Table 2.2 and Table 2.3).

That sustained inhibition was evoked across a broad range of frequencies within a cell's eBW could help to ensure that inhibition lasts sufficiently long to coincide with an offset-evoked excitatory input that plays a critical role in the coincidence detection mechanism of duration selectivity; the sustained inhibition would suppress spiking at stimulus durations outside the excitatory temporal bandwidth (Aubie et al. 2009, 2012). Sustained/persistent inhibition was longest at BEF but systematically decreased at non-BEFs. This effect appeared to be strongest for stimulus frequencies higher than BEF (Fig. 2.8*B* and Fig. 2.13). It seems possible that spectral tuning of the inhibitory inputs to a DTN simply reflects the asymmetric frequency tuning curves that primary auditory afferents (and other cells) inherit as a result of the asymmetric mechanical band-pass displacement tuning curves of the cochlea. In theory, if the duration of sustained inhibition in a DTN

changes with sound frequency then this may alter the cell's response to echolocation calls and echoes. Although some cells may lose their duration selectivity with increases in stimulus frequency above the BEF, the temporal selectivity of cells with higher BEFs could improve. Therefore, across the overall population of DTNs within the IC, duration selectivity will be reduced in some cells and enhanced in others, with the exact effect depending on the relative difference between stimulus frequency and each cell's BEF. Within bats, these effects may also differ between high-duty-cycle species that employ Doppler shift compensation and low-duty-cycle bats that do not (Macías et al. 2016).

The iFRA of a DTN is broadly tuned with the BIF centered on the BEF, ensuring the cell receives inhibition throughout its eFRA. Several studies have shown that inhibition is necessary for creating duration selectivity in the IC (Casseday et al. 1994, 2000; Fuzessery and Hall 1999; Jen and Feng 1999; Jen and Wu 2005; Yin et al. 2008). Broadband inhibition would also help to preserve duration tuning at non-BEFs. It is important to note that excitatory spectral tuning could be broader than what is measured from a cell's spiking discharge pattern (e.g., subthreshold excitation or suprathreshold excitation that is sculpted by inhibition; Xie et al. 2007). For temporal selectivity to be preserved across a wide range of frequencies, a DTN should receive an inhibitory input whose spectral tuning is as broad as or broader than the tuning of its excitatory input. This is exactly what we found: the iBWs of DTNs were significantly larger than their eBWs (Fig. 2.12).

Two previous studies found that the temporal response properties of some DTNs changed when cells were stimulated at non-BEFs (Brand et al. 2000; Macías et al. 2016).

In our study, 5 of 43 DTNs showed no evidence of inhibition when stimulated with NE tones set to the 1.5 H_{eBW} condition, and in the remaining 38 cells the average duration of the evoked inhibition was shorter than the duration of the NE tone stimulus (Fig. 2.8*B*). Computational circuit models and in vivo neuropharmacological experiments have both shown that when the sustained/persistent inhibition of a DTN is lost/blocked, duration selectivity becomes reduced or abolished (see Aubie et al. 2009; Casseday et al. 2000). Given the modulatory role of inhibition in temporal processing, it seems possible that the temporal selectivity of a DTN could change when stimulated at non-BEFs, and particularly at frequencies higher than BEF. In the mustached bat (*Pteronotus parnellii*) spike discharge patterns of resting-frequency DTNs changed for stimulation at different frequencies (Macías et al. 2016). This result differs somewhat from the temporal properties of inhibition observed in DTNs of *E. fuscus*, where the onset of leading inhibition was frequency independent but the duration of the sustained persistent inhibition was not. Alternatively, the properties (e.g., latency, discharge pattern) of excitation may also change when DTNs are stimulated with non-BEFs. Future studies should measure the temporal tuning profiles of DTNs at different sound frequencies.

2.5.4 – Persistent inhibition and recovery cycles

Persistent inhibition is a property of many IC neurons regardless of whether or not they are duration-tuned (Covey et al. 1996; Faingold et al. 1991; Faure et al. 2003; Klug et al. 1999; Kuwada et al. 1997; Pollak and Park 1993; Sayegh et al. 2014; Yin 1994). Two previous studies have discussed the role of persistent inhibition in determining the recovery cycle time for a DTN (Sayegh et al. 2012; Wu and Jen 2006). The recovery time of a neuron

is typically determined with paired-pulse stimulation and is measured as the minimum ISI required for the response (i.e., spike count or latency) evoked by a second stimulus to recover within a specified level of the response evoked by the first stimulus (Grinnell 1963). Paired-pulse stimulation is similar to the paired-tone stimulation paradigm that we employed, the difference being that in the latter the BD and NE tones differed in duration.

In our study, the duration of the sustained inhibition occurred on a timescale similar to the recovery cycle times of DTNs when the BD and NE tones were matched in frequency (Sayegh et al. 2012). The present results also show that the duration of the sustained inhibition evoked by the NE tone systematically decreased as the NE tone frequency moved away from the BEF. This finding predicts that a DTN stimulated at a non-BEF will have a shorter recovery cycle time compared with stimulation at the BEF. Other studies found that the frequency selectivity of DTNs sharpened during paired-pulse stimulation when the second tone was presented at short ISIs compared with longer ISIs (Wu and Jen 2008b, 2008c). These results are generally consistent with our findings (Fig. 2.8*B*). For a more direct comparison, future studies on DTNs should test the effect of varying the BD tone frequency during paired-tone stimulation. We acknowledge that the duration of the NE tone could also influence the strength of the inhibition evoked by it, as shown in computational (Aubie et al. 2009, 2012) and neurophysiological (Faure et al. 2003) studies.

2.5.5 – Frequency tuning of temporal masking

Psychophysical auditory temporal masking experiments are analogous to the paired-tone stimulation paradigm that we used to test DTNs from the IC of *E. fuscus*. The BD tone is analogous to the probe (or signal) tone, while the NE tone is analogous to the

masker (or suppressor) tone. Neural correlates of auditory temporal masking patterns have been identified in DTNs with paired-tone stimulation (Faure et al. 2003; Sayegh et al. 2014). Spike suppression when the BD tone preceded the NE tone is the neural equivalent of backward masking and occurred as a result of the leading inhibition evoked by the NE tone. Similarly, spike suppression when the BD tone overlapped with the NE tone to produce a composite stimulus is the neural equivalent of simultaneous masking and occurred as a result of the sustained inhibition evoked by the NE tone. Finally, spike suppression when the BD tone followed the NE tone is the neural equivalent of forward masking and occurred as a result of the persistent inhibition evoked by the NE tone.

We found that the onset-evoked, leading and sustained inhibition were stronger and more broadly tuned than the persistent inhibition evoked in the same cells (Fig. 2.8). Moreover, the low-frequency slope of a DTN's iFRA was shallower than its high-frequency slope (Fig. 2.13). Interestingly, psychophysical masking data show similar relationships in frequency selectivity to DTNs in paired-tone stimulation. Psychophysical tuning curves measured during simultaneous masking were broader than those of forward masking, with forward masking thresholds increasing more steeply at higher frequencies (Bacon and Moore 1986; Moore 1978; Soderquist et al. 1981). In contrast, psychophysical tuning curves measured in backward masking were more variable. Some human studies suggest that backward masking is more broadly tuned than forward masking (Dye and Yost 1981; Miyazaki and Takayuki 1984). One study found that human psychophysical tuning curves were equally broad in forward and backward masking, whereas in birds forward

masking psychophysical tuning curves were broader than their backward masking counterparts (Dooling and Searcy 1985).

2.6 – References

Aubie B, **Becker S**, **Faure PA**. Computational models of millisecond level duration tuning in neural circuits. *J Neurosci* 29: 9255–9270, 2009.

Aubie B, **Sayegh R**, **Faure PA**. Duration tuning across vertebrates. *J Neurosci* 32: 6373–6390, 2012.

Bacon SP, **Moore BC**. Temporal effects in simultaneous pure-tone masking: effects of signal frequency, masker/signal frequency ratio, and masker level. *Hear Res* 23: 257–266, 1986.

Barrio LC, **Araque A**, **Buno W**. Participation of voltage-gated conductances on the response succeeding inhibitory synaptic potentials in the crayfish slowly adapting stretch receptor neuron. *J Neurophysiol* 72: 1140–1151, 1994.

Brand A, **Urban R**, **Grothe B**. Duration tuning in the mouse auditory midbrain. *J Neurophysiol* 84: 1790–1799, 2000.

Carney LH, **Yin TC**. Responses of low-frequency cells in the inferior colliculus to interaural time differences of clicks: excitatory and inhibitory components. *J Neurophysiol* 62: 144–161, 1989.

Casseday JH, **Covey E**. Frequency tuning properties of neurons in the inferior colliculus of an FM bat. *J Comp Neurol* 319: 34–50, 1992.

Casseday JH, **Ehrlich D**, **Covey E**. Neural tuning for sound duration: role of inhibitory mechanisms in the inferior colliculus. *Science* 264: 847–850, 1994.

Casseday JH, **Ehrlich D**, **Covey E**. Neural measurement of sound duration: control by excitatory-inhibitory interactions in the inferior colliculus. *J Neurophysiol* 84: 1475–1487, 2000.

Chandler SH, **Hsaio CF**, **Inoue T**, **Goldberg LJ**. Electrophysiological properties of guinea pig trigeminal motoneurons recorded *in vitro*. *J Neurophysiol* 71: 129–145, 1994.

Covey E, **Casseday JH**. Connectional basis for frequency representation in the nuclei of the lateral lemniscus of the bat *Eptesicus fuscus*. *J Neurosci* 6: 2926–2940, 1986.

Covey E, **Casseday JH**. The monaural nuclei of the lateral lemniscus in an echolocating bat: parallel pathways for analyzing temporal features of sound. *J Neurosci* 11: 3456–3470, 1991.

Covey E, **Kauer JA**, **Casseday JH**. Whole-cell patch-clamp recording reveals subthreshold sound-evoked postsynaptic currents in the inferior colliculus of awake bats. *J Neurosci* 16: 3009–3018, 1996.

Dooling RJ, **Searcy MH**. Nonsimultaneous auditory masking in the budgerigar (*Melopsittacus undulatus*). *J Comp Psychol* 99: 226–230, 1985.

Duysens J, **Schaafsma SJ**, **Orban GA**. Cortical off response tuning for stimulus duration. *Vision Res* 36: 3243–3251, 1996.

Dye RH, **Yost WA**. A comparison of psychophysical tuning curves obtained in forward, backward, and combined forward-backward masking. *J Acoust Soc Am* 70: S87, 1981.

Ehrlich D, **Casseday JH**, **Covey E**. Neural tuning to sound duration in the inferior colliculus of the big brown bat, *Eptesicus fuscus*. *J Neurophysiol* 77: 2360–2372, 1997.

Faingold CL, **Boersma Anderson CA**, **Caspary DM**. Involvement of GABA in acoustically-evoked inhibition in inferior colliculus neurons. *Hear Res* 52: 201–216, 1991.

Faure PA, **Fremouw T**, **Casseday JH**, **Covey E**. Temporal masking reveals properties of sound-evoked inhibition in duration-tuned neurons of the inferior colliculus. *J Neurosci* 23: 3052–3065, 2003.

Fremouw T, **Faure PA**, **Casseday JH**, **Covey E**. Duration selectivity of neurons in the inferior colliculus of the big brown bat: tolerance to changes in sound level. *J Neurophysiol* 94: 1869–1878, 2005.

Fuzessery Z, **Razak K**, **Williams A**. Multiple mechanisms shape selectivity for FM sweep rate and direction in the pallid bat inferior colliculus and auditory cortex. *J Comp Physiol A* 197: 615–623, 2011.

Fuzessery ZM, **Feng AS**. Frequency selectivity in the anuran auditory midbrain: single unit responses to single and multiple tone stimulation. *J Comp Physiol A* 146: 471–484, 1982.

Fuzessery ZM, **Hall JC**. Sound duration selectivity in the pallid bat inferior colliculus. *Hear Res* 137: 137–154, 1999.

Galazyuk A V, **Feng AS**. Oscillation may play a role in time domain central auditory processing. *J Neurosci* 21: 147–147, 2001.

Galazyuk A V, **Lin W**, **Llano D**, **Feng AS**. Leading inhibition to neural oscillation is important for time-domain processing in the auditory midbrain. *J Neurophysiol* 94: 314-326, 2005.

Grinnell AD. The neurophysiology of audition in bats: temporal parameters. *J Physiol* 167: 67–96, 1963.

Grothe B, **Covey E**, **Casseday JH**. Medial superior olive of the big brown bat: neuronal responses to pure tones, amplitude modulations, and pulse trains. *J Neurophysiol* 86: 2219–2230, 2001.

Haplea S, **Covey E**, **Casseday JH**. Frequency tuning and response latencies at three levels in the brainstem of the echolocating bat, *Eptesicus fuscus*. *J Comp Physiol A* 174: 671–683, 1994.

He J, **Hashikawa T**, **Ojima H**, **Kinouchi Y**. Temporal integration and duration tuning in the dorsal zone of cat auditory cortex. *J Neurosci* 17: 2615–2625, 1997.

Hechavarría JC, **Cobo AT**, **Fernández Y**, **Macías S**, **Kössl M**, **Mora EC**. Sound-evoked oscillation and paradoxical latency shift in the inferior colliculus neurons of the big fruit-eating bat, *Artibeus jamaicensis*. *J Comp Physiol A* 197: 1159–1172, 2011.

Heil P. First-spike latency of auditory neurons revisited. *Curr. Opin. Neurobiol.* 14: 461–467, 2004.

Heil P, **Rajan R**, **Irvine DRF**. Sensitivity of neurons in cat primary auditory cortex to tones and frequency-modulated stimuli. II: Organization of response properties along the

"isofrequency" dimension. *Hear Res* 63: 135–156, 1992.

Hodgkin AL, **Huxley AF**. A quantitative description of membrane current and its application to conduction and excitation in nerve. *J Physiol* 117: 500–544, 1952.

Hu B, **Mooney DM**. Burst firing induces a slow after hyperpolarization in rat auditory thalamus. *Neurosci Lett* 375: 162–164, 2005.

Jen PH-S, **Feng RB**. Bicuculline application affects discharge pattern and pulse-duration tuning characteristics of bat inferior collicular neurons. *J Comp Physiol A* 184: 185–194, 1999.

Jen PH-S, Schlegel P. Auditory physiological properties of the neurones in the inferior colliculus of the big brown bat, *Eptesicus fuscus*. *J Comp Physiol A* 147: 351–363, 1982.

Jen PH-S, **Wu CH**. The role of GABAergic inhibition in shaping the response size and duration selectivity of bat inferior collicular neurons to sound pulses in rapid sequences. *Hear Res* 202: 222–234, 2005.

Jen PH-S, **Wu CH**. Duration selectivity organization in the inferior colliculus of the big brown bat, *Eptesicus fuscus*. *Brain Res* 1108: 76–87, 2006.

Klug A, **Bauer EE**, **Pollak GD**. Multiple components of ipsilaterally evoked inhibition in the inferior colliculus. *J Neurophysiol* 82: 593–610, 1999.

Klug A, **Khan A**, **Burger RM**, **Bauer EE**, **Hurley LM**, **Yang L**, **Grothe B**, **Halvorsen MB**, **Park TJ**. Latency as a function of intensity in auditory neurons: influences of central

processing. *Hear Res* 148: 107–123, 2000.

Koay G, **Heffner HE**, **Heffner RS**. Audiogram of the big brown bat (*Eptesicus fuscus*). *Hear Res* 105: 202–210, 1997.

Koch U, **Grothe B**. Hyperpolarization-activated current (I_h) in the inferior colliculus: distribution and contribution to temporal processing. *J Neurophysiol* 90: 3679–3687, 2003.

Kuwada S, **Batra R**, **Yin TCT**, **Oliver DL**, **Haberly LB**, **Stanford TR**. Intracellular recordings in response to monaural and binaural stimulation of neurons in the inferior colliculus of the cat. *J Neurosci* 17: 7565–7581, 1997.

Leary CJ, **Edwards CJ**, **Rose GJ**. Midbrain auditory neurons integrate excitation and inhibition to generate duration selectivity: an *in vivo* whole-cell patch study in anurans. *J Neurosci* 28: 5481–5493, 2008.

Ma X, Suga N. Corticofugal modulation of duration-tuned neurons in the midbrain auditory nucleus in bats. *Proc Natl Acad Sci* 98: 14060–14065, 2001.

Macías S, **Hechavarría JC**, **Kössl M**. Sharp temporal tuning in the bat auditory midbrain overcomes spectral-temporal trade-off imposed by cochlear mechanics. *Sci Rep* 6: 29129, 2016. doi: 10.1038/srep29129.

Macias S, **Hechavarria JC**, **Kossl M**, **Mora EC**. Neurons in the inferior colliculus of the mustached bat are tuned both to echo-delay and sound duration. *Neuroreport* 24: 404–409, 2013.

Macías S, **Mora EC**, **Hechavarría JC**, **Kössl M**. Properties of echo delay-tuning receptive fields in the inferior colliculus of the mustached bat. *Hear Res* 286: 1–8, 2012.

Mayberry HW, Faure PA. Morphological, olfactory, and vocal development in big brown bats. *Biol. Open* 4: 22–34, 2015. doi: 10.1242/bio.201410181.

Miyazaki K, **Takayuki S**. Pure-tone masking patterns in nonsimultaneous masking conditions. *Jpn Psychol Res* 26: 110–119, 1984.

Monroy JA, **Carter ME**, **Miller KE**, **Covey E**. Development of echolocation and communication vocalizations in the big brown bat, *Eptesicus fuscus*. *J Comp Physiol A* 197: 459–467, 2011.

Moore BC. Psychophysical tuning curves measured in simultaneous and forward masking. *J Acoust Soc Am* 63: 524–532, 1978.

Mörchen A, **Rheinlaender J**, **Schwartzkopff J**. Latency shift in insect auditory nerve fibers. *Naturwissenschaften* 65: 656–657, 1978.

Morrison JA, **Farzan F**, **Fremouw T**, **Sayegh R**, **Covey E**, **Faure PA**. Organization and trade-off of spectro-temporal tuning properties of duration-tuned neurons in the mammalian inferior colliculus. *J Neurophysiol* 111: 2047–60, 2014.

Moss CF, **Surlykke A**. Auditory scene analysis by echolocation in bats. *J Acoust Soc Am* 110: 2207–2226, 2001.

Narins PM, **Capranica RR**. Neural adaptations for processing the two-note call of the

Puerto Rican treefrog, *Eleutherodactylus coqui. Brain Behav Evol* 17: 48–66, 1980.

Owen DG, **Segal M**, **Barker JL**. A Ca-dependent Cl^- conductance in cultured mouse spinal neurones. *Nature* 311: 567–570, 1984.

Pérez-González D, **Malmierca MS**, **Moore JM**, **Hernández O**, **Covey E**. Duration selective neurons in the inferior colliculus of the rat: topographic distribution and relation of duration sensitivity to other response properties. *J Neurophysiol* 95: 823–836, 2006.

Pinheiro AD, **Wu M**, **Jen PS**. Encoding repetition rate and duration in the inferior colliculus of the big brown bat, *Eptesicus fuscus*. *J Comp Physiol A* 169: 69–85, 1991.

Pollak GD, **Park TJ**. The effects of GABAergic inhibition on monaural response properties of neurons in the mustache bat's inferior colliculus. *Hear Res* 65: 99–117, 1993.

Portfors C V, **Wenstrup JJ**. Delay-tuned neurons in the inferior colliculus of the mustached bat: implications for analyses of target distance. *J Neurophysiol* 82: 1326–1338, 1999.

Portfors C V., **Wenstrup JJ**. Topographical distribution of delay-tuned responses in the mustached bat inferior colliculus. *Hear Res* 151: 95–105, 2001.

Razak KA, **Fuzessery ZM**. Neural mechanisms underlying selectivity for the rate and direction of frequency-modulated sweeps in the auditory cortex of the pallid bat. *J Neurophysiol* 96: 1303–19, 2006.

Rose JE, **Greenwood DD**, **Goldberg JM**, **Hind JE**. Some discharge characteristics of

single neurons in the inferior colliculus of the cat. I. Tonotopical organization, relation of spike counts to tone intensity, and firing patterns of single elements. *J Neurophysiol* 26: 294–320, 1963.

Sah P. Ca^{2+}-activated K^+ currents in neurones: types, physiological roles and modulation. *TINS* 19: 150–154, 1996.

Sah P, **Faber ESL**. Channels underlying neuronal calcium-activated potassium currents. *Prog Neurobiol* 66: 345–353, 2002.

Sayegh R, **Aubie B**, **Faure PA**. Duration tuning in the auditory midbrain of echolocating and non-echolocating vertebrates. *J Comp Physiol A* 197: 571–583, 2011.

Sayegh R, **Aubie B**, **Fazel-Pour S**, **Faure PA**. Recovery cycles of inferior colliculus neurons in the big brown bat measured with spike counts and latencies. *Front Neural Circuits* 6: 56, 2012. doi: 10.3389/fncir.2012.00056.

Sayegh R, **Casseday JH**, **Covey E**, **Faure PA**. Monaural and binaural inhibition underlying duration-tuned neurons in the inferior colliculus. *J Neurosci* 34: 481–92, 2014.

Schnitzler H-U, **Kalko EK V**. Echolocation by insect-eating bats. *Bioscience* 51: 557–569, 2001.

Shannon R V, **Zeng FG**, **Kamath V**, **Wygonski J**, **Ekelid M**. Speech recognition with primarily temporal cues. *Science* 270: 303–304, 1995.

Soderquist DR, **Carstens AA**, **Frank GJ**. Backward, simultaneous, and forward masking

as a function of signal delay and frequency. *J Aud Res* 21: 227–245, 1981.

Suga N. Neural mechanisms of complex-sound processing for echolocation. *TINS.* 7: 20–27, 1984.

Sullivan WE. Possible neural mechanisms of target distance coding in auditory system of the echolocating bat *Myotis lucifugus*. *J Neurophysiol* 48: 1033–1047, 1982a.

Sullivan WE. Neural representation of target distance in auditory cortex of the echolocating bat Myotis lucifugus. *J Neurophysiol* 48: 1011–1032, 1982b.

Sutter ML, **Schreiner CE**, **McLean M**, **O'Connor K N**, **Loftus WC**. Organization of inhibitory frequency receptive fields in cat primary auditory cortex. *J Neurophysiol* 82: 2358–2371, 1999.

Tan X, **Wang X**, **Yang W**, **Xiao Z**. First spike latency and spike count as functions of tone amplitude and frequency in the inferior colliculus of mice. *Hear Res* 235: 90–104, 2008.

Tell F, **Bradley RM**. Whole-cell analysis of ionic currents underlying the firing pattern of neurons in the gustatory zone of the nucleus tractus solitarii. *J Neurophysiol* 71: 479-492, 1994.

Voytenko S V, **Galazyuk A V**. Timing of sound-evoked potentials and spike responses in the inferior colliculus of awake bats. *Neuroscience* 155: 923–936, 2008.

Wang J, **van Wijhe R**, **Chen Z**, **Yin S**. Is duration tuning a transient process in the inferior colliculus of guinea pigs? *Brain Res* 1114: 63–74, 2006.

Wu CH, **Jen PH-S**. GABA-mediated echo duration selectivity of inferior collicular neurons of *Eptesicus fuscus*, determined with single pulses and pulse-echo pairs. *J Comp Physiol A* 192: 985–1002, 2006.

Wu CH, **Jen PH-S**. Bat inferior collicular neurons have the greatest frequency selectivity when determined with best-duration pulses. *Neurosci Lett* 438: 362–367, 2008a.

Wu CH, **Jen PH-S**. Echo frequency selectivity of duration-tuned inferior collicular neurons of the big brown bat, *Eptesicus fuscus*, determined with pulse-echo pairs. *Neuroscience* 156: 1028–1038, 2008b.

Wu CH, **Jen PH-S**. Auditory frequency selectivity is better for expected than for unexpected sound duration. *Neuroreport* 19: 127–31, 2008c.

Xie R, **Gittelman JX**, **Pollak GD**. Rethinking tuning: *in vivo* whole-cell recordings of the inferior colliculus in awake bats. *J Neurosci* 27: 9469–9481, 2007.

Yavuzoglu A, **Schofield BR**, **Wenstrup JJ**. Circuitry underlying spectrotemporal integration in the auditory midbrain. *J Neurosci* 31: 14424–14435, 2011.

Yin S, **Chen Z**, **Yu D**, **Feng Y**, **Wang J**. Local inhibition shapes duration tuning in the inferior colliculus of guinea pigs. *Hear Res* 237: 32–48, 2008.

Yin TC. Physiological correlates of the precedence effect and summing localization in the inferior colliculus of the cat. *J. Neurosci.* 14: 5170–5186, 1994.

Zhou X, Jen PH-S. The effect of sound intensity on duration-tuning characteristics of bat

inferior colliculus neurons. *J Comp Physiol A* 187: 63–73, 2001.

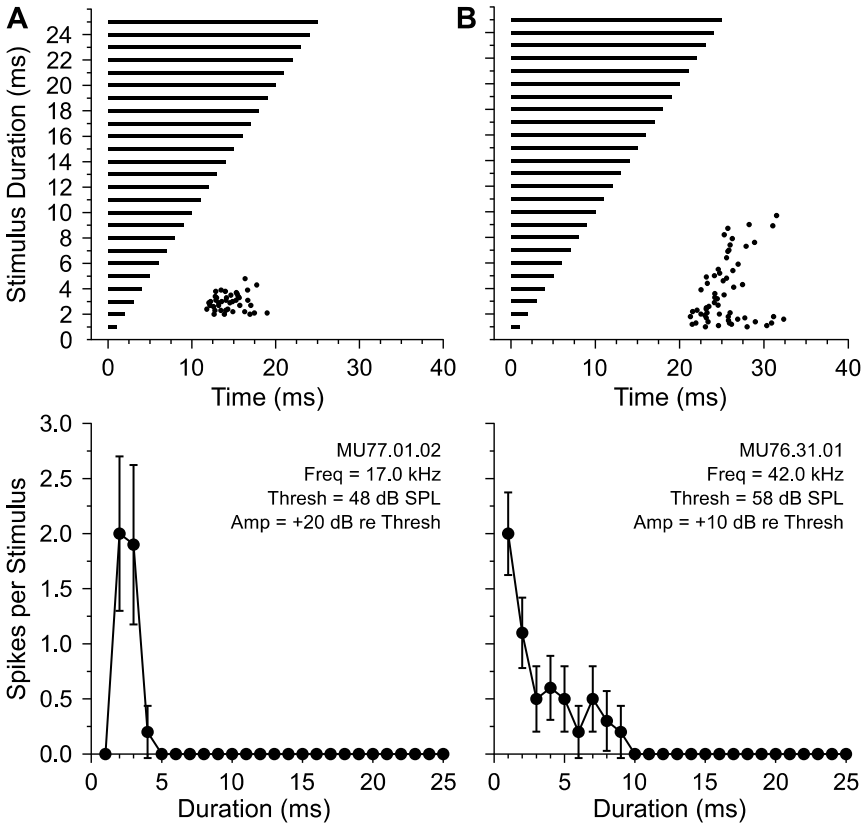

Fig. 2.1. Duration-tuned neurons (DTNs) from the inferior colliculus (IC) of the big brown bat.

A, Bandpass DTN with a best duration of 2 ms. ***B***, Short-pass DTN with a best duration of 1 ms. *Top row,* Dot raster displays showing the timing of action potentials in response to suprathreshold best excitatory frequency (BEF) tone pulses that were randomly varied in duration. *Bottom row,* Mean ± standard error (SE) spikes per stimulus as a function of stimulus duration for suprathreshold BEF tones. Stimulus level was **(*A*)** +20 dB and was **(*B*)** +10 dB re threshold. n = 10 trials per stimulus.

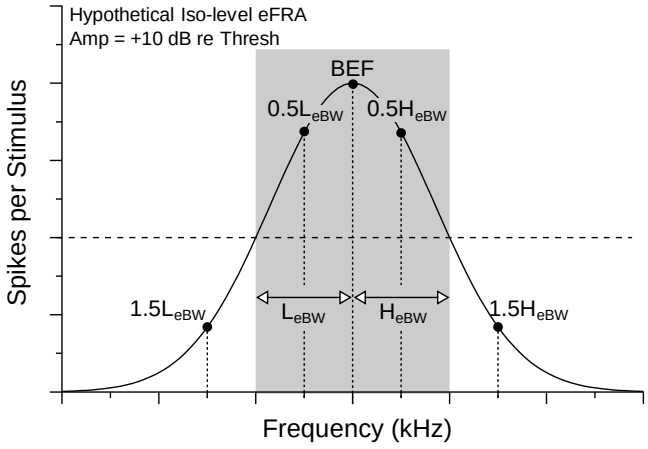

Fig. 2.2. Determining the five standardized NE tone frequencies.

Duration selective neurons were tested with paired tone stimulation using five NE tone frequencies that were standardized relative to the eBW (*grey box*) of each cell. The panel illustrates a hypothetical iso-level eFRA of a DTN, obtained by recording the number of spikes in response to single BD tones varied in frequency and presented at +10 dB above threshold. The cutoff frequencies (*edges of grey box*) of the eBW were defined as the lowest and highest stimuli evoking ≥50% (*horizontal dashed line*) of the maximum spike count measured at the BEF. The eBW was divided into lower (*L_{eBW}*) and higher (*H_{eBW}*) spectral partitions re BEF (*white arrows*), and five standardized NE tone frequencies (*black dots*) were selected as: (1) 1.5 times the L_{eBW} below the BEF (*$1.5L_{eBW}$*), (2) the midpoint of the L_{eBW} (*$0.5L_{eBW}$*), (3) the BEF, (4) the midpoint of the H_{eBW} (*$0.5H_{eBW}$*), and (5) 1.5 times the H_{eBW} above the BEF (*$1.5H_{eBW}$*). Thus, each cell was tested with at least three NE tone frequencies within its 50% eBW (*BEF, $0.5L_{eBW}$; $0.5H_{eBW}$*) and two NE tone frequencies outside its 50% eBW (*$1.5L_{eBW}$, $1.5H_{eBW}$*). Whenever possible, additional NE tone frequencies (not shown) were also tested.

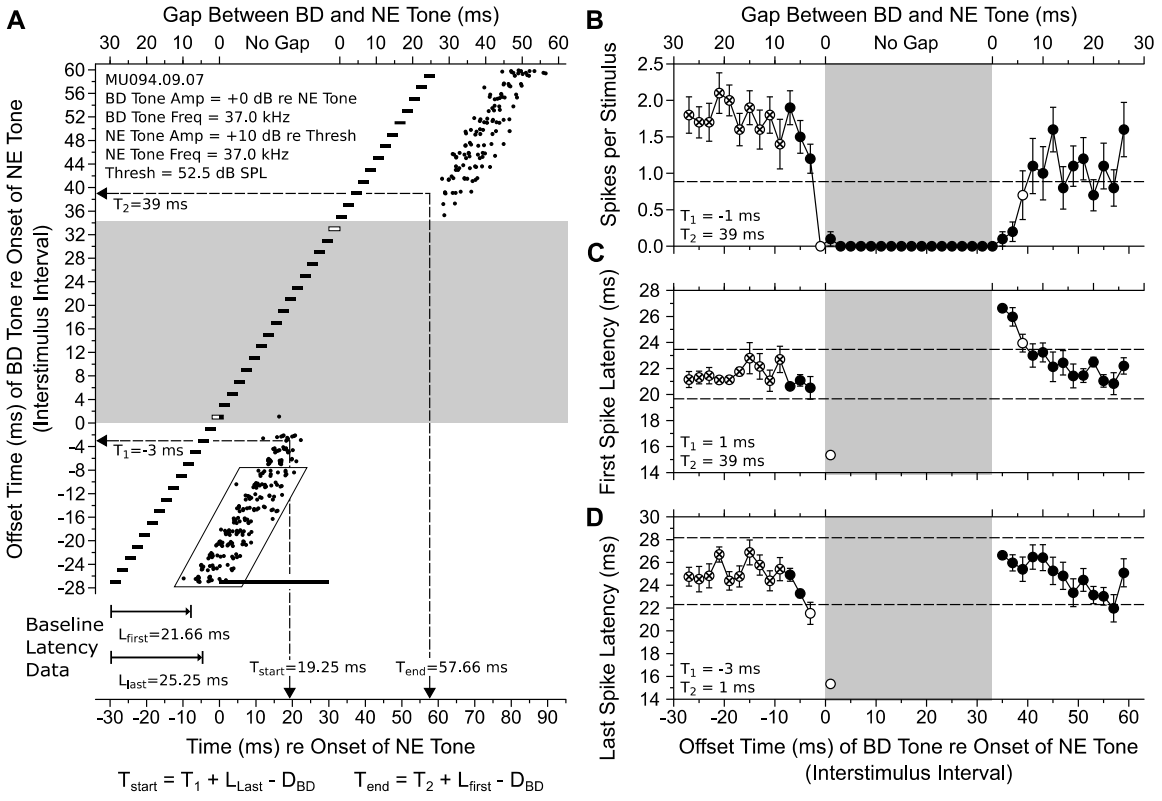

Fig. 2.3. Measuring the time course of inhibition with paired tone stimulation.

A, Dot raster display showing how changes in a cell's spike count and/or latencies in response to a roving BD tone were used to infer the time course of the synaptic inhibition evoked by the NE tone using the equations displayed at the bottom of the Figure. The onset time of the BD tone (*3 ms black bars*) was randomly varied relative to the onset of the NE Tone (*30 ms black bar;* drawn once for clarity). The bottom *x-axis* shows time relative to the onset of the NE tone, while the top *x-axis* shows the ISI or gap between BD and NE tones. The *y-axis* shows the offset time of the BD tone relative to the onset time of the NE tone. The two tones were electronically mixed and presented monaurally to the ear contralateral to the IC recorded. When the two tones were temporally contiguous or

overlapping (*grey box*), a single compound stimulus with an amplitude pedestal resulted. A BD tone bar with a *white fill* indicates when the BD and NE tones were contiguous. Responses from the first 10 trials with the longest ISI's (spikes in parallelogram) were used to calculate a mean ± SD baseline spike count (1.76 ± 0.80 spikes per stimulus), FSL (L_{first} = 21.66 ± 2.06 ms), and LSL (25.25 ± 2.93 ms); data points averaged in the baseline calculation are shown as *white circles with an X*. During paired tone stimulation BD tone evoked responses were suppressed by inhibition evoked by the NE tone. Three criteria were used to determine the effective onset (T_1) and offset (T_2) of the inhibition evoked by the NE tone using changes in spike count, FSL, and/or LSL. The first ISI with a significant deviation from the baseline spike count and/or latency was T_1 = -3 ms and was measured with a LSL criterion. The largest ISI with a significant deviation from the baseline spike count or latency was T_2 = 39 ms and was measured with either a spike count or FSL criterion. With the equations shown, T_{start} = 19.25 ms and T_{end} = 57.66 ms, resulting in an effective duration of inhibition of 38.41 ms. ***B,*** Mean ± standard error (SE) spikes per stimulus plotted as a function of the ISI between the BD and NE tones. The dashed line represents 50% of the baseline spike count. The leftmost *open circle* is the first ISI with an evoked spike count ≤ 50% of baseline spike count (T_1 = -1 ms). The rightmost *open circle* shows the last ISI with an evoked spike count ≤ 50% of baseline (T_2 = 39 ms). ***C,*** Mean ± SE FSL as a function of the ISI between the BD and NE tones. The dashed lines represent ±1 SD from the baseline FSL. The leftmost *open circle* shows the first ISI when the FSL deviated by >1 SD from baseline (T_1 = 1 ms). The rightmost *open circle* shows the last ISI when the FSL remained deviated by >1 SD from baseline (T_2 = 39 ms). ***D,*** Mean ± SE LSL

as a function of the ISI between the BD and NE tones. The dashed lines represent ±1 SD from the baseline LSL. The leftmost *open circle* shows the first ISI when the LSL deviated by >1 SD from baseline (T_1 = -3 ms). The rightmost *open circle* shows the last ISI when the LSL remained deviated by >1 SD from baseline (T_2 = 1 ms). The final values of T_1 (-3 ms) and T_2 (39 ms) were those that most sensitively reflected the time course of the NE tone evoked inhibition. 10 trials per stimulus.

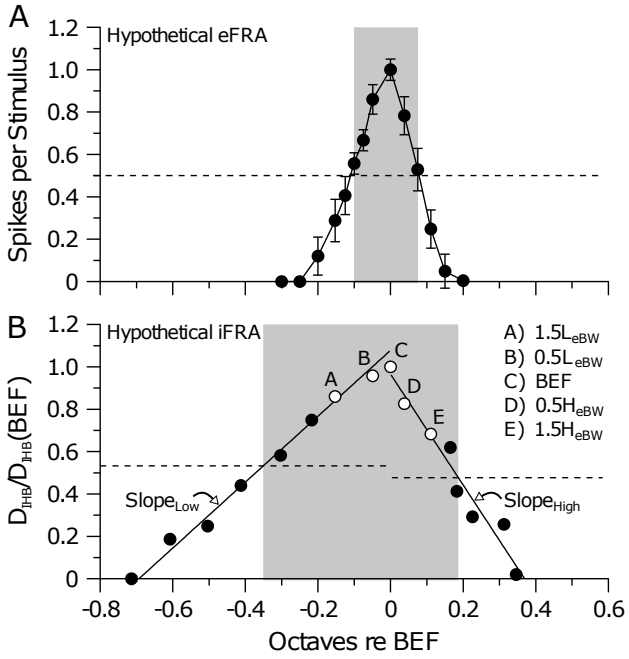

Fig. 2.4. Determining the inhibitory FRA, BIF, and iBW.

A, Hypothetical iso-level eFRA of a DTN showing the mean ± SD spikes per stimulus in response to single BD tones that were varied in frequency and presented at +10 dB above threshold (*filled circles*). The eBW (*grey box*) was determined with a 50% spike count criterion re BEF (*horizontal dashed line*). See Fig. 2.2 for additional details. ***B***, Hypothetical iso-level iFRA of the same cell, measured as the duration of inhibition (D_{IHB}) evoked at each NE tone frequency (relative to the BEF) at +10 dB above threshold and normalized by the duration of inhibition evoked at BEF [i.e. $D_{IHB}/D_{IHB}(BEF)$]. All cells were tested with at least 5 standardized NE tone frequencies described in Figure 2.2 (*open circles A-E*), and whenever possible additional NE tone frequencies were presented (*filled circles*). Except for the BEF, the number of NE tone frequencies tested was independent of the number of BD tone frequencies in the eFRA. The BIF was defined as the frequency

evoking the largest normalized duration of inhibition (*open circle C*). Separate linear regressions (*solid lines*) were computed for the low ($Slope_{Low}$) and high ($Slope_{High}$) frequency tuning slopes of the iFRA. Each regression was interpolated to 50% of its maximum normalized duration of inhibition at BIF, and this resulted in slightly different 50% criteria (*horizontal dashed lines*) to define the lowest and highest cutoff frequencies (*edges of grey box*) of the $Slope_{Low}$ and $Slope_{High}$ tuning slopes. For the hypothetical cell illustrated, the eBW ranged from -0.10 – 0.08 octaves (re BEF) and the iBW ranged from -0.35 – 0.19 octaves (re BEF).

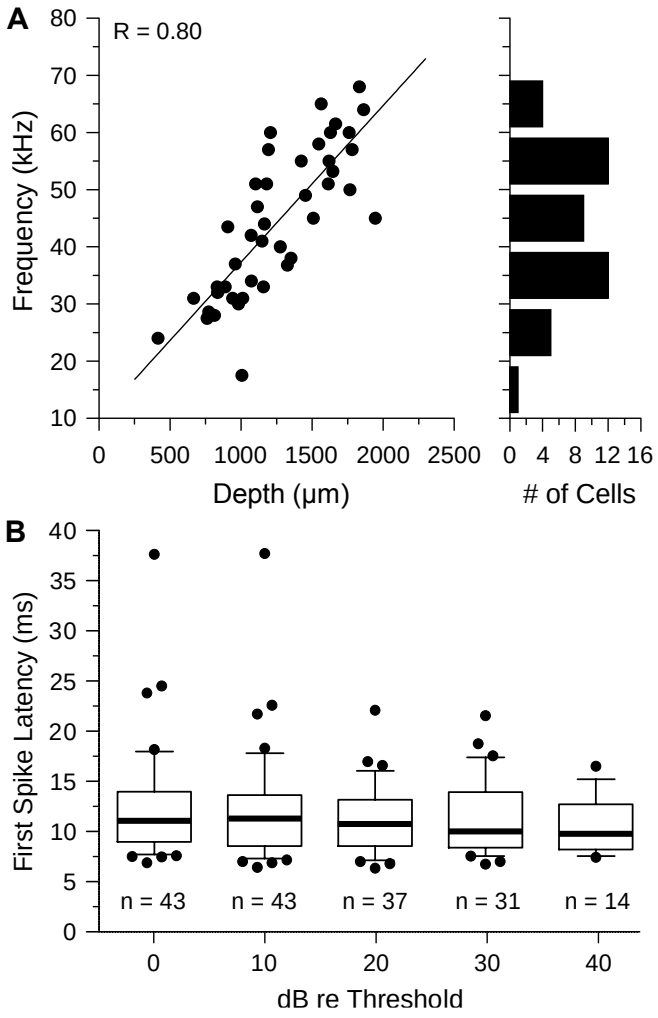

Fig. 2.5. Tonotopic organization and response latency of DTNs in the IC.

A, Topographical organization of DTN BEFs. *Left panel*: There was a strong positive correlation (R = 0.80) between recording electrode depth and neural BEF (measured at +10 dB re threshold), demonstrating that DTNs were tonotopically organized within the IC. *Right panel*: Histogram of BEFs (n = 43 cells; bin width = 10 kHz). ***B,*** First spike latency of DTNs as a function of sound level above threshold. Box plots illustrating the median (*bold line*), 25th and 75th percentiles (*horizontal edges of box*), interquartile range (*height of box*), 10th percentile (*bottom whisker)*, 90th percentile (*top whisker*), and data values

falling outside of these ranges (*black circles)*. The interquartile range is defined as the 3rd quartile (75th percentile) minus the 1st quartile (25th percentile). Sample sizes decrease with increasing SPL because cells with high thresholds and/or non-monotonic rate-level functions could not be tested at all SPLs.

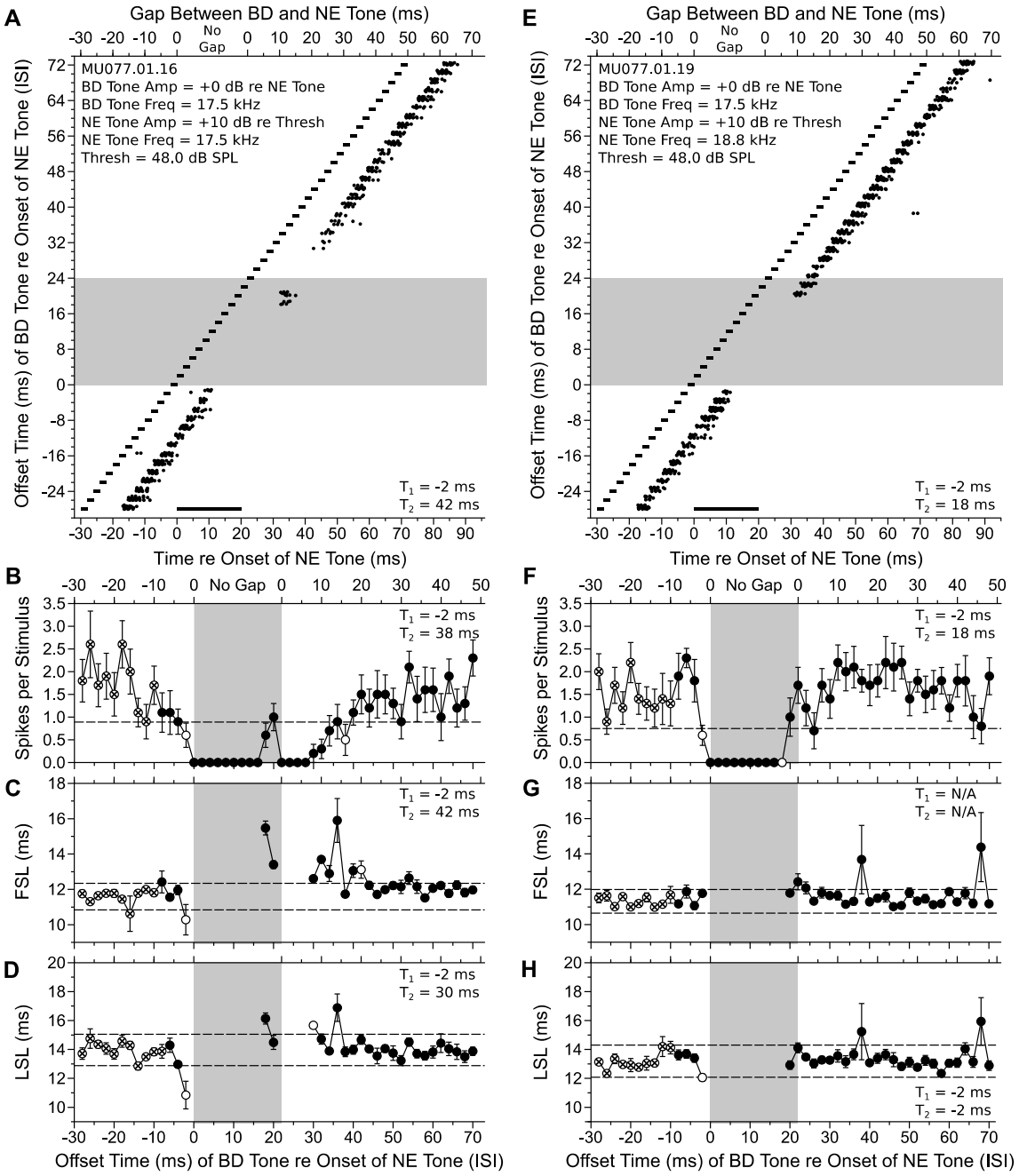

Fig. 2.6. Inhibition evoked at the BEF and at a non-BEF within the eBW.

Dot raster displays illustrating responses from a bandpass DTN with the NE tone presented at the cell's BEF (17.5 kHz; *left*) and at a non-BEF that was within the cell's eBW (18.8

kHz; *right*). ***A,*** When the BD and NE tones were matched in frequency, strong suppression was observed when the 2 ms BD tone and the 20 ms NE tone were sufficiently close in time. ***B,*** Mean ± SE spikes per stimulus as a function of the ISI between the BD and NE tones. The shortest ISI in which the spike count first dropped to ≤50% of baseline was T_1 = -2 ms (leftmost *open circle*). The longest ISI, starting from T_1, in which the spike count remained at ≤50% of baseline was T_2 = 38 ms (rightmost *open circle*). ***C,*** Mean ± SE FSL as a function of the ISI between the BD and NE tones. The shortest ISI in which the FSL deviated by >1 SD from baseline was T_1 = -2 ms (leftmost *open circle*), and the longest ISI in which the FSL deviated by >1 SD from baseline was T_2 = 42 ms (rightmost *open circle*). ***D,*** Mean ± SE LSL as a function of the ISI between the BD and NE tones. The shortest ISI in which the LSL deviated by >1 SD from baseline was T_1 = -2 ms (leftmost *open circle*), and the longest ISI in which the FSL deviated by >1 SD from baseline was T_2 = 30 ms (rightmost *open circle*). In the BEF condition, the final value of T_1 (-2 ms) was determined with all three criteria and the final value of T_2 (42 ms) was determined with a FSL criterion. In the matched condition, the onset of the NE tone evoked inhibition led the excitatory FSL by 1.63 ms, and the inhibition persisted 21.63 ms longer than the NE tone. ***E,*** Dot raster display illustrating responses from the same DTN when the BD and NE tones were not matched in frequency. ***F,*** Inhibition evoked by the NE tone also led to a reduction in the cell's spike count, although the effective duration of spike suppression was shorter, but almost no deviations in either the ***G,*** FSL and ***H,*** LSL. The final value of T_1 (-2 ms) was determined with either a spike count or LSL criterion, and the final value of T_2 (18 ms) was determined with a spike count criterion. In the non-BEF condition, the latency of inhibition

led the excitatory FSL by 2.14 ms, and the duration of inhibition was -1.86 ms shorter than the NE tone. The 10 data points that were averaged in the calculation of baseline spike counts and latencies are shown as *white circles with an X*. n = 10 trials per stimulus.

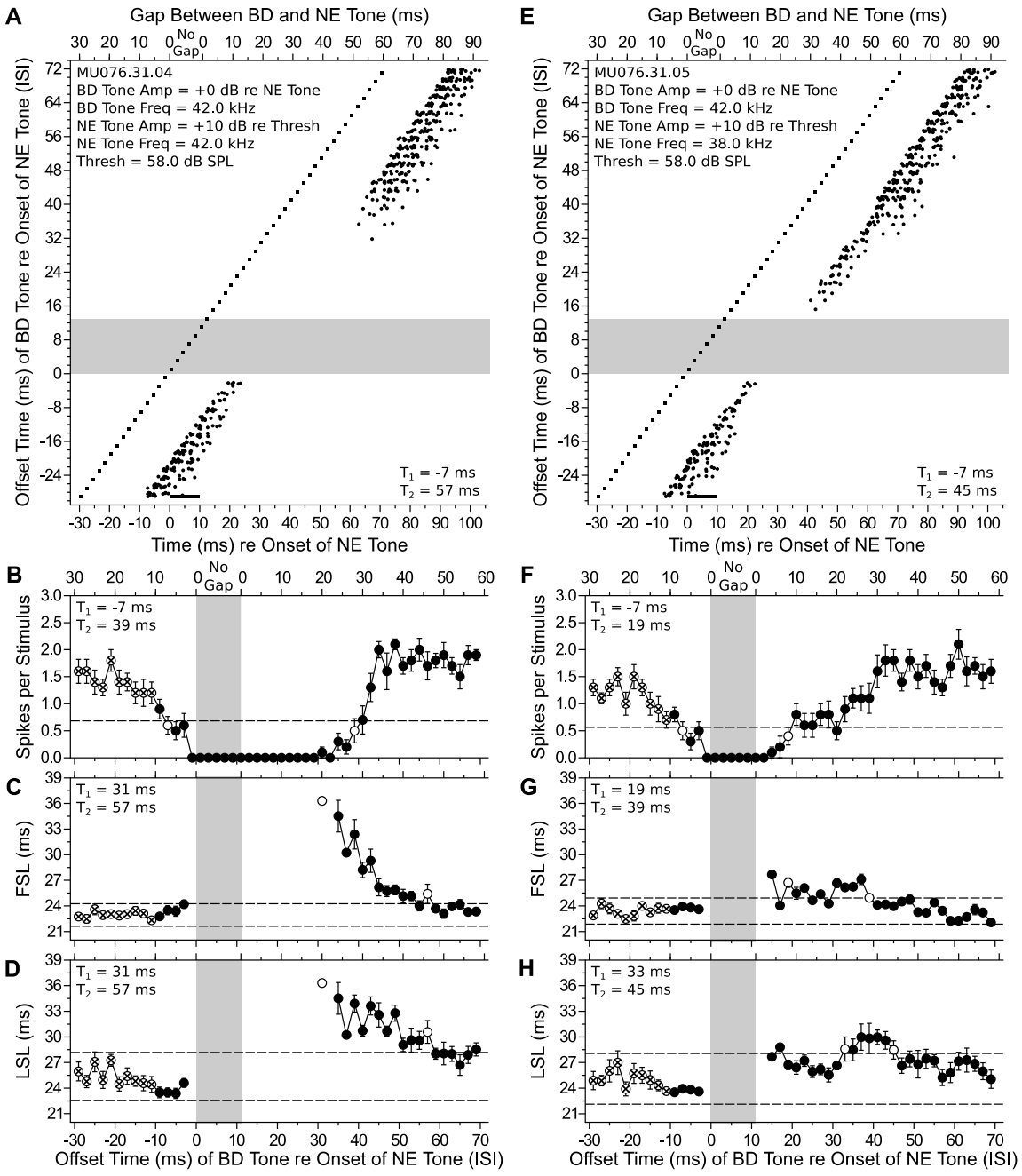

Fig. 2.7. Inhibition evoked at the BEF and at a non-BEF outside of the eBW.

Dot raster displays illustrating responses from a short-pass DTN with the NE tone presented at the cell's BEF (42 kHz; *left*) and at a non-BEF that was outside of the cell's

eBW (38 kHz; *right*). ***A,*** When the BD and NE tones were matched in frequency, strong suppression was observed when the 1 ms BD tone and the 10 ms NE tone were sufficiently close in time. ***B,*** Mean ± SE spikes per stimulus as a function of the ISI between the BD and NE tones. The shortest ISI in which the spike count first dropped to ≤50% of baseline was T_1 = -7 ms (leftmost *open circle*). The longest ISI, starting from T_1, in which the spike count remained ≤50% of baseline was T_2 = 39 ms (rightmost *open circle*). ***C,*** Mean ± SE FSL as a function of the ISI between the BD and NE tones. The shortest ISI in which the FSL deviated by >1 SD from baseline was T_1 = 31 ms (leftmost *open circle*), and the longest ISI in which the FSL deviated by >1 SD from baseline was T_2 = 57 ms (rightmost *open circle*). ***D,*** Mean ± SE LSL as a function of the ISI between the BD and NE tones. The shortest ISI in which the LSL deviated by >1 SD from baseline was T_1 = 31 ms (leftmost *open circle*), and the longest ISI in which the FSL deviated by >1 SD from baseline was T_2 = 57 ms (rightmost *open circle*). In the BEF condition, the final value of T_1 (-7 ms) was determined with a spike count criterion and the final value of T_2 (57 ms) was determined using either a FSL or LSL criterion. In the matched condition, the onset of the NE tone evoked inhibition led the excitatory FSL by 5.57 ms, and the inhibition persisted 51.57 ms longer than the NE tone. ***E,*** Dot raster display illustrating responses from the same DTN when the BD and NE tones were not matched in frequency. ***F,*** Inhibition evoked by the NE tone again caused a reduction in the cell's spike count and deviations in the ***G,*** FSL and ***H,*** LSL, although the effective duration of the altered response was shorter. The final value of T_1 (-7 ms) was determined with a spike count criterion, and the final value of T_2 (45 ms) was determined with either a FSL or LSL criterion. In the non-

BEF condition, the latency of inhibition led the excitatory FSL by 6.30 ms, and the duration of the inhibition was 40.30 ms longer than the NE tone. The 10 data points that were averaged in the calculation of baseline spike counts and latencies are shown as *white circles with an X*. n = 10 trials per stimulus.

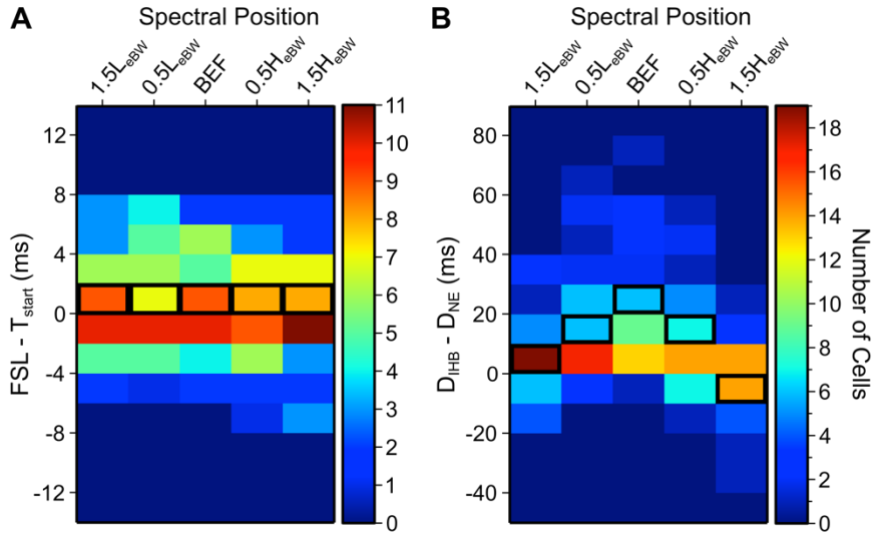

Fig. 2.8. Distribution of duration of leading/lagging and persistent inhibition across the five standardized NE tone frequencies.

Two dimensional histograms showing the distributions of leading/lagging inhibition and persistent inhibition in DTNs tested with paired tone stimulation at five standardized NE tone frequencies (re eBW). Mean duration at each NE tone frequency condition indicated by a *black box*, with the color scale showing the number of DTNs per bin. ***A,*** Distribution of the difference between the excitatory FSL and latency of inhibition (FSL – T_{start}) evoked by the NE tone. Cells with a positive difference have leading inhibition; cells with a negative difference have lagging inhibition. There was no difference in the distribution of FSL – T_{start} across NE tone frequencies, demonstrating a relatively constant latency of inhibition. ***B,*** Distribution of the difference between the duration of inhibition evoked by the NE tone and the duration of the NE tone stimulus (D_{IHB} – D_{NE}). Cells with a positive difference have persistent inhibition; cells with a negative difference have inhibition lasting less than the duration of the NE tone evoking the inhibition. The distribution of D_{IHB} – D_{NE}

differed across NE tone frequencies, with cells showing less persistent inhibition as the NE tone frequency moved away from the BEF (see Table 2.1). n = 38 cells.

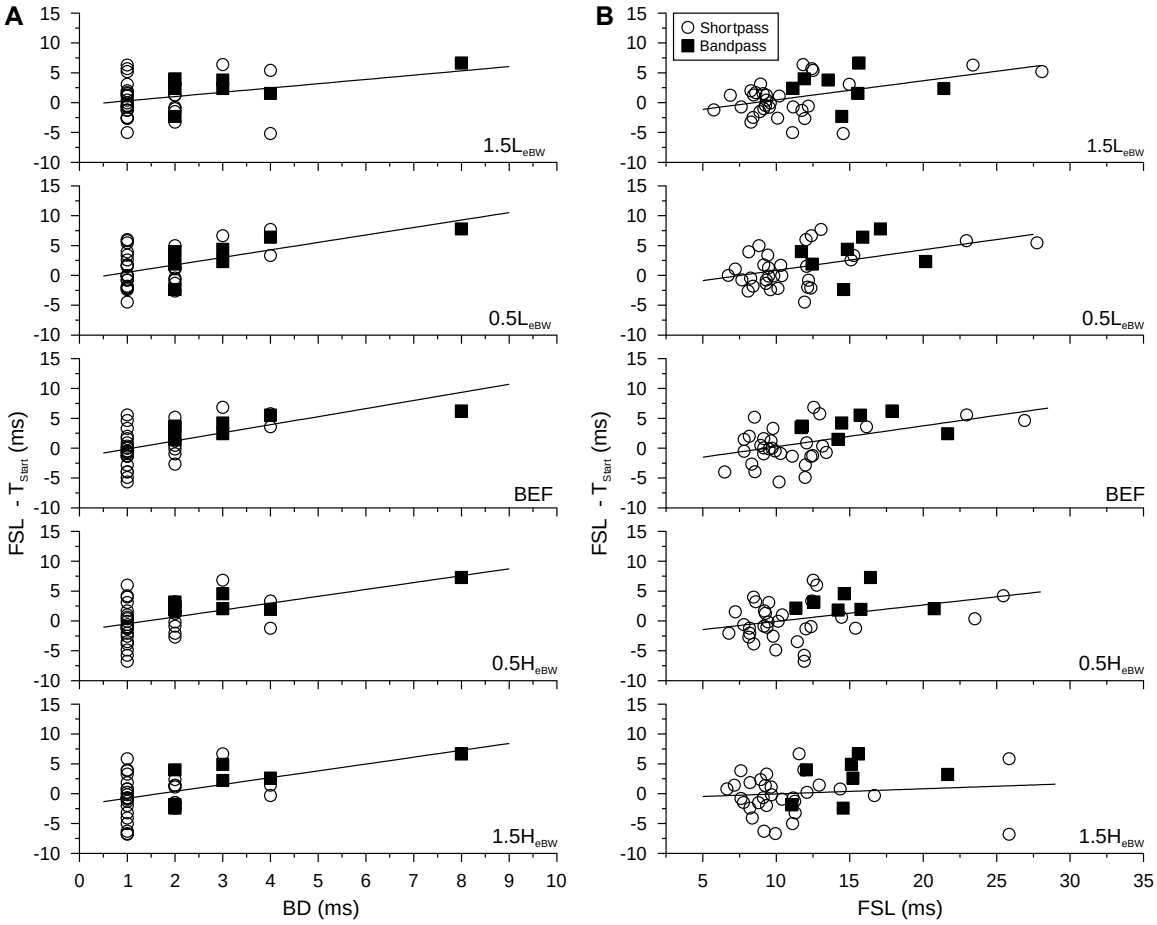

Fig. 2.9. Relationship of duration of leading/lagging inhibition to BD, FSL, and duration filter class.

Duration of inhibition measured using paired tone stimulation at five standardized NE tone frequencies relative to the eBW of short-pass and bandpass DTNs. ***A,*** Duration of leading inhibition increased in DTNs tuned to longer BDs at all NE tone frequencies. ***B,*** Duration of leading inhibition also increased in DTNs with longer FSLs at the four lowest NE tone frequencies; however, no correlation was observed at the highest NE tone frequency ($1.5H_{eBW}$). Regression equations, correlation coefficients (R), and p-values for each linear regression are listed in Table 2.2. n = 38 cells.

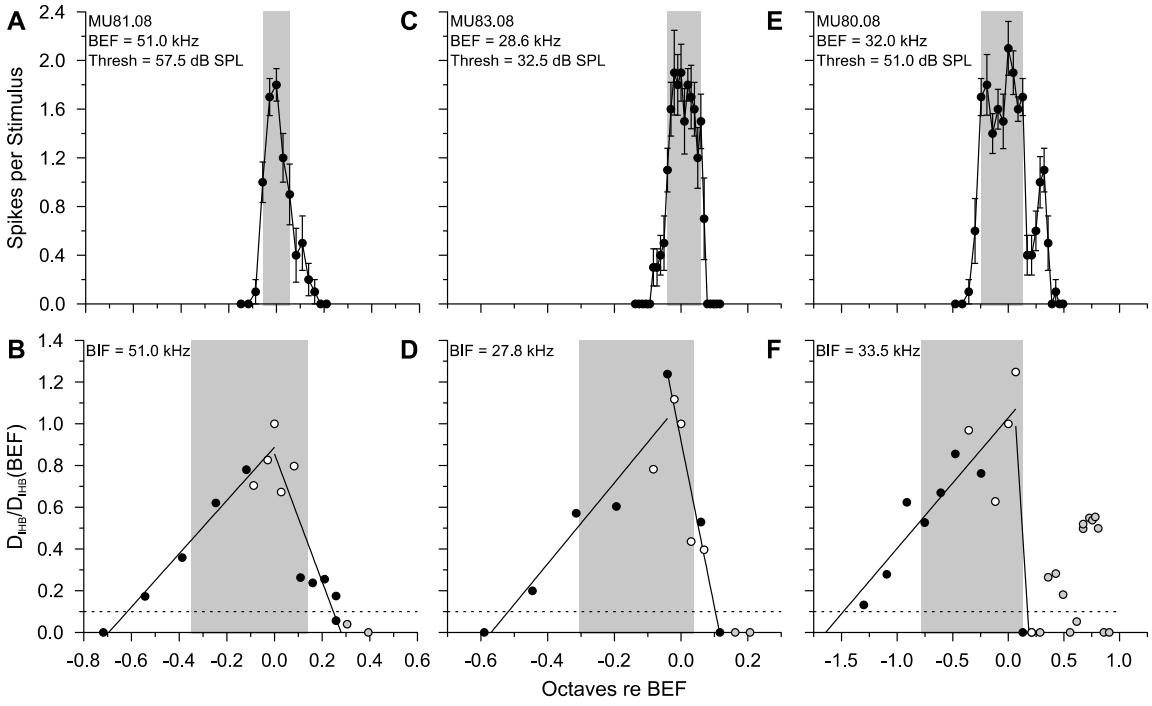

Fig. 2.10. Excitatory and inhibitory BFs, FRAs and BWs of DTNs.

Each column shows the (***top***) excitatory FRA of a DTN, plotted as the mean ± SD spike count as a function of different BD tone frequencies, and the (*bottom*) inhibitory FRA of the same DTN measured during paired tone stimulation, plotted as the normalized duration of inhibition in octaves (re BEF) as a function of NE tone frequency. ***A,*** The eFRA of a short-pass DTN with a 1 ms BD, BEF of 51.0 kHz, and an eBW ranging from 49.0–53.0 kHz illustrated as a *grey box* between -0.06–0.06 octaves (re BEF). ***B,*** Normalized iFRA of the same cell plotted as the duration of inhibition evoked by NE tones of different frequencies (re duration of inhibition evoked at BEF), including the 5 standardized NE tone frequencies (*open circles*). Note that the 5 standardized NE tone frequencies are the same ones described in Figure 2.2 and used in Figures 2.8 and 2.9. The BIF was defined as the

frequency evoking the longest duration of inhibition. We computed separate linear regressions, calculated for the low and high frequency slopes of the iFRA, to measure each cell's inhibitory bandwidth (iBW) with the cutoffs defined as the two frequencies where the regression line dropped to 50% of the regressed maximum. It is important to note that not every NE tone frequency was included in the linear regression calculations; in all cases, the lowest (or highest) frequency included was the first data point to reach ≤0.1 (*dotted line*), starting from the BIF and moving lower (or higher) in frequency. Data points not included in linear regression calculations are shown as *grey circles*. The BIF of this cell was 51.0 kHz and was matched to its BEF. The iBW ranged from 40.07–56.19 kHz or -0.31–0.14 octaves (re BEF). ***C,*** The eFRA of a short-pass DTN with a 1 ms BD, BEF of 28.6 kHz, and an eBW ranging from 27.8–29.8 kHz or -0.04–0.06 octaves (re BEF). ***D,*** Normalized iFRA of the same cell with a BIF of 27.8 kHz or -0.04 octaves below its BEF, and an iBW ranging from 23.15–29.35 kHz or -0.31–0.04 octaves (re BEF). ***E,*** The eFRA of a bandpass DTN with a 3 ms BD, BEF of 32.0 kHz, and a multi-peaked eFRA. The main peak ranging from 27.0–35.0 kHz or -0.25–0.13 octaves (re BEF). ***F,*** Normalized iFRA of the same cell showing a multi-peaked iFRA with a BIF of 33.5 kHz or 0.07 octaves re BEF. This cell had two secondary inhibitory tuning peaks between 41.0–45.0 kHz (0.36–0.49 octaves re BEF) and between 51.0–56.0 kHz (0.67–0.81 octaves re BEF) not included in the calculation of the iBW. The iBW ranged from 18.53–34.91 kHz or -0.79–0.13 octaves (re BEF), and there was 98.9% spectral overlap with the eBW. The rightmost *open circle* in panel *F* (at +0.21 octaves) was included in the regression of the low frequency tuning slope of the iFRA. Stimuli presented +10 dB (re BEF, BD threshold); 10 trials per stimulus.

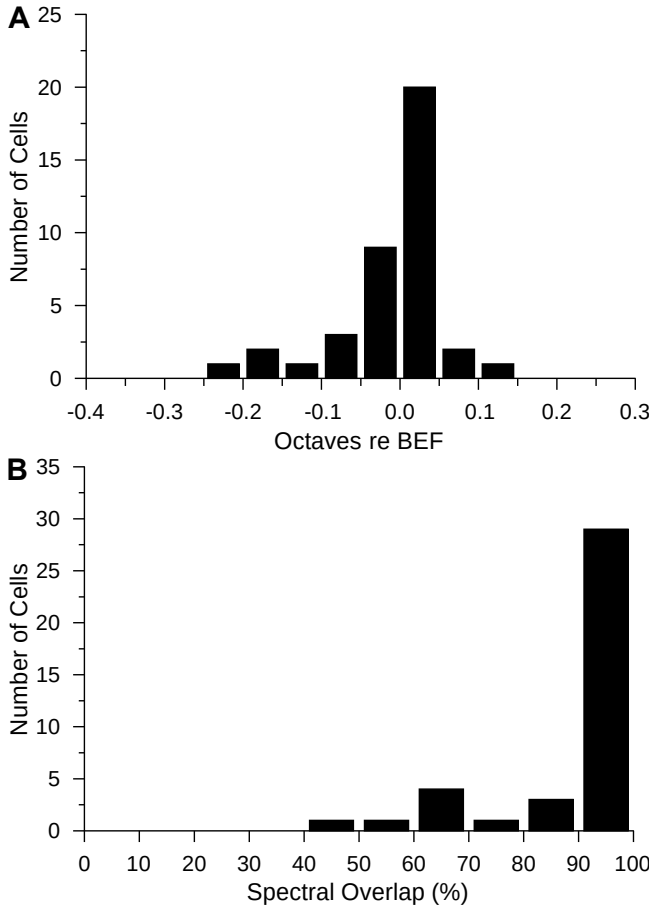

Fig. 2.11. Relation of BEF to BIF and correspondence in spectral tuning between excitation and inhibition in midbrain DTNs.

A, Distribution of the difference in octaves between the BEF and BIF. Cells with a positive difference had a higher BIF relative to their BEF, while cells with a negative difference had a lower BIF compared to their BEF. In most DTNs, the BIF closely corresponded to the BEF. Bin width = 0.05 octaves. ***B,*** Distribution of percent spectral overlap between the eBW and iBW. In the majority of DTNs, neural inhibition completely or nearly overlapped the entire bandwidth of neural excitation. Bin width = 10.0%; n = 39 cells.

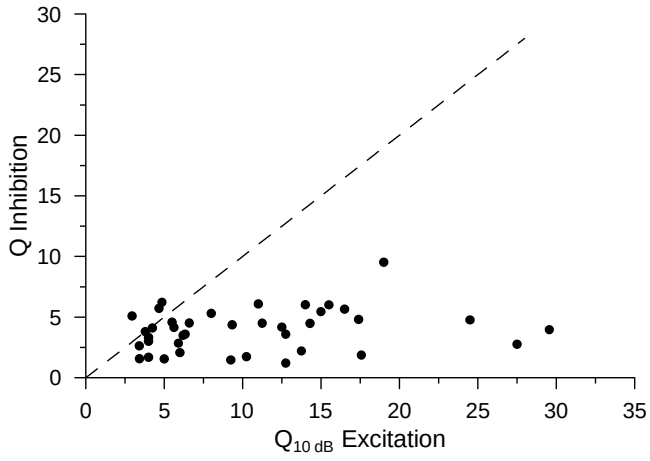

Fig. 2.12. Sharpness of excitatory and inhibitory tuning in DTNs.

Excitatory and inhibitory tuning sharpness plotted as quality (Q) factors measured at +10 dB (re excitatory threshold). Excitatory tuning sharpness measured as $Q_{10\ dB}$ = BEF/eBW; inhibitory tuning sharpness measured as Q = BIF/iBW. Most inhibitory Q factors were smaller than their corresponding excitatory $Q_{10\ dB}$ factors measured from the same cell, as demonstrated by the majority of points falling below the $y = x$ identity line. n = 39 cells.

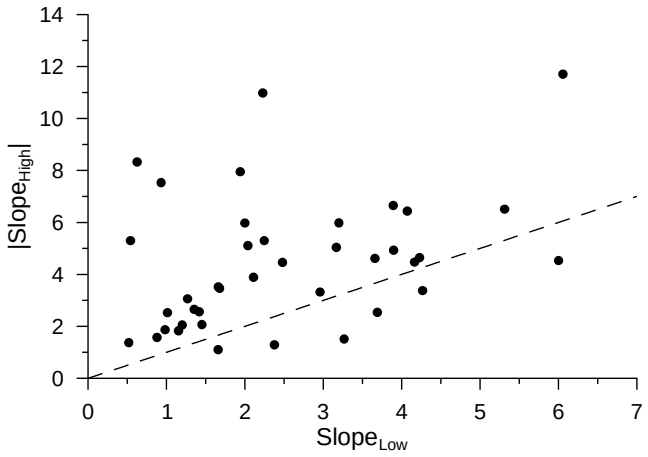

Fig. 2.13. Steepness of the low and high frequency tuning slopes of the normalized iFRA.

The absolute value of |Slope$_{High}$| vs. Slope$_{Low}$ are plotted as well as the identity line ($y = x$). Points above the identity line indicate cells with an iFRA with a steeper high frequency slope than low frequency slope, whereas points below the line indicate cells with an iFRA with a steeper low frequency slope than high frequency slope. Most DTNs had asymmetrical iFRAs with normalized durations of inhibition falling off more quickly at higher compared to lower frequencies. n = 39 cells.

Table 2.1.

Comparison of the proportion of DTNs showing persistent inhibition at five standardized NE tone frequencies relative to each cell's 50% eBW. Also shown are the results of Nemenyi post-hoc pairwise comparisons on the duration of persistent inhibition at each standardized NE tone frequency.

	% DTNs with persistent inhibition[1]	Pairwise comparisons of duration of persistent inhibition[2]				
		$1.5L_{eBW}$	$0.5L_{eBW}$	BEF	$0.5H_{eBW}$	$1.5H_{eBW}$
$1.5L_{eBW}$	73.7%	-	-	-	-	-
$0.5L_{eBW}$	92.1%	**<0.001**	-	-	-	-
BEF	97.4%	**<0.001**	0.977	-	-	-
$0.5H_{eBW}$	78.9%	0.366	0.218	0.056	-	-
$1.5H_{eBW}$	47.4%	0.162	**<0.001**	**<0.001**	**<0.001**	-

Statistically significant differences indicated in **bold face type**.

[1]Cochran Q test, $\chi^2(4) = 36.87$, $p << 0.001$, $n = 38$.

[2]Friedman test, $\chi^2(4) = 62.38$, $p << 0.001$, $n = 38$.

Table 2.2.

Linear relationships on the duration of leading inhibition (L_{first} – T_{start}) and BD or FSL at five standardized NE tone frequencies relative to each cell's 50% eBW (n = 38 cells).

Comparison	Frequency	Slope	Intercept	R	p-value
L_{first}-T_{start} (ms) *vs.* BD (ms)	$1.5L_{eBW}$	0.72	-0.41	0.320	**0.050**
	$0.5L_{eBW}$	1.25	-0.73	0.531	**<0.001**
	BEF	1.35	-1.48	0.580	**<0.001**
	$0.5H_{eBW}$	1.15	-1.63	0.481	**0.002**
	$1.5H_{eBW}$	1.13	-1.90	0.453	**0.004**
L_{first} -T_{start} (ms) *vs.* FSL (ms)	$1.5L_{eBW}$	0.30	-2.56	0.437	**0.007**
	$0.5L_{eBW}$	0.35	-2.64	0.473	**0.003**
	BEF	0.37	-3.44	0.497	**0.002**
	$0.5H_{eBW}$	0.29	-2.76	0.358	**0.027**
	$1.5H_{eBW}$	0.09	-0.96	0.108	0.518

Statistically significant correlations are indicated in **bold face type**.

Table 2.3.

Mann-Whitney U tests comparing the duration of leading inhibition ($L_{first} - T_{start}$) in short-pass (n = 31) and bandpass (n = 7) DTNs at five standardized NE tone frequencies relative to each cell's 50% excitatory bandwidth.

Frequency	Duration Filter Class: Median, [IQR] (ms)	U	p-value
$1.5L_{eBW}$	Short-pass: 0.039, [-1.23 – 3.08] Bandpass: 2.407, [1.54 – 4.00]	58.0	0.059
$0.5L_{eBW}$	Short-pass: 0.002, [-0.93 – 4.09] Bandpass: 4.000, [1.90 – 6.41]	62.0	0.083
BEF	Short-pass: 0.000, [-1.01 – 3.62] Bandpass: 3.701, [2.42 – 5.53]	37.0	**0.005**
$0.5H_{eBW}$	Short-pass: -0.606, [-1.50 – 3.11] Bandpass: 2.140, [1.94 – 4.57]	36.0	**0.005**
$1.5H_{eBW}$	Short-pass: -0.312, [-1.89 – 2.76] Bandpass: 2.608, [-1.85 – 4.91]	63.0	0.091

Statistically significant differences indicated in **bold face type**.

Chapter 3 – Effect of Sound Pressure Level on Contralateral Inhibition Underlying Duration-Tuned Neurons in the Mammalian Inferior Colliculus

3.1 – Abstract

Duration tuning in the mammalian inferior colliculus (IC) is created by the interaction of excitatory and inhibitory synaptic inputs. We used extracellular recording and paired-tone stimulation to measure the strength and time-course of the contralateral inhibition underlying duration-tuned neurons (DTNs) in the IC of the awake bat. The onset time of a short, best duration (BD), excitatory probe tone set to +10 dB (re threshold) was varied relative to the onset of a longer-duration, non-excitatory (NE) suppressor tone whose sound pressure level (SPL) was varied. Spikes evoked by the roving BD tone were suppressed when the stationary NE tone amplitude was at or above the BD tone threshold. When the NE tone was increased from 0 to +10 dB the inhibitory latency became shorter than the excitatory first spike latency and the duration of inhibition increased, but no further changes occurred at +20 dB (re BD tone threshold). We used the effective duration of inhibition as a function of the NE tone amplitude to obtain suppression-level functions that were used to estimate the inhibitory half-maximum SPL ($ISPL_{50}$). We also measured rate-level functions of DTNs with single BD tones varied in SPL and modeled the excitatory half-maximum SPL ($ESPL_{50}$). There was a correlation between the $ESPL_{50}$ and $ISPL_{50}$, and the dynamic range of excitation and inhibition were similar. We conclude that the strength of inhibition changes in proportion to excitation as a function of SPL, and this feature likely contributes to the amplitude tolerance of the responses of DTNs.

3.2 – Introduction

Sound duration conveys information vital for intraspecific sexual communication (Pollack and Hoy 1979), speech recognition (Denes 1955; Shannon et al. 1995), and echolocation in bats (Schnitzler and Kalko 2001). Within the vertebrate central auditory system, stimulus duration may be encoded by a class of neurons with electrophysiological response selectivity for sound duration. These so-called duration-tuned neurons (DTNs) were first identified in the auditory midbrain of frogs (Potter 1965; Narins and Capranica 1980), but have since been found in guinea pigs (Wang et al. 2006), mice (Brand et al. 2000; Xia et al. 2000), rats (Pérez-González et al. 2006), cats (He et al. 1997) and echolocating bats (Pinheiro et al. 1991; Ehrlich et al. 1997; Mora and Kössl 2004). Interestingly, neuronal best durations (BDs) of DTNs correlate well with species-typical vocalization durations, suggesting that DTNs are adapted to the sensory ecology of each organism (Sayegh et al. 2011).

Most biological sounds exhibit natural variation in amplitude and temporal features (Rosen 1992; Singh and Theunissen 2003). For example, aerially-hawking bats decrease the duration and amplitude of their echolocation calls during an approach to a target (Kick and Simmons 1984; Schnitzler and Kalko 2001). Moreover, echolocation calls and echoes experience distance dependent attenuation, all of which presents a challenge for the neural processing of pulse-echo pairs because both amplitude and/or duration alter the total energy of an acoustic stimulus ($Energy = Power \times Time$).

Previous studies have shown that the spiking responses of auditory DTNs—including a cell's BD, temporal bandwidth of duration tuning, duration filter class, and first-spike latency—remain remarkably stable and thus are tolerant to broad changes in sound pressure level (SPL) (Fremouw et al. 2005; Zhou and Jen 2001; but see Mora and Kössl 2004). This is thought to occur because the excitatory and inhibitory inputs that create DTNs remain stable in timing and/or strength as stimulus amplitude is varied. Because inhibitory inputs are known to play a crucial role in shaping the response properties of DTNs (Casseday et al. 1994; Ehrlich et al. 1997; Faure et al. 2003), it is important to understand how the properties of neural inhibition create and shape the responses of DTNs when stimulus amplitude is varied.

Here we used a modified version of paired-tone stimulation (Faure et al. 2003) to characterize the effect of stimulus amplitude on inhibitory inputs to DTNs in the mammalian IC. Cells were stimulated with a short duration, excitatory probe tone set to the cell's best duration (BD) and presented at +10 dB above the excitatory threshold. The onset time of the BD tone was varied relative to a longer duration, non-excitatory (NE) tone that was varied in amplitude. Spikes evoked by the BD tone were consistently suppressed when the amplitude of the NE tone was at or above the BD tone excitatory threshold. As the NE tone amplitude increased, the onset of inhibition shortened while the offset and duration of the NE tone-evoked inhibition increased. We used the effective duration of the NE tone-evoked inhibition at different SPLs (re BD tone threshold) to create a suppression-level response function from which we measured the inhibitory half-maximum SPL ($ISPL_{50}$) to the cell. We also modeled each cell's rate-level function to

measure the excitatory half-maximum SPL ($ESPL_{50}$). There was a strong correlation between $ESPL_{50}$ and $ISPL_{50}$, showing that the strengths of neural excitation and inhibition changed proportionately with SPL. We conclude that this balance of excitation and inhibition likely contributes to the preservation (tolerance) of duration tuning.

3.3 – Materials and Methods

Electrophysiological recordings were conducted at the University of Washington (UW) in Seattle, WA, USA, and at McMaster University (MU) in Hamilton, ON, Canada. Big brown bats (*Eptesicus fuscus*) at both institutions were housed in outdoor husbandry facilities where food and water were available *ad libitum* and the colony temperature and lighting corresponded to ambient conditions. All procedures were approved by the UW Laboratory Animal Care and Use Committee or the MU Animal Research Ethics Board, and were in accordance with the Guide to the Care and Use of Experimental Animals published by the Canadian Council on Animal Care.

3.3.1 – Surgical Procedures

Bats were brought indoors at least one day prior to surgery to acclimatize. Neural recordings were obtained from the IC of 24 *E. fuscus*, 17 big brown bats from MU (12 males, 5 females) and 7 big brown bats from UW (1 male, 6 females) Prior to recording, each bat underwent a preparatory surgery in which a stainless-steel post was glued to the anterior, dorsal portion of the skull. The post prevented the bat from moving its head during recording and allowed for precise replication of the head position between sessions. Bats at UW were anaesthetized with a subcutaneous (SQ) injection of a neuroleptic [0.3 ml 1:1 mixture of 0.025 mg/ml fentanyl citrate and 1.25 mg/ml Inapsine (droperidol); 19.1 mg/kg] followed by inhalation (1-5 min) of Metofane (methoxyflurane) in a bell jar. Bats at MU were anaesthetized with a SQ injection of buprenorphine (Temgesic; 0.03 ml; 0.045 mg/kg) followed by inhalation of an isoflurane-oxygen mixture (1-5%; flow rate = 1 L/min) in an induction chamber (12 × 10 × 10 cm, length x width x height). Once anaesthetized, bats

were placed in a foam-lined body restraint within a surgical stereotaxis apparatus (David Kopf Instruments Model 1900). The bat's upper canine teeth were placed into a custom bite bar with a gas mask to allow for continuous delivery of isoflurane, the level of which was adjusted according to changes in the bat's breathing patterns. The hair covering the skull was cut and the exposed skin was disinfected with a povidone-iodine (Betadine) surgical scrub. A SQ injection of local anaesthetic (0.05 ml of 2% lidocaine at UW; 0.2 ml of 5 mg/ml bupivacaine at MU) was administered prior to making a midline incision in the scalp. The exposed temporal muscles were reflected, and the skull was scraped clean and swabbed with 70%-100% ethanol. A stainless-steel post was glued to the skull with cyanoacrylate gel adhesive (Zap Gel; Pacer Technology) cured with liquid acrylic hardener (Jet Liquid, Lang Dental Manufacturing Company) at UW, or with cyanoacrylate superglue (Henkel Loctite Corporation) and liquid hardener (Zip Kicker; Pacer Technology) at MU. One end of a chloride silver wire, attached to the head post, was placed under the temporal muscles and served as a reference electrode. A piece of Gelfoam covered in Neosporin (UW) or Polysporin (MU) was placed over the wound to prevent infection. Following surgery, bats were housed individually in stainless steel cages (1/4-in mesh) in a temperature- and humidity-controlled room. Food and water were provided *ad libitum*.

3.3.2 – Electrophysiological Recordings

Bats were given 1-4 days to recover from surgery before recording. Each bat underwent 1-8 recording sessions, lasting 4-8 hours each and conducted on separate days. Recording sessions were terminated if the bat showed signs of discomfort. At the end of each session, the exposed skull was covered with a piece of contact lens and Gelfoam

coated in topical antibiotic to prevent infection. Neural recordings were conducted within a double-walled, sound attenuation booth with electrical shielding (Industrial Acoustics Corporation). Prior to recording, the bat was given a SQ injection of neuroleptic [0.3 ml; 1:1 (vol/vol) mixture of 0.025 mg/ml fentanyl citrate and 1.25 mg/ml Inapsine (droperidol); 19.1 mg/kg]. Once sedated, the bat was placed in a foam-lined body restraint that was suspended by springs within a custom small-animal stereotaxic frame (ASI Instruments) that rested atop an air vibration table (TMC Micro-G). To immobilize the bat's head, the head post was connected to a stainless-steel rod that was attached to a manual micromanipulator (ASI Instruments) mounted on the stereotaxic frame.

The IC can be visually identified as a white ellipse through the translucent skull. A scalpel blade was used to make a small opening in the skull, and the dura mater overlying the IC was removed with a sharp pin to allow for the insertion of microelectrodes. Single-unit extracellular recordings were collected with thin-wall borosilicate glass microelectrodes (outer diameter = 1.2 mm; A-M Systems) filled with 0.3-0.5 M (UW) or 1.5 M (MU) NaCl. Electrode resistances typically ranged between 15 - 30 MΩ. Electrodes were positioned over the opening of the skull with manual micromanipulators (ASI Instruments) and advanced into the IC with a stepping hydraulic micropositioner (David Kopf Instruments; model 650 at UW or model 2650 at MU). Action potentials were recorded with a neuroprobe amplifier (A-M Systems model 1600) whose 10x output was band-pass filtered and further amplified (500-1000x) by a spike preconditioner [Tucker Davis Technologies (TDT) PC1; low-pass filter cut-off frequency (f_c) = 7 kHz, high-pass f_c = 300 Hz]. The TDT PC1 output was passed to a spike discriminator (TDT SD1) and an

event timer (TDT ET1) synchronized to a timing generator (TDT TG6) to log spike times onto a computer.

3.3.3 – Stimulus Generation

Custom software was used to control stimulus generation and on-line data visualization. Spike times were displayed as dot rasters ordered by the acoustic parameter that was randomly varied. Sounds were digitally synthesized with a two-channel array processor (TDT Apos II; 357 kHz sampling rate) optically interfaced to two digital-to-analog converters (TDT DA3-2) whose individual outputs were passed to a low-pass antialiasing filter (TDT FT6-2; f_c = 120 kHz) and either two (TDT PA4, UW) or one programmable attenuators (TDT PA5, MU) before being fed to two signal mixers (TDT SM5) with equal weighting, a manual attenuator (Leader LAT-45), and power amplifier (Krohn-Hite model 7500).

Accoustic stimuli were broadcast with a Brüel & Kjær (B&K) ¼-in condenser microphone (Type 4939; protective grid on), altered for use as a loudspeaker with a transmitting adaptor (B&K Type UA-9020) to correct for nonlinearities in the transfer function (Frederiksen, 1977). The loudspeaker was positioned approximately 1 mm in front of the external auditory meatus. The output of the loudspeaker was measured with a B&K type 4138 ⅛-in condenser microphone (90° incidence; grid off), connected to a measuring amplifier (B&K type 2606) and a band-pass filter (Krone-Hite model 3500), quantified with a sound calibrator (B&K type 4231) and expressed in decibels sound pressure level (dB SPL re 20 µPa) equivalent to the peak amplitude of continuous tones of the same frequency. The loudspeaker function was flat ± 6 dB from 28 to 118 kHz, and there was at

least 30-dB attenuation at the ear opposite the source (Ehrlich et al. 1997). All stimuli were presented at a rate of 3 pulses/s and had rise/fall times of 0.4 ms shaped with a squared cosine function.

3.3.4 – Data Collection

Search stimuli consisted of two pure tones of different durations (typically 1 and 4 ms) with an interstimulus interval (ISI) ≥ 110 ms. Search stimuli were presented monaurally, contralateral to the IC being recorded. Upon isolating a unit, the cell's best excitatory frequency (BEF; 0.1-1 kHz resolution), BD (1-2 ms resolution), and duration filter class at the BEF were determined (Sayegh et al. 2011). Because this study focused specifically on DTNs, responses of other types of IC neurons were not recorded. Using stimuli at or near BEF and BD, we measured an excitatory rate-level function and minimum acoustic threshold (5 dB resolution) for all neurons in this study (n = 50 neurons). The acoustic threshold was defined as the lowest amplitude tested that evoked a ~0.5 spike probability.

Previous studies have categorized DTNs into three or more duration filter response classes depending on the relative number of spikes evoked across all stimulus durations tested. Our study focused exclusively on short-pass and band-pass DTNs (Fig. 3.1). Short-pass DTNs respond maximally at BD with spike counts dropping to ≤50% of the peak in response to stimulus durations that are longer, but not shorter, than BD. Band-pass DTNs also respond maximally at BD with spike counts dropping to ≤50% of the peak in response to stimulus durations both shorter and longer than BD.

Paired-tone stimulation was used to measure the latency, time course, and strength

of the inhibition in 50 DTNs. In this paradigm, a cell was stimulated with a pair of pure tone pulses set to the cell's BEF but differing in duration and ISI (Faure et al. 2003). The first tone was an excitatory probe set to the cell's BD (BD tone) and presented at +10 dB above the minimum acoustic threshold. The second tone was a suppressor set to a longer, non-excitatory duration (NE tone) that was typically 10 times the duration of the BD tone to ensure a constant energy relationship between the two signals. It is important to clarify that presentation of either the BD or the NE tones evoke both excitation and inhibition in a DTN, with the net response evoked by the BD tone being suprathreshold excitation (i.e. spiking) and the net response evoked by the NE tone being inhibition (i.e. spike suppression). The onset time of the NE tone was fixed, while the onset time of the BD tone was randomly varied (2 ms steps) re NE tone onset, so that the BD tone preceded, overlapped with, and followed the NE tone. At MU, the BD and NE tones were matched in starting phase so that whenever the two BEF tones temporally overlapped, they summated to form a single composite tone with a +6 dB amplitude pedestal. For a subset of cells recorded at UW, the BD and NE tones were not phase-matched, hence at some positions of signal overlap the resulting composite tone may have had an amplitude decrement. For these cases, cells were included in the final analysis only if the summed composite tone had an amplitude increment that was within 3 dB of the maximum theoretical amplitude increment expected from the summation of phase-matched tones of equal amplitude (see Faure et al. 2003).

3.3.5 – Varying NE Tone Amplitude

We used paired tone stimulation and varied the amplitude of NE tone (in 5-10 dB

steps) to measure the inhibition evoked at different SPLs (re BD tone threshold) in 50 DTNs. For every cell the initial NE tone amplitude was matched to the BD tone and set at +10 dB (re BD tone threshold). In 30 cells, the NE tone was presented at three standardized amplitudes (0 dB, +10 dB and +20 dB re BD tone threshold), and whenever possible additional NE tone amplitudes were tested. Responses from these 30 cells were used in the repeated measures statistical analysis. In the remaining 20 cells, responses were collected at +10 dB and at 2 (or more) NE tone amplitudes, but not at all three standardized amplitudes. In these cases, responses evoked at each NE tone amplitude were used to model an inhibitory suppression-level function, but the data were not included in the final repeated measures statistical analysis.

3.3.6 – Measuring the Strength and Time Course of Inhibition

We recorded the ISIs at which spike counts evoked by the BD tone decreased and/or were altered in latency. Spike counts and latencies were calculated off-line using custom software with an analysis window. The start and stop times of the window were anchored to the onset and offset of the BD tone, respectively, and the exact values were chosen to minimize the effects of spontaneous activity in each cell.

To measure the time course (duration) of the evoked inhibition, we quantified each cell's average baseline response to the BD tone over the 10 longest ISIs when the BD tone preceded the NE tone. The baseline response reflects activity evoked by the BD tone in the absence of NE tone-evoked inhibition (Fig. 3.2). For each cell, we calculated the mean ± standard deviation (SD) baseline spike count, baseline first spike latency (FSL), and baseline last spike latency (LSL). For the example short-pass DTN in Figure 3.2A, baseline

responses were measured from spikes falling within the parallelogram. The baseline spike count was 1.41 ± 0.72 spikes per stimulus, the baseline FSL was 29.61 ± 1.46 ms (re BD tone onset), and the baseline LSL was 32.33 ± 2.58 ms (re BD tone onset). Responses at each ISI were compared to these baseline values to determine when spike counts and/or latencies became suppressed and/or altered by NE tone-evoked inhibition based on three, separate criteria. Using a spike count criterion, a cell's responses were said to be suppressed when the mean spikes per stimulus decreased to ≤ 50% of the baseline spike count. The use of this criterion is illustrated in Figure 3.2B; data points falling below the dashed line, which represents 50% of the baseline spike count, were defined as suppressed. Using a FSL criterion, spiking was said to be altered when the mean FSL deviated by > 1 SD from the baseline FSL. The use of this criterion is depicted in Figure 3.2C; data points falling above or below the two dashed lines, which represent ± 1 SD of the baseline FSL, were defined as altered in latency. Lastly, using a LSL criterion, spiking was said to be altered when the mean LSL deviated by > 1 SD from the baseline LSL. The use of this criterion is shown in Figure 3.2D; data points falling above or below the dashed lines, which represent ± 1 SD of the baseline LSL, were defined as altered in latency.

Each criterion yielded a set of ISI's when BD tone-evoked spikes were suppressed and/or altered in latency. Two time points were obtained from the three sets of ISIs: the onset of spike suppression (T_1) and the offset of spike suppression (T_2). The value of T_1 was defined as the shortest ISI, starting from when the BD tone preceded the NE tone and moving toward larger positive ISI's, when the spike count and/or latency became altered and the next two consecutive ISI's remained deviated for a given criterion. The value of T_2

was defined as the shortest ISI, following T_1, when the spike count and/or latency remained altered and the next two consecutive ISI's had returned to within baseline values for a given criterion. Altogether, three pairs of T_1 and T_2 values were obtained from changes in spike count, FSL, and LSL for each cell. For the example cell in Figure 3.2, the values of T_1 and T_2 were -7 ms and 63 ms using a spike count criterion, 49 ms and 69 ms using a FSL criterion, and -7 ms for both T_1 and T_2 using a LSL criterion because the LSL never returned to within 1 SD over the ISIs measured.

The final values of T_1 and T_2 were chosen to be those most sensitive in capturing the time course of the altered response using a spike count and/or latency criterion (Faure et al. 2003; Sayegh et al. 2014; Valdizón-Rodríguez and Faure 2017). In cases where cells responded with only a single spike per stimulus (i.e. baseline FSL = baseline LSL), a change in spike count was typically used to obtain T_1 and T_2 because this criterion most accurately reflected the time course of spike suppression. For cells that responded with more than one spike per stimulus (i.e. baseline FSL < baseline LSL) or in cases where the spike count of the cell had recovered to within 50% of baseline even though the FSL and/or LSL remained deviated by > 1 SD from baseline, a change in spike latency was typically used to obtain T_1 and T_2 because this criterion most accurately reflected the time course of the cell's altered response. In cases where the mean spike count or latency did not return to $\geq$ 50% or < 1 SD of baseline, respectively, over the range of ISIs presented, T_2 was defined as the longest ISI tested. In all cases, the criterion used for selecting the final values of T_1 and T_2 was confirmed by visual inspection. For the cell in Figure 3.2, the final value of T_1 was -7 ms and could be obtained with either a spike count or LSL criterion, and the

final value of T_2 was 69 ms and was obtained with a FSL criterion.

The final T_1 and T_2 values were then used to calculate the effective start time (T_{start}), end time (T_{end}), and duration of inhibition (D_{IHB}) evoked by the NE tone with the equations:

$$T_{start} = T_1 + L_{last} - D_{BD}\ , \qquad (1)$$

$$T_{end} = T_2 + L_{first} - D_{BD}\ , \text{ and} \qquad (2)$$

$$D_{IHB} = T_{end} - T_{start}\ , \qquad (3)$$

where L_{first} is the baseline FSL, L_{last} is the baseline LSL, and D_{BD} is the duration of the BD tone. A cell was said to have leading inhibition when the onset of inhibition evoked by the NE tone was smaller than the FSL (i.e. $T_{start} < L_{first}$). A cell was said to have persistent inhibition when the duration of inhibition evoked by the NE tone was longer than the duration of the NE tone, D_{NE} (i.e. $D_{IHB} > D_{NE}$). For the cell in Figure 3.2, T_{start} = 20.33 ms, T_{end} = 93.61 ms, and D_{IHB} = 73.28 ms. The cell displayed leading inhibition because the latency of inhibition evoked by the NE tone was 9.28 ms shorter than the excitatory FSL ($L_{first} - T_{start}$ = 9.28 ms). This cell also displayed persistent inhibition because the duration of inhibition evoked by the NE tone was 23.28 ms longer than the duration of the 30 ms NE tone ($D_{IHB} - D_{NE}$ = 23.28 ms).

3.3.7 – Modelling Inhibitory and Excitatory Input-Output Functions

To model input-output (I/O) functions of excitation and inhibition as SPL was varied, we plotted neural responses measured from each cell against stimulus amplitude. Excitatory rate-level functions were normalized to the maximum spike count evoked by single BD tones (Fig. 3.3A). Similarly, inhibitory suppression-level functions were normalized to the maximum duration of NE tone-evoked inhibition [D_{IHB}(max)] during

paired tone stimulation with the BD tone at +10 dB re threshold (Fig. 3.3B).

Normalized plots from 50 DTNs were fit to a 3-parameter logistic function of the form

$$F(x) = (A)/(1 + (x/C)^B) , \qquad (4)$$

where x is the amplitude in dB SPL, A is the maximum asymptote, B is the slope factor, and C is the inflection point at 50% of the value of parameter A. Because A was a free parameter its value was not fixed (e.g. Fig. 3.3B); however, if the maximum asymptote was overestimated by the regression (A>1.3), its value was fixed to A = 1.0 (n = 4 excitatory rate-level functions, n = 10 inhibitory suppression-level functions). The value of C was used to estimate half-maximum response SPL. For excitation, the half-maximum response SPL was abbreviated as $ESPL_{50}$ while for inhibition it was abbreviated as $ISPL_{50}$. The minimum asymptote was fixed at zero for all cells to reflect the assumption that at sub-threshold SPLs spikes were neither evoked nor suppressed.

For the example short-pass DTN in Figure 3.3, the excitatory maximum asymptote was A = 0.980 while the inhibitory asymptote was A = 0.982. This suggests that the I/O functions were saturated near the maximum response for both the normalized functions. The excitatory slope factor was B = -9.80 (Fig. 3.3A), and the inhibitory slope factor was B = -13.68 (Fig. 3.3B). Hence, the inhibitory logistic function was steeper than the excitatory logistic function. Comparing the half-maximum response SPL, for excitation the $ESPL_{50}$ = 42.14 dB SPL while the inhibitory $ISPL_{50}$ = 38.30 dB SPL. This shows that inhibition was more sensitive at half maximum than excitation. Finally, we estimated the 10% and 90% response SPLs from each I/O model to define the dynamic range of

excitation ($ESPL_{90} - ESPL_{10}$) and inhibition ($ISPL_{90} - ISPL_{10}$) for a cell. For the example rate-level function shown in Figure 3.3A, $ESPL_{10}$ = 33.68 dB SPL and $ESPL_{90}$ = 52.73 dB SPL, resulting in a dynamic range of excitation of 19.05 dB. For the example inhibitory suppression-level function shown in Figure 3.3B, $ISPL_{10}$ = 32.62 dB SPL and $ISPL_{90}$ = 44.98 dB SPL, resulting in a dynamic range of inhibition of 12.36 dB.

We were interested in modelling only the monotonic portion of a cell's I/O function containing the largest dynamic range for the cell. Therefore, when a cell's excitatory rate-level function or inhibitory suppression-level function was non-monotonic some data points were excluded from the regression. If data points dropped to < 80% of the maximum spike count and remained under 80% for one additional consecutive point, these points along with all other data points at higher amplitudes were excluded from the model curve fitting and these cells were labelled as non-monotonic. The *crossed circles* in Figure 3.3A illustrate the use of this rule.

3.3.8 – Statistical Analyses

Unless otherwise stated, all data are reported as the mean ± SD. Data were first tested for normality and homogeneity of variances with Shapiro-Wilk and Bartlett tests, respectively. Parametric tests were used when the data were normally distributed with equal variances; otherwise, equivalent nonparametric statistical tests were used.

We used least squares regression to obtain best-fit models of excitatory and inhibitory I/O logistic functions (Fig. 3.3). When a model failed to converge on the data ($p>0.05$ or $R^2 <0.5$), the cell was excluded from statistical analysis (n = 1 excitatory rate-level function, n = 11 inhibitory suppression-level functions).

Linear regressions were used to evaluate the relationship between the: (1) onset of inhibition and BD at the three standardized NE tone amplitudes, (2) duration of inhibition and FSL at the three standardized NE tone amplitudes, (3) excitatory thresholds and $ESPL_{50}$, and (4) $ESPL_{50}$ and $ISPL_{50}$. Cochran's Q-test compared the proportion of cells showing leading/lagging or persistent inhibition at the three standardized NE tone amplitudes. The duration of leading/lagging or persistent inhibition at the three standardized NE tone amplitudes was compared with a Friedman test followed by Nemenyi post-hoc tests for all pairwise comparisons. A Mann-Whitney U-test compared the duration of leading/lagging inhibition in band-pass and short-pass DTNs. Wilcoxon Signed ranks test were used to compare the values of B and C obtained from 3-parameter logistic function (Equation 4), as well as the excitatory ($ESPL_{90} - ESPL_{10}$) and inhibitory ($ISPL_{90} - ISPL_{10}$) dynamic ranges measured from the modelled inhibitory and excitatory IO functions. The proportion of excitatory and inhibitory amplitude response types (i.e. monotonic, nonmonotonic) was compared using a McNemar test. All statistical tests were performed in IBM SPSS or R and used a test-wise type I error rate of $\alpha = 0.05$.

3.4 – Results

3.4.1 – Strength and Time Course of Inhibition Evoked at Different NE Tone Amplitudes

Spiking responses evoked from an example short-pass DTN using paired-tone stimulation with the BD tone amplitude at +10 dB (re threshold) and the NE tone amplitude at 0 dB and +10 dB (re BD tone threshold) are shown in Figure 3.4. The cell's BEF was 39.0 kHz and its acoustic threshold to single BD tones was 53.0 dB SPL. It is important to note that when the NE tone was presented at 0 dB, the BD and NE tones possessed approximately equal energy because the duration of the 10-ms NE tone was 10 times longer than the duration of the 1 ms BD tone (Fig. 3.4A). When the NE tone was at 0 dB there was a reduction in the cell's spike count (Fig. 3.4B), with no change in FSL (Fig. 3.4C), and deviations in the LSL (Fig. 3.4D) when the 1-ms BD tone and 10-ms NE tone were sufficiently close in time. This included ISIs when the BD tone preceded, overlapped with, and followed the NE tone. The final T_1 value was -1 ms and was obtained with a spike count criterion. The final T_2 value was 17 ms and was obtained with a LSL criterion. The effective duration of inhibition (D_{IHB}) was 16.83 ms. The cell had leading inhibition because the onset of inhibition (T_{start} = 11.26 ms) preceded the FSL (FSL = 12.09 ms) by 0.83 ms. The cell also exhibited persistent inhibition because D_{IHB} persisted 6.83 ms longer than the 10-ms NE tone.

When the NE tone amplitude was increased to +10 dB (re BD tone threshold) so that it was equal in amplitude (but not energy) to the BD tone (Fig. 3.4E), spike suppression was again detected; however, the duration of the changed response was noticeably longer

compared to the 0 dB condition (Fig. 3.4A), as evident from changes in the cell's spike count (Fig. 3.4F) and deviations in FSL (Fig. 3.4G) and LSL (Fig. 3.4H). The final T_1 value was -1 ms and this concurred across all three criteria. The final T_2 value was 27 ms and was obtained with a LSL criterion. The effective D_{IHB} was 27.10 ms. Leading inhibition was still evident because the onset of inhibition (T_{start} = 11.08 ms) preceded the FSL (FSL = 12.18 ms,) by 1.10 ms. The cell again displayed persistent inhibition because D_{IHB} lasted 17.10 ms longer than the 10-ms NE tone.

Comparing the two conditions, sustained inhibition was evoked at both NE tone amplitudes; however, the duration of inhibition increased at the higher NE tone amplitude. The onset of inhibition, which was similar across the two conditions, was within the measurement resolution of the stimulus paradigm (i.e. 2 ms). The fact that spike suppression was evident at ISIs where the BD tone preceded the NE tone indicates that the NE tone-evoked inhibition had a shorter latency than the BD tone-evoked excitation. Also, the duration of inhibition persisted longer at the higher NE tone amplitude, suggesting that the inhibition was stronger.

Responses evoked from a second short-pass DTN tested with paired-tone stimulation with the BD at +10 dB and the NE tone at +10 dB and +20 dB (re BD tone threshold) are shown in Figure 3.5. The neuron's BEF was 29.0 kHz and its BD tone threshold was 33.5 dB SPL. When the NE tone was at +10 dB (Fig. 3.5A), spike suppression (Fig. 3.5B) and deviations in both the FSL (Fig. 3.5C) and LSL (Fig. 3.5D) were observed when the 2-ms BD tone and 20-ms NE tone were sufficiently close in time. This included ISIs when the BD tone preceded, was simultaneous with, and followed the

NE tone. The final T_1 value was 0 ms and was obtained with a spike count criterion. The final T_2 value was 30 ms and was obtained with a FSL criterion. The effective duration of inhibition was 28.62 ms. The cell showed leading inhibition because the onset of inhibition (T_{start} = 10.20 ms) preceded the FSL (FSL = 10.82 ms) by 0.62 ms. This cell had persistent inhibition because the duration of inhibition (D_{IHB} = 28.62 ms) lasted 8.62 ms longer than the 20-ms NE tone. The transient increase in spike count (and deviations in spike latencies) near the offset of the NE tone at an ISI = 20 ms (Fig. 3.5, A-D) is an example of offset facilitation, which has previously been reported (Faure et al. 2003).

Spike suppression was again observed when the NE tone amplitude was increased (Fig. 3.5E). At +20 dB (re BD tone threshold) there was a reduction in spike count (Fig. 3.5F) and deviations in both the FSL (Fig. 3.5G) and LSL (Fig. 3.5H) when the two tones were sufficiently close in time. The final T_1 value was -2 ms and was obtained with a LSL criterion. The final T_2 value was 36 ms and was obtained with a FSL criterion. The effective duration of inhibition was 36.66 ms. This cell continued to show leading inhibition because the FSL = 10.80 ms and T_{start} = 8.14 ms, hence inhibition preceded excitation by 2.66 ms. Persistent inhibition was also observed because the duration of inhibition (36.66 ms) was 16.66 ms longer than the 20-ms NE tone.

Comparing the +10 dB and + 20 dB NE tone conditions, the onset of inhibition at +20 dB (T_{start} = 8.14 ms) was earlier than at +10 dB condition (T_{start} = 10.20 ms). The duration of the sustained inhibition was also longer at +20 dB condition (36.66 ms) that at +10 dB (28.62 ms), which also resulted in a longer duration of persistent inhibition +20 dB (16.66 ms) compared to +10 dB (8.62 ms).

We tested 30 DTNs with paired-tone stimulation with the NE tone amplitude at 0 dB, +10 dB and +20 dB (re BD tone threshold). Spike suppression could be measured in all 30 cells (100%) when the NE tone was at 0 dB, +10 dB, and at +20 dB re threshold. Leading inhibition was detected in 55 of 90 (61.11%) observations measured from 30 DTNs tested at the three standardized NE tone amplitudes. The proportion of cells with leading inhibition increased with NE tone amplitude (Figure 3.6A; Table 3.1). Moreover, the duration of leading/lagging inhibition differed across the three standardized amplitudes. Shorter durations of leading inhibition were measured when the NE tone amplitude was in the 0 dB condition compared to when the NE tone was at +20 dB condition. There was no difference between the +10 dB condition and the 0 dB or +20 dB conditions, however, there was a trend of observing more leading inhibition in the +10 dB condition compared to the 0 dB condition as demonstrated by the fact that the mean in the +10 dB condition shows leading inhibition while the mean in the 0 dB condition is lagging (Figure 3.6A; Table 3.1). These results demonstrate that the duration of the advance of inhibition relative to excitation (leading inhibition) evoked during paired-tone stimulation increased when the amplitude of the NE tone was presented above the BD tone threshold and remained relatively constant as amplitudes were increased further.

Persistent inhibition was observed in 75 of 90 (88.9%) observations from 30 DTNs tested at three standardized NE tone amplitudes. The proportion of cells with persistent inhibition varied as a function of NE tone amplitude (Figure 3.6B; Table 3.2), with fewer cells showing persistent inhibition at 0 dB, the threshold for the BD tone, and more cells at +10 dB and +20 dB. Moreover, the duration of persistent inhibition differed across the

three amplitude treatments (Figure 3.6B, black boxes; Table 3.2). Both the +10 and +20 dB conditions had significantly longer durations of persistent inhibition than the 0 dB condition, but there was no difference between the +10 and +20 dB conditions (Table 3.2). These results demonstrate that the duration and offset of the NE tone-evoked inhibition increased with SPL above threshold.

Overall, these findings demonstrate that the onset of inhibition was less affected by changes in the amplitude of the NE tone compared to the offset (and thus duration) of inhibition. Furthermore, these data suggest that time course of inhibition is most dynamic between the 0 dB and +10 dB conditions and becomes relatively constant as the NE tone amplitude was increased from +10 to +20 dB re threshold.

3.4.2 – Relationship of Leading Inhibition to BD, FSL, and Duration Filter Class

Conceptual and computational models, combined with evidence from electrophysiological recordings, indicate that a DTN's BD and duration filter response class depend, in part, on the amount of time that inhibition leads excitation (i.e. leading inhibition) (Aubie et al. 2009, 2012; Casseday et al. 1994, 2000; Ehrlich et al. 1997; Faure et al. 2003; Fremouw et al. 2005; Fuzessery and Hall, 1999). Previous studies have also reported a positive relation between the duration of leading inhibition and BD and/or FSL (Faure et al. 2003; Sayegh et al. 2014; Valdizón-Rodríguez and Faure 2017).

We performed linear regressions to determine the relationship between the duration of leading inhibition and BD, FSL, and duration filter class (Figure 3.7). There was no correlation between the duration of leading inhibition and BD when the NE tone amplitude

was 0 dB re BD tone threshold (Fig. 3.7A); however, a positive correlation was observed when the NE tone amplitude was at +10 and +20 dB re threshold conditions (Fig. 3.7B, C). The strongest correlation was observed for the +20 dB condition (Table 3.3). These results indicate that DTNs with shorter BDs have shorter durations of leading inhibition, but the effect is only evident when the amplitude of the NE tone was above the BD tone threshold (i.e. when NE tone energy was greater than BD tone energy).

There was no correlation between the duration of leading inhibition and FSL when the NE tone amplitude was at 0 dB re BD tone threshold (Fig. 3.7D); however, there was a positive correlation between the onset of inhibition and FSL in the +10 and +20 dB conditions (Fig. 3.7E, F). The strongest correlation occurred when the NE tone amplitude was +10 dB re BD tone threshold (Table 3.3). These results demonstrate that DTNs with shorter FSLs had shorter durations of leading inhibition when the amplitude of the NE tone was above the BD tone threshold.

We tested for a difference between the duration of leading/lagging inhibition and duration filter class across the three standardized NE tone amplitudes. There was no difference in the duration of leading/lagging inhibition between short-pass and band-pass DTNs when the NE tone amplitude was at 0 dB re threshold; however, the duration of leading inhibition differed between short-pass and band-pass DTNs in the +10 dB and +20 dB condition (Table 3.4). In general, short-pass cells had shorter durations of leading inhibition than band-pass cells in the +10 dB and +20 dB conditions. In addition to replicating the results from previous *in vivo* studies (Faure et al. 2003; Sayegh et al. 2014;

Valdizón-Rodríguez and Faure 2017), the present data demonstrate that the NE tone amplitude must be above the BD tone threshold for the relationship to be apparent.

Finally, we tested for a difference between a cell's BD or baseline FSL and duration filter class (shortpass or bandpass). There was a tendency for BDs to be shorter in short-pass cells (Mean ± SD = 1.64 ± 0.90 ms, n=22) than bandpass cells (Mean ± SD = 4.50 ± 1.60 ms, n=8) ($U = 10.00$, $p = 1.16 \times 10^{-4}$; Fig. 3.7A-C). Furthermore, short-pass cells had a shorter baseline FSL (Mean ± SD = 10.55 ± 3.52 ms, n = 22) than bandpass cells (Mean ± SD = 23.21 ± 5.61 ms, n = 8) when measured in the +10 dB condition ($U = 8.00$, $p = 1.76 \times 10^{-4}$; Fig. 3.5E); similar results were observed for both the 0 dB and +20 dB re threshold NE tone amplitude conditions (data not shown). These results replicate previous findings from Faure et al. (2003).

3.4.3 – Comparing Inhibitory and Excitatory Input-Output Functions

To compare excitatory and inhibitory amplitude I/O functions, we plotted the neural responses from each cell as a function of stimulus amplitude. Excitatory rate-level functions were obtained by randomly varying the amplitude of a single BD tone pulse plotting the normalized spike count evoked from the cell at each amplitude. The excitatory rate-level function and the inhibitory I/O function for an example cell are shown in Figure 3.8. The cell's BEF was 49.0 kHz and its excitatory threshold was 43.0 dB SPL. Figure 3.8A shows the normalized mean (± SE) spikes per stimulus plotted for various BD tone amplitudes. The solid line shows the best fit 3-parameter logistic model. The excitatory half-maximum SPL ($ESPL_{50}$) was 48.86 dB SPL, which was 5.86 dB louder than the

acoustic threshold determined online during recording. The maximum asymptote of the logistic function was A = 0.97 and the slope value of the sigmoid was B = -9.13 . The 10% ($ESPL_{10}$) and 90% ($ESPL_{90}$) response points were $ESPL_{10}$ = 38.41 dB SPL and $ESPL_{90}$ = 62.16 dB SPL, yielding a dynamic range of 23.75 dB (Fig. 3.8A). Because the cell was non-monotonic, two data points were removed from the logistic regression of the excitatory rate-level function (Fig. 3.8A, *crossed circles*) so that the regression only contained data points that were on the monotonic portion of the function.

Paired-tone stimulation data were used to construct an inhibitory I/O function (Fig. 3.8B) by plotting the normalized duration of inhibition [$D_{IHB}/D_{IHB}(max)$] as a function of NE tone amplitude and fitting a 3-parameter logistic curve to the data (Fig. 3.8B). Using the model we determined the half-maximum inhibitory SPL ($ISPL_{50}$) to be 51.25 dB SPL, the maximum asymptote was A = 1.08 and the slope of the sigmoid was B = -8.93, and the 10% ($ISPL_{10}$) and 90% ($ISPL_{90}$) response points were $ISPL_{10}$ = 40.07 dB SPL and $ISPL_{90}$ = 65.54 dB SPL, yielding a dynamic range of 25.47 dB (Fig. 3.8B).

The difference between the $ISPL_{50}$ and $ESPL_{50}$ was 2.38 dB SPL. Thus, inhibition and excitation had very similar inflection points with the $ISPL_{50}$ having a slightly higher value. The slope value of the sigmoid was larger for excitation, meaning that the dynamic portion of the logistic function covered a narrower range of amplitudes for excitation compared to inhibition as can be seen by the narrower 10 - 90% excitatory dynamic range (23.75 dB) compared to the 10 - 90% inhibitory dynamic range (25.47 dB). However, the difference between the two slopes was 0.20, which is a small difference, indicating that the

steepness of the inhibitory and excitatory logistic functions were similar to one another in this cell.

We obtained logistic models from both the excitatory rate-level and inhibitory suppression-level functions of 38 DTNs. To test the validity of the logistic regression in excitatory rate-level functions, we measured the relationship between the excitatory threshold measured online during recordings and the cell's $ESPL_{50}$. We found a strong linear relationship between the excitatory threshold (determined online) and $ESPL_{50}$ (slope = 0.908, y-intercept = 5.239; R = 0.962, $p = 1.00 \times 10^{-13}$), demonstrating that logistic functions model excitatory rate-level functions in a manner consistent with our estimate of acoustic threshold determined while recording from a cell. We compared the difference between the excitatory and inhibitory half-maximum SPL ($ISPL_{50} - ESPL_{50}$) measured from the same cell in 38 DTNs (Fig. 3.9); negative values suggest that $ISPL_{50}$ was more sensitive than $ESPL_{50}$. In 25 of 38 cells (65.79%), the $ISPL_{50} - ESPL_{50}$ difference was negative and the magnitude of the difference (median = -3.22 dB, IQR = -8.46 dB to 2.55 dB) was significantly different from zero (Z = -2.27, p = 0.023, n = 38). Altogether, these data demonstrate that in a majority of DTNs inhibition was more sensitive to stimulus amplitude than excitation; although, the difference in sensitivity was relatively small compared to the dynamic range of auditory neurons in general.

There was also a strong relationship between the $ISPL_{50}$ and $ESPL_{50}$ values measured from the same cell (Fig. 3.10; R = 0.730, $p = 1.93 \times 10^{-7}$, n= 38), indicating that the strength of excitation (quantified from the rate-level function with single BD tones)

increased in proportion to inhibition (measured with paired-tone stimulation with a +10 dB BD tone and variable amplitude NE tones). The slope of the linear regression in Figure 3.10 was less than 1, suggesting that thresholds of inhibition were lower than excitatory thresholds.

We examined the slopes of the excitatory and inhibitory logistic functions fit to each cell (Fig. 3.11). The median slope value obtained from the excitatory rate-level functions was -17.77 and the IQR was between -53.55 to -9.63. The median slope value obtained from the inhibitory suppression-level response function was -17.25 and the IQR was between -35.85 to -4.77. There was no difference between the slopes of the excitatory and inhibitory logistic functions ($Z = -1.080$, $p = 0.280$, $n = 38$). This comparison demonstrates that the excitatory and inhibitory sigmoid curves that we modeled did not differ with respect to the rate of change at which they reached their maximum asymptotes.

We also measured the 10% – 90% dynamic range from the modelled inhibitory and excitatory I/O functions. The distributions of dynamic ranges for excitation (Fig. 3.12A; median = 11.358 dB, IQR = 4.239 to 22.627) and inhibition (Fig. 3.12B; median = 11.549, IQR = 5.008 to 27.805) were quite similar ranges and not significantly different ($Z = -1.283$; $p = 0.199$, $n=38$). This demonstrates that changes in excitation and inhibition occurred over similar dynamic ranges in the same cell.

Finally, we classified the excitatory rate-level and inhibitory suppression-level response functions of the 38 DTNs as either monotonic (response increased with increasing SPL) or non-monotonic (either peaked or other). For example, the response-level functions

shown in Figs. 3.3B and 3.8B and were both monotonic while the functions shown in Figs. 3.3A and 3.8A were both non-monotonic. A minority of excitatory rate-level functions were monotonic (15 cells; 39.47%) while a majority of inhibitory suppression-level functions were monotonic (32 cells; 84.21%). Furthermore, the proportion of monotonic and non-monotonic functions differed between excitation and inhibition (Table 3.5).

3.5 – Discussion

3.5.1 – Strength and Time Course of Inhibition

Previous extracellular and intracellular recording studies have demonstrated that duration tuning arises from the summation of excitatory and inhibitory synaptic inputs that differ in latency (Brand et al. 2000; Casseday et al. 2000; Covey et al. 1996; Faure et al. 2003; Fuzzesery and Hall, 1999; Leary et al. 2008; Pérez-González et al. 2006; Valdizón-Rodríguez and Faure 2017). Furthermore, neuropharmacological studies have shown that duration selectivity was reduced or abolished after antagonists of inhibitory neurotransmitters were administered (Casseday et al. 1994, 2000; Fuzessery and Hall 1999; Jen and Feng, 1999; Jen and Wu, 2005; Yin et al. 2008), indicating that inhibition is necessary for duration selectivity. Single-unit and whole cell patch-clamp recordings have further shown that inhibition precedes excitation and is sustained for as long or longer than the duration of the stimulus (Casseday et al. 1994, 2000; Ehrlich et al. 1997; Faure et al. 2003; Leary et al. 2008; Valdizón-Rodríguez and Faure 2017). Altogether, these studies demonstrate inhibition is necessary for shaping the excitatory responses that create duration tuning.

In the range between threshold (0 dB) and +10 dB, the onset (i.e. latency) of inhibition shortened and led excitation, but between +10 and +20 dB it did not change and thus became amplitude tolerant. A similar trend was also observed for the offset (i.e. duration) of inhibition; between 0 and +10 dB (re threshold), the duration of inhibition lengthened, but between +10 and +20 dB it became amplitude tolerant. Compared to the onset of inhibition, the duration of inhibition changed more as the NE tone amplitude

increased. It is worth noting that this is the first study to characterize response properties of DTNs at the cell's excitatory threshold. We found that the largest changes in the onset and offset of inhibition occurred when the amplitude of the NE tone was between 0 dB and +10 dB re threshold (Fig. 3.6).

Our results can be compared with a previous, contrasting paired-tone stimulation study on DTNs by Faure et al. (2003) in which the BD tone amplitude was varied from 0 to + 20 dB (re NE tone) and the NE tone amplitude was typically set to +10 dB (re BD tone threshold). That study found that the amount of leading inhibition remained relatively constant, whereas the offset/duration of inhibition systematically decreased as the amplitude of the BD tone increased from +10 to +30 dB re BD tone threshold (or 0 to +20 dB re NE tone). Faure et al. (2003) suggested this occurred because the sustained inhibition evoked by the NE tone was strongest near signal onset but gradually waned in strength.

Our finding that the onset of inhibition remained level tolerant when the amplitude of the NE tone was varied between +10 and +20 dB re BD tone threshold (Fig. 3.6 and Table 3.1) is consistent with the results of Faure et al. (2003). Changes in the onset of leading inhibition were similar between the studies, with Faure et al. (2003) reporting an average decrease of 1.0 ms in leading inhibition when the BD tone amplitude increased from +10 dB to +20 dB, while the current study found a 0.69 ms increase in leading inhibition when the NE tone amplitude increased from +10 dB to +20 dB (Fig. 3.6A). Importantly, the latency changes reported in both studies were smaller than the 2-ms step-size (i.e. measurement resolution) used to vary the onset time of the roving BD tone, and were also smaller than the SD in any condition between the two studies (min SD = 2.9 ms,

max SD = 4.41 ms). We suggest two explanations for why changing the amplitude of either the BD tone or the NE tone did not greatly influence the onset of inhibition. First, the strengths of the BD tone excitation and the NE tone inhibition may have changed proportionately. Second, because the onset of inhibition was level tolerant between +10 and +20 dB, it may have reached maximum strength between 0 and +10 dB (re BD tone threshold). Evidence for the latter can be seen by noting the switch from lagging to leading inhibition between the 0 dB and +10 dB conditions, followed by a plateau in the duration of leading inhibition between the +10 and +20 dB conditions (Fig. 3.6A).

Conversely, changes in the offset/duration of NE tone evoked inhibition were stronger when the BD tone amplitude was varied (Faure et al. 2003) than when the NE tone amplitude was varied (current study). This is demonstrated by a greater change in the amount of persistent inhibition when the BD tone amplitude was increased (see Fig. 3.12 in Faure et al. 2003) than when the NE tone amplitude was increased (Fig. 3.6B). Faure et al. (2003) reported an increase in the duration of persistent inhibition of 9.2 ms when the BD tone amplitude increased from +10 dB and +20 dB (re BD tone threshold), compared to an increase of 2.9 ms in the present study when the NE tone amplitude went from +10 dB to +20 dB (re BD tone threshold). This implies that the increase in strength of excitation evoked by increasing the amplitude of the BD tone (Faure et al. 2003) was greater than the increase in the strength of inhibition evoked by increasing the NE tone amplitude near the offset of inhibition. Together, these findings suggest that when the tones were presented at +10 and +20 dB above threshold the strength of excitation evoked by the BD tone increased faster than the strength of inhibition evoked by the NE tone. Interestingly, Sayegh et al.

(2012) came to a similar conclusion although that study used paired pulse stimulation with pairs of BD tones (see *Effect of Stimulus Amplitude on Paired tone and Paired pulse Stimulation*).

The fact that the onset and offset of inhibition responded differently to increases in the amplitude of the BD tone (Faure et al. 2003) and/or the NE tone (this study) suggest that these inhibitory components may be caused by different inputs. This hypothesis was also suggested in a study that varied the frequency of the NE tone during paired tone stimulation and found that the onset of inhibition was frequency invariant whereas the offset/duration of inhibition shortened as the NE tone frequency departed from the BEF (Valdizón-Rodríguez and Faure 2017). That study also suggested that inputs from the VNLLc were a likely candidate for providing the strong, early inhibition seen in DTNs. Data from the current study also support the hypothesis that the VNLLc may provide inhibitory inputs to DTNs. First, neurons in the VNLLc project primarily to the IC (Covey et al. 1986). Second, VNLLc neurons have short response latencies (Covey and Casseday, 1991), a feature consistent with leading inhibition to DTNs (Figs. 3.6*A*, 3.7). Third, VNLLc neurons are known to have narrow dynamic ranges and respond maximally to small increases in SPL (Covey and Casseday, 1991). This feature is consistent with the level tolerance of leading inhibition at SPLs ≥+10 dB re BD tone threshold (Fig. 3.6A), and the narrow dynamic ranges of the inhibitory suppression-level functions that we measured in our sample population of DTNs (Fig. 3.12B). Fourth, a majority of VNLLc neurons have monotonic rate-level functions (Covey and Casseday, 1991), and this was also true for the inhibitory suppression-level functions measured in DTNs (Table 3.5). Fifth, the responses

of VNLLc neurons are primarily monaural (Covey et al. 1991), and in the IC duration tuning is created monaurally (Sayegh et al. 2014). Finally, that VNLLc neurons may be the source of the onset-evoked, leading inhibition to DTNs is also supported by another study that measured duration selectivity changes before and after iontophoretic application of bicuculline and strychnine, inhibitory neurotransmitter antagonists to γ-aminobutyric acid (GABA) and glycine, respectively. When GABAergic inhibition was blocked, sustained spiking was revealed more frequently than when glycinergic inhibition was blocked (Casseday et al. 2000), suggesting that GABAergic inhibition plays a stronger role during the ongoing portion of the inhibitory response, while glycinergic inhibition may be strongest in the early, onset-evoked portion of the inhibitory response.

3.5.2 – Level Tolerance in DTNs is Created by a Balance of Excitation and Inhibition

A DTN's FSL, BD, and duration filter class do not vary with increases in stimulus amplitude (Zhou and Jen, 2001; Fremouw et al., 2005; Valdizón-Rodríguez and Faure, 2017), except near threshold (Fig. 3.6A), suggesting that the strengths of excitation and inhibition remain balanced with increasing stimulus amplitude. If the strength of excitation increased faster than that of inhibition, FSLs would be expected to decrease at louder SPLs as is the case for most central auditory neurons (Heil, 2004; Klug et al. 2000; Mörchen et al. 1978; Rose et al. 1963; Tan et al. 2008). If the strength of inhibition increased faster than that of excitation, FSLs should lengthen and the cell should demonstrate a paradoxical latency shift (PLS) at increasing SPLs (Covey et al. 1996; Galazyuk et al. 2005; Galazyuk and Feng, 2001; Hechavarría et al. 2011; Hechavarría and Kössl, 2014; Klug et al. 2000; Macías et al. 2016; Sullivan, 1982a, 1982b). Two conditions must be met for a neuron to

display PLS: 1) the onset of inhibition must precede or begin simultaneously with the onset of excitation, and 2) the strength of inhibition must increase more rapidly than the strength of excitation with increasing stimulus energy (Fremouw et al. 2005; Galazyuk and Feng, 2001). To the best of our knowledge, shortpass and bandpass DTNs do not exhibit PLS (Zhou and Jen 2001; Fremouw et al. 2005; Valdizón-Rodríguez and Faure 2017).

Our results demonstrate that the onset of inhibition remained relatively constant when the amplitude of the NE tone was between +10 and +20 dB re BD tone threshold (Fig. 3.6A). Moreover, our measures of the $ESPL_{50}$ and $ISPL_{50}$ were positively correlated (Fig. 3.10), and the dynamic ranges of excitation and inhibition were matched (Figs. 3.11, 3.12). Altogether, these findings suggest that excitation and inhibition are balanced in DTNs. This hypothesis is supported by whole-cell patch clamp recordings from DTNs in mammals and amphibians which have revealed a short, phasic inhibitory event that occurs near stimulus onset and offset but not during the ongoing portion (Casseday et al. 1994; Leary et al. 2008). That DTNs receive sustained inhibition has been repeatedly demonstrated with single-unit recording and application of inhibitory neurotransmitter antagonists (Casseday et al. 1994, 2000) or paired-tone stimulation (Faure et al. 2003; Sayegh et al. 2014; Valdizón-Rodríguez and Faure 2017). If excitation and inhibition are more-or-less in balance during the ongoing portion of a stimulus, this would explain why intracellular studies were unable to detect a net tonic inhibition—because it is counteracted by excitation. This explanation is consistent with the present findings.

3.5.3 – Modelling Inhibitory and Excitatory Input-Output Functions

We used logistic regression to model I/O functions of DTNs, which allowed us to compare excitation and inhibition as a function of SPL. The strong, positive correlation between the measured excitatory threshold (determined online while recording from the cell) and $ESPL_{50}$ gives us confidence that a logistic function models excitatory rate-level functions in a manner that consistent with how acoustic threshold was determined. Our modelled inhibitory and excitatory I/O functions revealed that $ISPL_{50}$ values were significantly lower than $ESPL_{50}$ values (Fig. 3.9). This result supports previous findings (see Fig. 3.12 in Faure et al. 2003) and our observation that near the offset of inhibition the strength of excitation increased faster than the strength of inhibition when a DTN was presented with tones between +10 and +20 dB re threshold (Fig. 3.6). We suggest this occurs because a cell's excitatory rate-level function is offset from and has a higher threshold relative to its inhibitory suppression-level function. Consequently, when the stimulus is 10 or 20 dB above threshold, the inhibitory function will be near its asymptote while the excitatory function may still be within its dynamic range. Therefore, for a near threshold stimulus, the recruitment of synaptic excitation will be faster than for inhibition.

Another possible reason why $ISPL_{50}$ values were lower than $ESPL_{50}$ values is the difference in stimulus energy between the NE and BD tones. In our study the duration of the NE tone was always ten times the duration of the BD tone. Thus, even when the two tones were equal in amplitude the NE tone possessed 10 dB more energy than the BD tone (i.e. $Energy = Power \times Time$; $\Delta dB = 10 \times \log_{10}[10]$). Therefore, at lower SPLs the NE

tone would surpass the threshold of inhibition sooner than the BD tone passed its threshold of excitation, yielding a higher excitatory acoustic threshold.

Finally, it is also possible that the differences between $ISPL_{50}$ and $ESPL_{50}$ values resulted from different methods of data collection prior to the model fits for estimating half-maximal SPLs. Inhibitory I/O functions, which served as a proxy for the strength of inhibition, were derived from the normalized duration of inhibition evoked by the NE tone during paired-tone stimulation. In contrast, excitatory I/O functions, which served as a proxy for the strength of excitation, were derived from each cell's excitatory rate-level function with a single BD tone. Despite these methodological differences, the $ISPL_{50}$ and $ESPL_{50}$ values we obtained were strongly and positively correlated (Fig. 3.10).

3.5.4 – Effect of Stimulus Amplitude on Paired tone and Paired pulse stimulation

The recovery cycle of a neuron is determined with paired-pulse stimulation and is measured as the minimum ISI between two pulses that is required for the spike count or latency evoked by the second pulse to recover to within a specified amount of the response evoked by the first pulse (Grinnell, 1963). The technique of paired-pulse stimulation and paired-tone stimulation are similar, but unlike paired-tone stimulation, paired-pulse stimulation uses equal duration tone pairs (Sayegh et al. 2012). Previous studies have demonstrated that application of GABA-antagonist bicuculline broadens the duration tuning curves of the second tone in the pair (Casseday et al. 1994; Jen and Feng, 1999) and shortens recovery cycles times in most IC neurons (Lu et al. 1997; Zhou and Jen, 2003). It has also been shown that band-pass cells have significantly longer recovery cycle times

than non-duration selective neurons (Sayegh et al. 2012). These studies illustrate that inhibitory inputs play a role in recovery cycles of DTNs.

Our study demonstrated that the duration of NE tone evoked inhibition increased as the amplitude of the NE tone increased. These results suggest that the recovery time of a DTN will increase as the amplitude of the first tone pulse increases because the first tone will evoke longer persistent inhibition. A similar result has been observed in auditory neurons from the IC where recovery times decreased as the amplitude of the first tone pulse decreased relative to the second tone pulse (Friend et al. 1966).

Sayegh et al. (2012) found that recovery cycle times shortened when the amplitude of both tones increased together. They proposed the idea that the strength of excitation increases faster than the strength of inhibition when cells are stimulated with tones at +10 and +20 dB re threshold, because the excitation evoked by the second tone can overcome the inhibition evoked by the first tone. This result is consistent with our finding that excitation increased in strength faster than inhibition near the offset of inhibition as the amplitude was increased from +10 to +20 dB re threshold (see discussion section (see *Strength and Time Course of Inhibition*).

3.5.5 – Masker Amplitude and Temporal Masking

The paired-tone stimulation paradigm that we used to stimulate DTNs yield neurophysiological results that were analogous to the results of auditory psychophysical temporal masking experiments. The BD tone is comparable to a probe tone and the NE tone is comparable to a masker tone. Neurophysiological equivalents of auditory temporal

masking patterns have been observed in DTNs during paired-tone stimulation (Faure et al. 2003; Sayegh et al. 2014; Valdizón-Rodríguez and Faure 2017). Spike suppression that occurred when the BD tone preceded the NE tone is the neural equivalent of backward masking and is caused by the arrival of early, leading inhibition evoked by the NE tone. Spike suppression that occurred when the BD tone was contiguous and/or overlapping with the NE tone is the neural equivalent of simultaneous masking and is caused by the sustained inhibition evoked by the NE tone. Lastly, spike suppression that occurred when the BD tone followed the NE tone is the neural equivalent of forward masking and is caused by the persistent inhibition evoked by the NE tone.

We found that the effects of leading and sustained inhibition could be observed at lower amplitudes than persistent inhibition evoked in the same cell (Fig. 3.6). This leads to the prediction that backward and simultaneous masking should have lower thresholds than forward masking. Temporal masking data from human and non-human animals supports this prediction. Moore (1978) found that in a majority of subjects, thresholds for simultaneous masking were lower than forward masking. Dooling and Searcy (1985) found that backward masking thresholds were lower than forward masking thresholds. The similarity between our results and the results of temporal masking experiments suggest that leading, sustained, and persistent inhibition may provide a neural mechanism to explain temporal masking phenomena. Our results are also consistent with other neural studies on temporal masking (Nelson et al., 2009).

3.6 – References

Aubie B, Becker S, Faure PA. Computational models of millisecond level duration tuning in neural circuits. *J Neurosci 29*(29), 9255–9270, 2009.

Aubie B, Sayegh R, Faure PA. Duration tuning across vertebrates. *J Neurosci 32*(18), 6373–6390, 2012.

Brand A, Urban R, Grothe B. Duration tuning in the mouse auditory midbrain. *J Neurophysiol 84*(4), 1790–1799, 2000.

Casseday JH, Ehrlich D, Covey E. Neural tuning for sound duration: role of inhibitory mechanisms in the inferior colliculus. *Science, 264*(5160), 847–850, 1994.

Casseday JH, Ehrlich D, Covey E. Neural measurement of sound duration: control by excitatory-inhibitory interactions in the inferior colliculus. *J Neurophysiol 84*(3), 1475–1487, 2000.

Covey E, Casseday JH. Connectional basis for frequency representation in the nuclei of the lateral lemniscus of the bat Eptesicus fuscus. *J Neurosci* 6:2926–2940, 1986.

Covey E, Casseday JH. The monaural nuclei of the lateral lemniscus in an echolocating bat: parallel pathways for analyzing temporal features of sound. *J Neurosci* 11:3456–3470, 1991.

Covey E, Kauer JA, Casseday JH. Whole-cell patch-clamp recording reveals subthreshold sound-evoked postsynaptic currents in the inferior colliculus of awake bats. *J Neurosci 16*(9), 3009–3018, 1996.

Denes P. Effect of duration on the perception of voicing. *J Acoust Soc Am 27*(4), 761–764, 1955.

Dooling RJ, Searcy MH. Nonsimultaneous auditory masking in the budgerigar (*Melopsittacus undulatus*). *J Comp Psychol 99*(2), 226–230, 1985.

Ehrlich D, Casseday JH, Covey E. Neural tuning to sound duration in the inferior colliculus of the big brown bat, *Eptesicus fuscus*. *J Neurophysiol* 77:2360–2372, 1997.

Faure PA, Fremouw T, Casseday JH, Covey E. Temporal masking reveals properties of sound-evoked inhibition in duration-tuned neurons in the inferior colliculus. *J Neurosci 23*(7), 3052–3065, 2003.

Fremouw T, Faure PA, Casseday JH, Covey E. Duration selectivity of neurons in the inferior colliculus of the big brown bat: tolerance to changes in sound level. *J Neurophysiol 94*(3), 1869–1878, 2005.

Friend JH, Suga N, Suthers RA. Neural responses in the inferior colliculus of echolocating bats to artificial orientation sounds and echoes. *J Cell Physiol 67*(2), 319–332, 1966.

Fuzessery ZM, Hall JC. Sound duration selectivity in the pallid bat inferior colliculus. *Hear Res 137*(1-2), 137–154, 1999.

Galazyuk AV, Feng AS. Oscillation may play a role in time domain central auditory processing. *J Neurosci 21*(11), RC147, 2001.

Galazyuk AV, Lin W, Llano D, Feng AS. Leading inhibition to neural oscillation is important for time-domain processing in the auditory midbrain. *J Neurophysiol 94*(1), 314–326, 2005.

Grinnell AD. The neurophysiology of audition in bats: temporal parameters. *J Physiol 167*(1), 67–96, 1963.

He J, Hashikawa T, Ojima H, Kinouchi Y. Temporal integration and duration tuning in the dorsal zone of cat auditory cortex. *J Neurosci* 17:2615–2625, 1997.

Hechavarría JC, Cobo AT, Fernández Y, Macías S, Kössl M, Mora EC. Sound-evoked oscillation and paradoxical latency shift in the inferior colliculus neurons of the big fruit-eating bat, *Artibeus jamaicensis*. *J Comp Physiol A 197*(12), 1159–1172, 2011.

Hechavarría JC, Kössl M. Footprints of inhibition in the response of cortical delay-tuned neurons of bats. *J Neurophysiol 111*(8), 1703–1716, 2014.

Heil P. First-spike latency of auditory neurons revisited. *Curr Opin Neurobiol 14*(4), 461–467, 2004.

Jen PH-S, Feng RB. Bicuculline application affects discharge pattern and pulse-duration tuning characteristics of bat inferior collicular neurons. *J Comp Physiol A 184*(2), 185–194, 1999.

Jen PH-S, Wu CH. The role of GABAergic inhibition in shaping the response size and duration selectivity of bat inferior collicular neurons to sound pulses in rapid sequences. *Hear Res 202*(1-2), 222–234, 2005.

Klug A, Khan A, Burger RM, Bauer EE, Hurley LM, Yang L, Grothe B, Halvorsen MB, Park TJ. Latency as a function of intensity in auditory neurons: influences of central processing. *Hear Res 148*(1-2), 107–123, 2000.

Leary CJ, Edwards CJ, Rose GJ. Midbrain auditory neurons integrate excitation and inhibition to generate duration selectivity: an *in vivo* whole-cell patch study in anurans. *J Neurosci 28*(21), 5481–5493, 2008.

Lu Y, Jen PH-S, Zheng Q-Y. GABAergic disinhibition changes the recovery cycle of bat inferior collicular neurons. *J Comp Physiol A 181*(4), 331–341, 1997.

Macías S, Hechavarría JC, Kössl M. Sharp temporal tuning in the bat auditory midbrain overcomes spectral-temporal trade-off imposed by cochlear mechanics. *Sci Rep 6*, 29129, 2016.

Moore BC. Psychophysical tuning curves measured in simultaneous and forward masking. *J Acoust Soc Am 63*(2), 524–532, 1978.

Mora EC, Kössl M. Ambiguities in sound-duration selectivity by neurons in the inferior colliculus of the bat *Molossus molossus* from Cuba. *J Neurophysiol 91*(5), 2215–2226, 2004.

Mörchen A, Rheinlaender J, Schwartzkopff J. Latency shift in insect auditory nerve fibers. *Naturwissenschaften, 65*(12), 656–657, 1978.

Narins PM, Capranica RR. Neural adaptations for processing the two-tone call of the Puerto Rican treefrog, *Eleutherodactylus coqui*. *Brain, Behavior and Evolution, 17*(1), 48–66, 1980.

Nelson PC, Smith ZM, Young ED Wide-dynamic-range forward suppression in marmoset inferior colliculus neurons is generated centrally and accounts for perceptual masking. *J Neurosci* 29(8), 2553–2562, 2009.

Pérez-González D, Malmierca MS, Moore JM, Hernández O, Covey E. Duration selective neurons in the inferior colliculus of the rat: topographic distribution and relation of duration sensitivity to other response properties. *J Neurophysiol 95*(2), 823–836, 2006.

Pinheiro AD, Wu M, Jen PH-S. Encoding repetition rate and duration in the inferior colliculus of the big brown bat, *Eptesicus fuscus*. *J Comp Physiol A 169*(1), 69–85, 1991.

Pollack GS, Hoy RR. Temporal pattern as a cue for species-specific calling song recognition in crickets. *Science* 204:429–432, 1979.

Potter HD. Patterns of acoustically-evoked discharges of neurons in the mesencephalon of the bullfrog. *J Neurophysiol 28*, 1155–1184, 1965.

Rose JE, Greenwood DD, Goldberg JM, Hind JE. Some discharge characteristics of single neurons in the inferior colliculus of the cat. I. Tonotopical organization, relation of spike counts to tone intensity, and firing patterns of single elements. *J Neurophysiol 26*(2), 294–320, 1963.

Rosen S. Temporal information in speech: acoustic, auditory and linguistic aspects. *Philos Trans R Soc London Ser B: Biol Sci* 336:367–373, 1992.

Sayegh R, Aubie B, Faure PA. Duration tuning in the auditory midbrain of echolocating and non-echolocating vertebrates. *J Comp Physiol A 197*(5), 571–583, 2011.

Sayegh R, Casseday JH, Covey E, Faure PA. Monoaural and binaural inhibition underlying duration-tuned neurons in the inferior colliculus. *J Neurosci 34*(2), 481–492, 2014.

Schnitzler H-U, Kalko EKV. Echolocation by insect-eating bats. *Bioscience* 51:557–569,

2001.

Shannon RV, Zeng FG, Kamath V, Wygonski J, Ekelid M. Speech recognition with primarily temporal cues. *Science* 270:303–304, 1995.

Singh NC, Theunissen FE. Modulation spectra of natural sounds and ethological theories of auditory processing. *J Acoust Soc Am* 114:3394–3411, 2003.

Sullivan WE III. Possible neural mechanisms of target distance coding in auditory system of the echolocating bat *Myotis lucifugus*. *J Neurophysiol 48*(4), 1033–1047, 1982a.

Sullivan WE III. Neural representation of target distance in auditory cortex of the echolocating bat *Myotis lucifugus*. *J Neurophysiol 48*(4), 1011–1032, 1982b.

Tan X, Wang X, Yang W, Xiao Z. First spike latency and spike count as functions of tone amplitude and frequency in the inferior colliculus of mice. *Hear Res 235*(1-2), 90–104, 2008.

Valdizón-Rodríguez R, Faure PA. Frequency tuning of synaptic inhibition underlying duration-tuned neurons in the mammalian inferior colliculus. *J Neurophysiol 117*(4), 1636–1656, 2017.

Wang J, van Wijhe R, Chen Z, Yin S. Is duration tuning a transient process in the inferior colliculus of guinea pigs? *Brain Res 1114*(1), 63–74, 2006.

Xia YF, Qi ZH, Shen JX. Neural representation of sound duration in the inferior colliculus of the mouse. *Acta Otolaryngol* 120:638–643, 2000.

Yin S, Chen Z, Yu D, Feng Y, Wang J. Local inhibition shapes duration tuning in the inferior colliculus of guinea pigs. *Hear Res 237*(1-2), 32–48, 2008.

Zhou X, Jen PH-S. The effect of sound intensity on duration-tuning characteristics of bat inferior collicular neurons. *J Comp Physiol A 187*(1), 63–73, 2001

Zhou X, Jen PH-S (2003) The effect of bicuculline application on azimuth-dependent recovery cycle of inferior collicular neurons of the big brown bat, *Eptesicus fuscus*. *Brain Res* 973:131–141.

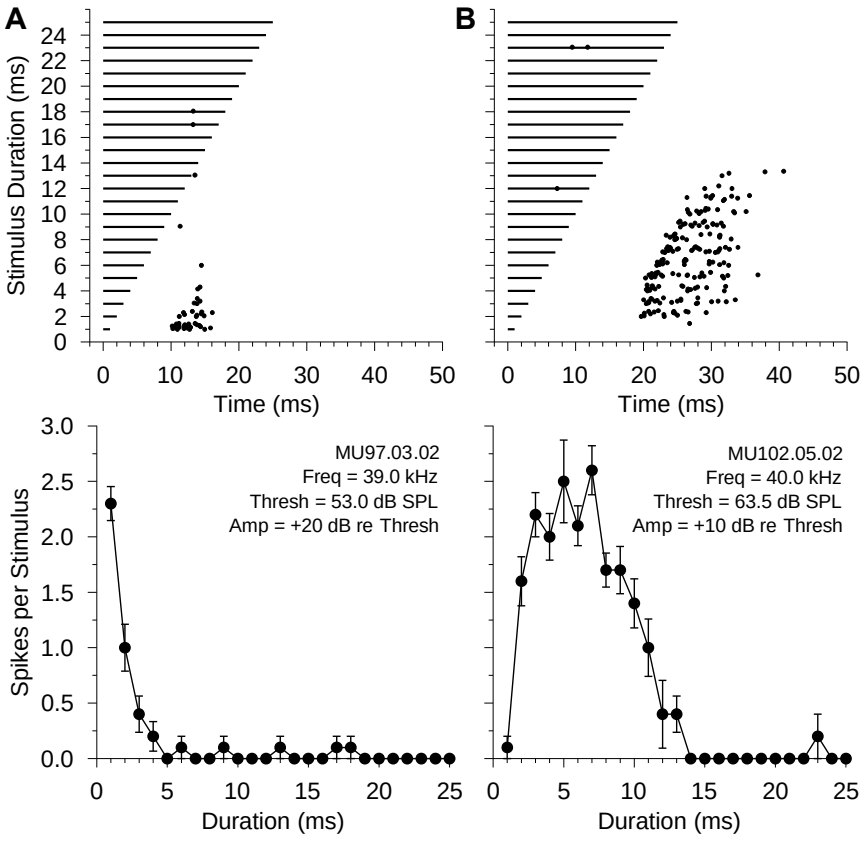

Figure 3.1. Band-pass and short-pass DTNs from the IC of the big brown bat.

A: Short-pass DTN with a BD of 1 ms. B: Band-pass DTN with a BD of 7 ms. *Top row*: dot raster displays showing the timing of action potentials (*black dots*) in response to BEF tone pulses (*black bars*) randomly varied in duration. *Bottom row*: mean ± standard error (SE) spikes per stimulus as a function of stimulus duration for suprathreshold BEF tones. Insets shows bat and cell identification, BEF, acoustic threshold, and stimulus level above threshold. n = 10 trials per stimulus.

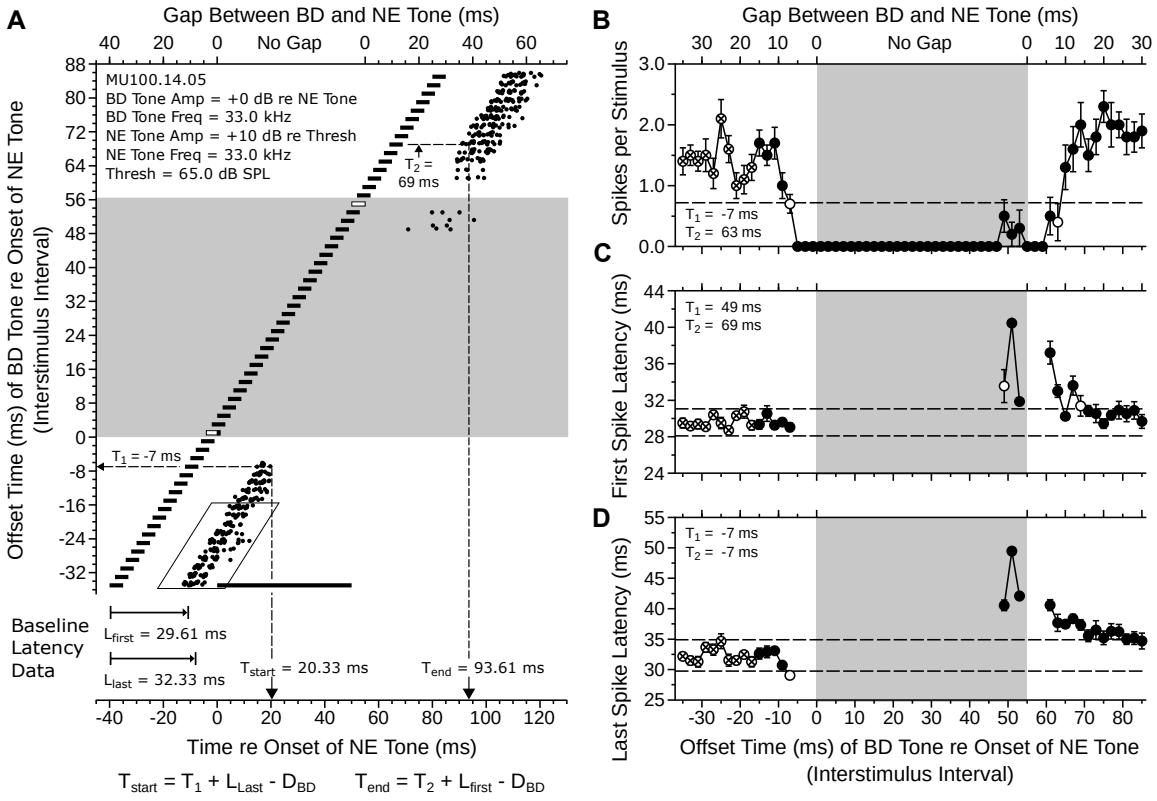

Figure 3.2. Measuring inhibition with paired-tone stimulation.

A: Dot raster display from a short-pass DTN demonstrating how the time course of inhibition evoked by the NE tone was measured using changes in the cell's spike count and/or latencies in response to a roving BD tone. In this example, the BD and NE tones were matched in frequency and amplitude but differed in duration. The onset time of the NE tone (50 ms *black bar*, drawn once for clarity) was constant whereas the onset time of the BD tone (5 ms *black bars*) was randomly varied relative to NE tone onset. The top *x-axis* shows the gap (ISI) between the BD and NE tones. The bottom *x-axis* shows time relative to the onset of the NE tone. The *y-axis* shows the offset time of the BD tone relative to the onset time of the NE tone (i.e. the ISI). The BD and NE tones were electronically

mixed and presented monaurally to the ear contralateral to the recorded IC. When the two tones temporally overlapped (*gray box*), a single compound stimulus with an amplitude pedestal resulted. The BD tone bars with a *white fill* display ISIs when the BD and NE tones overlapped or were contiguous. Spikes evoked by the BD tone at the 10 longest ISIs when the BD tone preceded the NE tone (spikes in *parallelogram*) were used to calculate the mean ± SD baseline spike count (1.41 ± 0.72 spikes per stimulus), baseline FSL (L_{first} = 29.61 ± 1.46 ms), and baseline LSL (L_{last} = 32.33 ± 2.58 ms). Note how BD tone-evoked responses were suppressed by NE tone-evoked inhibition when the two tones where sufficiently close in time. Three separate criteria regarding changes to the spike count, FSL, and/or LSL were used to determine the onset (T_1) and offset (T_2) of inhibition evoked by the NE tone. The shortest ISI with a significant deviation from the baseline spike count and/or latency was T_1 = -7 ms and was obtained using either a spike count or LSL criterion. The longest positive ISI with a significant deviation from the baseline spike count and/or latency was T_2 = 69 ms and could be obtained using a FSL criterion. Using the equations shown, T_{start} = 20.33 ms, T_{end} = 93.61 ms, and the duration of inhibition ($T_{end} - T_{start}$) = 73.28 ms. B: Mean ± SE spikes per stimulus as a function of the ISI between the BD and NE tones. The *dashed line* represents 50% of the baseline spike count. The left *open circle* shows the first ISI with a spike count below 50% of baseline (T_1 = -7 ms). The right *open circle* shows the last ISI with a spike count below 50% of baseline (T_2 = 63 ms). C: Mean ± SE FSL as a function of the ISI between the BD and NE tones. The *dashed lines* represent ± 1 SD from the baseline FSL. The left *open circle* shows the first ISI when the FSL deviated by > 1 SD from baseline (T_1 = 49 ms). The right *open circle* shows the last ISI

when the FSL remained deviated by > 1 SD from baseline (T_2 = 69 ms). D: Mean ± SE LSL as a function of the ISI between the BD and NE tones. The *dashed lines* represent ± 1 SD from the baseline LSL. The left *open circle* shows the first ISI when the LSL deviated by > 1 SD from baseline (T_1 = -7 ms) and the LSL remained deviated by > 1 SD from baseline across all ISIs tested. *Crossed circles* show the 10 longest ISIs when the BD tone preceded the NE tone, and these data points were used to calculate the mean ± SD baseline (B) spike count, (C) FSL, and (D) LSL. n = 10 trials per stimulus.

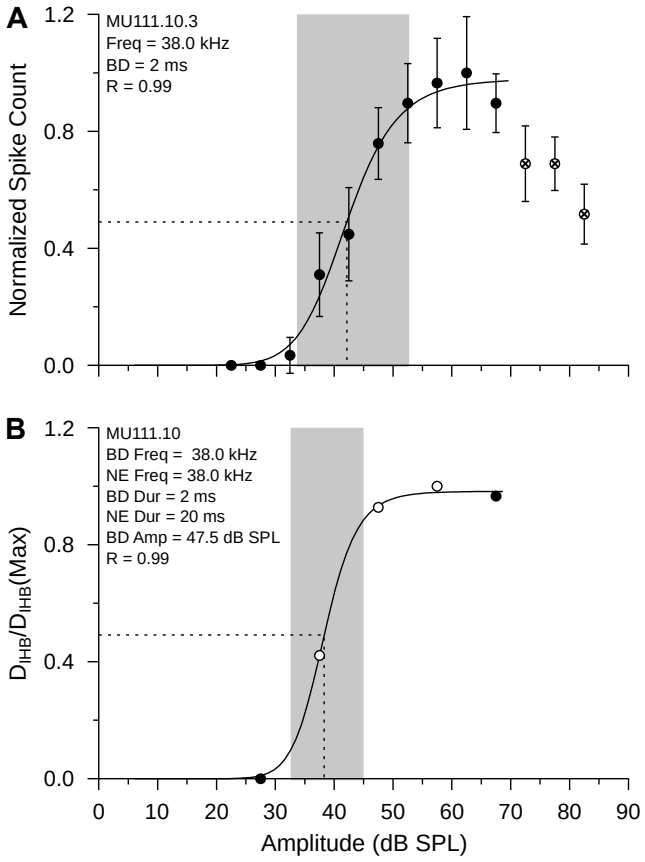

Figure 3.3. Modelling excitatory and inhibitory input-output (I/O) functions in DTNs. A 3-parameter logistic function was used to model an **excitatory and inhibitory** I/O function (*black line*). (A) Normalized spike counts evoked by BD tones at different SPLs. *Crossed circles* indicate points that were excluded from the logistic regression because they fell below 80% of the maximum response and remained decreased for at least one consecutive point. (B) Normalized duration of inhibition [$D_{IHB}/D_{IHB}(Max)$] measured with paired-tone stimulation at different NE tone amplitude, with the three standardized NE tone amplitudes (0, +10, and +20 dB re BD tone threshold) illustrated (*open circles*). The *grey box* illustrates the 10-90% dynamic range of each I/O function. The *dashed lines* indicate the 50% inflection points of each function, which were used to estimate the excitatory half-

maximal SPL ($ESPL_{50}$ = 42.14 dB SPL) from the rate-level function, and the inhibitory half-maximal SPL($ISPL_{50}$ = 38.31 dB SPL) from the suppression-level function. n = 10 trials per stimulus in A, B.

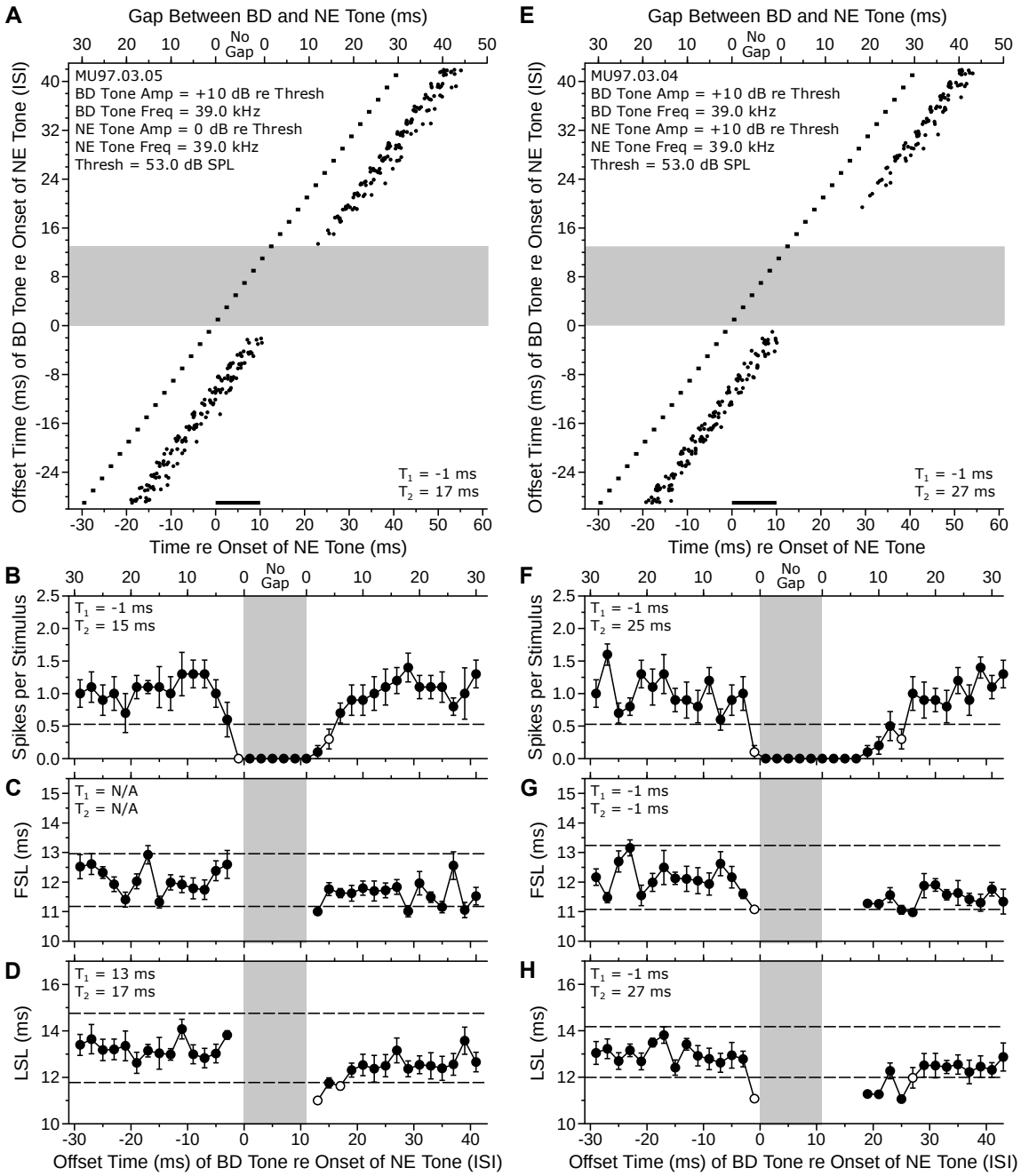

Figure 3.4. Inhibition evoked with the NE tone at 0 dB and +10 dB.

Dot raster displays demonstrate spiking responses from a short-pass DTN tested with paired-tone stimulation, with the 1-ms BD tone presented at +10 dB and the 10-ms NE tone

presented at 0 dB and +10 dB re BD tone threshold. Data points with *crossed circles* show the 10 longest ISIs used to calculate the mean ± SD baseline (B,F) spike count, (C,G) FSL, and (D,H) LSL. A: When the NE tone was presented at 0 dB (re BD tone threshold), spiking was suppressed by the NE tone-evoked inhibition when the two tones were sufficiently close in time. B: Mean ± SE spikes per stimulus as a function of the ISI between the BD and NE tones. The shortest ISI with a spike count < 50% of the baseline count (*dashed line*) was T_1 = -1 ms (leftmost *open circle*). The longest ISI, starting from T_1, with a spike count < 50% of the baseline count was T_2 = 15 ms (rightmost *open circle*). C: Mean ± SE FSL as a function of the ISI between the BD and NE tones. The values of T_1 or T_2 could not be measured because the FSL never deviated by > 1 SD from baseline (*dashed lines*). D: Mean ± SE LSL as a function of the ISI between the BD and NE tones. The shortest ISI when the LSL deviated by > 1 SD from baseline (*dashed lines*) was T_1 = 13 ms (leftmost *open circle*), and the longest ISI when the LSL remained deviated by > 1 SD from baseline was T_2 = 17 ms. When the NE tone was presented at 0 dB (re BD tone threshold; A-D), the final T_1 value (T_1 = -1 ms) was calculated with a spike count criterion and the final T_2 value (T_2 = 17 ms) was calculated with a LSL criterion. The onset of inhibition preceded the excitatory FSL by 0.83 ms, and the inhibition persisted 6.83 ms longer than the duration of the NE tone. E: When the BD and NE tones were both presented at +10 dB re BD tone threshold, strong spike suppression was observed when the 1-ms BD tone and 10-ms NE tone were sufficiently close in time. F: Mean ± SE spikes per stimulus as a function of the ISI between the BD and NE tones. NE tone-evoked inhibition led to a reduction in spike count, and the effective duration of spike suppression was longer. G: Mean ± SE FSL as a

function of the ISI between the BD and NE tones. The shortest and longest ISIs in which the FSL deviated by > 1 SD from the baseline FSL was $T_1 = T_2 = -1$ ms. H: Mean ± SE LSL as a function of the ISI between the BD and NE tones. Deviations in LSL were also detected and the effective duration of the altered response was longer. When the NE tone was presented at the same amplitude as the BD tone (E-H), the final T_1 value ($T_1 = -1$ ms) could be determined by all three criteria and the final T_2 value ($T_2 = 27$ ms) was obtained with a LSL criterion. Also, in this condition the onset of the NE tone-evoked inhibition preceded the excitatory FSL by 1.10 ms, and the duration of inhibition persisted 17.10 ms longer than the duration of the NE tone. n = 10 trials per stimulus.

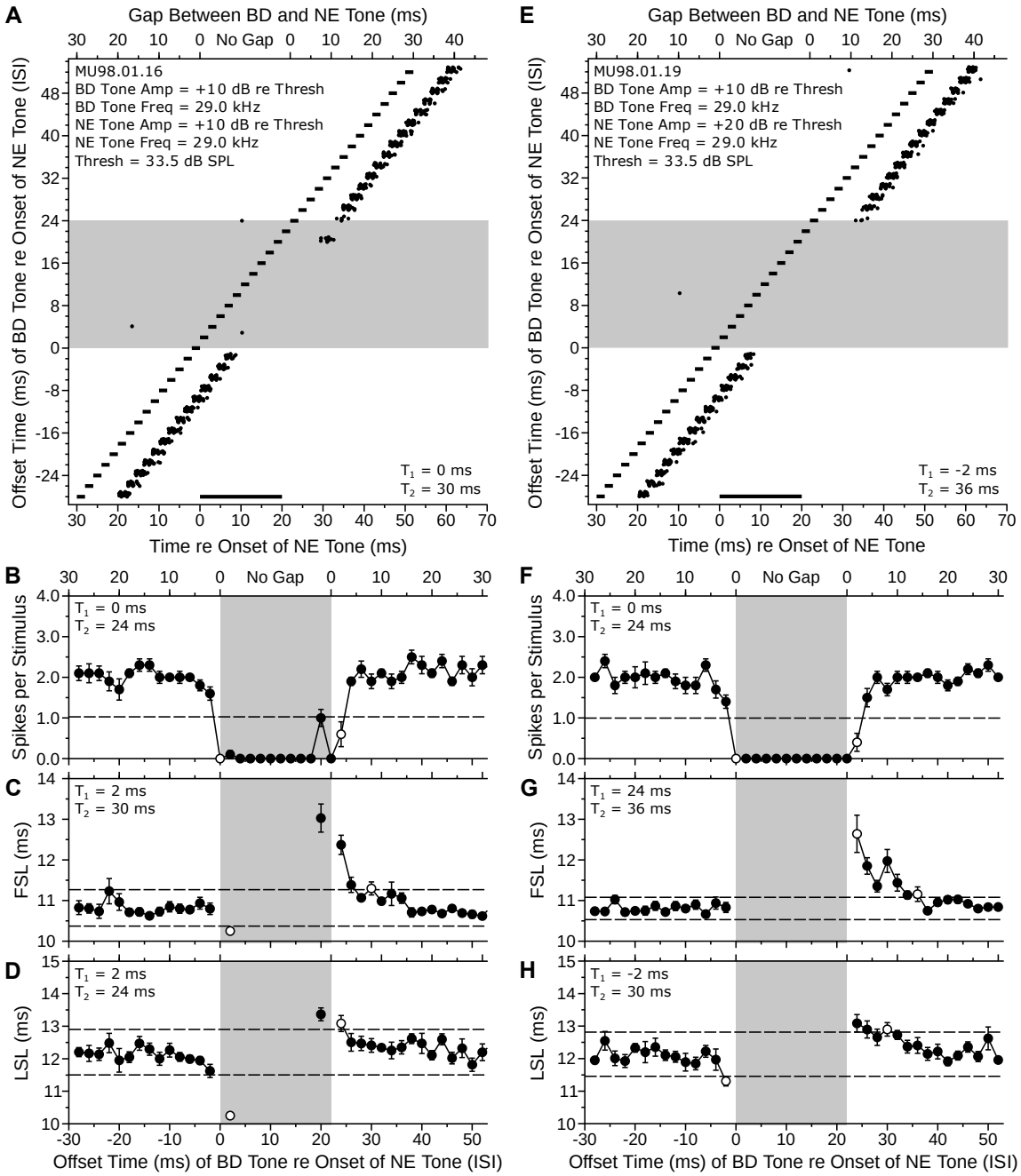

Figure 3.5. Inhibition evoked with the NE tone at +10 dB and +20 dB.

Dot raster displays demonstrate spiking responses from a short-pass DTN tested with paired-tone stimulation, with the 2-ms BD tone presented at +10 dB and the NE tone

presented at +10 dB and +20 dB re BD tone threshold. Data points with *crossed circles* show the 10 longest ISIs used to calculate the mean ± SD baseline (B,F) spike count, (C,G) FSL, and (D,H) LSL. A: When the BD and NE tones were both presented at +10 dB (re BD tone threshold), spiking was suppressed by the NE tone-evoked inhibition when the two tones were sufficiently close in time. B: Mean ± SE spikes per stimulus as a function of the ISI between the BD and NE tones. T_1 = 0 ms (leftmost *open circle*) and T_2 = 24 ms (rightmost *open circle*). C: Mean ± SE FSL as a function of the ISI between the BD and NE tones. T_1 = 2 ms (leftmost *open circle*) and T_2 = 30 ms (rightmost *open circle*). D: Mean ± SE LSL as a function of the ISI between the BD and NE tones. T_1 = 2 ms (leftmost *open circle*) and T_2 = 24 ms (rightmost *open circle*). When the NE tone was presented at the same amplitude as the BD tone (A-D), the final T_1 value (T_1 = 0 ms) was calculated with a spike count criterion and the final T_2 value (T_2 = 30 ms) was calculated with a FSL criterion. The onset of inhibition preceded the excitatory FSL by 0.62 ms, and the inhibition persisted 8.62 ms longer than the duration of the NE tone. E: When the NE tone was presented at +20 dB (re BD tone threshold), strong spike suppression was observed when the 2-ms BD tone and 20-ms NE tone were sufficiently close in time. F: Mean ± SE spikes per stimulus as a function of the ISI between the BD and NE tones. The effective duration of spike suppression was the same as in the +10 dB condition. G: Mean ± SE FSL as a function of the ISI between the BD and NE tones. Deviations in FSL were detected and T_2 was larger. H: Mean ± SE LSL as a function of the ISI between the BD and NE tones. Deviations in LSL were also detected and the effective duration of the altered response was longer. When the NE tone was presented at +20 dB re BD tone threshold (E-H), the final

T_1 value (T_1 = -2 ms) was obtained with a LSL criterion and the final T_2 value (T_2 = 36 ms) was obtained with a FSL criterion. The onset of the NE tone-evoked inhibition preceded the excitatory FSL by 2.66 ms, and the duration of inhibition persisted 16.66 ms longer than the duration of the NE tone. n = 10 trials per stimulus.

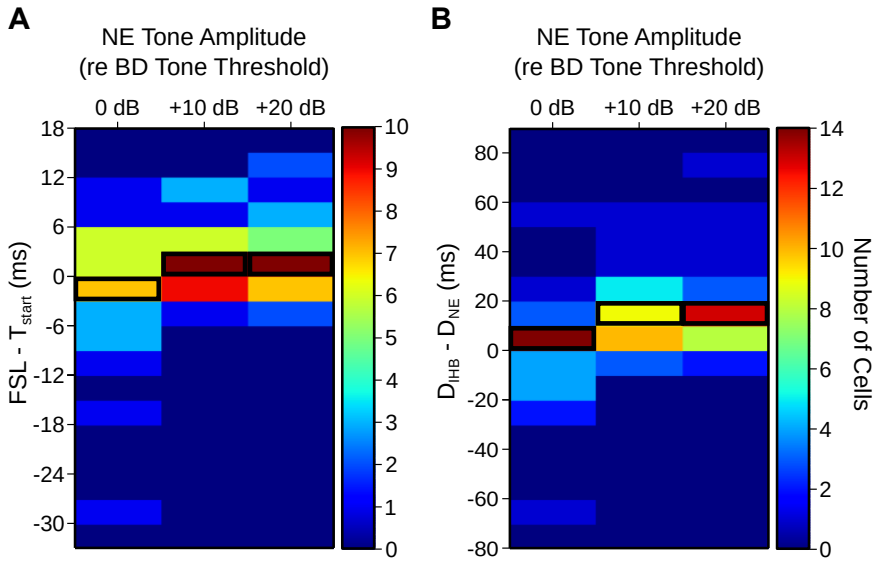

Figure 3.6. Onset and duration of inhibition at 3 standardized NE tone amplitudes.

Two-dimensional histograms show the distributions of the durations of leading/lagging inhibition and persistent inhibition in DTNs tested with paired tone stimulation at 3 standardized NE tone amplitudes: 0, +10, and +20 dB (re BD tone threshold). Mean value of each column shown by a *black box*, with the *colour scale* defining the number of cells per bin. A: Distribution of the difference between FSL and latency of NE tone-evoked inhibition (FSL - T_{start}). Cells with a positive difference have leading inhibition; cells with a negative difference have lagging inhibition. There was a significant increase in the duration of leading inhibition from 0 dB to +20 dB, but not between 0 dB and +10 dB or +10 dB and + 20 dB (see Table 3.1 for statistics). B: Distribution of the difference between the duration of inhibition evoked by the NE tone and the NE tone duration (D_{IHB} - D_{NE}). Cells with a positive difference have persistent inhibition; cells with a negative difference have inhibition that lasts shorter than the duration of the NE tone that evoked it. Duration

of inhibition increased significantly from 0 dB to +10 dB but was constant between +10 dB and +20 dB (see Table 3.2 for statistics). n = 30 cells.

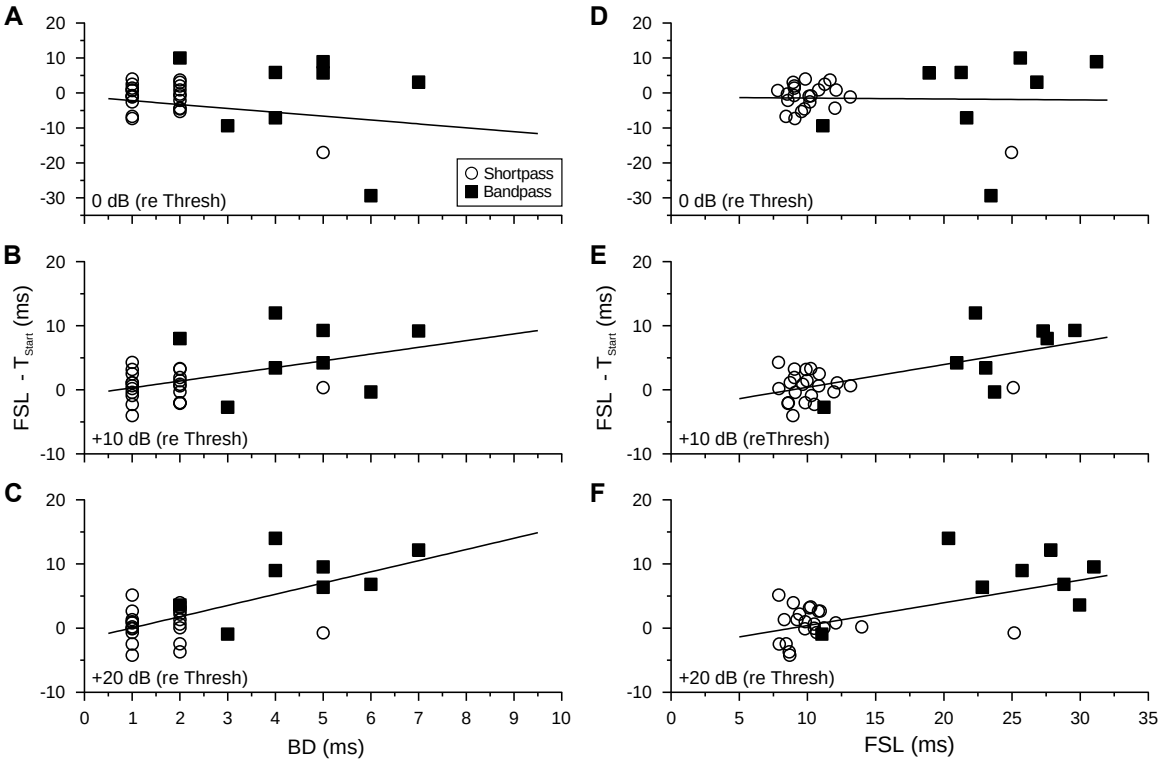

Figure 3.7. Relation of onset of inhibition to BD, FSL, and duration class filter.

Plots show onset of inhibition measured with paired tone stimulation at 3 standardized NE tone amplitudes in short-pass and band-pass DTNs. A: No correlation was observed between the onset of inhibition and BD when the NE tone amplitude was at 0 dB (re BD tone threshold). The duration of leading inhibition increased in cells with longer BDs when the NE tone amplitude was at (B) +10 dB and (C) +20 dB (re BD tone threshold). D: No correlation was observed between the onset of inhibition and FSL when the NE tone amplitude was at 0 dB; however, the duration of leading inhibition increased in DTNs with longer FSLs when the NE tone amplitude was increased to (E) +10 dB, and (F) +20 dB re BD tone threshold. In general, short-pass DTNs had less leading inhibition than band-pass

DTNs, but the relationship was significant only when the NE tone amplitude was at +20 dB (re BD tone threshold). Regression equations, correlation coefficients (R), and p-values for each regression are listed in Table 3.3. n = 30 cells.

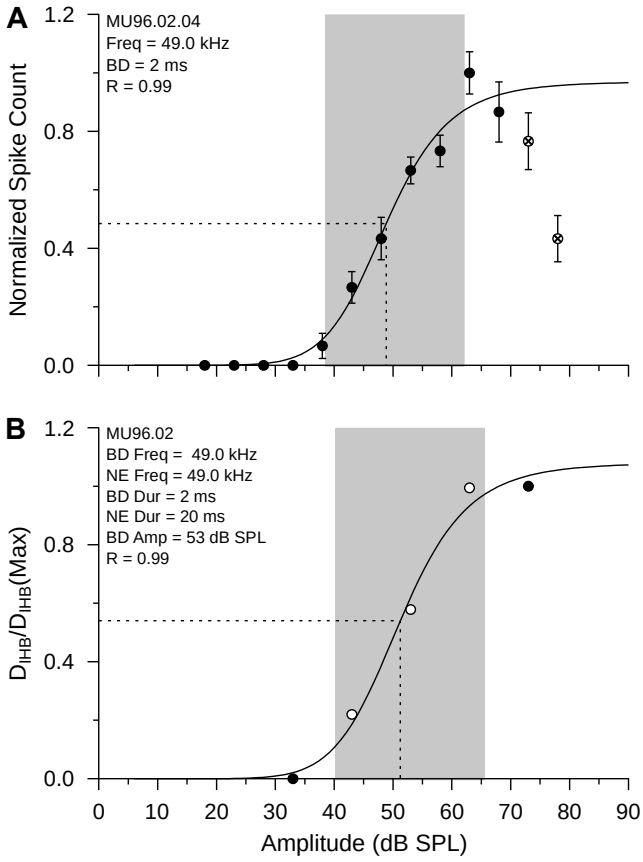

Figure 3.8. Excitatory and inhibitory I/O functions in a short-pass DTN.

Three-parameter logistic function model fit to an excitatory rate-level function, and an inhibitory suppression-level function measured with paired-tone stimulation. A: Normalized mean ± SE spikes per stimulus as a function BD tone amplitude. The fitted model is shown as a *black line*. *Crossed circles* indicate points that were excluded from regression. The excitatory half-maximum SPL ($ESPL_{50}$), measured from inflection point (*dashed lines*), was 48.86 dB SPL. B: Normalized duration of inhibition [$D_{IHB}/D_{IHB}(Max)$] as a function of NE tone amplitude. For reference, the three standardized NE tone amplitudes are also illustrated as *open circles*. The inhibitory half-maximum SPL ($ISPL_{50}$),

measured from inflection point (*dashed lines*), was 51.25 dB SPL. In both panels the 10-90% dynamic range for each I/O function is illustrated as a *grey box*. n = 10 trials per stimulus in A, B.

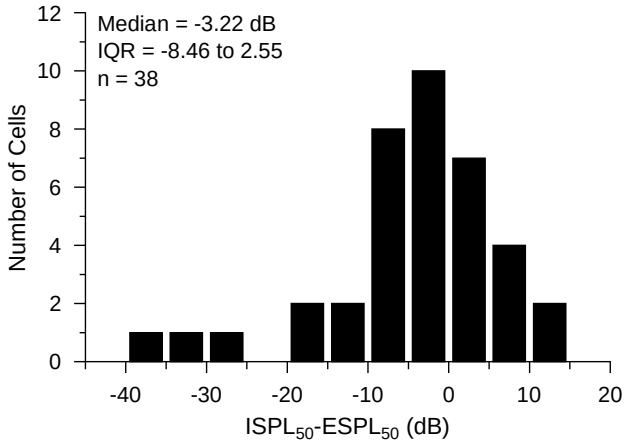

Figure 3.9. Difference between the inhibitory half-maximum SPL and excitatory half-maximum SPL ($ISPL_{50} – ESPL_{50}$).

The distribution differed significantly from a value of zero, therefore $ISPL_{50}$ was lower than $ESPL_{50}$. Bin width = 5 dB. n = 38 cells.

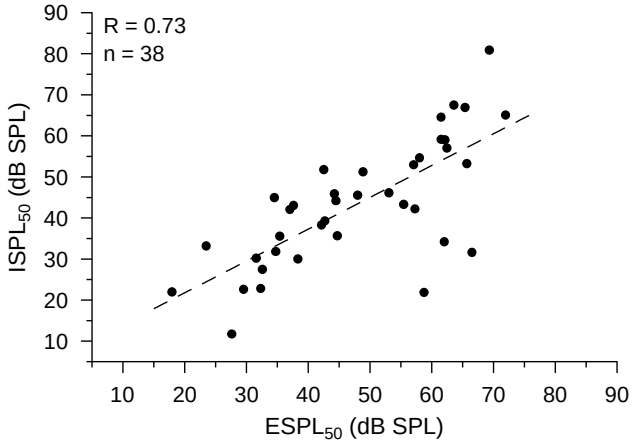

Figure 3.10. Relationship between the inhibitory half-maximum SPL (ISPL50) and excitatory half-maximum SPL (ESPL50).

Data were estimated from the 50% inflection point of a 3-parameter logistic function fit to excitatory rate-level functions and inhibitory suppression-level responses functions. The slope of the line was 0.775 and the y-intercept was 6.276. There was a strong, positive correlation between $ISPL_{50}$ and $ESPL_{50}$.

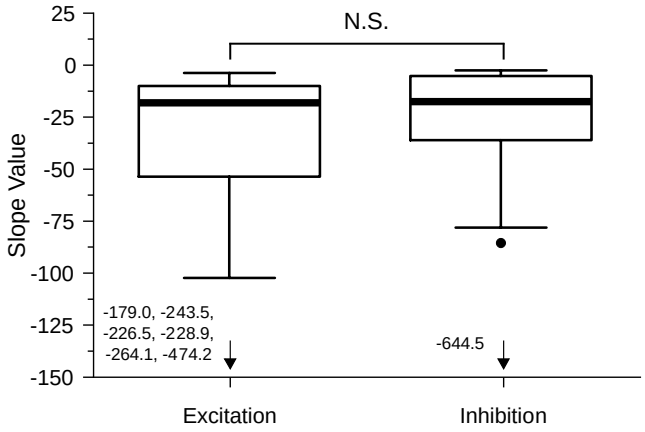

Figure 3.11. Comparison of excitatory and inhibitory response-level slopes.

Box plots illustrate the median (bold line in box), 25th and 75th percentiles (edges of box), and interquartile range (IQR, height of box) of slope values obtained from the modeled logistic regressions of excitatory rate-level functions and inhibitory suppression-level functions from 38 DTNs (see Fig. 3.8). The IQR is defined as the 75th percentile minus the 25th percentile. The whiskers were calculated with the Tukey method; the top whisker indicates the largest value less than the sum of the 75th percentile plus 1.5 times the IQR, while the bottom whisker represents the difference of the smallest value greater than the 25th percentile minus 1.5 times the IQR. Data points falling outside of these ranges are illustrated as *black circles* or their *y-values* are shown in parentheses. There was no difference between excitatory and inhibitory logistic function slope values. N.S. = Not significant.

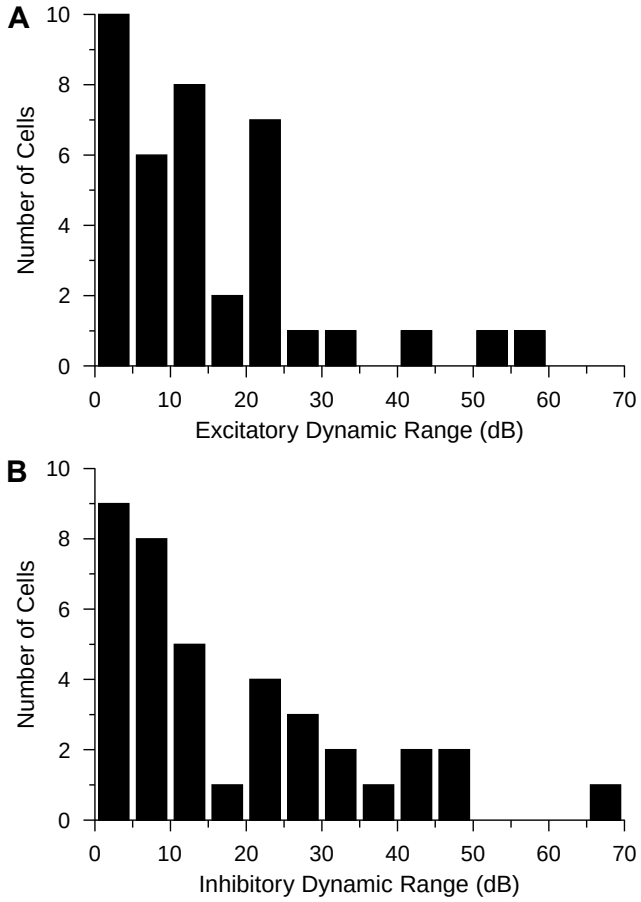

Figure 3.12. Distribution of excitatory and inhibitory amplitude dynamic ranges.

Dynamic range measured from modeled logistic regressions of (A) excitatory rate-level functions, and (B) inhibitory suppression-level functions. Dynamic range defined as SPL between 10% to 90% of maximum asymptote. The dynamic ranges measured from excitatory rate-level functions and inhibitory suppression-level functions were not significantly different. Bin width = 5 dB. n=38 cells.

Table 3.1.

Duration of leading inhibition as a function of NE tone amplitude. The proportion of DTNs exhibiting leading inhibition increased across the three standardized NE tone amplitudes. Also shown are Nemenyi post-hoc pairwise comparisons on the duration of leading inhibition at each NE tone amplitude.

NE Tone Amplitude (re Thresh)	% DTNs with Leading Inhibition*	Pairwise Comparisons of Duration of Leading Inhibition**		
		0 dB (re Thresh.)	+10 dB (re Thresh.)	+20 dB (re Thresh.)
0 dB	46.7			
+10 dB	66.7	0.167		
+20 dB	70.0	**0.013**	0.556	

Statistically significant differences indicated in **boldface**.
Cochran Q-test, $X^2(2) = 8.60$, $p = 0.016$, $n = 30$.
**Friedman test, $X^2(2) = 1.867$, $p = 0.393$, $n = 30$.

Table 3.2.

Duration of persistent inhibition as a function of NE tone amplitude. The proportion of DTNs exhibiting persistent inhibition increased across the three standardized NE tone amplitudes. Also shown are Nemenyi post-hoc pairwise comparisons on the duration of persistent inhibition at each NE tone amplitude.

NE Tone Amplitude (re Thresh)	% DTNs with Persistent Inhibition*	Pairwise Comparisons of Duration of Persistent Inhibition**		
		0 dB (re Thresh.)	+10 dB (re Thresh.)	+20 dB (re Thresh.)
0 dB	63.3			
+10 dB	90.0	**0.0014**		
+20 dB	93.3	**2.50×10^{-6}**	0.597	

Statistically significant differences indicated in **boldface**.
*Cochran Q-test, $\chi^2(2) = 11.231$, $p = 0.004$, $n = 30$.
**Friedman test, $\chi^2(2) = 22.134$, $p = 1.56 \times 10^{-5}$, $n = 30$.

Table 3.3.

Relation between the duration of leading inhibition and BD or FSL. Shown are the slope, intercept, R, and p-values for the linear relationships between the duration of leading inhibition (FSL – T_{start}) and BD or FSL at the 3 standardized NE tone amplitudes.

Comparison	Amplitude (re Thresh)	Slope	Intercept	R	p-value
FSL – T_{start} (ms) vs. BD (ms)	0 dB	-1.1079	1.10914	0.2446	0.1927
	+10 dB	1.0498	-0.7232	0.4672	**0.0092**
	+20 dB	1.7466	-1.7062	0.6705	**5.0×10^{-5}**
FSL – T_{start} (ms) vs. FSL (ms)	0 dB	-0.0258	-1.2107	0.0228	0.9047
	+10 dB	0.3545	3.1416	0.6534	**9.1×10^{-5}**
	+20 dB	0.3786	2.9524	0.6635	**6.4×10^{-5}**

Statistically significant correlations indicated in **boldface**.

Table 3.4.

Duration of leading inhibition in short-pass and band-pass DTNs. Shown are the results of Mann-Whitney U-tests comparing the duration of leading inhibition (FSL – T_{start}) in short-pass (n = 22) and band-pass (n = 8) DTNs at the 3 standardized NE tone amplitudes.

Amplitude (re Thresh)	Duration Filter Class	Median, [IQR], ms	U	p-value
0 dB	Short-pass	-0.78, [-4.40 to 1.55]	65	0.281
	Band-pass	4.41, [-8.81 to 8.17]		
+10 dB	Short-pass	0.63, [-1.17 to 2.08]	38	**0.018**
	Band-pass	6.11, [0.61 to 9.26]		
+20 dB	Short-pass	0.78, [-0.71 to 2.65]	20	**0.001**
	Band-pass	7.90, [4.30 to 11.53]		

Statistically significant comparisons indicated in **boldface**.

Table 3.5.

Characterization of excitatory and inhibitory response functions in DTNs. Amplitude response functions measured from excitatory (rate-level response functions) and inhibitory (suppression-level response function) data were classified as monotonic, non-monotonic. n = 38 DTNs. See methods for definitions.

	Excitatory	Inhibitory
Monotonic	15	32
Non-monotonic	23	6
McNemar Test, χ = 11.130, p = 4.88×10^{-4}		

Chapter 4 – Response Properties of Offset Facilitation in Duration-Tuned Neurons

4.1 – Abstract

Duration-tuned neurons (DTNs) are created through the convergence and temporal interaction of excitatory and inhibitory synaptic inputs that are offset in time. Previous studies have used paired tone stimulation to measure the strength and time course of the synaptic inhibition acting on DTNs by randomly varying the onset time of a short, best duration (BD), excitatory probe tone relative to the onset of a longer duration, non-excitatory (NE) suppressor tone and noting when BD tone-evoked spikes were suppressed. Here we describe the properties of an offset-evoked, facilitation in spiking observed as a transient increase in the BD tone-evoked response during or following NE tone suppression. Conceptual models of duration tuning suggest the mechanism of spike facilitation is an offset-evoked, excitation to the cell, caused by either a separate excitatory synaptic input or post-excitatory rebound from sustained inhibition. We used paired tone stimulation and extracellular recording in the inferior colliculus of the big brown bat (*Eptesicus fuscus*) to measure the response properties of this spike facilitation in a population of DTNs. Offset-locked, spike facilitation was observed in 66 of 204 (32.4%) DTNs tested with paired tone stimulation. We observed that facilitation typically occurred before the offset of inhibition. Furthermore, when NE tone amplitude/frequency and/or BD tone amplitude were varied, the latency of facilitation remained relatively constant similar to the onset of inhibition but unlike the offset of inhibition. These data indicate that the mechanism of spike facilitation was a separate excitatory synaptic input and was not caused by post-inhibitory rebound excitation at the offset of inhibition.

4.2 – Introduction

Stimulus duration provides information important for a wide range of auditory animal behaviors, including human speech recognition (Shannon et al., 1995), discrimination of mating vocalizations (Narins and Capranica, 1980), detection of prey/predators (Fremouw et al., 2005) and echolocation by bats (Schnitzler and Kalko, 2001). Within the vertebrate central auditory system there exists a class of cells, called duration-tuned neurons (DTNs), with neurophysiological responses selective for signal duration. That DTNs exist in all vertebrates examined for this response feature, including frogs (Potter, 1965; Gooler and Feng, 1992; Leary et al., 2008), guinea pigs (Wang et al., 2006), chinchillas (Chen 1998), mice (Brand et al., 2000), rats (Pérez-González et al., 2006), cats (He et al., 1997) and bats (Ehrlich et al., 1997; Mora and Kössl, 2004), suggests that duration tuning is an important and highly conserved component of auditory temporal processing.

Single-unit extracellular recordings, intracellular recordings, and neuropharmacological experiments from DTNs suggest that duration selectivity is created *de novo* in the auditory midbrain through the convergence and temporal interaction of excitatory and inhibitory synaptic inputs that are offset in time (Narins and Capranica, 1980; Casseday et al., 1994, 2000; Covey et al., 1996; Ehrlich et al., 1997; Faure et al., 2003; Leary et al., 2008). This evidence has been used to generate conceptual and computational circuit models explaining neural tuning to stimulus duration (e.g. Aubie et al., 2009, 2012). For example, the coincidence detection mechanism of duration tuning (Fig. 4.1) consists of three components: (1) a delayed, transient subthreshold onset evoked excitatory post-synaptic potential (EPSP), (2) a transient subthreshold offset-evoked EPSP,

and (3) a sustained onset-evoked inhibitory post-synaptic potential (IPSP) whose latency is as short or shorter than components (1) or (2), and tracks stimulus duration. In this model, spiking occurs when the onset- and offset-evoked EPSPs (components 1 and 2) coincide to produce a suprathreshold response. When the stimulus duration is too short or too long, the latency of the offset-evoked EPSP (component 2) no longer coincides with the latency of the onset-evoked EPSP (component 1), hence the neuron fails to produce action potentials because that net sum of all post-synaptic potentials remains subthreshold. In the coincidence mechanism of duration tuning, the offset-evoked EPSP (component 2) can arise from a separate excitatory synaptic input or from post-inhibitory rebound excitation (Aubie et al., 2009, 2012; Casseday et al., 2000; Sayegh et al., 2011).

There is increasing evidence for the existence of an offset timing pathway in the mammalian central auditory system (Kopp-Scheinplug et al., 2018). In addition to being offset responding themselves, DTNs are known to receive offset excitation (Covey et al., 1996; Leary et al., 2008). Recordings of DTNs from the bat auditory midbrain occasionally reveal an offset-evoked facilitation in spiking from cells tested with paired tone stimulation. Facilitation often occurs over a transient window and lasting only a few milliseconds during or after long lasting inhibition, ruling out the possibility that it is caused by long lasting excitation (Faure et al. 2003; Sayegh et al., 2014; Valdizón-Rodríguez and Faure 2017). For example, offset-evoked spike facilitation was observed in both short-pass and bandpass neurons tested with this paradigm (Faure et al., 2003). In paired tone stimulation DTNs are presented with a pair of pure tone pulses: a short duration, excitatory probe tone set to the cell's best duration (BD) and best excitatory frequency

(BEF), and a longer duration, non-excitatory (NE) suppressor tone typically of the same frequency and amplitude (Fig. 4.2A). By varying the interstimulus interval (ISI) of the tone pair and measuring the range of ISIs over which BD tone-evoked spikes become suppressed and/or facilitated, it is possible to measure the time course of neural inhibition and/or spike facilitation (Fig. 4.2B).

Assuming an offset-evoked excitation underlies the mechanism of duration tuning, then a facilitation in spiking in response to the BD tone should be observed at ISIs near the offset of the NE tone (Fig. 4.2B). This excitatory event could either break though the cell's long lasting inhibition or immediately follow it as illustrated in Fig. 4.2B. The purpose of this study was to examine properties of the offset-evoked facilitation in spiking in DTNs tested with paired tone stimulation. Our goal was to disambiguate whether the offset-evoked facilitation was caused by an explicit excitatory synaptic input or if it resulted from post-inhibitory rebound excitation. However, it should be noted that not all DTNs show clear evidence for an offset evoked excitation; these cells have often been thought to be produced by anti-coincidence mechanism first proposed by Fuzessery and Hall in 1999 – with an increasing body of evidence (Leary et al., 2008; Alluri et al., 2016). Offset-evoked, spike facilitation was observed in 66 of 204 (32.4%) DTNs tested with paired tone stimulation. The latency of facilitation (re NE tone onset), typically occurred before the offset of inhibition and changes in the latency of facilitation were more related to the changes in the onset of inhibition than the offset of inhibition when the NE tone amplitude/frequency and/or BD tone amplitude were varied. These data suggest that spike

facilitation resulted from a separate excitatory synaptic input and was not caused by post-inhibitory rebound excitation.

4.3 – Materials and Methods

Electrophysiological recordings were conducted at the University of Washington (UW) and McMaster University (MU). All procedures were approved by the Laboratory Animal Care and Use Committee (UW) or the Animal Research Ethics Board (MU) and were in accordance with the Guide to the Care and Use of Experimental Animals published by the Canadian Council on Animal Care. Animals at both institutions were housed in outdoor husbandry facilities where lighting and temperature corresponded to ambient, and food and water were available *ad libitum*.

4.3.1 – Surgical Procedures

Neural recordings were obtained from the inferior colliculus (IC) of 52 (25 from UW, 43 from MU) awake big brown bats (*Eptesicus fuscus*) of both sexes. Bats were brought into the laboratory 1 to 3 days prior to surgery to allow animals to acclimatize. Prior to recording, each animal underwent a preparatory surgery in which a small post was glued to the dorsal-anterior portion of the skull. The post prevented movement of the bat's head during recording and ensured replication of head-position between recording sessions. Animals at the UW were anesthetized by a combination of a subcutaneous injection of a neuroleptic [0.3 mL; 1:1 v/v mixture of 0.025 mg/mL fentanyl citrate and 1.25 mg/mL droperidol; 19.1 mg/kg] followed by gaseous inhalation (1–5 min) of Metofane (methoxyflurane) in a bell jar. Bats at MU were anesthetized with a subcutaneous (SQ) injection of buprenorphine (Temgesic; 0.03 mL; 0.025–0.045 mg/kg) followed by inhalation of an isoflurane:oxygen inhalation (1–5%; flow rate = 1–5 L/min) in an induction chamber (12 x 10 x 10 cm; length x width x height). Once anaesthetized, bats were placed

in a foam-lined body restraint within a surgical stereotaxis apparatus (David Kopf Instruments Model 1900). The bat's upper canine teeth were placed into a custom bite bar with a gas mask to allow for continuous delivery of isoflurane, the level of which was adjusted according to the animal's breathing pattern. The hair overlying the skull was shaved and the skin was disinfected with a povidone-iodine (Betadine) surgical scrub. A SQ injection of local anaesthetic (0.05 mL lidocaine, 20 mg/mL at UW; 0.2 mL bupivacaine, 5mg/mL at MU) was administered prior to making a midline incision in the scalp. The exposed temporal muscles were then reflected to reveal the dorsal surface of the skull, which was scraped clean with 70–100% ethanol:water. After drying, a stainless-steel post was glued to the skull with cyanoacrylate gel adhesive (Zap Gel; Pacer Technology) cured with liquid acrylic hardener (Jet Liquid, Lang Dental Manufacturing Company) at UW, or with cyanoacrylate superglue (Henkel Loctite Corporation) and liquid hardener (Zip Kicker; Pacer Technology) at MU. One end of a chlorided silver wire attached to the head post, was placed under the temporal musculature and served as a reference electrode. The wound was covered with a piece of Gelfoam® coated with Polysporin® to prevent infection. Following surgery, bats were housed individually in stainless steel cages (¼-in mesh) located in a temperature and humidity controlled room, and were provided with food and water *ad libidum*

4.3.2 – Electrophysiological Recordings

Neural recordings began 1–2 days after surgery. Each bat was used in 1–8 recording sessions, lasting 4–8 hrs each and conducted on separate days. Neural recordings were terminated if the bat showed any signs of discomfort. Between sessions, the electrode

penetration site was covered with a piece of contact lens and Gelfoam® coated in Polysporin®. Recordings were conducted inside a double-walled, sound attenuation booth with electrical shielding (Industrial Acoustics Co., Inc.). Before recording, bats were given a SQ injection of a neuroleptic (0.3 mL; 1:1 v/v mixture of 0.025 mg/mL fentanyl citrate and 1.25 mg/mL Inapsine [droperidol]; 19.1 mg/kg). Once sedated, bats were placed in a foam lined body restraint that was suspended by springs within a small animal stereotaxic frame customized for bats (ASI Instruments). The entire apparatus was set atop an air vibration table (TMC Micro-G). The bat's head was immobilized by securing the distal portion of the head to a stainless-steel rod attached to a manual micromanipulator (ASI instruments) mounted on the stereotaxic frame (David Kopf Instruments).

The IC can be visually identified as two white ellipses below the translucent skull. A craniotomy was performed with a scalpel blade, and the dura mater over the dorsal portion of the IC was removed with a sharp pin for the insertion of recording electrodes. Single-unit extracellular recordings were obtained with thin-walled, borosilicate glass microelectrodes (outside diameter = 1.2 mm; A-M Systems, Inc.) filled with 0.3-0.5 M (UW) or 1.5 M NaCl (MU). Typical electrode resistances ranged between 15–30 MΩ. Electrodes were positioned over the exposed IC with a manual micromanipulator (ASI Instruments) and advanced into the brain with a stepping hydraulic micropositioner (David Kopf Instruments; model 650 at UW or model 2650 at MU). Action potentials were recorded with a neuroprobe amplifier (A-M Systems model 1600) whose 10x output was bandpass filtered and further amplified (500–1000x) by a Tucker Davis Technologies (TDT) spike pre-conditioner (TDT PC1; lowpass f_c = 7 kHz; high-pass f_c = 300 Hz). Spike

times were logged onto a computer by passing the TDT PC1 output to a spike discriminator (TDT SD1) and then an event timer (TDT ET1) synchronized to a timing generator (TDT TG6).

4.3.3 – Stimulus Generation and Data Collection

Stimulus generation and on-line data collection were controlled with custom software that shows spike-times as dot raster displays ordered by the acoustic parameter that was varied. Stimuli were digitally generated with a two-channel array processor (TDT Apos II; 357 kHz sampling rate) optically interfaced to two digital-to-analog (D/A) converters (TDT DA3-2) whose individual outputs were fed to a low-pass anti-aliasing filter (TDT FT6-2; f_c = 120 kHz), and either one (TDT PA5, MU) or two programmable attenuators (TDT PA4, UW) before being fed to two signal mixers (TDT SM5) with equal weighting, a manual attenuator (Leader LAT-45), and power amplifier (Krohn-Hite model 7500).

Stimuli were presented monaurally with a Brüel & Kjær (B&K) ¼-in condenser microphone (Type 4939; protective grid on), modified for use as a loudspeaker with a transmitting adaptor (B&K Type UA-9020) to correct for nonlinearities in its transfer function. The loudspeaker was positioned ca. 1 mm in front of the external auditory meatus. The output of the speaker, measured with a B&K Type 4138 ⅛-inch condenser microphone (90° incidence; grid off) connected to a measuring amplifier (B&K Type 2606) and bandpass filter (Krone-Hite model 3500), was quantified with a sound calibrator (B&K Type 4231) and expressed in decibels sound pressure level (dB SPL re 20 µPa) equivalent to the peak amplitude of continuous tones of the same carrier frequency. The loudspeaker

transfer function was flat ±6 dB from 28–118 kHz, and there was at least 30 dB attenuation at the ear opposite the source (Ehrlich et al., 1997). All stimuli had rise/fall times of 0.4 ms, shaped with a squared cosine function, and were presented at a rate of 3 Hz.

Search stimuli consisted of two pure tones that differed in duration (typically 1 and 4 ms) with an interstimulus interval (ISI) ≥ 110 ms). Search signals were presented monaurally to the contralateral ear of the IC being recorded. Upon isolating a unit, the cell's best excitatory frequency (BEF; 0.1-1 kHz resolution), BD (1-2 ms resolution), and duration filter class at BEF were determined (Sayegh et al., 2011). Duration selective neurons can be categorized into at least three duration filter response classes, depending on the relative number of spikes evoked across all stimulus durations. In this study, we focused exclusively on the responses of short-pass and bandpass DTNs (Fig. 4.3). Short-pass DTNs respond maximally at BD with spike counts dropping to ≤50% of the peak in response to stimulus durations that are longer, but not shorter, than BD. Band-pass DTNs also respond maximally at BD with spike counts dropping to ≤50% of the peak in response to stimulus durations both shorter and longer than BD.

Using BEF and BD stimuli, we measured a cell's minimum acoustic threshold (dB SPL; 5 dB resolution) and excitatory rate-level function. By varying the BD tone frequency we measured each cell's frequency response area at +10 dB re threshold to determine its excitatory spectral tuning bandwidth (eBW), defined as the lowest and highest frequencies eliciting ≥50% of the maximum spike count at the BEF.

4.3.4 – Paired Tone Stimulation

We used paired tone stimulation to measure the strength and time course of spike suppression and/or spike facilitation. The paradigm consisted of stimulating a cell with a pair of pure tone pulses that differed in duration and ISI (Faure et al., 2003). The BD tone was set to the cell's BD and BEF to evoke maximal excitation. The NE tone was set to a non-excitatory duration that was typically ten times the duration of the BD tone. We did this to ensure that the NE tone would be non-excitatory and to keep a constant energy relationship between the two signals, regardless of each cell's actual BD. The onset time of the NE tone was fixed between stimulus presentations, while the onset time of the BD tone was randomly varied in 2-4 ms steps so that it preceded, overlapped with, and followed the NE tone. The two tones were electronically mixed and presented to the contralateral ear at +10 dB re minimum acoustic threshold. The BD and NE tones were matched in starting phase and could constructively or destructively interfere when they overlapped. When the BD and NE tones were matched in frequency and amplitude the two signals always constructively interfered, resulting in a composite signal with an amplitude pedestal of +6 dB for the duration of overlap. When the BD and NE tone frequencies were not matched, the resultant signal contained an amplitude pedestal that was sinusoidally amplitude modulated with a modulation index = 1.

To quantify offset-evoked spike facilitation, cells were tested with monotic (contralateral ear) paired tone stimulation with BD and NE tones set to the same frequency (i.e. BEF) and amplitude (i.e. +10 dB re BD tone threshold). In a subset of cells, we varied the duration, amplitude, and/or frequency of the NE tone. The NE tone duration was varied

in integer multiples (5–35) of the BD tone, the NE tone amplitude was varied between 5-10 dB steps, and the NE tone frequency was presented between 15 – 85 kHz. In a subset of cells the BD tone amplitude was varied in 3-10 dB steps. Some cells were tested with dichotic paired-tone stimulation, with the NE tone presented to the ipsilateral ear and the BD tone presented to the contralateral ear (re IC being recorded).

4.3.5 – Measuring the Time Course of Inhibition

We measured the duration and latency of the inhibition evoked by the NE tone by observing time points when BD tone-evoked spikes became suppressed and/or altered in latency using the same criteria as Sayegh et al. (2014). To measure the time-course of the NE tone-evoked inhibition, we first quantified the cell's baseline response evoked by the BD tone at the ten longest ISI's when the BD tone preceded the NE tone (see baseline data points in Fig. 4.4). This baseline reflects responses evoked by the BD tone in the absence of inhibition evoked by the NE tone. For each cell, we calculated the mean ± standard deviation (SD) baseline spike count, first spike latency (FSL), and last spike latency (LSL). For the example shortpass DTN in Figure 4.4*A*, baseline spiking was measured from responses falling within the parallelogram. The baseline spike count was 1.70 ± 1.02 spikes per stimulus, the baseline FSL was 13.85 ± 1.19 ms, and the baseline LSL was 16.09 ± 1.40 ms.

Using three criteria, we compared baseline responses with those obtained at each ISI to determine when spike counts and/or latencies became altered by NE tone-evoked inhibition. Using a spike count criterion, spiking was said to be suppressed when the mean spikes per stimulus decreased to ≤50% of baseline. The use of this criterion is depicted in

Figure 4.4*B*; data points below the dashed line, which represents 50% of the baseline spike count, were defined as suppressed. Using a FSL criterion, spiking was said to be altered when the mean FSL deviated by >1 SD from baseline. The use of this criterion is depicted in Figure 4.4*C*; data points falling outside of the area between the two dashed lines, which represent ±1 SD of the baseline FSL, were defined as altered. Finally, using a LSL criterion, spiking was said to be altered when the mean LSL deviated by >1 SD from baseline. The use of this criterion is depicted in Figure 4.4*D*; data points falling outside of the area between the two dashed lines, which represent ±1 SD of the baseline LSL, were defined as altered.

Each criterion yielded a pair of ISI's indicating when a cell's BD tone evoked responses first became suppressed and/or altered in latency due to the presentation of the NE tone, and when the responses had recovered to within baseline. These two time points, representing the onset of spike suppression (T_1) and the offset of spike suppression (T_2), were each calculated from a spike count, FSL, and LSL criterion. The value of T_1 was defined as the shortest ISI, starting from when the BD tone preceded the NE tone and moving toward larger positive ISIs, when the spike count and/or latency became suppressed and/or altered and the next two consecutive ISI's also deviated for a given criterion. The value of T_2 was defined as the shortest ISI, following T_1, when the spike count and/or latency remained suppressed and/or altered and the responses for the next two consecutive ISI's had returned to within baseline values for a given criterion. Ideally, three values of T_1 and T_2 were obtained from changes in the spike count, FSL, and LSL for each cell. For the example cell in Figure 4.4, the values of T_1 and T_2 were -3 ms and 37 ms using

only a spike count criterion, 25 ms and 37 ms using only a FSL criterion, and -5 ms and 37 ms using only a LSL criterion.

The final values of T_1 and T_2 were chosen to be those which were most sensitive in capturing the time course of the suppressed/altered response evoked by the NE tone using either a spike count and/or spike latency criterion. The use of spike counts or spike latencies (or both) to quantify changes in a neuron's responsiveness has previously been validated (Faure et al., 2003; Sayegh et al., 2012, 2014; Valdizón-Rodríguez and Faure 2017). In cases where cells responded with only a single spike per stimulus (i.e. $L_{first} = L_{last}$), a change in spike count was used for selecting T_1 and T_2 because this criterion was more accurate in reflecting the time course of the evoked inhibition. For cells that responded with more than one spike per stimulus (i.e. $L_{first} < L_{last}$) or in cases where the spike count of the cell had recovered to within 50% of baseline even though L_{first} or L_{last} (or both) were still deviated by >1 SD from baseline, a change in spike latency was typically used for selecting T_1 and T_2 because this criterion was more sensitive in reflecting the time course of the evoked inhibition. In cases where the mean spike count or latency had not returned to within 50% or 1 SD of baseline, respectively, over the range of ISIs presented, T_2 was conservatively estimated as the longest ISI tested. For the example cell shown in Figure 4.4, the final value of T_1 was -5 ms and was obtained using a LSL criterion, whereas the final value of T_2 was 37 ms and could be obtained using a spike count, LSL, or FSL criterion. In all instances, the final choice of criterion was confirmed by visual inspection.

The final values T_1 and T_2 were used to calculate the effective start time (T_{start}), end time (T_{end}), and duration of inhibition (D_{IHB}) evoked by the NE tone as:

$$T_{start} = T_1 + L_{last} - D_{BD} ,$$

$$T_{end} = T_2 + L_{first} - D_{BD} , \text{ and}$$

$$D_{IHB} = T_{end} - T_{start} ,$$

where L_{first} was the baseline FSL, L_{last} was the baseline LSL, and D_{BD} was the duration of the BD tone. A DTN was said to have leading inhibition when the onset of inhibition evoked by the NE tone occurred before the FSL (i.e. $T_{start} < L_{first}$), but was said to have lagging inhibition when the onset of NE tone evoked inhibition occurred after the FSL (i.e. $T_{start} > L_{first}$). A DTN was said to have persistent inhibition when D_{IHB} was longer than the NE tone duration (D_{NE}) evoking the suppression (i.e. $D_{IHB} > D_{NE}$). For the example cell shown in Figure 4.4, T_{start} = 8.09 ms, T_{end} = 47.85 ms, and D_{IHB} = 39.76 ms. The cell showed leading inhibition because the latency of inhibition evoked by the NE tone occurred 5.76 ms before the 13.85 ms FSL ($L_{first} - T_{start}$ = 5.76 ms). The cell also showed persistent inhibition because the effective duration of inhibition was 9.76 ms longer than the duration of the 30 ms NE tone ($D_{IHB} - D_{NE}$ = 9.76 ms). Note that this cell also shows spike facilitation at an ISI of 27 ms (Fig. 4.4A transient recovery shown with *blue circles,* and Fig. 4.4B, *blue circle*).

4.3.6 – Measuring the Strength and Time Course of Facilitation

To quantify the strength and latency of facilitation, we observed the time points when the evoked spike count showed a transient increase relative to the (1) suppressed spike count during the effective duration of NE tone-evoked inhibition, or (2) baseline spike count when the facilitation in spiking occurred after the offset of NE tone-evoked

inhibition. In both cases, the facilitation in spiking had to be transient, with spike counts returning to their suppressed or baseline values for both detection criteria. We did this to ensure that the recovery in response after the end of NE tone-evoked inhibition was not counted as spike facilitation. In all cases, the detection of spike facilitation was confirmed by visual inspection.

We divided the ISIs tested with paired tone stimulation into two ranges: Range 1 was defined to detect spike facilitation that occurred between the effective onset (T_1) and offset (T_2) of inhibition evoked by the NE tone, as measured with a spike count criterion. Hence, Range 1 detected facilitation in spiking that occurred during spike suppression by the NE tone. Figure 4.5A shows an example of a bandpass DTN tested with paired tone stimulation. Range 1 can be visualized as the set of ISIs in the *parallelogram* labelled with a *white circle 1*. In Figure 4.5B, Range 1 is the span of ISIs under the *dashed line* with a *white circle 1*. We detected spike facilitation in Range 1 by comparing the evoked spike count at each ISI to the mean + 1 SD spike count calculated from the first 5 trials within Range 1 starting from the onset (T_1) of inhibition (Fig. 4.5B, *five squares*). However, to minimize the possibility of classifying stray spikes as being facilitated, we used a spike count of 0.2 spikes per stimulus as a minimum criterion for classifying facilitation in Range 1. Thus, when the mean + 1 SD spike count in the first five ISIs within Range 1 was $\leq$0.2 spikes per stimulus, a criterion of >0.2 spikes per stimulus was employed instead. For the example cell in Figure 4.5, the mean + 1 SD spike count over the first 5 trials within Range 1 was 0.02 + 0.061 spikes per stimulus = 0.081 spikes per stimulus (Fig. 4.5B). Because this value was <0.2 spikes per stimulus, spike counts were not scored as being facilitated

unless they exceeded >0.2 spikes per stimulus within Range 1 (Figure 4.5B, height of *dashed line 1*).

Range 2 detected spike facilitation that occurred after the effective offset (T_2) of inhibition evoked by the NE tone, as measured with a spike count criterion. Hence, Range 2 detected facilitation in spiking that occurred when responses of the cell were recovering to baseline levels. Figure 4.5A shows Range 2 as the set of ISIs in the *parallelogram* labelled with a *white circle 2,* while Figure 4.5B shows Range 2 as the span of ISIs under the *dashed line* with a *white circle 2*. The criterion for detecting spike facilitation in Range 2 was the mean + 1 SD baseline spike count at the 10 longest ISIs when the BD tone preceded the NE tone (Figure 4.5B, *crossed circles*). For the example cell in Figure 4.5A and B, the mean + 1 SD baseline spike count was 1.26 + 0.896 spikes per stimulus, and this yielded a spike facilitation detection criterion of 2.156 spikes per stimulus. Thus, spike facilitation was detected whenever spike counts in Range 2 exceed 2.156 spikes per stimulus (Figure 4.5B, height of *dashed line 1*).

To find the effective onset (F_1) and offset (F_2) times of spike facilitation and time of maximum facilitation (F_{Max}), we compared the evoked spike count at each ISI within Range 1 and Range 2 with its detection criterion value. Spike counts were said to be facilitated when the mean count at a given ISI exceeded its corresponding detection criterion. We defined F_1 as the shortest positive ISI to become deviated above its criterion. We defined F_2 as the longest positive consecutive ISI, following F_1, that remained deviated above its criterion. Finally, we defined F_{Max} as the ISI with the highest spike count between F_1 and F_2. For the example DTN shown in Figure 4.5A and B, spike facilitation was

detected in Range 1. The onset of facilitation was at F_1 = 29 ms, the offset of facilitation was at F_2 = 31 ms, and the peak facilitation was 0.7 spikes per stimulus at F_{Max} = 29 ms.

Figure 4.5 C and D shows an example shortpass DTN where a facilitation in spiking was detected in Range 2 after the offset of NE tone evoked inhibition. The mean + 1 SD spike count over the first five ISIs within Range 1 was 0.04 + 0.084 = 0.124 spikes per stimulus. Because 0.124 was <0.2 spikes per stimulus, a value of > 0.2 spikes per stimulus was used as the criterion to detect spike facilitation. Consequently, no spike facilitation was detected within Range 1 (Fig. 4.5C, *parallelogram 1*; Fig. 4.5D, *dashed line 1*). The cell's mean ± SD baseline spike count at the 10 longest ISI's when the BD tone preceded the NE tone (*crossed circles* in Fig. 4.5C) was 2.01 + 0.719 spikes per stimulus, yielding a spike facilitation detection criterion of 2.729 spikes per stimulus within Range 2 (Fig. 4.5D, *dashed line 2*). The first ISI with a spike count above this criterion within Range 2 was F_1 = 13 ms. This was also the last consecutive ISI with a spike count above this criterion (i.e. F_2 = 13 ms). Correspondingly, the peak facilitated spike count between F_1 and F_2 was also at F_{Max} = 13 ms and was 3.2 spikes per stimulus.

The value of F_1 was also used to measure the effective latency of spike facilitation (F_{start}) as the average FSL relative to the onset of the NE Tone. For the example cell in Fig. 4.5A and B, F_{start} = 44.06 ms, and for the example cell in Fig. 4.5 C and D, F_{start} = 22.89 ms.

4.3.7 – Comparing the Timing of Facilitation to the Onset and Offset of Inhibition

For each cell, we assessed whether F_{start} was related to changes in T_{start} or T_{end} by measuring their time of occurrence as a function of NE tone amplitude, BD tone amplitude, and/or NE tone frequency with the equations:

$$\delta_{start} = \frac{\sum_{i=1}^{n} \left| \left(T_{start(i)} - \overline{T}_{start} \right) - \left(F_{start(i)} - \overline{F}_{start} \right) \right|}{n}$$

$$\delta_{end} = \frac{\sum_{i=1}^{n} \left| \left(T_{end(i)} - \overline{T}_{end} \right) - \left(F_{start(i)} - \overline{F}_{start} \right) \right|}{n}$$

where n is the number of values in a given parameter (i.e. the number of NE tone amplitudes, or BD tone amplitudes, or NE tone frequencies measured), i is the index of summation (starts at 1 and goes to n), $\overline{T}_{start}$ is the mean onset of inhibition, $\overline{T}_{end}$ is the mean offset of inhibition, and $\overline{F}_{start}$ is the mean latency of facilitation. The variables δ_{start} and δ_{end} measure how closely changes in F_{start} followed changes in T_{start} or T_{end}, relative to each of their respective means. A smaller δ_{start} compared to δ_{end} indicates that F_{start} was more strongly correlated to T_{start}, whereas a larger δ_{start} compared to δ_{end} indicates that F_{start} was more strongly correlated to T_{end} as a given stimulus property was varied.

4.3.8 – Disambiguating the Source of Offset Facilitation

To disambiguate whether the facilitation in spiking during paired tone stimulation was caused by post-inhibitory rebound excitation or by a separate excitatory synaptic input to DTNs, we conducted a linear regression on the strength of spike facilitation or its latency (F_{start}) as a function of NE tone amplitude, BD tone amplitude, and/or NE tone frequency.

These regressions produced slope values that represented the linear change in the average spike count or latency of facilitation (F_{start}) per unit change in NE tone amplitude, BD tone amplitude, and/or NE tone frequency. For a subset of cells, multiple slope values were obtained as a function of NE tone amplitude, BD tone amplitude, and/or NE tone frequency because these cells were tested in combination with variations in other stimulus properties. When this occurred, all slope values calculated for a given cell were included in our analysis.

For cells tested with paired tone stimulation with a changing NE tone frequency, the range of test frequencies was divided into lower and higher partitions relative to the BEF. A linear regression was performed separately on the lower and higher partitions for each cell to represent the change in the average spike count during facilitation or F_{start} as the NE tone frequency moved below and above the BEF, respectively. Because slope values calculated from the lower frequency partition were opposite in sign, they were multiplied by -1 to make them directly comparable to the slope values calculated from the higher frequency partition.

4.3.9 – Statistical Analyses

Unless otherwise stated, all data are reported as the mean ± SD. Chi-squared tests were used to determine if the proportion of cells showing facilitation in our population of DTNs differed from that reported in Faure et al., 2003, and if the proportion cells showing facilitation differed between MU and UW. Chi-squared tests were also used to test whether there was a difference in the number of cells in Range 1 and Range 2. Linear regressions were used to evaluate the relationship between F_{start} and NE tone duration – for each

observation from each cell – to determine if F_{start} in a given cell was locked to stimulus offset; a one-sample t-test was used to determine if the slope values generated from the population of cells differed from a slope = 1.0 $ms_{Fstart}/ms_{NE\text{-}Tone}$. A paired samples t-test was used to compare the difference between the two sets of mean difference scores, δ_{start} and δ_{end}. A Chi-squared test was used to determine whether the proportion of observations showing facilitation in either monotic condition, the dichotic condition, or both was different from chance. A Chi-squared test was used to determine whether the proportion of cells showing inhibition in the dichotic condition was different than the proportion reported by Sayegh *et al.* (2014). For observations that showed inhibition in the dichotic condition, a binomial test was used to determine if the proportion of observations with facilitation was different from a chance value of 50%. Linear regressions were performed between F_{start} and baseline FSL, BD, and leading inhibition. Linear regression was also used to measure the relationship between spike count at F_{Max} OR the onset of facilitation (F_{start}) and one of the following stimulus properties for each cell: NE tone amplitude, BD tone amplitude, and NE tone frequency; one-sample t-tests were performed on these slope values to test whether they were different from zero; chi-squared tests were used determine if the number of slopes above or below zero was significantly different from chance. A Linear regression was performed between F_{start} (re BD tone onset) and the baseline FSL and two more regressions were calculated on this data when datapoints were split by whether they occurred in Range 1 or Range 2. Linear regressions were performed between baseline FSL and BD, and baseline FSL and leading inhibition. An ANCOVA evaluated whether the

mean F_{start} (re BD tone onset) was equal between cells occurring in Range 1 or Range 2, after controlling for the effect of other the covariate – baseline FSL.

All statistical tests were performed in IBM SPSS or R and used a test-wise type I error rate of $\alpha = 0.05$.

4.4 – Results

4.4.1 – Prevalence of Spike Facilitation

Data were collected from a database of 204 DTNs, 92 recorded at UW and 112 at MU. Spike facilitation near the offset of the NE tone was observed in 66 DTNs (32.4%), and this proportion did not differ from the number of cells exhibiting offset facilitation in Faure et al. (2003) [10/37 = 27.0%; $X^2(1) = 0.411$, p = 0.570]. Importantly, there was no difference in the proportion of cells with offset facilitation for recordings collected at UW (33/93 = 35.5%) compared to those conducted at MU [33/112 = 29.5%; $X^2(1) = 0.843$, p = 0.372].

Of the 66 DTNs we determined the number of DTNs that showed facilitation in Range 1 (during NE tone evoked spike suppression; i.e. Fig. 4.5A and B) or Range 2 (following NE tone evoked spike suppression; Fig. 4.5C and D). If facilitation occurs during Range 1, this supports the hypothesis (H1) that facilitation is a separate excitatory input, independent from inhibition because inhibition is still acting on the cell even after facilitation has occurred. However, if facilitation occurs during Range 2, then this supports the hypothesis (H2) that facilitation is a rebound from inhibition since it is occurring after the offset of inhibition. We found that the majority of DTNs (51/66 = 77.3%) with facilitation showed spiking that occurred during Range 1 and this proportion was significantly different from the proportion of cells showing facilitation during Range 2 (15/66 = 22.7%) [$X^2(1) = 19.64$, p = 9.37×10^{-6}]. Thus, the majority cells support the first hypothesis (H1) that facilitation is a separate excitatory synaptic input and not a rebound following inhibition.

Of the 51 DTNs with evidence for spike facilitation that occurred during Range 1, 38 DTNs (74.5%) used a criterion where spiking was considered facilitated when spike counts were greater than the mean +1 SD, whereas the remaining 13 cells used a criterion of >0.2 spikes per stimulus because spiking during inhibition was low (i.e. Fig. 4.5).

4.4.2 – Spike Facilitation is Time-Locked to Stimulus Offset

Both conceptual and computational models of duration selectivity predict that a DTN receives two excitatory inputs: one locked to stimulus onset and another locked stimulus offset (Casseday et al., 1994, 2000; Aubie et al., 2009, 2012; Fig. 4.1). To disambiguate whether the latency of spike facilitation was time-locked to stimulus onset *versus* stimulus offset, we varied the duration of the NE tone during paired tone stimulation.

Responses from a short-pass DTN (BD tone = 2 ms) with the NE tone set to two different durations are shown in Figure 4.6. When the NE tone was set to 30 ms (Fig. 4.6*A*) there was a large reduction in the spike count (Fig. 4.6*B*) and significant deviations in both the FSL and LSL (Fig. 4.6*C,D*) when the BD and NE tone were sufficiently close in time. This included ISI's when the BD tone immediately preceded, was simultaneous with, and immediately followed the NE tone. The final value for the onset of inhibition evoked by the NE tone was T_1 = -8 ms and was determined with a deviation in LSL. The final value for the offset of inhibition evoked by the NE tone was T_2 = 34 ms and was derived from a change in the cell's spike count and a deviation in FSL. The effective duration of inhibition was D_{IHB} = 37.20 ms. This neuron showed leading inhibition because L_{first} = 10.00 ms and T_{start} = 4.80 ms, hence the onset of inhibition preceded the cell's FSL by 5.20 ms. The cell also showed persistent inhibition because the effective duration of spike suppression lasted

7.20 ms longer than the 30 ms NE tone that evoked it. Spike facilitation was observed at an ISI of F_{Max} = 30 ms with a peak spike count of 1.13 spikes per stimulus, which was more than 1 SD above the cell's spike count of 0.31 ± 0.20 spikes per stimulus measured from the first five ISIs during spike suppression. The latency of spike facilitation was F_{start} = 40.93 ms re NE tone onset.

When the duration of the stationary NE tone was increased to 40 ms, spike suppression was again observed (Fig. 4.6*E*). The duration of suppression increased as measured by changes in the cell's spike count, but not FSL and LSL (Fig. 4.6*F-H*). The final value for T_1 was -6 ms and was derived from a change in LSL. The final value for T_2 was 44 ms and was derived from a change in spike count. This resulted in an D_{IHB} = 44.24 ms, which was 7.04 ms longer than when the NE tone was 30 ms in duration. The cell still showed leading inhibition in the 30 ms NE tone condition because L_{first} = 9.85 ms and T_{start} = 7.61 ms, hence the onset of inhibition preceded the cell's FSL by 2.24 ms. The cell also showed persistent inhibition because the D_{IHB} was 4.24 ms longer than the duration of the 40 ms NE tone. Spike facilitation was again observed near the offset of the NE tone and during the ongoing portion of spike suppression. Peak facilitation was F_{Max} = 40 ms with a spike count of 2.20 ± 0.77 spikes per stimulus, which was more than 1 SD above the initial spike count in the first five ISIs from T_1 (0.29 + 0.22 = 0.51 spikes per stimulus). The latency of the facilitated response was F_{start} = 48.92 ms re NE tone onset.

The onset of inhibition was similar regardless of whether the NE tone duration was 30 ms (T_{start} = 4.80 ms) or 40 ms (T_{start} = 7.61 ms); however, the offset of inhibition was 9.85 ms longer when the NE tone duration was 40 ms (T_{end} = 51.85 ms) than when it was

30 ms (T_{end} = 42.00 ms). These data demonstrate that the offset of inhibition increased in proportion to the duration of the NE tone. Spike facilitation was observed when the NE tone was set to 30 ms (F_{Max} = 30 ms) and 40 ms (F_{Max} = 40 ms), with the ISI of the facilitated response (F_{Max}) increasing directly with the NE tone duration. To investigate whether spike latencies increased in proportion with NE tone duration, we performed a linear regression of spike latency re: NE tone onset (F_{start}) as a function of NE tone duration. The slope for this example was 0.80 $ms_{Fstart}/ms_{NE\text{-}Tone}$.

For 17 DTNs showing spike facilitation, we collected 31 measurements at varying NE tone durations. For each measurement, we calculated a slope of the linear regression of F_{start} (re NE tone onset) plotted as a function of NE tone duration. The mean ± SD slope across all observations was 1.00 ± 0.11 $ms_{Fstart}/ms_{NE\text{-}Tone}$ and this was not significantly different from a slope of 1.00 $ms_{Fstart}/ms_{NE\text{-}Tone}$ [$t(30) = 0.44$, $p = 0.965$; Fig. 4.7]. This demonstrates that spike facilitation during paired tone stimulation was time-locked to the offset of the NE tone. Furthermore, of 66 DTNs with spike facilitation, the latency of facilitated spikes relative to the onset of the NE tone (F_{start}) was greater than the duration of the tone that evoked it (D_{NE}) in every cell tested with paired tone stimulation. This demonstrates that facilitation occurred after the offset of the tone evoking it.

4.4.3 – Effect of NE Tone Frequency on Timing of Facilitation

We evaluated how the timing of spike facilitation changed during paired tone stimulation as we varied the NE tone frequency relative to the onset and offset of inhibition. Figure 4.8A shows a dot raster display of spiking from a short-pass DTN tested with paired tone stimulation with the 1-ms BD tone and 10-ms NE tone set to +10 dB above the BD

tone threshold. In this example cell, the BD tone was set to the cell's BEF of 51.0 kHz, and the NE tone was set to a non-BEF of 75.0 kHz (Fig. 4.8A *left panel*). When the BD and NE tone were sufficiently close in time this resulted in a reduction in the cell's spike count (Fig. 4.8A *right panel*) and significant deviations in both the FSL and LSL (data not shown). This included ISI's when the BD tone immediately preceded, was simultaneous with, and immediately followed the NE tone. The final value of T_1 was -3 ms and the final value for T_2 was 13 ms, and both were derived from changes in the cell's FSL. The effective duration of spike suppression was 15.50 ms. This neuron showed leading inhibition because L_{first} = 11.69 ms and T_{start} = 8.19 ms, hence the onset of inhibition preceded the cell's FSL by 3.50 ms. The cell showed persistent inhibition because the effective duration of spike suppression was 5.50 ms longer than the duration of the 10-ms NE tone. Facilitation was observed at an ISI of F_{Max} = 17 ms with a spike count of 1.70 ± 0.674 spikes per stimulus, which was more than 1 SD greater than the average evoked count from the initial five ISIs starting from T_1 (0.89 + 0.59 spikes per stimulus = 1.48 spikes per stimulus). The latency of spike facilitation at this ISI was F_{start} = 26.84 ms re NE tone offset.

A plot of how spike counts changed during paired tone stimulation as a function of NE tone frequency is shown in Figure 4.8B for the same cell. The 10-ms NE tone was varied between 15.0 – 85.0 kHz. Across 18 frequencies tested, the ISI indicating the onset of inhibition (T_1) was detected remained relatively constant (Fig. 4.8B, *red dashed line*), while the offset of inhibition (T_2) decreased systematically as the NE tone frequency moved above and below from the BEF (Fig. 4.8B, *white dashed line*). This pattern has previously been described by Valdizón-Rodríguez and Faure (2017), but not with respect to the

strength or timing of spike facilitation. Based on these data, we generated two hypotheses about F_{start}. The first hypothesis (H1) is that F_{start} follows a pattern similar to T_{start}, because a cell's BD and duration filter class depend, in part, on the relative latency difference between the onset of inhibition (T_{start}) and the onset of excitation (FSL) (Casseday et al., 1994, 2000; Ehrlich et al., 1997; Faure et al., 2003; Aubie et al., 2009, 2012). To preserve a cell's temporal tuning and response properties across changes in stimulus frequency, the relative latency between T_{start} and F_{start} should remain constant. Alternatively (H2), the coincidence detection model of duration tuning hypothesizes that offset-locked excitation (Fig. 4.1) arises from post-inhibitory rebound excitation following sustained hyperpolarization of the cell (Casseday et al., 1994, 2000; Casseday and Covey, 1995; Covey et al., 1996; Ehrlich et al., 1997). If facilitation is caused by post-inhibitory rebound excitation, then the timing of F_{start} should mirror the offset of inhibition and be independent of the latency difference between T_{start} and F_{start}.

We tested these contrasting hypotheses in DTNs using paired tone stimulation where the NE tone frequency was varied and we assessed whether the latency of spike facilitation, F_{start}, was related to changes in T_{start} or T_{end} using the variables δ_{start} and δ_{end} that quantify how changes in F_{start} vary with changes in T_{start} or T_{end} across the entire stimulus set presented (see Materials and Methods *Comparing the Timing of Facilitation to the Onset and Offset of Inhibition*).

For the example DTN in Figure 4.8B, F_{Max} (*dashed blue line*) remained relatively constant across changes in BD tone amplitude, demonstrating that the onset of facilitation

behaved more similarly (i.e. was more parallel) to the onset of inhibition (Fig. 4.8B, *red line*) than the offset of inhibition (Fig. 4.8B, *blue line*), especially at frequencies between 41 – 55 kHz where facilitation precedes the offset of inhibition. For this cell, F_{start} deviated from changes in T_{start} by an average of δ_{start} = 3.71 ms across changes in NE tone frequency. On the other hand, changes in F_{start} deviated from changes in T_{end} by an average of δ_{end} = 22.10 ms. Thus, for this cell, changes in F_{start} related more to T_{start} than T_{end} as the NE tone frequency was varied.

We measured δ_{start} and δ_{end} for 19 observations (n = 19 DTNs) that showed spike facilitation when the NE tone frequency was varied (Fig. 4.9A). There was a significant difference between the mean ± SD δ_{start} (2.91 ± 1.57 ms) and δ_{end} (5.79 ± 5.77 ms; $t(18) = 2.133$, $p = 0.047$). Moreover, δ_{start} was smaller than δ_{end} in a majority of observations (13/19 = 68.4%), although not significantly different from chance [$X^2(1) = 6.26$, $p = 0.10$], thus demonstrating that a greater proportion of F_{start} values related more to T_{start} than to T_{end}. Overall, these results demonstrate that changes in the latency of spike facilitation (re NE tone onset) related more to changes in T_{start} than T_{end} when frequency was varied. These data are consistent with the hypothesis that F_{start} follows a pattern more similar to T_{start} than T_{end}, supporting the notion that a cell's BD and duration filter response class—which depend, in part, on the relative latency difference between the onset of inhibition and excitation—will be preserved across different frequencies of stimulation (Casseday et al., 1994, 2000; Ehrlich et al., 1997; Faure et al., 2003; Aubie et al., 2009, 2012).

4.4.4 – Effect of NE Tone Frequency on Strength of Facilitation

In this section we examine the role the NE tone frequency plays in modulating the spike count of offset facilitation. Like most central auditory neurons, the number of spikes evoked by a DTN changes with stimulus frequency (Pinheiro et al., 1991; Wu and Jen, 2006a; Morrison et al., 2014; Valdizón-Rodríguez and Faure, 2017). We evaluated two hypotheses by assessing how the strength of facilitation varies during paired tone stimulation with changes in NE tone frequency. (H1) If offset facilitation is caused by a separate excitatory input, then spike counts should increase as NE tone frequency departs from BEF because the strength of inhibition evoked by the NE tone decreases away from the BEF (Valdizón-Rodríguez and Faure, 2017), this will change the relative balance of excitation and inhibition. (H2) In contrast, if offset facilitation is caused by post-inhibitory rebound excitation, then facilitated spike counts during paired tone stimulation should peak at the BEF where inhibition is strongest (i.e. rebound from inhibition will be at a maximum at the BEF) and decrease as the NE tone frequency moves away from the BEF.

The example cell in Figure 4.8C shows the mean facilitated spike count plotted as a function of NE tone frequency deviation (re BEF). When the NE tone frequency was below the cell's BEF, we found a linear regression slope of 0.033 spikes/kHz. When the NE tone frequency was above the BEF, the slope of the relationship increased to 0.035 spikes/kHz. Note that the slope measured when the NE tone frequency was varied below the BEF was sign inverted so that it could be directly compared to the slope when the NE tone frequency was varied above the BEF. These data demonstrate that facilitated spike

counts increase as the NE tone frequency departs from the cell's BEF, and support hypothesis H1 that offset facilitation is caused by a separate excitatory input.

We performed a similar regression analyses on the strength of facilitation on 18 DTNs that showed offset facilitation when the NE tone frequency was varied (n = 16 observations below BEF and n = 13 observations above BEF; Fig. 4.9B). The mean ± SD slope was 0.082 ± 0.437 spikes/kHz for frequencies below the BEF and was 0.166 ± 0.281 spikes/kHz for frequencies above the BEF. Because the distributions of slopes above and below BEF did not differ [t(27) = -0.598, p = 0.915], we pooled the datasets, calculated a combined slope of 0.120 ± 0.372 spikes/kHz, and found that it did not differ from a slope of zero [t(49) = 1.74, p = 0.09]. However, the effect almost reached statistical significance in the direction predicted by H1. Individually, 18 of the 29 (62%) slopes were greater than zero [$X^2(1) = 1.690$, p = 0.194] despite having a majority of slopes in the direction of H1. Together, these data fail to show that the strength of facilitation changed during paired tone stimulation when the NE tone frequency departed from the BEF. The data do not support either (H1) the hypothesis that offset facilitation is caused by a separate input or (H2) the hypothesis that facilitation is a rebound from inhibition – however, it should be noted that the pattern predicted by H1 was nearly significant.

4.4.5 – Effect of NE Tone Frequency on Latency of Facilitation (F_{start})

Many auditory neurons show a change in spike latency as stimulus frequency is varied (Brugge et al., 1969; Heil, 1997, 2004). Furthermore, a number of studies have suggested that changes in a cell's first spike latency as a function of stimulus amplitude or frequency are caused by an imbalance in the strength of excitation and inhibition (Park and

Pollak, 1993; Covey et al., 1996; Galazyuk and Feng, 1997; Kuwada et al., 1997; Faure et al., 2003; Fremouw et al., 2005; Voytenko and Galazyuk, 2008; Valdizón-Rodríguez and Faure, 2017). We generated two hypotheses regarding changes in the FSL of spike facilitation (F_{start}) as a function of NE tone frequency. (H1) If offset facilitation is caused by a separate excitatory input, then F_{start} should remain constant or decrease as the NE tone frequency moves away from the BEF. This is because the strength of the NE tone-evoked inhibition decreases as frequency departs from the cell's BEF and thus allows early excitation that was previously suppressed to be suprathreshold. However, (H2) if F_{start} is caused by post-inhibitory rebound, then excitation following rebound should be strongest and occur with its shortest FSL when the NE tone is set to the BEF (i.e. Sun and Wu 2008). Therefore, the FSL of the facilitated response, F_{start}, should increase as the NE tone frequency moves away from BEF.

The example cell in Figure 4.8D plots F_{start} as a function of the deviation of the NE tone frequency from BEF. Using linear regression, the slope of the data below BEF was -0.153 ms/kHz, and was -0.307 ms/kHz for the data above BEF. Note that the slope measured when the NE tone frequency was varied below BEF was sign inverted so that it could be directly compared to the slope when the NE tone frequency was varied above BEF.

We performed a linear regression analysis on the FSL of facilitation (F_{start}) on 18 DTNs that showed offset facilitation when the NE tone frequency was varied (n = 16 observations below BEF and n = 13 observations above BEF; Fig. 4.9C). The mean ± SD slope was -0.81 ± 1.35 ms/kHz for frequencies below the BEF, and was -1.07 ± 1.37

ms/kHz for frequencies above the BEF. Because the distribution of slopes above and below the BEF did not differ [t(27) = 0.519, p = 0.608], we pooled the datasets, calculated a combined slope of -0.926 ± 1.34 ms/kHz, and found that it differed from a slope of zero [t(28) = -3.71, p = 0.001]. Moreover, 23 of 29 (79.3%) individual slopes were less than zero [$X^2(1) = 9.996$, p = 0.002] showing that the majority of observations had a negative slope. Altogether, these data demonstrate that the FSL of facilitation decreased as the NE tone frequency was varied above and below a cell's BEF. Together, the data support the hypothesis that offset facilitation is caused by a separate input and not by rebound from inhibition.

4.4.6 – Effect of NE Tone Amplitude on Timing of Facilitation

In this section we evaluate how the timing of spike facilitation changed relative to the onset and offset of inhibition during paired tone stimulation as we varied the NE tone amplitude. Figure 4.10A (*left panel*) shows a dot raster display of spiking from a short-pass DTN tested with paired tone stimulation with both tones presented at the cell's BEF. In this example cell, the 1-ms BD tone amplitude was set to +10 dB re threshold (69.0 dB SPL), and the 10-ms NE tone amplitude was set to -10 dB re BD tone threshold (49 dB SPL). When the BD and NE tone were sufficiently close in time this resulted in a large reduction in spike count (Fig. 4.10*A right panel*) and significant deviations in both the FSL and LSL (data not shown). This included ISI's when the BD tone immediately preceded, was simultaneous with, and immediately followed the NE tone. The final value for T_1 was -1 ms and was derived from a change in spike count. The final value for T_2 was 19 ms and was derived from a change in LSL. The effective duration of spike suppression was 19.10

ms. This neuron showed leading inhibition because L_{first} = 10.16 ms and T_{start} = 9.06 ms, hence the onset of inhibition preceded the cell's FSL by 1.10 ms. The cell showed persistent inhibition because the effective duration of spike suppression was 9.10 ms longer than the duration of the 10-ms NE tone. Spike facilitation was observed at an ISI of F_{Max} = 15 ms with a peak spike count of 3.20 ± 0.63 spikes per stimulus, which was more than 1 SD above the cell's baseline spike count of 1.49 ± 0.68 spikes per stimulus. The FSL of the facilitated response was F_{start} = 20.86 ms re NE tone onset.

We evaluated how spike counts at each ISI changed for the same cell during paired tone stimulation as the amplitude of the 10-ms NE tone was varied between -40 – + 20 dB re BD tone threshold (i.e. 19.0 – 79.0 dB SPL; 10 dB steps; Fig. 4.10*B*). In this cell, the onset of inhibition (T_1) remained relatively constant (Fig. 4.10B, *red dashed line*); however, the offset of inhibition (T_2) systematically increased with the amplitude of the NE tone (Fig. 4.10B, *white dashed line*). We generated two hypotheses about F_{start}. The first hypothesis (H1) is that F_{start} follows a pattern similar to T_{start}, because a cell's BD and duration filter class depend, in part, on the relative latency difference between the onset of inhibition (T_{start}) and the onset of excitation (FSL) (Casseday et al., 1994, 2000; Ehrlich et al., 1997; Faure et al., 2003; Aubie et al., 2009, 2012). To preserve a cell's temporal tuning and response properties across changes in stimulus frequency, the relative latency between T_{start} and F_{start} should remain constant. Alternatively (H2), the coincidence detection model of duration tuning hypothesizes that offset-locked excitation (Fig. 4.1) arises from post-inhibitory rebound excitation following sustained hyperpolarization of the cell (Casseday et al., 1994, 2000; Casseday and Covey, 1995; Covey et al., 1996; Ehrlich et al., 1997). If

facilitation is caused by post-inhibitory rebound excitation, then the timing of F_{start} should mirror the offset of inhibition.

We next assessed whether the latency of spike facilitation, F_{start}, related to changes in T_{start} or T_{end} using the variables δ_{start} and δ_{end} across the entire stimulus set presented (see Materials and Methods *Comparing the Timing of Facilitation to the Onset and Offset of Inhibition*). For example the DTN in Figure 4.10B, the onset of inhibition or F_{Max} (*blue dashed line*) remained relatively constant as a function of NE tone amplitude, suggesting that the onset of facilitation behaved similarly to the onset of inhibition (Fig. 4.10B, *red dashed line*) compared to the offset of inhibition (Fig. 4.10B, *blue dashed line*). Changes in F_{start} deviated from changes in T_{start} by an average of δ_{start} = 2.23 ms across the seven BD tone amplitudes tested (-40 to 20 dB re BD tone threshold), which was near the measurement error for data collected with a roving BD tone whose ISI was randomly varied in 2-ms steps. On the other hand, changes in F_{start} deviated from changes in T_{end} by an average of δ_{end} = 5.24 ms. Although the facilitation (*blue line*) in Fig. 4.10B was intermediate between the onset (*red line*) and offset (*white line*) of inhibition, the evidence suggests it was more related to the onset of inhibition. It is possible that the latency of facilitation was delayed by the increasing strength of inhibition as stimulus amplitude is increased. Consequently, for this cell changes in F_{start} correlated more with T_{start} than T_{end} as the NE tone amplitude was varied.

We measured δ_{start} and δ_{end} in 20 observations (n = 15 DTNs) that showed spike facilitation when the NE tone amplitude was varied (Fig. 4.11A). There was a significant

difference between the mean ± SD δ_{start} (2.19 ± 1.92 ms) and δ_{end} (6.14 ± 6.14 ms; t(24) = 2.61, p = 0.017]. Additionally, δ_{start} was smaller than δ_{end} in 15 of 20 (75%) observations, demonstrating that a greater proportion of F_{start} values were more related to T_{start} than T_{end} [$X^2(1) = 5.00$, p = 0.025]. Overall, these results are consistent with the hypothesis that F_{start} follows a pattern more similar to T_{start} than to T_{end}, supporting the notion that a cell's BD and duration filter response class— which depend on the relative latency difference between the onset inhibition and excitation—will be preserved across different amplitudes of stimulation (Zhou and Jen, 2001; Fremouw et al., 2005).

4.4.7 – Effect of NE Tone Amplitude on Strength of Facilitation

We generated two hypotheses regarding changes in the facilitated spike count as a function of NE tone amplitude. HI: If facilitation was caused by a separate excitatory input, then spike counts should decrease with increasing NE tone amplitude because the strength of the inhibition would increase changing the relative balance of excitation and inhibition. H2: However, if facilitation is caused by a rebound from the offset of NE tone-evoked inhibition, then the strength of offset facilitation should increase as the amplitude of the NE tone increases because this would also increase the strength of post-inhibitory rebound excitation; spike counts would therefore increase as the NE tone amplitude was increased.

The example cell in Figure 4.10C plots the facilitated spike count evoked during paired tone stimulation as a function of NE tone amplitude. The strength of facilitation at first increases and then decreases with increasing level of the NE tone. A linear regression of these data reveals a slope of -0.012 spikes/$dB_{NE\ Tone}$. Note that the cell in Fig. 4.10C does

not respond strongly to amplitudes between 19 and 29 dB SPL, resulting in a concave shaped rate-level function for facilitation. Because both amplitudes were below the cell's excitatory threshold of 59 dB SPL, these stimuli likely did not contain sufficient energy to evoke facilitation in the cell. However, amplitudes >39 dB SPL illustrate the pattern much more strongly.

We performed a linear regression analysis on the strength of spike facilitation for 15 DTNs that showed offset facilitation when the NE tone amplitude was varied (n = 20 observations; Fig. 4.11B). Across all observations, the average slope was -0.008 ± 0.036 spikes/$dB_{NE\ Tone}$ and this did not differ from a slope of zero [t(19) = 1.034, p = 0.314]. Individually, 9 of 20 (45%) were less than zero [$X^2(1) = 0.2$, p = 0.655]. Overall, these data indicate that the strength of facilitation did not change with increasing NE tone amplitude, and thus did not support either (H1) the hypothesis that offset facilitation was caused by a separate excitatory input and or (H2) the hypothesis that it was a rebound from inhibition.

4.4.8 – Effect of NE Tone Amplitude on Latency of Facilitation (F_{start})

Most auditory neurons show a decrease in latency when stimulus amplitude is increased (Mörchen et al., 1978; Heil, 2004; Tan et al., 2008). Furthermore, many studies have suggested that changes in FSL as a function of stimulus amplitude or frequency can occur due to an imbalance in the strengths of excitation and inhibition (Park and Pollak, 1993; Covey et al., 1996; Galazyuk and Feng, 1997; Kuwada et al., 1997; Faure et al., 2003; Fremouw et al., 2005; Voytenko and Galazyuk, 2008; Valdizón-Rodríguez and Faure, 2017). We generated two hypotheses regarding changes in the FSL of facilitation (F_{start}) as a function of NE tone amplitude. H1: if spike facilitation is caused by a separate

excitatory input linked to stimulus offset, then the FSL of facilitated spikes should increase with increasing NE tone amplitude. This occurs because increased NE tone-evoked inhibition would suppress earlier responses. However, (H2) if facilitation is caused by excitatory rebound from the offset of inhibition, then F_{start} could decrease with increasing NE tone amplitude owing to a stronger (faster) rebound from inhibition (i.e. Sun and Wu 2008).

For the example cell shown in Figure 4.10D, we plotted F_{start} as a function of NE tone amplitude and calculated a linear regression slope of 0.016 ms/$dB_{NE\ Tone}$ indicating that the latency of facilitation was increasing as a function of NE tone amplitude.

We performed a similar analysis on F_{start} for 15 DTNs that showed offset facilitation when the NE tone amplitude was varied (n = 20 observations; Fig. 4.11C). The average slope was 0.179 ± 0.270 ms/$dB_{NE\ Tone}$ and was significantly different from a slope of zero [t(19) = 2.97, p = 0.008]. These population data indicate that the FSL of facilitation increased with NE tone amplitude. Individually, 16 of 20 (80%) of slopes were greater than zero and this proportion differed from a chance value of 50% [$X^2(1) = 7.20$, p = 0.007]. Together, the data support the hypothesis that offset facilitation is caused by a separate excitatory input and not by rebound from inhibition.

4.4.9 – Effect of BD Tone Amplitude on Timing of Facilitation

In this section we evaluate how the timing of spike facilitation changed relative to the onset and offset of inhibition during paired tone stimulation as we varied the BD tone amplitude. A dot raster display of responses from a bandpass DTN evoked during paired

tone stimulation with a 5-ms BD tone and 20-ms NE tone is shown in Figure 4.12*A* (*left panel*). In this example, the amplitude of the BD tone was set to +30 dB (re threshold) and the amplitude of the NE tone was set to 0 dB (re BD tone threshold). When the BD and NE tone were sufficiently close in time, again there was a marked decrease in the evoked spike count (Fig. 4.12*B right panel*) and significant deviations in both the FSL and LSL (data not shown). The final value for T_1 was -9 ms and the final value for T_2 was 3 ms and both were derived from a change in spike count. When the BD tone was +30 dB re NE tone, the effective duration of spike suppression was only 10.43 ms. This neuron showed leading inhibition because L_{first} = 25.50 ms and T_{start} = 13.07 ms, hence the onset of inhibition preceded the FSL by 12.43 ms. The cell did not show persistent inhibition because the effective duration of inhibition was 9.57 ms shorter than the duration of the 20-ms NE tone. A facilitation in spiking was observed at an ISI of F_{Max} = 15 ms with a peak spike count of 2.00 ± 0.47 spikes per stimulus, which was >1 SD above the cell's baseline spike count of 0.88 ± 0.72 spikes per stimulus measured over the first 5 responses. The latency of the facilitated spikes evoked at the onset of facilitation was F_{start} = 33.32 ms re NE tone onset.

We then examined how spike counts at each ISI changed as a function of BD tone amplitude (Fig. 4.12*B*). When the 5-ms BD tone was varied between 0 and +30 dB re threshold (21.5 – 51.5 dB SPL; 4 amplitude steps) and the amplitude of 20-ms NE tone was held constant at 0 dB (re BD tone threshold), the ISI for the onset of inhibition (T_1) remained relatively constant (Fig. 4.12B, *red dashed line*) whereas the ISI indicating the offset of inhibition (T_2) systematically decreased with increasing BD tone amplitude (Fig. 4.12B, *white dashed line*). This pattern was previously described (Faure et al., 2003). We

generated two hypotheses about the onset of spike facilitation, F_{start}, in DTNs tested with paired tone stimulation and variable BD tone amplitudes. H1: if a cell's BD and duration filter class depend, in part, on the relative latency difference between T_{start} and FSL (Casseday et al., 1994, 2000; Ehrlich et al., 1997; Faure et al., 2003; Aubie et al., 2009, 2012), then F_{start} should follow a pattern similar to T_{start}. H2: if offset facilitation is caused by a rebound from inhibition, then F_{start} should vary with the offset of inhibition.

We assessed these contrasting hypotheses in DTNs tested with paired tone stimulation and variable BD tone amplitudes by calculating δ_{start} and δ_{end} across the entire stimulus set presented. For the example cell in Figure 4.12*B*, F_{Max} (*blue dashed line*) remained relatively constant as a function of BD tone amplitude. The data for the onset of spike facilitation followed a pattern that was more similar to the onset of inhibition (Fig. 4.12B, *red dashed line*) than the offset of inhibition (Fig. 4.8B, *blue dashed line*). Changes in the value of F_{start} deviated from changes in T_{start} by an average of δ_{start} = 3.46 ms over the BD tone amplitudes tested (0 – 30 dB re threshold). Importantly, δ_{start} was similar to the measurement error (i.e. ISI step size of 2 ms) for the roving BD tone. On the other hand, changes in F_{start} deviated from changes in T_{end} by an average of δ_{end} = 18.25 ms. Therefore, in this cell, changes in F_{start} correlated with T_{start} rather than T_{end} when the BD tone amplitude was varied.

We measured δ_{start} and δ_{end} in 38 observations (n = 22 DTNs) that showed offset facilitation when the BD tone amplitude was varied (Fig. 4.13A). There was a significant difference between δ_{start} (2.72 ± 2.13 ms) and δ_{end} (4.86 ± 4.92 ms [$t(37) = 2.684$, $p =$

0.011]). Although δ_{start} was smaller than δ_{end} in 24 of 38 (63.2%) observations, there was no difference in the proportion of F_{start} values related to T_{start} than T_{end} [$X^2(1) = 2.632$, $p = 0.105$]. Overall, these results suggest that changes in F_{start} were corelated to changes in T_{start} rather than T_{end} when the BD tone amplitude was varied, which supports the hypothesis that F_{start} follows a pattern more similar to T_{start} than T_{end}.

4.4.10 – Effect of BD Tone Amplitude on Strength of Facilitation

In this section we examine how changes in the amplitude of the BD tone modulate offset facilitation spike counts during paired tone stimulation. The strength of the evoked excitation typically increased as BD tone amplitude increased. Because the NE tone amplitude was not varied, contributions to the strength of facilitation from the NE tone should remain the same. Therefore, we generated two hypotheses regarding changes in the facilitated spike count as a function of BD tone amplitude. H1: If facilitation is caused by a separate excitatory input, then spike counts should increase with increasing BD tone amplitude owing to increased BD tone evoked excitation. H2: However, if facilitation is caused by a post-inhibitory rebound excitation, then the strength of facilitation should decrease because increased BD tone-evoked excitation would summate with and weaken the strength of inhibition, moving the membrane potential away from the reversal potential for inhibition, thus weakening post-inhibitory rebound excitation. Spike counts would therefore decrease as the BD tone amplitude was increased.

The cell in Figure 4.12C shows that the average number of spikes per stimulus evoked during offset facilitation increased as a function of BD tone amplitude with a slope of 0.03 Spikes/$dB_{BD\ Tone}$ thus supporting H1.

We performed a similar regression analyses on 22 DTNs that showed offset facilitation when the BD tone amplitude was varied (n = 38 observations; Fig. 4.13B). The mean ± SD slope was 0.027 ± 0.062 spikes/$dB_{BD\ Tone}$ and was significantly different from a slope of zero [t(37) = 2.73, p = 0.01]. Moreover, the slopes were greater than zero in a majority (26/38; 68.4%) of the observations [X^2(1) = 5.16, p = 0.023]. The population data demonstrate that the strength of offset facilitation increased as the amplitude of the BD tone increased. Thus, these data are consistent with the hypothesis that offset facilitation is caused by a separate excitatory input (H1).

4.4.11 – Effect of BD Tone Amplitude on Latency of Facilitation (F_{start})

In this section we explore how changes in the amplitude of the BD tone during paired tone stimulation influence the FSL of facilitated spikes. As the BD tone amplitude increased, the latency of the excitation evoked by the BD tone decreases (Faure et al., 2003). Furthermore, because the NE tone amplitude was not varied, its contributions to the timing of offset-evoked spike facilitation would stay the same. We generated two hypotheses regarding changes in the FSL of facilitation (F_{start}) as a function of BD tone amplitude. H1: if spike facilitation is caused by a separate excitatory input linked to stimulus offset, then the FSL of facilitated spikes should decrease with increasing BD tone amplitude. This occurs because increased BD tone-evoked excitation would reveal earlier responses that were previously subthreshold. However, (H2) if facilitation is caused by a

post-inhibitory rebound excitation, then the latency of facilitation should increase because increased BD tone-evoked excitation would summate with and weaken the strength of inhibition, moving it further away from its reversal potential, thus reducing the strength post-inhibitory rebound. If post-inhibitory rebound is weaker, early spikes that were previously suprathreshold will become subthreshold and thus only later spiking at the peak of facilitation will be observed.

Evidence to support H1 is shown by the example cell in Figure 4.12D, which plots decreasing values of F_{start} as a function of increasing BD tone amplitude. The slope of the linear regression was -0.26ms/$dB_{BD\ Tone}$. The data are consistent with the hypothesis that offset facilitation in DTNs is evoked by a separate excitatory input.

We performed a similar analysis on F_{start} as a function of BD tone amplitude for 22 DTNs (n = 38 observations; Fig. 4.13C). The average slope across the population was -0.29 ± 0.39 ms/$dB_{BD\ Tone}$ and was significantly different from a slope of zero [t(37) = 4.57, $p = 5.2x10^{-5}$]. Individually, a majority of observations (30/38, 78.9%) had slopes less than zero, and this proportion differed from 50% due to chance [$X^2(1) = 12.74$, $p = 3.6x10^{-4}$]. These data demonstrate that the FSL of offset facilitation decreased with increasing BD tone amplitude, and support the hypothesis that offset facilitation is caused by a separate excitatory input (H1).

4.4.12 – Effect of Monotic and Dichotic Stimulation on Facilitation

In this section we evaluate how facilitation changed when DTNs were presented with monotic or dichotic paired tone stimulation. Dot raster displays of responses from a

shortpass DTN evoked during paired tone stimulation with a 1-ms BD tone and 20-ms NE tone are shown in Figure 4.14. When the BD tone and NE tone were presented monotically to the contralateral ear (re: IC recorded), spike suppression was observed (Fig. 4.14A). There was a marked decrease in the evoked spike count (Fig. 4.14*B*) however, we did not observe significant deviations in FSL (Fig. 4.14C) and LSL (Fig. 4.14D). The final value for T_1 was -1 ms and the final value for T_2 was 23 ms and both were derived with a spike count criterion. In the monotic condition, the effective duration of spike suppression was 23.63 ms. This neuron showed leading inhibition because L_{first} = 12.38 ms and T_{start} = 10.75 ms, hence the onset of inhibition preceded the FSL by 1.63 ms. The cell also showed persistent inhibition because the effective duration of inhibition was 3.63 ms longer than the duration of the 20-ms NE tone. A facilitation in spiking was observed at an ISI of F_{Max} = 29 ms with a peak spike count of 1.55 ± 0.76 spikes per stimulus, which was >1 SD above the cell's baseline spike count of 0.58 ± 0.65 spikes per stimulus measured over the first 10 responses. The latency of the facilitated spikes evoked at the onset of facilitation was F_{start} = 36.01 ms re NE tone onset.

When the cell was stimulated dichotically (ipsilateral NE tone re: IC recorded), spike suppression was again observed (Fig. 4.14E). There was a decrease in the evoked inhibition measured with a spike count criterion (Fig. 4.14*F*) and significant deviations in FSL (Fig. 4.14G) and LSL (Fig. 4.14H) were not observed. The final value for T_1 was -1 ms and the final value for T_2 was 23 ms and both were derived from with a spike count criterion. In the dichotic condition, the effective duration of spike suppression was 13.57 ms. This neuron showed lagging inhibition because L_{first} = 12.50 ms and T_{start} = 14.93 ms,

hence the onset of inhibition lagged the FSL by 2.43 ms. The cell did not show persistent inhibition because the effective duration of inhibition was 6.43 ms shorter than the duration of the 20-ms NE tone. Importantly, the dichotic condition did show any evidence of offset evoked spike facilitation.

Comparing the monotic and dichotic condition, the onset of inhibition was shorter in the monotic (T_{start} = 10.75 ms) than in the dichotic condition (T_{start} = 14.93 ms) and duration of inhibition was 10.06 ms longer in the monotic condition (T_{end} = 34.38 ms; D_{IHB} = 23.63 ms) than in the dichotic condition (T_{end} = 28.50 ms; D_{IHB} = 13.57 ms). These data demonstrate inhibition was stronger, earlier, and longer lasting in the monotic condition compared to the dichotic condition and this result has been reported previously by Sayegh *et al.* (2014) but not with respect to facilitation. We generated two hypotheses about the timing of facilitation in the monotic condition compared to the dichotic condition. The first hypothesis is (H1) if facilitation results from a separate excitatory synaptic input, then observing facilitation should be independent of whether or not inhibition is observed in monotic or dichotic condition. However, (H2) if facilitation is a rebound from inhibition, then cells that show inhibition in both the monotic and dichotic conditions, should also show facilitation in both conditions. The data collected from this cell support H1 because facilitation is only observed in the monotic condition even though inhibition could be measured in both the monotic and dichotic conditions.

We recorded from 18 DTNs (20 observations) that showed facilitation recorded during either monotic or dichotic paired tone stimulation. In the majority of observations (17/20 = 85%) facilitation was observed when DTNs were stimulated with monotic but not

dichotic paired tone stimulation. In two observations (10%) offset facilitation was observed in the dichotic condition but not in the monotic condition, and in one observation (5%) facilitation was observed in both conditions. These data show that the facilitation is primarily observed when DTNs are tested with monotic paired-tone stimulation to the contralateral ear re: IC recorded [$X^2(2) = 24.10$, $p = 5.85 \times 10^{-6}$].

When cells were tested monaurally, 20 of 20 (100%) observations showed evidence of inhibition evoked from the contralateral ear. Ipsilateral (binaural) inhibition could only be measured in 35% of observations (7 of 20), which was not significantly different from the proportion of cells reported by Sayegh et al. (2014) [47.6%; $X^2(1) = 1.277$, $p = 0.258$]. In the 7 cases with ipsilateral inhibition, none (0%) of the observations showed spike facilitation, and this was significantly different from a chance value of 50% (binomial test, $p = 0.016$). Furthermore, in the three cases (3/20 =15%) where facilitation was observed in the dichotic condition, ipsilaterally evoked inhibition was not observed, showing that facilitation can occur without the presence of inhibition. These data demonstrate facilitation did not occur together with inhibition which supports the hypothesis that offset facilitation is caused by a separate excitatory input (H1) and is not a rebound from inhibition.

4.4.13 – Relationship between Latency of Offset Facilitation and Leading Inhibition, FSL, and BD

If facilitation is involved in creating the response properties of DTNs (i.e. Fig. 4.1 – trace labeled *OFF EPSP*; Fig. 4.2), then we hypothesized that the latency of facilitation (F_{start}) should correlate to a DTN's baseline FSL. For the 66 DTNs with offset facilitation, we found a strong, positive correlation between F_{start} and baseline FSL [Fig. 4.15*A*; R^2 =

0.44, $F(1,64) = 51.19$, $p = 9.95 \times 10^{-10}$]. These data apply to paired tone stimulation when the BD and NE tones were at (or very near) the same BEF, equal in amplitude (+10 dB re threshold), and the NE tone was 10 times longer in duration than the BD. These results suggest that F_{start} is working under a similar time course as the excitatory FSL of the cell.

We plotted the latency of facilitation (F_{start}) – calculated with respect to the onset of the BD tone that evoked it – as a function of the cell's baseline FSL and found a strong relationship [Fig. 4.15B – regression line not shown; $R^2 = 0.80$, $F(1,64) = 249.71$, $p = 1.00 \times 10^{-13}$]. This relationship is expected because it is the combination of responses evoked by the BD tone and NE tones that cause facilitation. We then split cells by whether spike facilitation occurred in Range 1 or Range 2 (i.e. Fig. 4.5). We found that the slope of the relationship for cells with facilitation in Range 1 was greater than 1 (Fig. 4.15B, *diamonds* and *solid line*, slope = 1.13). These results demonstrate that the latency of facilitation (F_{start} re BD tone onset) occurring in Range 1 was longer than the cell's baseline FSL. Conversely, when facilitation occurred in Range 2, the slope of the relationship decreased (Fig. 4.15B, *triangles* and *dashed line*, slope = 0.88), showing that F_{start} (re BD tone onset) was shorter than the cell's baseline FSL. Furthermore, the average latency of spike facilitation (F_{start}) was longer in Range 1 than in Range 2 [$F(1,63) = 6.81$, $p = 0.011$] after controlling for the linear association between F_{start} (re BD tone onset) and baseline first spike latency [$F(1,63) = 272.38$, $p = 2.0 \times 10^{-16}$]. That facilitated spikes occurring in Range 1 and were delayed relative to the baseline FSL demonstrates that offset facilitation was not caused by post-inhibitory rebound excitation in a majority of DTNs. That facilitated spikes occurring in Range 2 had shorter FSLs relative to their baseline FSL suggests that

post-inhibitory rebound could possibly be responsible for facilitation in these cells, however, they are a minority.

Previous studies have consistently reported that DTNs with longer BDs have longer FSLs (e.g. Faure et al. 2003; Sayegh et al., 2014; Valdizón-Rodríguez and Faure 2017). This result was also observed in DTNs that showed facilitation during paired tone stimulation – where the baseline FSL was related to a given cell's BD [Fig. 4.15*C*; R^2 = 0.501, F(1,64) = 64.195, p = 3.08×10^{-11}]. Given that facilitation is thought to be involved in creating DTN response properties of DTNs (Fig. 4.1 – trace labeled *OFF EPSP*; Fig. 4.2) we predicted that cells with longer BD's would also have longer F_{start} re NE tone onset. In support of this prediction, there was a positive correlation between F_{start} and BD [Fig. 4.15*D*; R^2 = 0.34, F(1,64) = 32.37, p = 3.42×10^{-7}].

Computational and conceptual models of duration tuning have shown that a DTN's FSL, BD, duration filter class, and range of temporal selectivity are controlled, in part, by the amount of time that onset-evoked inhibition leads excitation (Fig.1 – note that there is less leading inhibition in the 1-ms BD, short FSL, shortpass cell compared to the 4-ms BD, longer FSL, band pass cell). Previous studies have reported that baseline FSL is related to the amount of leading inhibition (e.g. Faure et al. 2003; Sayegh et al., 2014; Valdizón-Rodríguez and Faure 2017). This result was also observed in DTNs that showed facilitation during paired tone stimulation – where the baseline FSL was related to a the amount of leading inhibition measured from a DTN [Fig. 4.15*E*; R^2 = 0.41, F(1,64) = 43.78, p = 8.71×10^{-9}]. If facilitation plays a role in creating these response properties of DTNs, we predicted that F_{start} should be correlated to the duration of leading inhibition (i.e. the

difference in the onset latency of inhibition and excitation). Indeed, we found a positive correlation between F_{start} and the duration of leading inhibition in the population of DTNs with offset facilitation [Fig. 4.15*E*; $R^2 = 0.19$, $F(1,64) = 15.03$, $p = 2.52 \times 10^{-4}$].

Finally, Faure et al. (2003) found that duration filter class also relates to a cell's response class, with short-pass DTNs having shorter FSLs than bandpass DTNs. We replicated this finding in our sample of 66 DTNs with offset facilitation, of which 41 were short-pass DTNs and 25 were bandpass DTNs. The distribution of the baseline FSL differed between short-pass (11.12 ± 2.19 ms) and bandpass cells (19.27 ± 6.44 ms; [$t(64) = 7.46$, $p = 2.91 \times 10^{-10}$]). We hypothesized that if facilitation is involved in creating the response properties of duration tuning, then by extension bandpass DTNs should have facilitated spikes with longer F_{start} than short-pass DTNs. Across the population of 66 DTNs, the value of F_{start} differed between short-pass (30.13 ± 7.89 ms) and bandpass cells (47.08 ± 19.05 ms; [$t(64) = 5.049$, $p = 3.94 \times 10^{-6}$]).

4.5 – Discussion

4.5.1 – Relationship and Temporal Sequence of Inhibition and Excitation

Previous research suggests that duration tuning is an emergent electrophysiological response property that is created in the auditory midbrain through the convergence and temporal interaction of sound-evoked excitatory and inhibitory synaptic inputs that are offset in time (Ehrlich et al., 1997; Faure et al., 2003). Conceptual models have been created show how duration selectivity could arise in the mammalian IC. For instance, the coincidence detection model of duration tuning illustrates how two subthreshold excitatory inputs can summate to become suprathreshold at some stimulus durations but not at others (Fig. 4.1). Note that inhibition is not a necessary component of the coincidence detection model (Narins and Capranica, 1980), since an interaction between the two subthreshold excitatory inputs could be sufficient to generate a duration selective circuit. However, we know that inhibition is a necessary component of duration tuning because when pharmacological antagonists of inhibitory neurotransmitters were iontophoretically applied to DTNs, duration selectivity was broadened or completely abolished (Casseday et al., 1994; Casseday et al., 2000; Fuzessery & Hall, 1999; Jen & Wu, 2005; Jen & Feng, 1999). Furthermore, extracellular single unit recordings and whole-cell patch-clamp recordings confirm the presence of an onset-evoked inhibitory input to DTNs that precedes excitation and is sustained for at least as long or longer than the duration of the stimulus that evoked it (Casseday et al., 1994; Faure et al., 2003; Leary et al., 2008, Alluri et al., 2016). However, it is unclear how the strength and latency of inhibition shapes and modulates the excitatory components of duration selectivity.

This study reveals important relationships between offset evoked facilitation and sustained inhibition that are involved in generating duration selectivity in the mammalian IC. First, the data reveal that facilitation, which followed the offset of the NE tone (Fig. 4.7), typically preceded the offset of inhibition (i.e. the majority of facilitated cells responded with facilitation in Range 1 and not Range 2). This pattern has been observed in previous studies using paired tone stimulation even though facilitation was not the focus of the investigations. For instance, Valdizón-Rodríguez et al. (2017; *their* Fig. 6A) and Sayegh et al. (2014 *their* Fig. 1A and Fig. 3A) both showed cases of facilitation in Range 1. On the other hand, Faure et al. (2003; *their* Fig. 11) showed an example of a cell that was facilitated in Range 2. Range 1 and Range 2 type categories have also been described outside of paired tone stimulation. For example, Range 1 type facilitation has been reported from DTNs in the IC of *E. fuscus* using paired pulse stimulation (Sayegh et al., 2012). In delay-tuned neurons from the IC of the mustached bat (*Pteronotus parnellii*), both Range 1 and Range 2 type facilitation were observed and, much like our results, authors report that the time between facilitation and the offset of inhibition was not related to the cell's best delay (Portfors and Wenstrup, 1999). These data suggest that these two Ranges of facilitation are generally observed in the mammalian IC. To our knowledge, we are the first study to formally divide these two kinds of facilitation into separate categories, and develop different criteria for assessing the presence of facilitation in either Range.

Second, that F_{start} is offset locked and is related to the response properties observed at the cell's BD, suggests that excitation and inhibition interact, and retain their response properties, even at long, non-excitatory durations. Computational and conceptual models

of DTNs predict that the BD and range of duration selectivity will depend, in part, on the amount of time by which inhibition leads excitation (Casseday et al., 1994, 2000; Aubie et al., 2009, 2012). Furthermore, blocking of GABA or glycine receptors shortens the response latency of many IC neurons, including duration-tuned neurons, showing that the response properties of IC neurons are, at least in part, under inhibitory control (Casseday et al., 2000; Fuzessery and Hall, 1999). Previous studies have shown that baseline FSL is related to the amount of leading inhibition, BD, and duration filter class (Faure et al., 2003; Sayegh et al., 2014; Valdizón-Rodríguez and Faure, 2017). We replicated these findings and showed that the latency of facilitation (F_{start}) was also related to the amount of leading inhibition, BD, and duration filter class (Fig. 4.15). That these relationships were replicated suggests (1) that F_{start} is linked to an offset-locked excitatory input that influences the duration selective response properties of DTNs, and (2) that the excitatory and inhibitory responses of DTNs interact in a similar way across stimulus duration. In other words, individual synaptic inputs will scale their responses across stimulus duration so that no individual component of duration selectivity behaves differently at any given duration. This implies that it is the *interaction* of the unbiased components that generates duration tuning rather than a special case at the BD. Thus, the intrinsic and extrinsic synaptic components creating duration tuning behave the same way at their BD as they would at a non-excitatory duration.

Third, when the NE tone frequency, NE tone amplitude or BD tone amplitude amplitude were varied, changes to F_{Start} were more related to the onset of inhibition than the offset of inhibition (NE tone frequency – Fig. 4.9A, NE tone amplitude – Fig. 4.11A,

BD tone amplitude – Fig. 4.13A). This property is thought to play a role in preserving duration selectivity across sound frequency and amplitude. For example, Valdizón-Rodríguez and Faure (2017), report that the onset of inhibition had a relatively constant latency as frequency was varied and was broadly frequency tuned while the offset of inhibition decreased and was more narrowly tuned as the frequency was varied away from the BEF. Similarly, Faure et al. (2003) reported that the onset of inhibition was level tolerant as the BD tone amplitude was varied, whereas the offset of inhibition systematically became shorter as the BD tone amplitude increased. We hypothesize that this feature could help to retain DTN response properties as stimulus properties are varied. This is because the difference in latency between inhibition and excitation plays a role in shaping the BD, duration filter class (i.e. short-pass or bandpass), temporal bandwidth of duration tuning, and FSL (Casseday et al. 1994, 2000; Covey et al. 1996; Fuzessery and Hall, 1999; Faure et al. 2003; Aubie et al. 2009, 2012; Sayegh et al. 2014). Thus, if the timing and amplitude of offset-locked facilitation varies with the onset of inhibition during variations in stimulus properties, duration selectivity should be maintained. In support of this observation, the FSL, BD, and tuning class of DTNs were shown to be level tolerant (Fremouw et al., 2005).

Finally, our results showed that offset facilitation was virtually absent in the dichotic condition independent of whether or not inhibition was observed. The lack of offset facilitation observed in the dichotic condition suggests that monaural, contralateral neural pathways are responsible for the offset-locked excitation necessary to create duration tuning. This finding is in accordance with previous studies that have suggested

that inhibition evoked by the ipsilateral ear (re IC recorded) is shorter, weaker, and delayed compared to inhibition evoked by the contralateral ear, and is therefore unlikely to be involved in duration tuning (Sayegh et al., 2014). Future research should investigate whether DTNs can be excited when stimulated by the ipsilateral ear, and whether those excitatory responses are duration-tuned.

4.5.2 – Mechanism of Duration Selectivity

The coincidence detection model for duration-tuning (Fig. 4.1) was first proposed by Narins and Capranica following the initial discovery of duration selective neurons in the torus semicircularis of anurans (Narins and Capranica 1980). In this model, the authors propose that a transient, subtreshold, onset evoked synaptic input and a transient, subthreshold, offset evoked synaptic input to DTNs would generate suprathreshold spiking responses for a particular range of stimulus durations when the inputs were coincident. However, at longer durations or shorter durations, these inputs would fail to coincide and be subthreshold.

Other models of duration tuning have also been proposed, such as the anti-coincidence mechanism, which was first proposed to explain short-pass cells that responded to stimulus onset in the IC of the pallid bat (Fuzessery & Hall, 1999). This mechanism proposes the temporal interaction of two synaptic inputs: (1) a delayed, long latency, onset-evoked, transient excitation that is suprathreshold on its own; and an (2) an onset-evoked, sustained inhibition that precedes excitation, and lasts as long or longer than the duration of the stimulus that evoked it. The sustained inhibition only renders the onset evoked excitation subthreshold when the inputs temporally overlap. At short stimulus

durations, the latency of the onset evoked excitation is longer than the offset of the sustained inhibition, hence the excitation is suprathreshold because it does not overlap with sustained inhibition. At longer durations, spikes fail to be evoked because the sustained inhibition temporally overlaps with the excitation. Because spikes are evoked by the onset-locked excitatory synaptic input, the anti-coincidence mechanism of duration tuning accounts for onset-locked responses in short-pass DTNs.

In the mammalian IC, shortpass and bandpass DTNs exhibit phasic spiking, with first spike latencies that increase as a function of stimulus duration in a majority of cells (Casseday et al. 1994, 2000; Ehrlich et al. 1997; Fuzessery and Hall 1999; Faure et al. 2003) including the two example DTNs shown in this study (Fig. 4.3); and this observation supports the coincidence detection model of duration tuning. However, for cells that respond to a narrow range of the durations tested (i.e. Sayegh et al., 2011, *their* Fig. 2A, or Valdizón-Rodríguez and Faure 2017, *their* Fig. 1A) it is difficult to attribute an increase in latency to an offset-locked excitatory input or to a decrease in the strength of excitation which would also change the latency of a DTN (Casseday et al., 2000; Fuzessery and Hall, 1999; Alluri et. al, 2016).

Our study shows that at least one third of DTNs received an excitatory input which was offset-locked to the NE tone (Fig. 4.7) and whose responses are related to a DTN's baseline FSL (Fig. 4.15A), BD (Fig. 4.15D), amount of leading inhibition (Fig. 4.15F), and duration filter response type (shortpass vs. bandpass). This data provides strong support for the coincidence detection mechanism. In the remaining cells that did not show facilitation, it is possible that inhibition is too strong for the BD tone to reveal individual inputs of a

DTN. This is especially likely because facilitation typically occurred in Range 1 while inhibition was still occuring. Another possibility is that cells had a signal to noise ratio that was too low for facilitation to be detected – given our criteria. Finally, it is possible that some cells are using an anticoincidence mechanism. Indeed, previous studies have reported that all DTNs tested with paired tone stimulation reveal sustained inhibition that leads excitation – suggesting that all the necessary components for an anticoincidence detection model are present in most DTNs (Faure et al. 2003; Sayegh et al., 2014; Valdizón-Rodríguez and Faure 2017).

4.5.3 – Offset Locked Excitation in DTNs is Not a Rebound From Inhibition

The coincidence detection model requires an offset-locked, transient depolarization that could either be (1) a separate excitatory input from an afferent pathway to the IC or (2) an intrinsic property of the synapse such as a rebound from sustained inhibition (Fig. 4.1 – *third trace*). Whole-cell patch-clamp recordings from DTNs revealed an outward, inhibitory post-synaptic current (IPSC) that was followed by an inward excitatory post-synaptic current (EPSC) linked to stimulus offset (Casseday et al., 1994; Covey et al., 1996). In these studies, the the size of the EPSC decreased as stimulus duration increased. This was taken as evidence for a rebound from inhibition because at long durations, the IPSC would have had more time to decay and would therefore produce a weaker rebound from inhibition. Rebound from inhibition has been observed from neurons in the IC (Peruzzi et al. 2000; Koch and Grothe, 2003; Tan et al., 2007, Sun and Wu 2008). However, offset responding cells have also been found in the mammalian superior olivary complex (Grothe, 1994; Kuwada and Batra, 1999), and in the superior paraolivary nucleus (Kadner

et al., 2006) *in vivo*, both of which project to the IC (*also see* Kopp-Scheinplug et al., 2018 for review).

We found no evidence to suggest that the offset-locked, transient depolarization – measured as facilitation– was a rebound from inhibition in our study. There were multiple lines of evidence for this: first, facilitation preceded the offset of inhibition in a majority of DTNs. Second, when NE tone frequency, NE tone amplitude, or BD tone amplitude were varied, we found that the timing of facilitation was more related to the onset of inhibition (which had a relatively constant latency) than the offset of inhibition, and the strength and latency of facilitation was altered in a way that either supported OR changed in the direction of a separate, extrinsic excitatory input. Furthermore, when DTNs showed evidence of ipsilateral inhibition during dichotic paired tone stimulation, ipsilateral facilitation was never observed and, conversely, ipsilateral facilitation was sometimes observed without inhibition – this evidence shows that facilitation occurred independent of inhibition. Finally, we found that the latency of facilitation (re BD tone onset) was longer than the cell's baseline FSL in most neurons – which suggests that excitation was delayed by inhibition. That we could not find a single piece of evidence in favour of a rebound from inhibition shows that it is not a likely candidate for the offset-locked, transient depolarization required by the coincidence detection model. Rather, a separate excitatory synaptic input from an afferent pathway that projects to IC is more likely.

Extracellular recordings have revealed that an offset locked excitatory response was observed in DTNs even after blocking inhibition (Casseday et al., 2000). In support of our conclusion, the authors argue that this could be evidence of separate, excitatory input to

DTNs. Moreover, *in vivo*, whole-cell recordings from duration-selective neurons in the anuran torus semicircularis also suggest that a rebound from inhibition is not present in DTNs (Leary et al., 2008). The authors show that sustained inhibition showed no evidence of postinhibitory rebound when stimulus frequency and/or duration were varied in either shortpass or bandpass cells. Another study measuring *in vivo*, whole-cell recordings from DTNs in the torus semicircularis, isolated inhibition by iontophoresing pharmacological antangonists to block AMPA and NMDA glutamate receptors, thereby attenuating excitation (Alluri et al., 2016). Again, the study found no evidence of a rebound from inhibition. However, both of these studies showed evidence for an anti-coincidence mechanism of duration selectivity; which cannot explain offset-locked facilitation.

Computational modelling of the coincidence detection mechanism using a postinhibitory rebound showed that the resulting responses gave band-reject duration selectivity and not bandpass or shortpass selectivity. This occurred because the postinhibitory rebound failed to produce suprathreshold excitation in the model cell at the shortest durations – except at some intermediate durations when it overlapped with the onset evoked excitation. However, post-inhibitory rebound at much longer durations became sufficiently strong to evoke spiking (Aubie et al., 2009). This resulted in a band of intermediate durations that did not evoke spiking. The same study showed that when the offset evoked, excitatory input was a separate, extrinsic component in the model, many of the response properties recorded *in vivo* from DTNs were reproduced. Our observations provide support for the the predictions made by this model.

4.5.4 – Level-Tolerance of DTNs is Incompatible with a Rebound from Inhibition

Previous research on DTNs has shown that a cell's FSL, BD, and duration filter class do not vary as a function of stimulus level (Zhou and Jen 2001; Fremouw et al. 2005; Valdizón-Rodríguez and Faure 2017). This suggests that inhibition and excitation are balanced across sound pressure level. If the strength of inhibition increased faster than that of excitation, FSLs should lengthen and the cell should demonstrate a paradoxical latency shift (PLS) at increasing SPLs (Covey et al. 1996; Galazyuk et al. 2005; Galazyuk and Feng, 2001; Hechavarría et al. 2011; Hechavarría and Kössl, 2014; Klug et al. 2000; Macías et al. 2016; Sullivan, 1982a, 1982b). Conversely, if the strength of excitation increased faster than that of inhibition, FSLs would be expected to decrease at louder SPLs as is the case for most central auditory neurons (Heil, 2004; Klug et al. 2000; Mörchen et al. 1978; Rose et al. 1963; Tan et al. 2008).

Our data shows that the latency of facilitation (F_{start}) increases as the amplitude was NE tone increases. This shows that the latency of facilitation was under inhibitory control and was not level tolerant. However, one must remember that it is only when the offset-locked, excitatory input (Fig. 4.1 – trace labeled *OFF EPSP*) coincides with the onset-locked, excitatory input (Fig. 4.1 – trace labeled *ON EPSP*) that spiking becomes suprathreshold and thus level tolerant. This shows that level tolerance is created and calibrated in the IC by a combination of inputs that are modulated by inhibition.

Finally, we hypothesize that if a rebound from inhibition were a component of duration selective circuits, level tolerance (or alternatively PLS) observed in DTNs would

be unlikely for two reasons. The first is that both the onset-evoked excitation and post-inhibitory rebound would shorten their response latency as stimulus level is increased (Heil, 2004; Sun and Wu 2008). Secondly, spiking would follow release from inhibition (i.e. "post-inhibitory" rebound) and thus excitation would have little or no modulation by inhibition. Thus, the cell's first spike latency could only decrease as stimulus amplitude was increased. This pattern is displayed by most auditory neurons – wherein a cell's first spike latency becomes shorter as stimulus level is increased. However, this type of latency change is not supported by the literature on duration selectivity. Thus, having inhibition as a separate, modulatory input is more parsimonious than a post-inhibitory rebound, even though fewer temporally coordinated inputs would be required by the latter.

4.5.5 – Facilitation in recovery cycles

The recovery time of a neuron is measured using paired pulse stimulation and is defined as the shortest ISI required for a neuron's response to a second stimulus to recover within a specified criterion (i.e. spike count or latency) of the response evoked by a first stimulus (Grinnell 1963). Indeed, paired tone stimulation, used in the present study, is very similar to paired-pulse stimulation, except that paired-pulse stimulation uses equal duration stimuli whereas paired tone stimulation has different durations for the NE and BD tones.

Facilitation has been observed during paired-pulse stimulation of DTNs and non-DTNs in the IC of *E. fuscus* (Sayegh et al., 2012). The authors report that when the cell was stimulated with tone pairs, both set to the cell's BD, and randomly varied in ISI, a brief facilitatory response was observed, followed by spike suppression. However, the combined proportion of DTNs and non-DTNs showing facilitation was very low (9/132 = 6.8%). This

proportion is very different from the nearly one third of DTNs observed in this study. This suggests that facilitation observed during recovery cycles is fundamentally different than that observed during paired tone stimulation. This result can be understood by recalling that facilitation is the result the of a subthreshold, offset-locked, excitatory input (Fig. 4.1 – trace labeled *OFF EPSP*) that coincides with a subthreshold, onset-locked, excitatory input (Fig. 4.1 – trace labeled *ON EPSP*) to elicit suprathreshold spiking at the cell's BD – as predicted by the coincidence detection model. This implies that offset-locked facilitation should be nearly absent during paired-pulse stimulation because both tones are set to the cell's BD and therefore the offset-locked excitatory input would be coincident and indiscernible from the onset evoked excitatory input. Thus the rarity of facilitation reported by Sayegh et al. (2012) supports our conclusion that offset-locked facilitation is related to the offset-locked depolarization in the coincidence detection mechanism.

Another study utilized a paradigm that mirrored pulse-echo pairs during echolocation, and found that a number of DTNs in the inferior colliculus of the mustached bat (*Pteronotus parnellii*) were also delay-tuned (Macías et al., 2013). These cells showed facilitation at some pulse-echo delays when they were tested with equal duration, BD pulse-echo tones – with the pulse played at a non-excitatory harmonic of the BEF, and the echo played at BEF and varied in amplitude. The authors found that a cell's BD was strongly related to that cell's best delay. Our results can help to elucidate a mechanism for this observation. We found that as the NE tone frequency was moved away from a DTN's BEF, the latency of facilitation became longer. It is possible that a delay is created in one or both of the excitatory components when stimulating at a non-excitatory frequency. This is

especially likely since inhibition is much more broadly tuned than excitation in DTNs (Leary et al., 2008; Valdizón-Rodríguez and Faure, 2017) and thus non-excitatory frequencies would have more inhibition than excitation. Therefore facilitation would be observed as delay tuning. The fact that the cell's best delay was related to BD further supports this hypothesis given that we found that F_{start} was related to a cell's BD (Fig. 4.15D). This kind of feature would allow DTNs to analyze sonar targets along multiple dimensions.

4.6 – References

Alluri RK, **Rose GJ**, **Hanson JL**, **Leary CJ**, **Vasquez-Opazo GA**, **Graham JA**, **Wilkerson J**. Phasic, suprathreshold excitation and sustained inhibition underlie neuronal selectivity for short-duration sounds. *Proc Natl Acad Sci* 113: E1927–E1935, 2016.

Aubie B, **Becker S**, **Faure PA**. Computational models of millisecond level duration tuning in neural circuits. *J Neurosci* 29: 9255–9270, 2009.

Aubie B, **Sayegh R**, **Faure PA**. Duration tuning across vertebrates. *J Neurosci* 32: 6373–6390, 2012.

Brand A, **Urban R**, **Grothe B**. Duration tuning in the mouse auditory midbrain. *J Neurophysiol* 84: 1790–1799, 2000.

Brugge JF, **Dubrovsky NA**, **Aitkin LM**, **Anderson DJ**. Sensitivity of single neurons in auditory cortex of cat to binaural tonal stimulation; effects of varying interaural time and intensity. *J Neurophysiol* 32: 1005–1024, 1969.

Casseday JH, **Covey E**. Mechanisms for analysis of auditory temporal patterns in the brainstem of echolocating bats. In: *Neural Representation of Temporal Patterns*, edited by Covey E, Hawkins HL, Port RF. Boston, MA: Springer US, 1995, p. 25–51.

Casseday JH, **Ehrlich D**, **Covey E**. Neural tuning for sound duration: role of inhibitory mechanisms in the inferior colliculus. *Science* 264: 847–850, 1994.

Casseday JH, **Ehrlich D**, **Covey E**. Neural measurement of sound duration: control by excitatory-inhibitory interactions in the inferior colliculus. *J Neurophysiol* 84: 1475–1487, 2000.

Chen G-D. Effects of stimulus duration on responses of neurons in the chinchilla inferior

colliculus. *Hear Res* 122: 142–150, 1998.

Covey E, **Kauer JA**, **Casseday JH**. Whole-cell patch-clamp recording reveals subthreshold sound-evoked postsynaptic currents in the inferior colliculus of awake bats. *J Neurosci* 16: 3009–3018, 1996.

Ehrlich D, **Casseday JH**, **Covey E**. Neural tuning to sound duration in the inferior colliculus of the big brown bat, *Eptesicus fuscus*. *J Neurophysiol* 77: 2360–2372, 1997.

Faure PA, **Fremouw T**, **Casseday JH**, **Covey E**. Temporal masking reveals properties of sound-evoked inhibition in duration-tuned neurons of the inferior colliculus. *J Neurosci* 23: 3052–3065, 2003.

Fremouw T, **Faure PA**, **Casseday JH**, **Covey E**. Duration selectivity of neurons in the inferior colliculus of the big brown bat: tolerance to changes in sound level. *J Neurophysiol* 94: 1869–1878, 2005.

Fuzessery ZM, **Hall JC**. Sound duration selectivity in the pallid bat inferior colliculus. *Hear Res* 137: 137–154, 1999.

Galazyuk A V, **Feng AS**. Encoding of sound duration by neurons in the auditory cortex of the little brown bat, *Myotis lucifugus*. *J Comp Physiol A* 180: 301–311, 1997.

Galazyuk A V, **Feng AS**. Oscillation may play a role in time domain central auditory processing. *J Neurosci* 21: 147–147, 2001.

Galazyuk A V, **Lin W**, **Llano D**, **Feng AS**. Leading inhibition to neural oscillation is important for time-domain processing in the auditory midbrain. *J Neurophysiol* 94: 314–326, 2005.

Gooler DM, **Feng AS**. Temporal coding in the frog auditory midbrain: the influence of

duration and rise-fall time on the processing of complex amplitude-modulated stimuli. *J Neurophysiol* 67: 1–22, 1992.

Grinnell AD. The neurophysiology of audition in bats: temporal parameters. *J Physiol* 167: 67–96, 1963.

Grothe B. Interaction of excitation and inhibition in processing of pure tone and amplitude-modulated stimuli in the medial superior olive of the mustached bat. *J Neurophysiol* 71: 706–721, 1994.

He J, **Hashikawa T**, **Ojima H**, **Kinouchi Y**. Temporal integration and duration tuning in the dorsal zone of cat auditory cortex. *J Neurosci* 17: 2615–2625, 1997.

Hechavarría JC, **Cobo AT**, **Fernández Y**, **Macías S**, **Kössl M**, **Mora EC**. Sound-evoked oscillation and paradoxical latency shift in the inferior colliculus neurons of the big fruit-eating bat, *Artibeus jamaicensis*. *J Comp Physiol A* 197: 1159–1172, 2011.

Hechavarría JC, **Kössl M**. Footprints of inhibition in the response of cortical delay-tuned neurons of bats. *J Neurophysiol* 111: 1703–1716, 2014.

Heil P. Auditory cortical onset responses revisited. I. first-spike timing. *J Neurophysiol* 77: 2616–2641, 1997.

Heil P. First-spike latency of auditory neurons revisited. *Curr. Opin. Neurobiol.* 14: 461–467, 2004.

Jen PH-S, **Feng RB**. Bicuculline application affects discharge pattern and pulse-duration tuning characteristics of bat inferior collicular neurons. *J Comp Physiol A* 184: 185–194, 1999.

Jen PH-S, **Wu CH**. The role of GABAergic inhibition in shaping the response size and

duration selectivity of bat inferior collicular neurons to sound pulses in rapid sequences. *Hear Res* 202: 222–234, 2005.

Kadner A, **Kulesza RJ**, **Berrebi AS**. Neurons in the medial nucleus of the trapezoid body and superior paraolivary nucleus of the rat may play a role in sound duration coding. *J Neurophysiol* 95: 1499–1508, 2006.

Klug A, **Khan A**, **Burger RM**, **Bauer EE**, **Hurley LM**, **Yang L**, **Grothe B**, **Halvorsen MB**, **Park TJ**. Latency as a function of intensity in auditory neurons: influences of central processing. *Hear Res* 148: 107–123, 2000.

Koch U, **Grothe B**. Hyperpolarization-Activated Current (I_h) in the Inferior Colliculus: Distribution and Contribution to Temporal Processing. *J Neurophysiol* 90: 3679–3687, 2003.

Kopp-Scheinpflug C, **Sinclair JL**, **Linden JF**. When Sound Stops: Offset Responses in the Auditory System. *TINS* 41: 712–728, 2018.

Kuwada S, **Batra R**. Coding of sound envelopes by inhibitory rebound in neurons of the superior olivary complex in the unanesthetized rabbit. *J Neurosci* 19: 2273–2287, 1999.

Kuwada S, **Batra R**, **Yin TCT**, **Oliver DL**, **Haberly LB**, **Stanford TR**. Intracellular recordings in response to monaural and binaural stimulation of neurons in the inferior colliculus of the cat. *J Neurosci* 17: 7565–7581, 1997.

Leary CJ, **Edwards CJ**, **Rose GJ**. Midbrain auditory neurons integrate excitation and inhibition to generate duration selectivity: an in vivo whole-cell patch study in anurans. *J Neurosci* 28: 5481–5493, 2008.

Macías S, **Hechavarría JC**, **Kössl M**. Sharp temporal tuning in the bat auditory

midbrain overcomes spectral-temporal trade-off imposed by cochlear mechanics. *Sci Rep* 6, 2016.

Macias S, **Hechavarria JC**, **Kossl M**, **Mora EC**. Neurons in the inferior colliculus of the mustached bat are tuned both to echo-delay and sound duration. *Neuroreport* 24: 404–409, 2013.

Mora EC, **Kössl M**. Ambiguities in sound-duration selectivity by neurons in the inferior colliculus of the bat Molossus molossus from Cuba. *J Neurophysiol* 91: 2215–2226, 2004.

Mörchen A, **Rheinlaender J**, **Schwartzkopff J**. Latency shift in insect auditory nerve fibers. *Naturwissenschaften* 65: 656–657, 1978.

Morrison JA, **Farzan F**, **Fremouw T**, **Sayegh R**, **Covey E**, **Faure PA**. Organization and trade-off of spectro-temporal tuning properties of duration-tuned neurons in the mammalian inferior colliculus. *J Neurophysiol* 111: 2047–60, 2014.

Narins PM, **Capranica RR**. Neural adaptations for processing the two-note call of the Puerto Rican treefrog, Eleutherodactylus coqui. *Brain. Behav. Evol.* 17: 48–66, 1980.

Park TJ, **Pollak GD**. GABA shapes a topographic organization of response latency in the mustache bat's inferior colliculus. *J Neurosci* 13: 5172–5187, 1993.

Pérez-González D, **Malmierca MS**, **Moore JM**, **Hernández O**, **Covey E**. Duration selective neurons in the inferior colliculus of the rat: topographic distribution and relation of duration sensitivity to other response properties. *J Neurophysiol* 95: 823–836, 2006.

Peruzzi D, **Sivaramakrishnan S**, **Oliver DL**. Identification of cell types in brain slices of the inferior colliculus. *Neuroscience* 101: 403–416, 2000.

Pinheiro AD, **Wu M**, **Jen PS**. Encoding repetition rate and duration in the inferior colliculus of the big brown bat, *Eptesicus fuscus*. *J Comp Physiol A* 169: 69–85, 1991.

Portfors C V, **Wenstrup JJ**. Delay-tuned neurons in the inferior colliculus of the mustached bat: implications for analyses of target distance. *J Neurophysiol* 82: 1326–1338, 1999.

Potter HD. Patterns of acoustically evoked discharges of neurons in the mesencephalon of the bullfrog. *J Neurophysiol* 28: 1155–1184, 1965.

Rose JE, **Greenwood DD**, **Goldberg JM**, **Hind JE**. Some discharge characteristics of single neurons in the inferior colliculus of the cat. I. Tonotopical organization, relation of spike counts to tone intensity, and firing patterns of single elements. *J Neurophysiol* 26: 294–320, 1963.

Sayegh R, **Aubie B**, **Faure PA**. Duration tuning in the auditory midbrain of echolocating and non-echolocating vertebrates. *J Comp Physiol A* 197: 571–583, 2011.

Sayegh R, **Aubie B**, **Fazel-Pour S**, **Faure PA**. Recovery cycles of inferior colliculus neurons in the big brown bat measured with spike counts and latencies. *Front Neural Circuits* 6: 56, 2012.

Sayegh R, **Casseday JH**, **Covey E**, **Faure PA**. Monaural and binaural inhibition underlying duration-tuned neurons in the inferior colliculus. *J Neurosci* 34: 481–92, 2014.

Schnitzler H-U, **Kalko EK V**. Echolocation by insect-eating bats. *Bioscience* 51: 557–569, 2001.

Shannon R V, **Zeng FG**, **Kamath V**, **Wygonski J**, **Ekelid M**. Speech recognition with

primarily temporal cues. *Science* 270: 303–304, 1995.

Sullivan WE. Possible neural mechanisms of target distance coding in auditory system of the echolocating bat *Myotis lucifugus*. *J Neurophysiol* 48: 1033–1047, 1982a.

Sullivan WE. Neural representation of target distance in auditory cortex of the echolocating bat *Myotis lucifugus*. *J Neurophysiol* 48: 1011–1032, 1982b.

Sun H, **Wu SH**. Physiological characteristics of postinhibitory rebound depolarization in neurons of the rat's dorsal cortex of the inferior colliculus studied in vitro. *Brain Res* 1226: 70–81, 2008.

Tan ML, **Theeuwes HP**, **Feenstra L**, **Borst JGG**. Membrane properties and firing patterns of inferior colliculus neurons: an in vivo patch-clamp study in rodents. *J Neurophysiol* 98: 443–453, 2007.

Tan X, **Wang X**, **Yang W**, **Xiao Z**. First spike latency and spike count as functions of tone amplitude and frequency in the inferior colliculus of mice. *Hear Res* 235: 90–104, 2008.

Valdizón-Rodríguez R, **Faure PA**. Frequency tuning of synaptic inhibition underlying duration-tuned neurons in the mammalian inferior colliculus. *J Neurophysiol* 117: 1636–1656, 2017.

Voytenko S V, **Galazyuk A V**. Timing of sound-evoked potentials and spike responses in the inferior colliculus of awake bats. *Neuroscience* 155: 923–936, 2008.

Wang J, **van Wijhe R**, **Chen Z**, **Yin S**. Is duration tuning a transient process in the inferior colliculus of guinea pigs? *Brain Res* 1114: 63–74, 2006.

Wu C-H, **Jen PH-S**. The role of GABAergic inhibition in shaping duration selectivity of

bat inferior collicular neurons determined with temporally patterned sound trains. *Hear Res* 215: 56–66, 2006a.

Wu CH, **Jen PH-S**. GABA-mediated echo duration selectivity of inferior collicular neurons of Eptesicus fuscus, determined with single pulses and pulse-echo pairs. *J Comp Physiol A Neuroethol Sensory, Neural, Behav Physiol* 192: 985–1002, 2006b.

Zhou X, **Jen PH-S**. The effect of sound intensity on duration-tuning characteristics of bat inferior collicular neurons. *J Comp Physiol A Sensory, Neural, Behav Physiol* 187: 63–73, 2001.

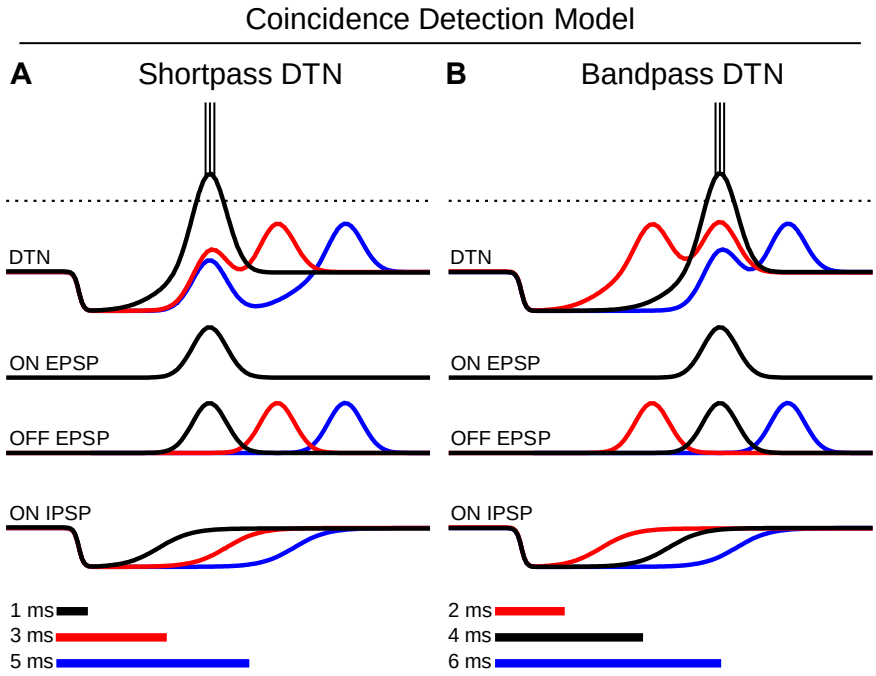

Figure 4.1. Coincidence detection model for duration selectivity in a short-pass and a bandpass DTN.

The bottom of each panel shows three stimuli of different stimulus durations represented with different *colors*. The hypothetical trace of the postsynaptic potentials resulting from the presentation of each stimulus to a DTN is shown in the corresponding color. The BD stimulus and response of the cell to a BD tone are shown in *black*. In each column, the *top trace* shows the net postsynaptic change in the membrane potential of the DTN and, if suprathreshold, its spike output (the spiking threshold of the DTN is indicated by a *dotted line*). The model has three components illustrated: (1) a delayed, transient onset-evoked, subthreshold EPSP (ON EPSP; *second trace*); (2) a transient offset-evoked EPSP (OFF EPSP; *third trace*) and (3) an onset-evoked sustained IPSP (ON IPSP; *bottom trace*). A DTN only spikes when the ON EPSP coincides with the OFF EPSP. The BD and temporal

range of duration selectivity of the cell is determined by the duration of the ON EPSP and its latency relative to the IPSP. Panel *A* shows a shortpass DTN with a BD = 1ms. When the cell is presented with a 1 ms stimulus (*black bar*), the ON EPSP coincides with the OFF EPSP (*middle black trace*), and the net postsynaptic membrane potential for the cell is suprathreshold (*top black trace*). When the cell is presented with a 3 ms tone (r*ed bar*) or a 5 ms tone (*blue bar*), the ON and OFF EPSPs do not coincide and are rendered subthreshold by the ON IPSP. Panel *B* shows a bandpass DTN with a BD = 4ms. For the 2 ms tone, the OFF EPSP occurs before the ON EPSP (*red bar and traces*). For the 4 ms tone, the OFF EPSP coincides with the ON EPSP, and the summation pushes the membrane potential of the cell above spike threshold (*black bar and traces*). For the 6 ms tone, the ON EPSP occurs before the OFF EPSP and is rendered subthreshold by the sustained inhibition (*blue bar and traces*). Models were adapted and modified from Faure et al. (2003), Leary et al., (2008), and Aubie et al. (2009, 2012).

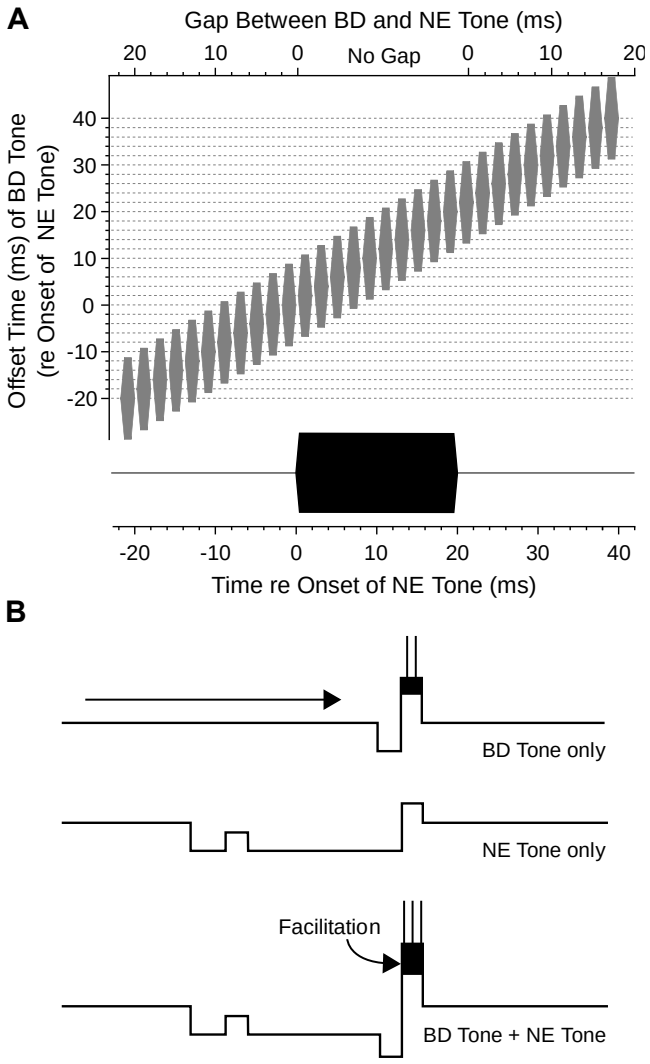

Figure 4.2. Paired tone stimulation and theoretical model of offset facilitation in DTNs.

A, Illustration of the temporal relationships between sound stimuli during paired tone stimulation. The onset time of the NE tone (*20 ms black pulse*) was fixed in time across stimulus presentations whereas the onset time of the BD tone (*2 ms grey pulses*) was randomly varied relative to the onset of the NE tone. A single composite tone resulted when

the two tones temporally overlapped and summed. *B*, Hypothetical postsynaptic membrane potentials of a duration-tuned neuron in response to a 2 ms BD tone by itself (*top trace*) that was varied in temporal position (*black arrow*) relative to a 20 ms NE tone by itself (*middle trace*) and the sum of the membrane potentials evoked from each of the two tones (*bottom trace*). As the temporal position of the BD tone is roved with regard to the onset of the NE tone, an interaction between the membrane potentials evoked from the two tones results in a facilitated EPSP. This would typically result when the BD tone is near the offset of the NE tone. Thus, the time and strength of the underlying excitatory (or inhibitory) inputs to DTNs can be measured when the evoked responses from the BD and NE tones overlapped with the NE tone evoked response. Each of the three traces are inferred from models shown in **Figure 4.1**. The membrane potentials in this figure are drawn as square waves which are meant to illustrate the temporal sequence of events during paired tone stimulation rather than the exact strength of the inputs. The *black* portion of the *BD Tone only trace* indicates the suprathreshold portion of the postsynaptic potentials which resulted in spiking.

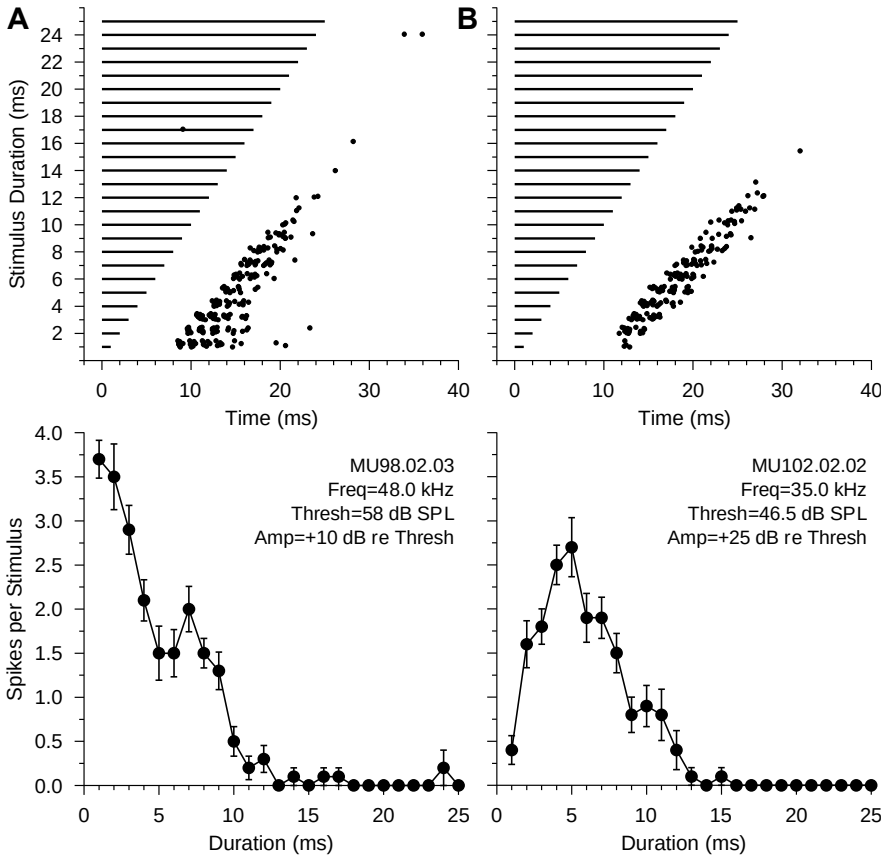

Figure 4.3. Bandpass and shortpass duration-tuned neurons from the inferior colliculus (IC) of the big brown bat.

A, Duration tuning response profile of a shortpass DTN with BD = 1 ms. *B*, Duration tuning response profile of a bandpass DTN with BD = 5ms. The *top row* shows dot raster displays illustrating the timing of the spikes recorded from DTNs in response to a series BEF tones of variable duration randomly presented. The *bottom row* shows the mean ± SE spikes per stimulus as a function of stimulus duration (n=10 trials per stimulus).

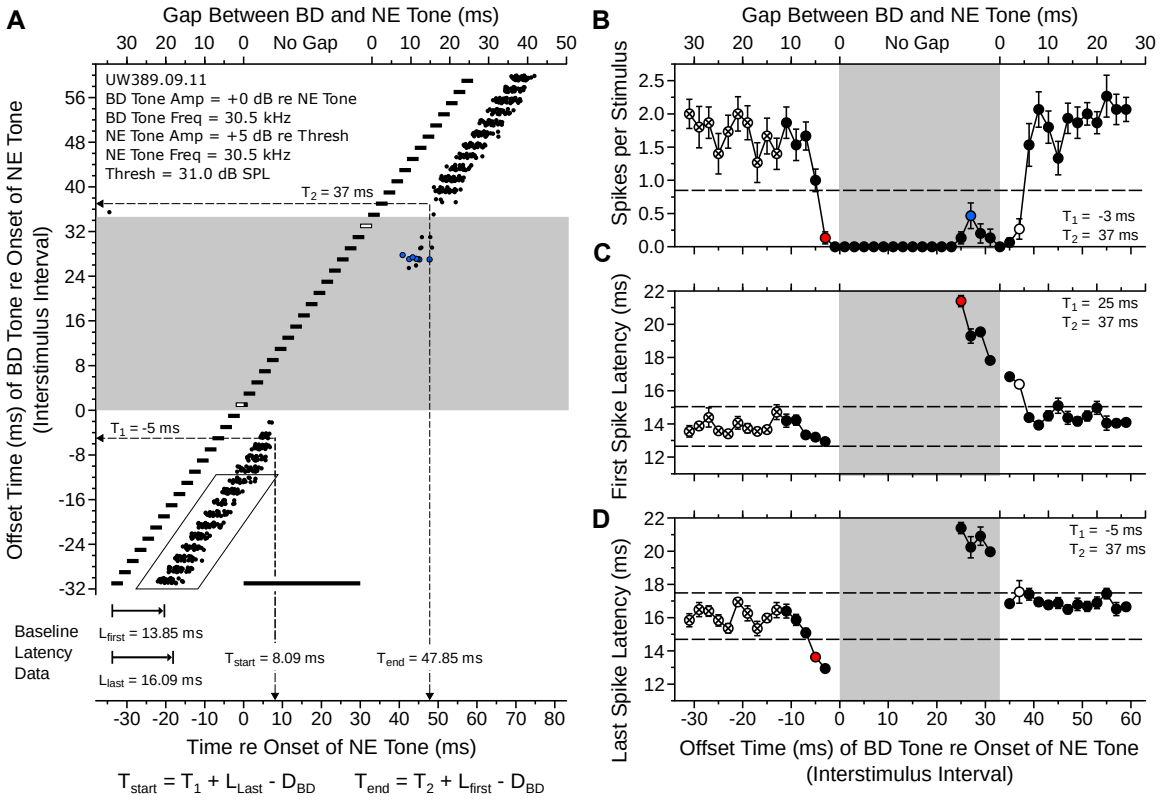

Figure 4.4. Measuring inhibition with paired tone stimulation.

A, Dot raster display from a short-pass DTN demonstrating how the time course of inhibition evoked by the NE tone was measured using changes in the cell's spike count and/or latencies in response to a roving BD tone. In this example, the BD and NE tones were matched in frequency and amplitude but differed in duration. The onset time of the NE tone (30 ms *black bar*, drawn once for clarity) was constant whereas the onset time of the BD tone (3 ms *black bars*) was randomly varied relative to NE tone onset. The top *x-axis* shows the gap (ISI) between the BD and NE tones. The bottom *x-axis* shows time relative to the onset of the NE tone. The *y-axis* shows the offset time of the BD tone relative to the onset time of the NE tone (i.e. the ISI). The BD and NE tones were electronically

mixed and presented monaurally to the ear contralateral to the recorded IC. When the two tones temporally overlapped (*gray box*), a single compound stimulus with an amplitude pedestal resulted. The BD tone bars with a *white fill* display ISIs when the BD and NE tones overlapped or were contiguous. Spikes evoked by the BD tone at the 10 longest ISIs when the BD tone preceded the NE tone (spikes in *parallelogram*) were used to calculate the mean ± SD baseline spike count (1.70 ± 1.02 spikes per stimulus), baseline FSL (L_{first} = 13.85 ± 1.19 ms), and baseline LSL (L_{last} = 16.09 ± 1.40 ms). Note how BD tone-evoked responses were suppressed by NE tone-evoked inhibition when the two tones where sufficiently close in time. Three separate criteria regarding changes to the spike count, FSL, and/or LSL were used to determine the onset (T_1) and offset (T_2) of inhibition evoked by the NE tone. The shortest ISI with a significant deviation from the baseline spike count and/or latency was T_1 = -5 ms and was obtained with a LSL criterion. The longest positive ISI with a significant deviation from the baseline spike count and/or latency was T_2 = 37 ms and could be obtained using either a spike count, LSL, or FSL criterion. Using the equations shown, T_{start} = 8.09 ms, T_{end} = 47.85 ms, and the duration of inhibition (T_{end} – T_{start}) = 39.76 ms. *Blue circles* show facilitated spikes. *B*, Mean ± SE spikes per stimulus as a function of the ISI between the BD and NE tones. The *dashed line* represents 50% of the baseline spike count. The *red circle* shows the first ISI with a spike count below 50% of baseline (T_1 = -5 ms). The *open circle* shows the last ISI with a spike count below 50% of baseline (T_2 = 37 ms). This cell showed facilitation at an ISI = 27 ms shown by the *blue circle*. *C*, Mean ± SE FSL as a function of the ISI between the BD and NE tones. The *dashed lines* represent ± 1 SD from the baseline FSL. The *red circle* shows the first ISI

when the FSL deviated by > 1 SD from baseline (T_1 = 25 ms). The *open circle* shows the last ISI when the FSL remained deviated by > 1 SD from baseline (T_2 = 37 ms). *D*, Mean ± SE LSL as a function of the ISI between the BD and NE tones. The *dashed lines* represent ± 1 SD from the baseline LSL. The *red circle* shows the first ISI when the LSL deviated by > 1 SD from baseline (T_1 = -5 ms). The *open circle* shows the last ISI when the LSL remained deviated by > 1 SD from baseline (T_2 = 37 ms). *Crossed circles* show the 10 longest ISIs when the BD tone preceded the NE tone, and these data points were used to calculate the mean ± SD baseline (*B*) spike count, (*C*) FSL, and (*D*) LSL. n = 10 trials per stimulus.

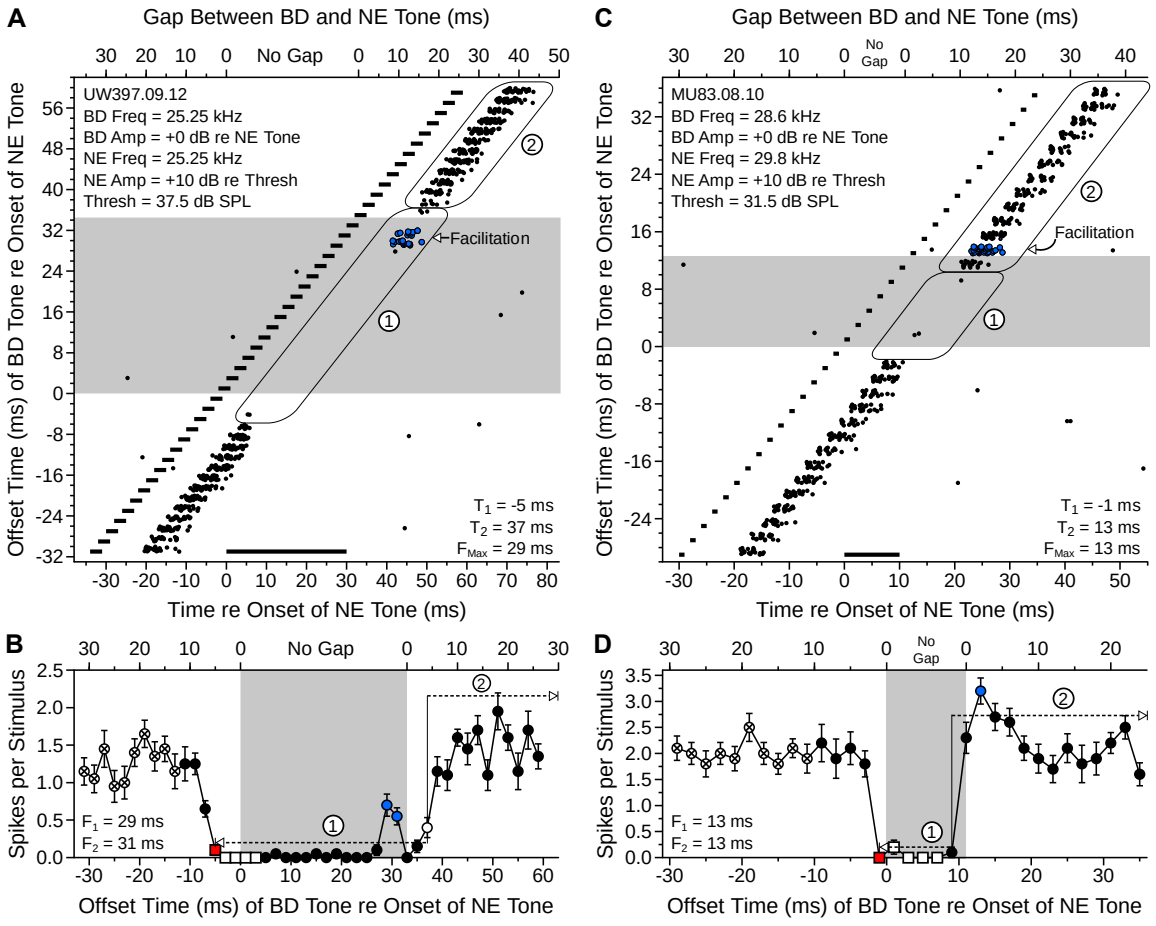

Figure 4.5. Measuring the strength and time course of facilitation with paired tone stimulation.

The *top panels* show dot raster displays of spikes evoked from two different shortpass DTNs presented with paired tone stimulation. The *bottom panels* show the mean ± SE spikes per stimulus plotted as a function of the interstimulus interval between the BD and NE tones. *A,* To quantify the time we applied different criteria to two different ranges of ISIs that were measured. To setup our threshold criteria, we divided the ISIs measured during paired tone stimulation into two ranges: Range 1 (*parallelogram 1*) contained ISIs

that occurred during NE tone-evoked inhibition (i.e. between, T_1 and T_2 obtained with a spike count criterion), and Range 2 (*parallelogram 2*) contained ISIs that occurred after the offset of inhibition (i.e. the longest positive ISIs starting at and including T2 obtained with a spike count criterion). These ranges were used to find the effective onset (F_1) and offset (F_2) of facilitation evoked by the NE tone (*blue filled circles*). *B,* For Range 1 (*dashed line 1*) spike counts were said to be facilitated if the average spike count at a given ISI was >1 SD above the mean spike count measured from the five (5) shortest ISIs following T1 measured with a spike count criterion (*5 squares* under *dashed line 1*) OR a criterion of > 0.2 spikes per stimulus with the more conservative criterion between the two being used. In this case the mean + 1 SD criterion was 0.02 + 0.061 = 0.081 spikes per stimulus, thus responses had to be >0.2 spikes per stimulus to be considered as facilitated during Range 1. For Range 2 (*dashed line 2*) spike counts were said to be facilitated if the average spike count at a given ISI was >1 SD above the mean spike count measured from the ten (10) longest negative ISIs (*10 leftmost crossed circles*), illustrating that spike counts during Range 2 had to be > mean + 1 SD = 1.26 + 0.896 = 2.156 spikes per stimulus to be considered facilitated. The leftmost *blue circle* shows first ISI to be deviated by >1 SD above the basline spike count (F_1 = 29 ms). The rightmost *blue circle* shows the largest consecutive ISI with a significant deviation from the baseline spike count (F_2 = 31 ms). In this cell, facilitation was concurrent with NE tone-evoked inhibition and thus occurred during Range 1. The ISI with the largest, facilitated spike count (F_{Max}) occurred at 29 ms. Inhibtion was also measured in this cell; the final value of T_1 = -5 ms is shown with a *red square*, and the final value of T_2 = 37 ms shown is shown with an *open circle*. C, For this

cell, Range 1 (*parallelogram 1*) did not contain facilitation while Range 2 (*parallelogram 2*) showed facilitation shown by the *blue circles* on the raster plot. *D,* Mean spike count + 1 SD measured from the five (5) shortest ISIs following T_1 measured with a spike count criterion (*5 squares* under *dashed line 1*) was less than 0.2 (Mean spike count + 1 SD = 0.04 + 0.084 spikes per stimulus = 0.124 spikes per stimulus) therefore a criterion of > 0.2 spikes per stimulus was used to detect facilitation (*dashed line 1*). For Range 2 (*dashed line 2*) spike counts were said to be facilitated if the average spike count at a given ISI was >1 SD above the mean spike count measured from the ten (10) longest negative ISIs (*10 leftmost crossed circles*), thus spike counts during Range 2 had to be > mean + 1 SD = 2.01 + 0.719 spikes per stimulus = 2.729 spikes per stimulus to be considered facilitated. The *open circle* shows the first and last ISIs deviated from the baseline spike count ($F_1 = F_2 = F_{Max}$ = 13 ms). In this cell, facilitation occurred in Range 2 after the end of the NE tone-evoked inhibition. Inhibtion was also measured in this cell; the final value of T_1 = -1 ms is shown with a *red square*, and the final value of T_2 = 37 ms overlaps with facilitation which is shown with a *blue circle*.

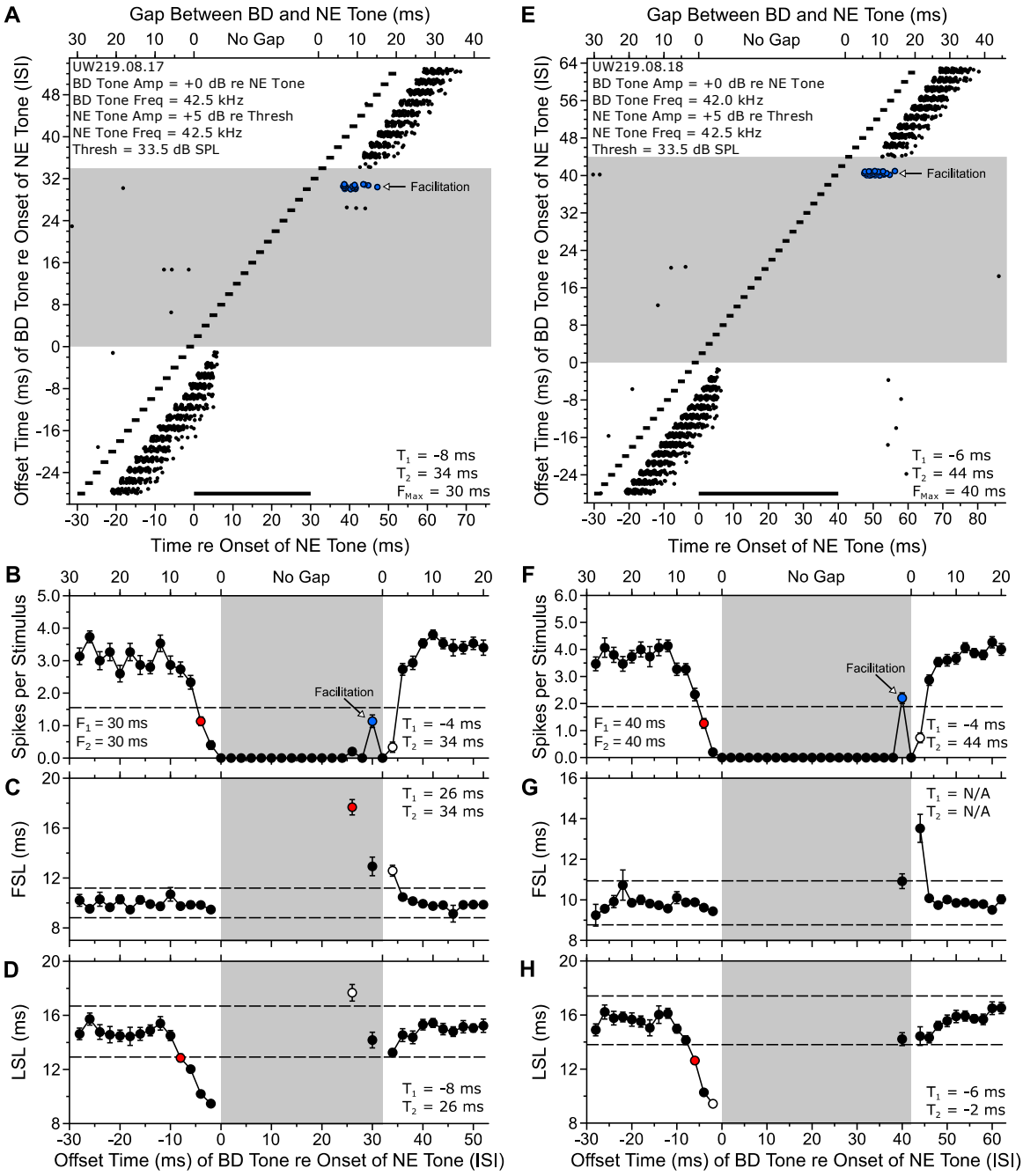

Figure 4.6. Inhibition and facilitation evoked with NE tones of different durations.

Dot raster displays illustrating responses from a shortpass DTN with the NE tone presented at 30 ms (left) and at 40 ms (right). A, When the NE tone was presented with a duration of

30 ms and the BD tone was presented with a duration of 2 ms, strong suppression was observed when the two tones were sufficiently close in time. Blue circles on raster plot show where facilitation occurred. B, Mean ± SE spikes per stimulus as a function of the ISI between the BD and NE tones. The shortest ISI in which the spike count first dropped to ≤50% of baseline was T_1 = -4 ms (red circle). The longest ISI, starting from T_1, in which the spike count remained at ≤50% of baseline was T_2 = 34 ms (open circle). Facilitation was also observed at an ISI of $F_1 = F_2 = F_{Max}$ = 30 ms (blue circle) with a spike count of 1.13 spikes per stimulus which was more than 1 SD above the baseline spike count measured during inhibition of 0.31 ± 0.20 spikes per stimulus. The latency of spikes (re NE tone onset) at this ISI was Fstart = 40.93 ms relative to the onset of the NE tone. C, Mean ± SE FSL as a function of the ISI between the BD and NE tones. The shortest ISI in which the FSL deviated by >1 SD from baseline was T_1 = 26 ms (red circle), and the longest ISI in which the FSL deviated by >1 SD from baseline was T_2 = 34 ms (open circle). D, Mean ± SE LSL as a function of the ISI between the BD and NE tones. The shortest ISI in which the LSL deviated by >1 SD from baseline was T_1 = -8 ms (red circle), and the longest ISI in which the FSL deviated by >1 SD from baseline was T_2 = 26 ms (open circle). In the 30 ms condition, the final value of T_1 (-8 ms) was determined with a LSL criteria and the final value of T_2 (34 ms) was determined with a spike count and FSL criterion. The onset of the NE tone evoked inhibition led the excitatory FSL by 5.20 ms, and the inhibition persisted 7.20 ms longer than the NE tone. E, Dot raster display illustrating responses from the same DTN when the duration of the NE tone was increased to 40 ms. Blue circles on raster plot show where facilitation occurred. F, Inhibition evoked by the NE tone also led

to a reduction in the cell's spike count . H, Deviations in LSL were also observed, but no changes in G, FSL could be measured. The final value of T_1 (-6 ms) was determined with a LSL criterion, and the final value of T_2 (44 ms) was determined with a spike count criterion. In the 40 ms NE tone condition, the latency of inhibition led the excitatory FSL by 2.24 ms, and the duration of inhibition was 4.24 ms longer than the NE tone. Facilitation was also observed at an ISI of F_{Max} = 40 ms with a spike count of 2.2 spikes per stimulus which was more than 1 SD above the baseline spike count measured during inhibition, which was 0.29 ± 0.22 spikes per stimulus. The latency of spikes (re NE tone onset) at this ISI was F_{start} = 48.92 ms relative to the onset of the NE tone. n = 15 trials per stimulus.

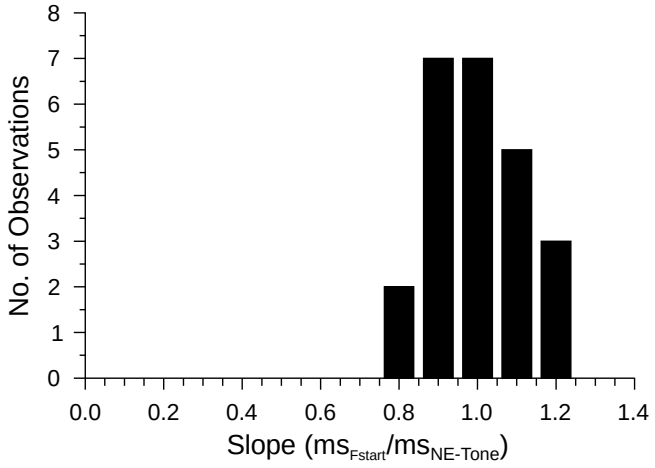

Figure 4.7. Characterizing the timing of offset facilitation as NE tone duration is varied.

Histogram showing distribution of slopes from the linear regression of the timing of spike facilitation (F_{Start}) with NE tone duration. This measure allows us to characterize temporal properties offset facilitation and distinguish it from other types of facilitation. Slope values represent the change in latency of facilitation (F_{start}) per change in NE tone duration (ms), with a slope value of 1.0 $ms_{Fstart}/ms_{NE\text{-}Tone}$ indicating a directly proportional relationship. These data demonstrate that the timing of spike facilitation was largely time-locked with respect to the offset of the NE tone. n = 24 observations from 14 DTNs.

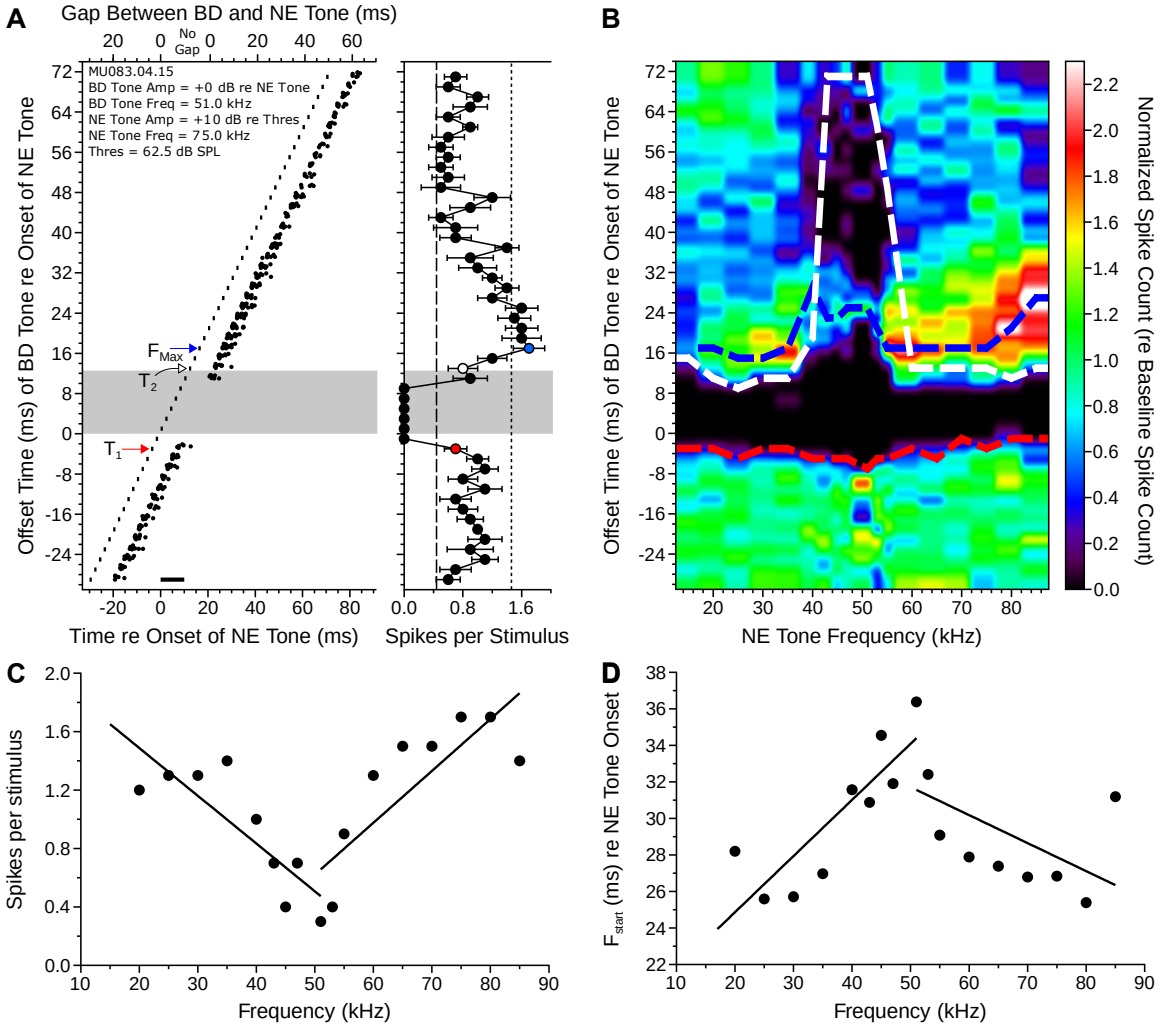

Figure 4.8. Time course of inhibition and facilitation as a function of changes in NE tone frequency.

A, left: Dot raster display illustrating responses from a short-pass DTN with the 1 ms BD tone presented at the cell's BEF (51.0 kHz) and the 10 ms NE tone was presented at a non-BEF that was outside of the cell's eBW (75.0 kHz). Strong suppression was observed when the BD tone and NE tone were sufficiently close in time. *Right,* Mean ± SE spikes per stimulus as a function of the ISI between the BD and NE tones. *Leftmost dashed line*: 50%

baseline spike count, *rightmost dashed line:* mean baseline spike count + 1 SD. *Left and right:* The final value for T_1 (-3 ms) was derived from a change in FSL and is shown with a *red arrow* (*left*) and a *red filled circle* (*right*). The final value for T_2 (13 ms) was also derived from a change in FSL and is shown with a *white arrow* (*left*) and a *white filled circle* (*right*). The effective duration of spike suppression was 15.50 ms. This neuron showed 3.50 ms of leading inhibition and was 5.50 ms longer than the duration of the 10 ms NE tone that evoked it. Facilitation was observed at an ISI of F_{Max} = 17 ms with a spike count of 1.70 spikes per stimulus and is shown with a *blue arrow* (*left*) and a *blue filled circle* (*right*) which was more than 1 SD above baseline spike count measurement of 0.89 + 0.61 spikes per stimulus (*right, rightmost dashed line*). The latency of spikes evoked at this ISI was F_{start} = 26.84 ms relative to the onset of the NE tone. *B,* Spike counts evoked at each ISI during paired tone stimulation as a function of the NE tone frequency for the same cell are shown. For this cell, the 10 ms NE tone was presented at +10 dB re threshold and was varied in frequency between between 15.0 – 85.0 kHz (18 frequencies) and the 1 ms BD tone was fixed at the cell's BEF (51.0 kHz) and +10 dB re threshold. The final ISI value at which the onset of inhibition is detected (T_1) is shown as a *red dashed line* and was observed to remain relatively constant as the NE tone frequency was varied for this cell. The final offset time of inhibition (T_2), shown as a *white dashed line*, decreased systematically as the NE tone frequency was moved away from the BEF for this cell. The ISI at which maximum spike facilitation was observed (F_{Max}) is shown as a *blue dashed line* and was observed to be relatively constant, similar to the onset of inhibition. *C,* Plot of the average number of spikes per stimulus evoked at F_{Max} vs. the NE tone frequency. A

linear regression was performed on this data and a slope of 0.033 spikes/kHz was found when the NE tone frequency was varied below the BEF, while a slope of 0.035 spikes/kHz was measured when the NE tone frequency was varied above the BEF. *D*, A plot of the latency of facilitation re NE tone onset (F_{start}) vs. the NE tone frequency; a linear regression was performed on this data and a slope of -0.307 ms/kHz was measured when the NE tone frequency was varied below the BEF, while a slope of -0.153 ms/kHz was measured when the NE tone frequency was varied above the BEF. Note: the slopes measured in panels C and D when NE tone frequency was below BEF were sign inverted so they could be directly compared to the slopes when the NE tone frequency was above BEF.

Figure 4.9. Characterizing changes in facilitation as a function of NE tone frequency *(following page).*

A, Boxplot showing distribution of δ_{start} and δ_{end} measured using the equations described in the methods section titled *Comparing the timing of facilitation to the onset and offset of inhibition*. These variables quantified how closely changes in F_{start} were associated with changes in T_{start} or T_{end} on average, over the stimulus set that was presented. Box plots illustrating the median (*horizontal middle line*), 25th and 75th percentiles (*horizontal edges of box*), interquartile range (*height of box*), 10th percentile (*bottom whisker)*, 90th percentile (*top whisker*), and data values falling outside of these ranges (*black circles)*. The interquartile range is defined as the 3rd quartile (75th percentile) minus the 1st quartile (25th percentile). n = 19 observations from 19 DTNs for both boxplots. *B*, Histogram showing distribution of slope values generated by performing a linear regression on the spike count measured at facilitation vs the deviation of the NE tone frequency from BEF (spikes/kHz). Measuring the distribution of slope values allows us to characterize how the strength of facilitation changes as a function of the NE tone frequency. n = 29 observations from 18 DTNs. *C*, Histogram showing distribution of slope values generated by performing a linear regression on the latency of facilitation (F_{start}) vs the deviation of the NE tone frequency from BEF (ms/kHz). Measuring the distribution of slope values allows us to characterize how the latency of facilitation changes as a function of the NE tone frequency. n = 29 observations from 18 DTNs.

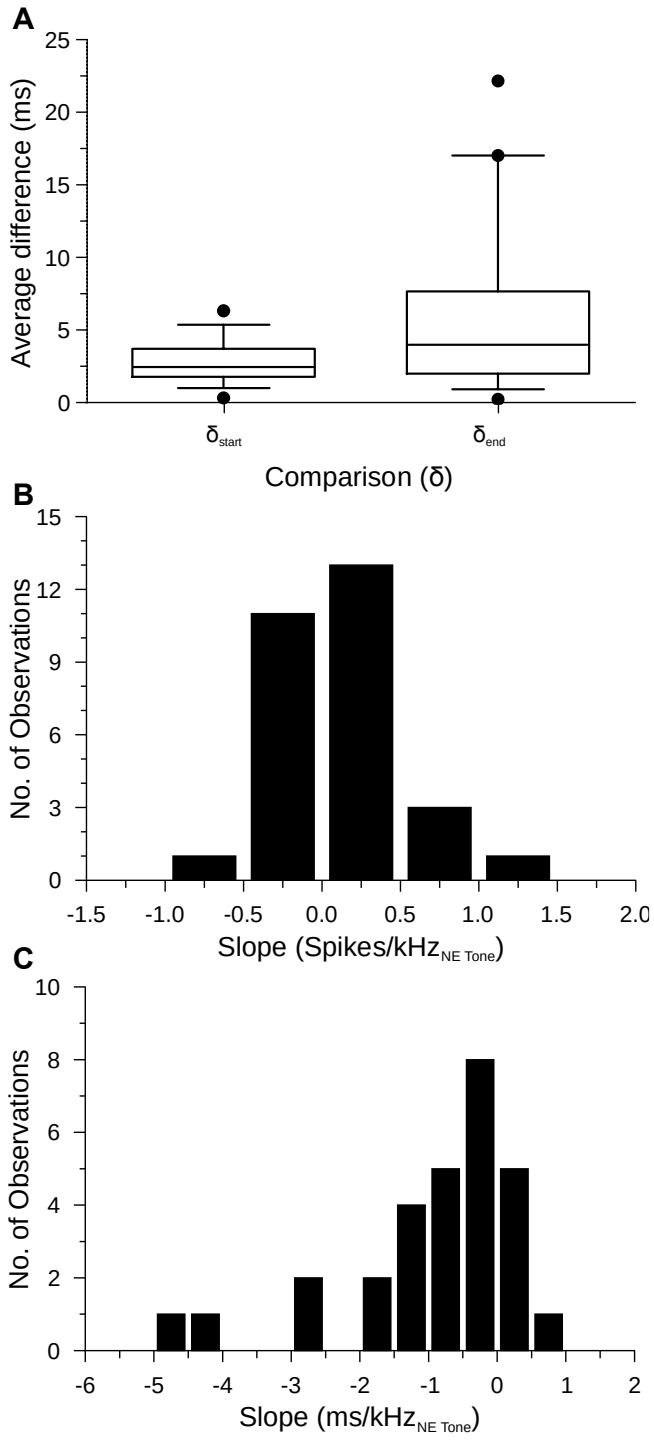
A
Average difference (ms)
25
20
15
10
5
0
δstart
δend
Comparison (δ)
B
No. of Observations
15
12
9
6
3
0
-1.5
-1.0
-0.5
0.0
0.5
1.0
1.5
2.0
Slope (Spikes/kHzNE Tone)
C
No. of Observations
10
8
6
4
2
0
-6
-5
-4
-3
-2
-1
0
1
2
Slope (ms/kHzNE Tone)

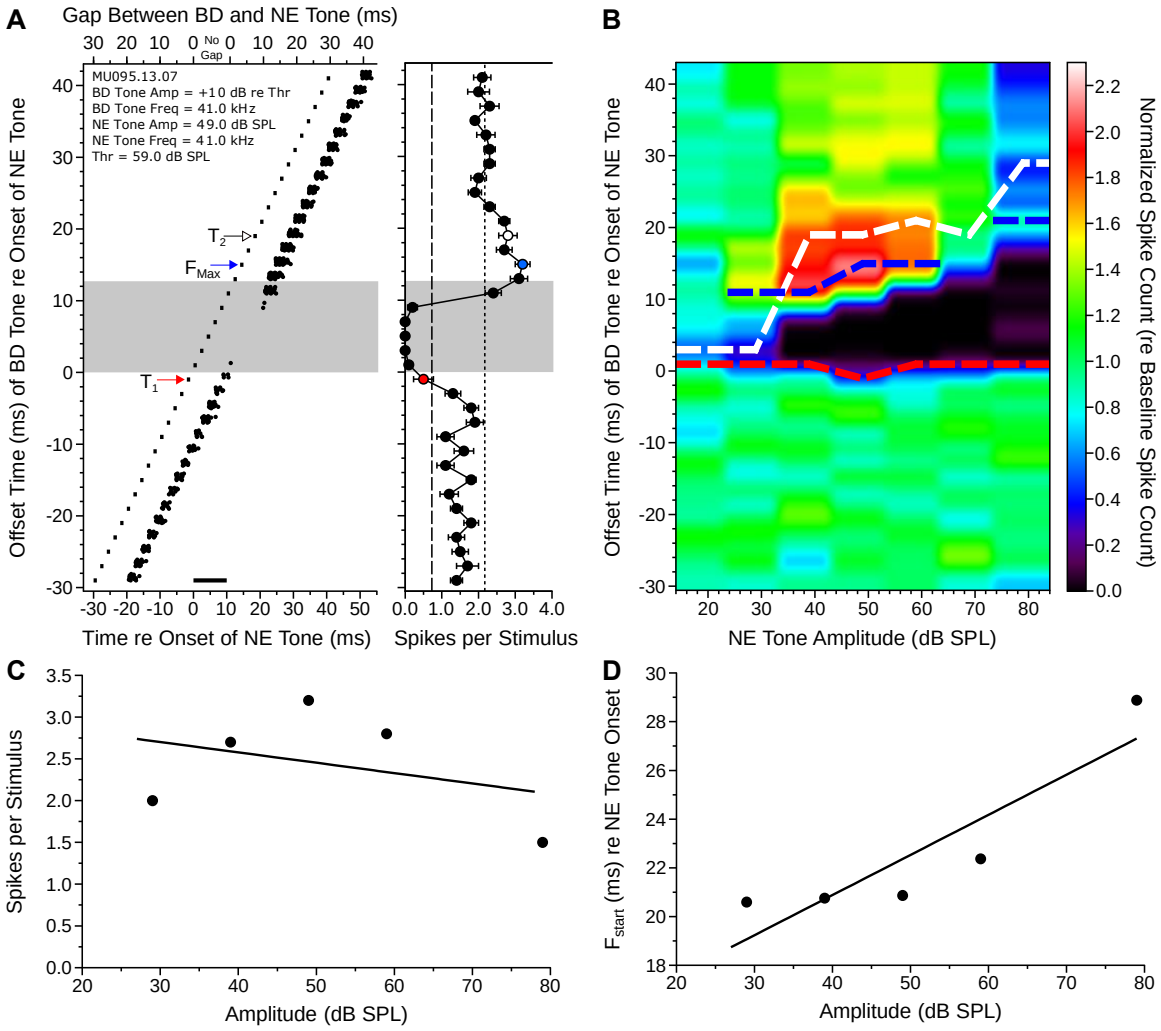

Figure 4.10. Time course of inhibition and facilitation as a function of changes in NE tone amplitude.

A, *left*: Dot raster display illustrating responses from a short-pass DTN with the 1 ms BD tone presented at +10 dB re threshold and the 10 ms NE tone was presented at amplitude -10 dB re threshold. Strong suppression was observed when the BD tone and NE tone were sufficiently close in time. *Right*, Mean ± SE spikes per stimulus as a function of the ISI between the BD and NE tones. Leftmost dashed line: 50% baseline spike count, rightmost

dashed line: mean baseline spike count + 1 SD. *Left and right:* The final value for T_1 (-1 ms) was derived from a change in spike count and is shown with a *red arrow* (*left*) and a *red filled circle* (*right*). The final value for T_2 (19 ms) was derived from a change in LSL and is shown with a *white arrow* (*left*) and a *white filled circle* (*right*). The effective duration of spike suppression was 19.10 ms. This neuron showed 1.10 ms of leading inhibition and was 9.10 ms longer than the duration of the 10 ms NE tone that evoked it. Facilitation was observed at an ISI of F_{Max} = 15 ms with a spike count of 3.20 ± 0.63 spikes per stimulus and is shown with a *blue arrow* (*left*) and a *blue filled circle* (*right*) which was more than 1 SD above baseline spike count measurement of 1.49 + 0.68 spikes per stimulus. The latency of spikes evoked at this ISI was F_{start} = 20.86 ms relative to the onset of the NE tone. *B*, Spike counts evoked at each ISI during paired tone stimulation as a function of the NE tone amplitude for the same cell are shown. For this cell, the 10 ms NE tone was presented at +10 dB re threshold and was varied in NE tone amplitude between -40 – 20 dB above threshold (19.0 – 79.0 dB SPL; 7 amplitudes) and the 1 ms BD tone was fixed at +10 dB above threshold. The final ISI value at which the onset of inhibition is detected (T_1) is shown as a *red dashed line* and was observed to remain relatively constant as the NE tone amplitude was varied for this cell. The final offset time of inhibition (T_2) is shown as a *white dashed line* and was observed to increase systematically as the NE tone amplitude was increased. The ISI at which maximum spike facilitation was measured (F_{Max}), shown as a *blue dashed line*, was relatively constant, similar to the onset of inhibition. *C*, Plot of the average number of spikes per stimulus evoked during facilitation vs. the NE tone amplitude was plotted. A linear regression was performed on this data and

a slope of of -0.012 spikes/$dB_{NE\ Tone}$ was found. *D*, A plot of the latency of facilitation (F_{start}) vs. the NE tone amplitude; a linear regression was performed on this data and a slope of 0.016 ms/$dB_{NE\ Tone}$ was measured.

Figure 4.11. Characterizing changes in facilitation as a function of NE tone amplitude *(following page).*

A, Boxplot showing distribution of δ_{start} and δ_{end} measured using the equations described in the methods section titled *Comparing the timing of facilitation to the onset and offset of inhibition*. These variables quantified how closely changes in F_{start} were associated with changes in T_{start} or T_{end} on average, over the stimulus set that was presented. Box plots illustrating the median (*horizontal middle line*), 25th and 75th percentiles (*horizontal edges of box*), interquartile range (*height of box*), 10th percentile (*bottom whisker)*, 90th percentile (*top whisker*), and data values falling outside of these ranges (*black circles)*. The interquartile range is defined as the 3rd quartile (75th percentile) minus the 1st quartile (25th percentile). n = 20 observations from 15 DTNs for both boxplots. *B*, Histogram showing distribution of slope values generated by performing a linear regression on the spike count measured at facilitation vs the deviation of the NE tone amplitude (spikes/$dB_{NE\ Tone}$). Measuring the distribution of slope values allows us to characterize how the strength of facilitation changes as a function of the NE tone amplitude. n = 20 observations from 15 DTNs. *C*, Histogram showing distribution of slope values generated by performing a linear regression on the latency of facilitation (F_{start}) vs NE tone amplitude (ms/$dB_{NE\ Tone}$). Measuring the distribution of slope values allows us to characterize how the latency of facilitation changes as a function of the NE tone amplitude. n = 20 observations from 15 DTNs.

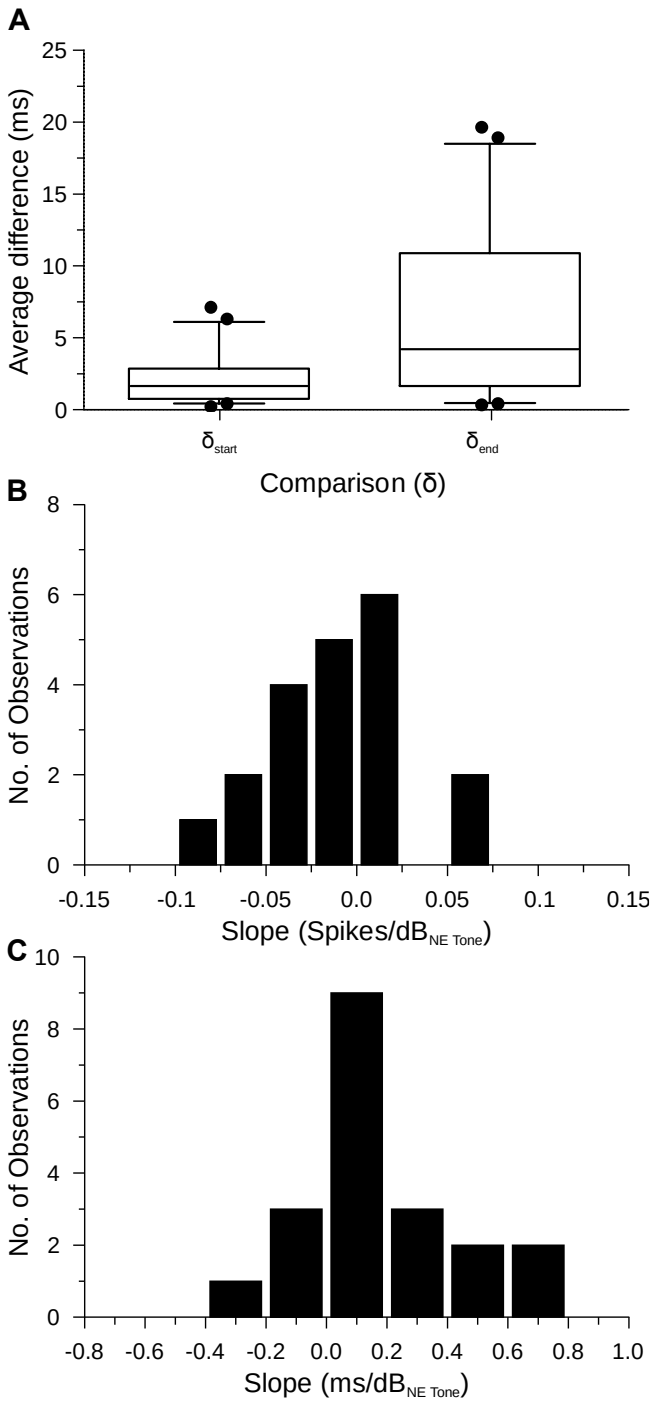
A
Average difference (ms)
25
20
15
10
5
0
δstart
δend
Comparison (δ)
B
No. of Observations
8
6
4
2
0
-0.15
-0.1
-0.05
0.0
0.05
0.1
0.15
Slope (Spikes/dBNE Tone)
C
No. of Observations
10
8
6
4
2
0
-0.8
-0.6
-0.4
-0.2
0.0
0.2
0.4
0.6
0.8
1.0
Slope (ms/dBNE Tone)

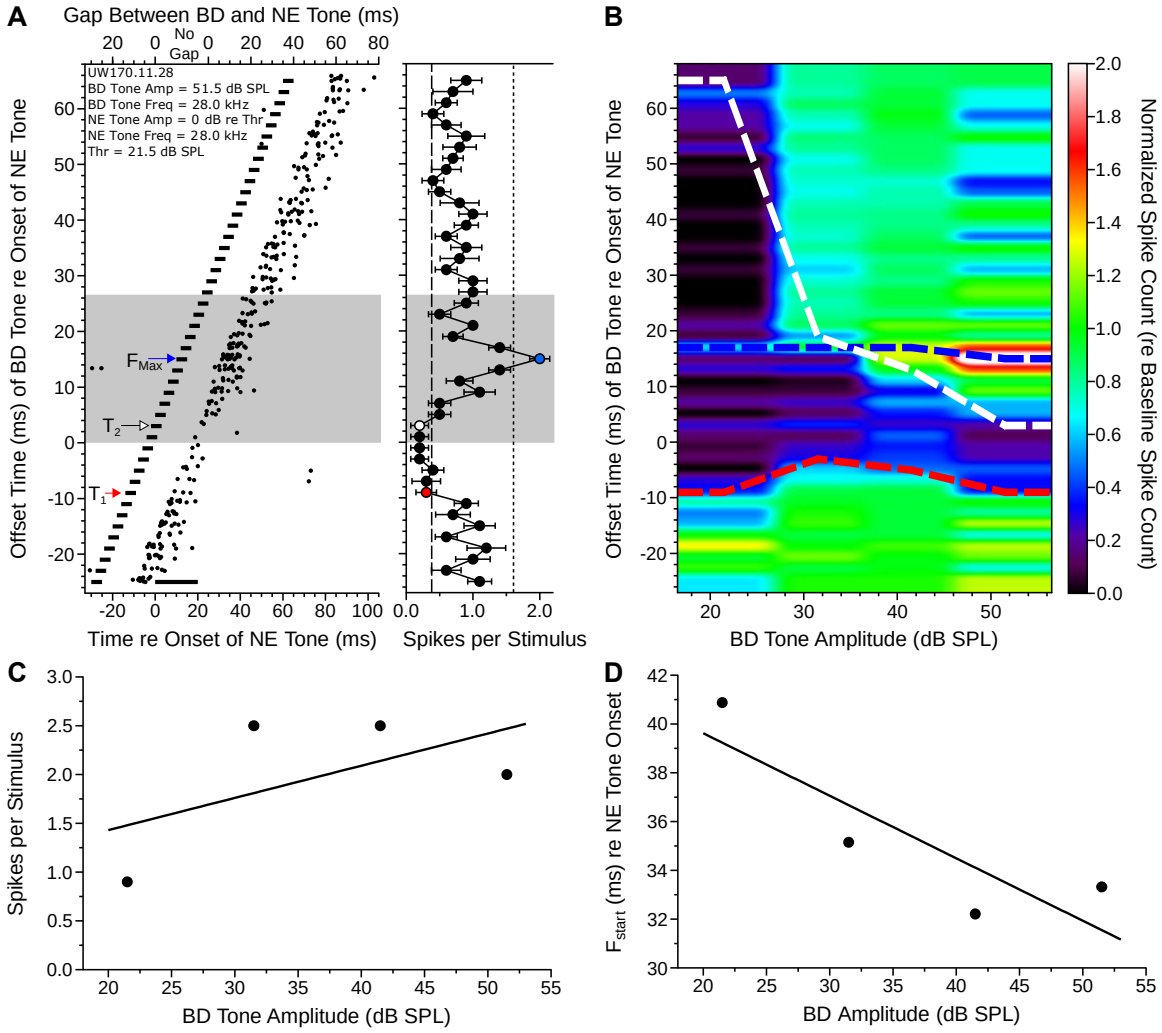

Figure 4.12. Time course of inhibition and facilitation as a function of changes in BD tone amplitude.

A, left: Dot raster display illustrating responses from a bandpass DTN with the 5 ms BD tone presented at +30 dB re threshold and the 20 ms NE tone was presented at amplitude 0 dB re threshold. Some suppression was observed when the BD tone and NE tone were sufficiently close in time. *Right*, Mean ± SE spikes per stimulus as a function of the ISI between the BD and NE tones. Leftmost dashed line: 50% baseline spike count, rightmost

dashed line: mean baseline spike count + 1 SD. *Left and right:* The final value for T_1 (-9 ms) was derived from a change in spike count and is shown with a *red arrow* (*left*) and a *red filled circle* (*right*). The final value for T_2 (3 ms) was also derived from a change in spike counts and is shown with a *white arrow* (*left*) and a *white filled circle* (*right*). The effective duration of spike suppression was 10.43 ms. This neuron showed 12.43 ms of leading inhibition and was 9.57 ms shorter than the duration of the 20 ms NE tone that evoked it. Facilitation was observed at an ISI of F_{Max} = 15 ms with a spike count of 2.00 ± 0.47 spikes per stimulus and is shown with a *blue arrow* (*left*) and a *blue filled circle* (*right*) which was more than 1 SD above baseline spike count measurement of 0.88 ± 0.72 spikes per stimulus. The latency of spikes evoked at this ISI was F_{start} = 33.32 ms re: onset of NE tone. *B*, Spike counts evoked at each ISI during paired tone stimulation as a function of the NE tone amplitude for the same cell shown are shown. For this cell, the 20 ms NE tone was presented at 0 dB re threshold while the 5 ms BD tone was varied between 0 – 30 dB above threshold (21.5 – 51.5 dB SPL; 4 amplitudes) and the 20 ms NE tone was fixed at 0 dB above threshold. The final ISI value at which the onset of inhibition is detected (T_1) is shown as a *red dashed line* and was observed to remain relatively constant as the BD tone amplitude was varied for this cell. The final offset time of inhibition (T_2) is shown as a *white dashed line* and was observed to decrease systematically as the BD tone amplitude was increased. It should be noted that strength and timing of T_2 did not change. Rather a weaker (stronger) BD probe tone revealed more (less) of the time course of inhibition. The ISI at which maximum spike facilitation was measured (F_{Max}) is shown as a *blue dashed line* and was observed to be relatively constant, similar to the onset of inhibition. *C*, Plot

of the average number of spikes per stimulus evoked during facilitation vs. the NE tone amplitude was plotted. A linear regression was performed on this data and a slope of 0.03 spikes/$dB_{BD\ Tone}$ was found. *D*, A plot of the latency of facilitation (F_{start}) vs. the BD tone amplitude; a linear regression was performed on this data and a slope of -0.26ms/$dB_{BD\ Tone}$ was measured.

Figure 4.13. Characterizing changes in facilitation as a function of BD tone amplitude *(following page)*.

A, Boxplot showing distribution of δstart and δend measured using the equations described in the methods section titled Comparing the timing of facilitation to the onset and offset of inhibition. These variables quantified how closely changes in Fstart were associated with changes in Tstart or Tend on average, over the stimulus set that was presented. Box plots illustrating the median (horizontal middle line), 25th and 75th percentiles (horizontal edges of box), interquartile range (height of box), 10th percentile (bottom whisker), 90th percentile (top whisker), and data values falling outside of these ranges (black circles). The interquartile range is defined as the 3rd quartile (75th percentile) minus the 1st quartile (25th percentile). n = 38 observations from 22 DTNs for both boxplots. B, Histogram showing distribution of slope values generated by performing a linear regression on the spike count measured at facilitation vs the deviation of the BD tone amplitude (spikes/dBBD Tone). Measuring the distribution of slope values allows us to characterize how the strength of facilitation changes as a function of the BD tone amplitude. n = 38 observations from 22 DTNs. C, Histogram showing distribution of slope values generated by performing a linear regression on the latency of facilitation (Fstart) vs NE tone amplitude (ms/dBNE Tone). Measuring the distribution of slope values allows us to characterize how the latency of facilitation changes as a function of the BD tone amplitude. n = 38 observations from 22 DTNs.

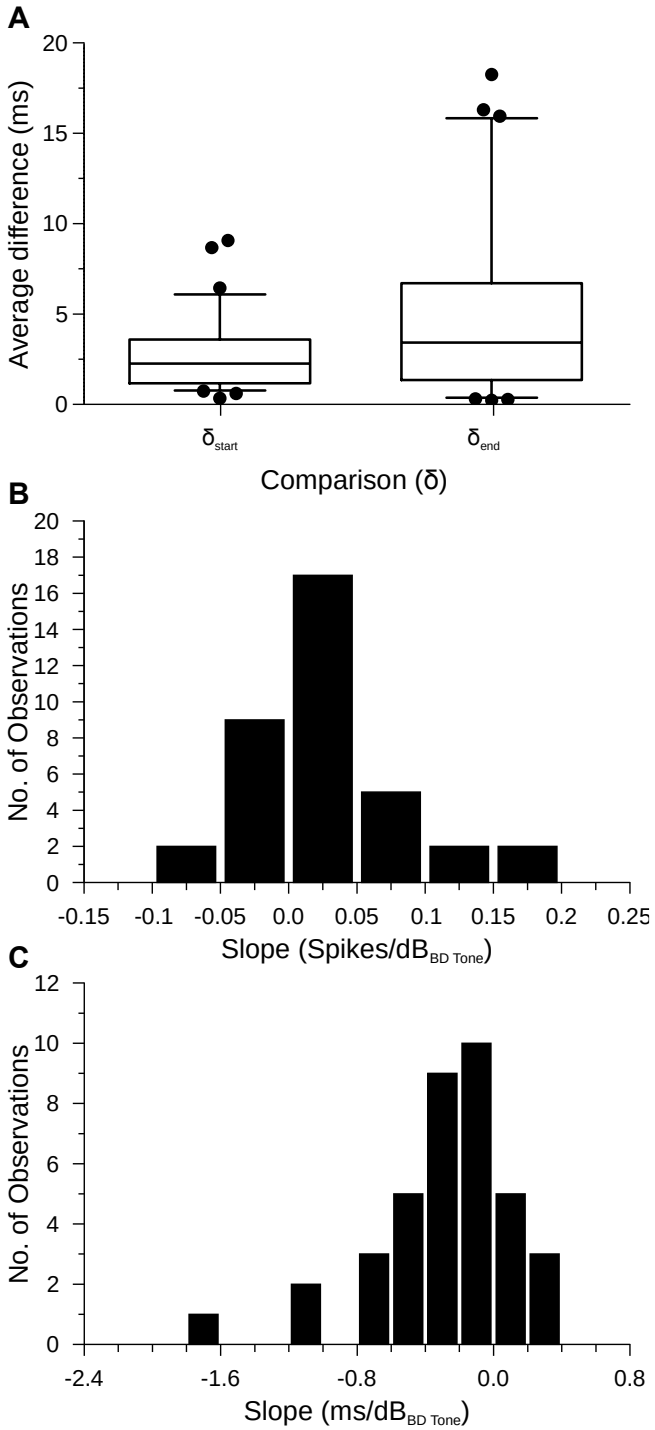
A
Average difference (ms)
20
15
10
5
0
δstart
δend
Comparison (δ)
B
No. of Observations
20
18
16
14
12
10
8
6
4
2
0
-0.15
-0.1
-0.05
0.0
0.05
0.1
0.15
0.2
0.25
Slope (Spikes/dBBD Tone)
C
No. of Observations
12
10
8
6
4
2
0
-2.4
-1.6
-0.8
0.0
0.8
Slope (ms/dBBD Tone)

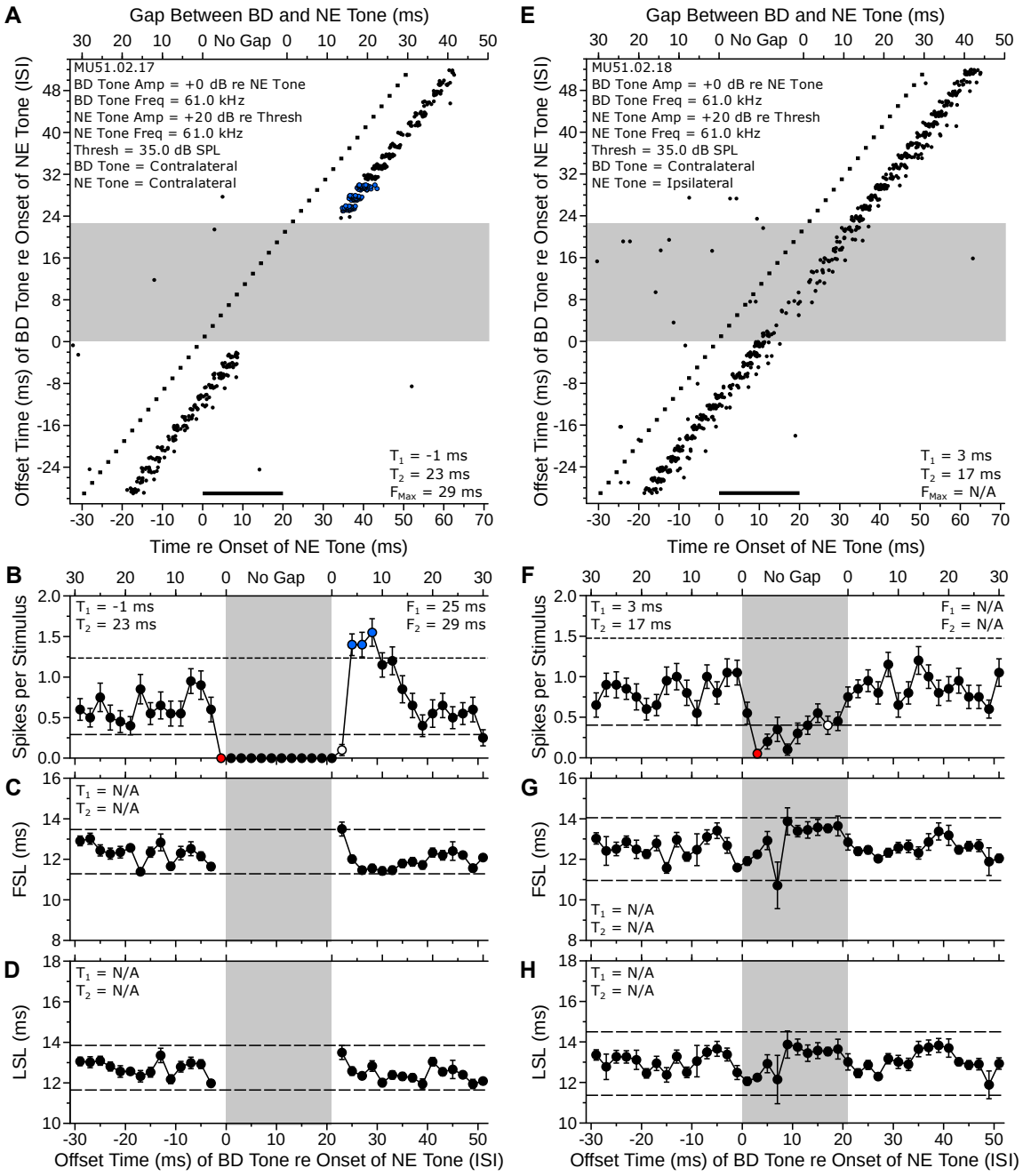

Figure 4.14. Inhibition and facilitation evoked with NE tones presented monotically and dichotically.

Dot raster displays illustrating responses from a shortpass DTN with the NE tone presented with monotic (*left*) and dichotic (*right*) paired tone stimulation. *A,* When both the 20-ms

NE tone and the 1-ms BD tone were presented monotically to the contralateral ear re: IC recorded, strong suppression was observed when the two tones were sufficiently close in time. Facilitation also occurred near the offset of the NE tone shown by the *blue circles* on raster plot. *B,* Mean ± SE spikes per stimulus as a function of the ISI between the BD and NE tones. The shortest ISI in which the spike count first dropped to ≤50% of baseline was T_1 = -1 ms (*red circle*). The longest ISI, starting from T_1, in which the spike count remained at ≤50% of baseline was T_2 = 23 ms (*open circle*). Facilitation was also observed at an ISI of F_1 = 25 ms, F_2 = 29 ms, and F_{Max} = 29 ms (*blue circles*). F_{max} had a spike count of 1.55 ± 0.76 spikes per stimulus which was more than 1 SD above the baseline spike count measured during inhibition of 0.58 ± 0.65 spikes per stimulus. The latency of spikes (re NE tone onset) at this ISI was F_{start} = 36.01 ms. *C,* Mean ± SE FSL as a function of the ISI between the BD and NE tones. We did not measure a deviation in FSL. *D,* Mean ± SE LSL as a function of the ISI between the BD and NE tones. We did not measure a significant deviation in LSL. In the contralateral condition, the final value of T_1 (-1 ms) and the final value of T_2 (23 ms) and both were determined using a spike count criterion. The onset of the NE tone evoked inhibition led the excitatory FSL by 1.63 ms, and the inhibition persisted 3.63 ms longer than the 20-ms NE tone. *E,* Dot raster display illustrating responses from the same DTN during dichotic paired tone stimulation with the NE tone was presented ipsilaterally re: IC recorded. *F,* Inhibition evoked when the NE tone was presented ipsilaterally also led to a reduction in the cell's spike count, although the effective duration of spike suppression was shorter and inhibition was weaker than the monotic condition. Deviations in *H,* LSL and *G,* FSL again could not be measured. The final value

of T_1 (3 ms) and the final value of T_2 (17 ms) were both determined with a spike count criterion. In the ipsilateral NE tone condition, the latency of inhibition lagged the excitatory FSL by 2.43 ms, and the duration of inhibition was 6.43 ms shorter than the 20-ms NE tone. Even though inhibition was observed when the NE tone was presented to the ipsilateral ear (re IC recorded) facilitation was not observed, suggesting that facilitation is not a rebound from inhibition in this cell. n = 20 trials per stimulus.

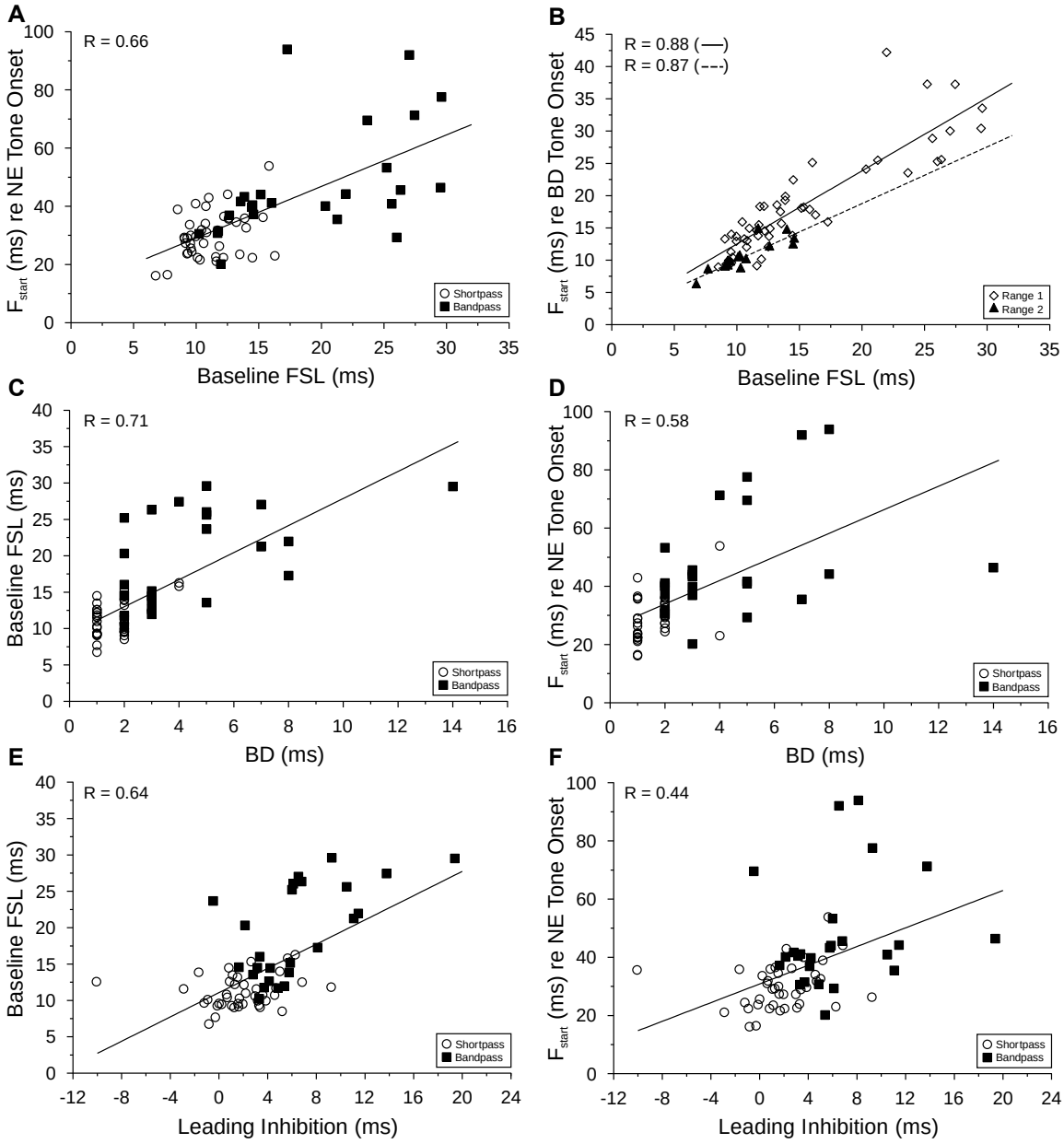

Figure 4.15. Relationships in response properties of temporally tuned cells that showed facilitation.

A, The latency of spike facilitation re NE tone onset, F_{start}, was significantly correlated with a cell's baseline FSL. *B*, The latency of spike facilitation re BD tone onset, was

significantly correlated with a cell's baseline FSL for both for cells whose facilitation occurred in Range 1, and Range 2; a linear regression was performed on Range 1 data (*solid line*) and Range 2 data (*dashed line*) separately. *C,* A positive relationship was found between F_{start} and a given DTN's BD. *D,* A positive relationship was found between a cell's baseline FSL and its BD. *E,* F_{start} was positively correlated with the amount of leading inhibition measured from each cell. *F,* A cell's baseline FSL was positively correlated with the amount of leading inhibition measured from each cell. In each panel the correlation coefficient (R) is shown. n = 66 cells.

Chapter 5 – Discussion

5.1 – Significance of Dissertation

The role that sound frequency and amplitude play on neural mechanisms of temporal processing within the central auditory nervous system (CANS) is of great relevance given that most auditory neurons trade-off spike timing as stimulus frequency and amplitude are varied (Rose et al. 1963; Mörchen et al. 1978; Heil 1997, 2004; Klug et al. 2000; Tan et al. 2008). For the majority of neurons in the CANS, stimuli that are lower in SPL and/or not centered on the neuronal BEF typically evoke longer first spike latencies, which in turn could lead to a confound in the encoding of temporal patterns because these neurons rely on the fidelity of their synaptic inputs to correctly demarcate time.

For example, consider echolocation in aerial hawking insectivorous bats. While hunting, bats emit outgoing calls and then listen for returning echoes to create a neural image of their surrounding environment. Bats co-vary call duration, frequency, and amplitude during the different stages of hunting (Schnitzler and Kalko 2001). Returning echoes are modified in amplitude (e.g. high frequencies attenuate more rapidly in the environment compared to low frequencies) and frequency (e.g. echoes become Doppler-shifted and/or their spectral pattern changes owing to acoustic interference with reflections from the target). For a CANS trying to encode temporal properties of an echo (e.g. pulse-echo delay), it would be very difficult to disambiguate whether a given response latency occurred because an object was more distant in space or because the echo frequency and/or amplitude was modified by sound reflection. Furthermore, our own experience with language also suggests that the perception of a given phoneme or morpheme does not

depend on the loudness or frequency of the sound, as long as these acoustic parameters are within the appropriate biological range of hearing.

In this thesis I report several specializations of the inputs to duration-tuned neurons (DTNs) that enable them to show the response property of level tolerance (Zhou and Jen 2001; Fremouw et al. 2005; Valdizón-Rodríguez and Faure 2017). These specializations also enable us to hypothesize which central auditory nuclei which could project synaptic inputs with these properties to the IC. In Chapters 2 and 3, I found that the onset of neural inhibition to DTNs was frequency and level tolerant and proposed the columnar division of the ventral nucleus of the lateral lemniscus (VNLLc) as a possible origin of inhibitory inputs to DTNs located in the auditory midbrain. The VNLLc is comprised of a matrix of neurons which receive projections from the anteroventral cochlear nucleus (AVCN). A large number of AVCN inputs, tuned to different frequencies, converge onto a small number of VNLLc neurons and form calyceal endings (Covey and Casseday, 1986). This anatomical and synaptic arrangement results in VNLLc neurons having wide spectral selectivity but high temporal precision (Covey and Casseday 1991).

The response properties of DTNs observed in Chapters 2 and 3 support the VNLLc as a candidate region to provide broadband inhibition to DTNs in the IC. First, the VNLLc projects primarily to the IC (Covey et al. 1986). Second, cells in the VNLLc have a short response latency (Covey et al. 1991), which is a feature of leading inhibition in DTNs (discussed in Chapters 2 and 3). Third, VNLLc neurons are broadly tuned in frequency and have threshold tuning curves that are asymmetrical, with steep high frequency flanks and more shallow low frequency flanks (Covey and Casseday 1991). Similar spectral tuning

was observed in the spectral tuning of the inhibition acting on DTNs during paired tone stimulation, where neural inhibition was much more broadly tuned than excitation and the strength of the inhibition decreased more quickly for frequencies above compared to frequencies below the cell's BEF (Chapter 2). Fourth, VNLLc neurons are known to have narrow dynamic ranges and respond maximally to small increases in SPL (Covey and Casseday, 1991). This feature is analogous to the narrow dynamic ranges of the inhibitory suppression-level functions (Chapter 3). Fifth, a majority of VNLLc neurons have monotonic rate-level functions (Covey and Casseday, 1991), and this is also true for the inhibitory suppression-level functions measured in DTNs (Chapter 3). Sixth, the responses of VNLLc neurons are primarily monaural (Covey et al. 1991), and in the IC the response property of duration tuning is also created monaurally (Sayegh et al. 2014). Finally, that VNLLc neurons may be the source of the onset-evoked, leading inhibition to DTNs is supported by another study that measured duration selectivity changes before and after iontophoretic application of bicuculline and strychnine, inhibitory neurotransmitter antagonists to γ-aminobutyric acid (GABA) and glycine, respectively. When GABAergic inhibition was blocked, sustained spiking was revealed more frequently than when glycinergic inhibition was blocked (Casseday et al. 2000), suggesting that GABAergic inhibition is stronger during the ongoing portion of an inhibitory response, while glycinergic inhibition is strongest in the onset-evoked portion of the inhibitory response.

In Chapter 4, I reported an offset-locked excitatory input to DTNs characterized as a transient facilitation in spiking observed during paired tone stimulation. This excitation was thought to be involved in the coincidence detection mechanism of duration tuning and

has certain features that make it well suited for temporal processing and the level tolerance of evoked responses. First, we showed that the latency of the offset-locked facilitation evoked by a long duration tone was related to the response properties of the cell when stimulated at the neuron's BD (Fig. 4.15). This reveals that the excitatory and inhibitory inputs of a DTN interact the same way at the BD as they would at a non-excitatory duration. This finding is important because paired tone stimulation reveals properties of the inputs to a DTN that are evoked by a non-excitatory tone. This feature gives us confidence in observations made from neurons stimulated at durations longer than a cell's BD. Second, we showed that the latency of offset-locked spike facilitation changed in a way that was more related to the onset of inhibition than the offset of inhibition when stimulus frequency and/or amplitude were varied. This result relates to earlier findings (see Chapters 2 and 3) where I showed that the onset (latency) of inhibition remained constant as NE tone frequency (Chapter 2) and/or amplitude were varied (Chapter 3), whereas the offset of inhibition decreased systematically when the NE tone was presented away from the BEF and/or at a lower SPLs. In Chapter 4, I showed that the latency of offset-locked facilitation followed changes in the onset of inhibition more closely than the offset of inhibition when stimulus amplitude and frequency were varied. These results indicate that the excitatory input underlying facilitation was not caused by a post-inhibitory rebound excitation, but rather a separate excitatory input. Finally, in the majority of cells we found that spike facilitation preceded the offset of inhibition—a finding that reveals that the offset-evoked excitation in the coincidence detection model of duration tuning is unlikely to be post-excitatory rebound from inhibition.

Altogether, my findings reveal a map of the response properties of the inhibitory and excitatory synaptic inputs to DTNs as frequency and amplitude are varied. These data provide a contextual framework for understanding previous studies that measured the response properties of DTNs through stimulation with single frequency, BD tones. Characterizing how changes in stimulus frequency and amplitude map on to the responses of inhibitory and excitatory synaptic inputs to DTNs furthers our understanding of the neural mechanisms and circuits of temporal processing and duration tuning in the mammalian central auditory system.

5.2 – References

Alluri RK, **Rose GJ**, **Hanson JL**, **Leary CJ**, **Vasquez-Opazo GA**, **Graham JA**, **Wilkerson J**. Phasic, suprathreshold excitation and sustained inhibition underlie neuronal selectivity for short-duration sounds. *Proc Natl Acad Sci* 113: E1927--E1935, 2016.

Aubie B, **Becker S**, **Faure PA**. Computational models of millisecond level duration tuning in neural circuits. *J Neurosci* 29: 9255–9270, 2009.

Aubie B, **Sayegh R**, **Faure PA**. Duration tuning across vertebrates. *J Neurosci* 32: 6373–6390, 2012.

Brand A, **Urban R**, **Grothe B**. Duration tuning in the mouse auditory midbrain. *J Neurophysiol* 84: 1790–1799, 2000.

Casseday JH, **Ehrlich D**, **Covey E**. Neural tuning for sound duration: role of inhibitory mechanisms in the inferior colliculus. *Science* 264: 847–850, 1994.

Casseday JH, **Ehrlich D**, **Covey E**. Neural measurement of sound duration: control by excitatory-inhibitory interactions in the inferior colliculus. *J Neurophysiol* 84: 1475–1487, 2000.

Chan AAY-H, **David Stahlman W**, **Garlick D**, **Fast CD**, **Blumstein DT**, **Blaisdell AP**. Increased amplitude and duration of acoustic stimuli enhance distraction. *Anim Behav* 80: 1075–1079, 2010.

Chen G-D. Effects of stimulus duration on responses of neurons in the chinchilla inferior colliculus. *Hear Res* 122: 142–150, 1998.

Covey E, **Casseday JH**. Connectional basis for frequency representation in the nuclei of the lateral lemniscus of the bat Eptesicus fuscus. *J Neurosci* 6: 2926–2940, 1986.

Covey E, **Casseday JH**. The monaural nuclei of the lateral lemniscus in an echolocating bat: parallel pathways for analyzing temporal features of sound. *J Neurosci* 11: 3456–3470, 1991.

Covey E, **Kauer JA**, **Casseday JH**. Whole-cell patch-clamp recording reveals subthreshold sound-evoked postsynaptic currents in the inferior colliculus of awake bats. *J Neurosci* 16: 3009–3018, 1996.

Denes P. Effect of Duration on the Perception of Voicing. *J Acoust Soc Am* 27: 761–764, 1955.

Duysens J, **Schaafsma SJ**, **Orban GA**. Cortical off response tuning for stimulus duration. *Vision Res* 36: 3243–3251, 1996.

Ehrlich D, **Casseday JH**, **Covey E**. Neural tuning to sound duration in the inferior colliculus of the big brown bat, Eptesicus fuscus. *J Neurophysiol* 77: 2360–2372, 1997.

Faure PA, **Fremouw T**, **Casseday JH**, **Covey E**. Temporal masking reveals properties of sound-evoked inhibition in duration-tuned neurons of the inferior colliculus. *J Neurosci* 23: 3052–3065, 2003.

Faure PA, **Fullard JH**, **Barclay RMR**. The response of tympanate moths to the echolocation calls of a substrate gleaning bat, Myotis evotis. *J Comp Physiol A* 166: 843–849, 1990.

Fremouw T, **Faure PA**, **Casseday JH**, **Covey E**. Duration selectivity of neurons in the inferior colliculus of the big brown bat: tolerance to changes in sound level. *J Neurophysiol* 94: 1869–1878, 2005.

Fuzessery ZM. Response selectivity for multiple dimensions of frequency sweeps in the pallid bat inferior colliculus. *J Neurophysiol* 72: 1061–1079, 1994.

Fuzessery ZM, **Hall JC**. Sound duration selectivity in the pallid bat inferior colliculus. *Hear Res* 137: 137–154, 1999.

Galazyuk A V, **Feng AS**. Encoding of sound duration by neurons in the auditory cortex of the little brown bat, Myotis lucifugus. *J Comp Physiol A* 180: 301–311, 1997.

Gooler DM, **Feng AS**. Temporal coding in the frog auditory midbrain: the influence of duration and rise-fall time on the processing of complex amplitude-modulated stimuli. *J Neurophysiol* 67: 1–22, 1992.

He J. off Responses in the Auditory Thalamus of the Guinea Pig. *J Neurophysiol* 88: 2377–2386, 2002.

He J, **Hashikawa T**, **Ojima H**, **Kinouchi Y**. Temporal integration and duration tuning in the dorsal zone of cat auditory cortex. *J Neurosci* 17: 2615–2625, 1997.

Heil P. Auditory cortical onset responses revisited. I. first-spike timing. *J Neurophysiol* 77: 2616–2641, 1997.

Heil P. First-spike latency of auditory neurons revisited. *Curr. Opin. Neurobiol.* 14: 461–

467, 2004.

Jen PH-S, **Feng RB**. Bicuculline application affects discharge pattern and pulse-duration tuning characteristics of bat inferior collicular neurons. *J Comp Physiol A* 184: 185–194, 1999.

Jen PH-S, **Schlegel P**. Auditory physiological properties of the neurones in the inferior colliculus of the big brown bat,Eptesicus fuscus. *J Comp Physiol A* 147: 351–363, 1982.

Jen PH-S, **Wu CH**. The role of GABAergic inhibition in shaping the response size and duration selectivity of bat inferior collicular neurons to sound pulses in rapid sequences. *Hear Res* 202: 222–234, 2005.

Jen PH-S, **Zhou XM**. Temporally patterned pulse trains affect duration tuning characteristics of bat inferior collicular neurons. *J Comp Physiol A* 185: 471–478, 1999.

Klug A, **Khan A**, **Burger RM**, **Bauer EE**, **Hurley LM**, **Yang L**, **Grothe B**, **Halvorsen MB**, **Park TJ**. Latency as a function of intensity in auditory neurons: influences of central processing. *Hear Res* 148: 107–123, 2000.

Leary CJ, **Edwards CJ**, **Rose GJ**. Midbrain auditory neurons integrate excitation and inhibition to generate duration selectivity: an in vivo whole-cell patch study in anurans. *J Neurosci* 28: 5481–5493, 2008.

Luo F, **Metzner W**, **Wu FJ**, **Zhang SY**, **Chen QC**. Duration-Sensitive Neurons in the Inferior Colliculus of Horseshoe Bats: Adaptations for Using CF-FM Echolocation Pulses. *J Neurophysiol* 99: 284–296, 2008.

Lyons-Warren AM, **Hollmann M**, **Carlson BA**. Sensory receptor diversity establishes a peripheral population code for stimulus duration at low intensities. *J Exp Biol* 215: 2586–2600, 2012.

Macias S, **Hechavarria JC**, **Kossl M**, **Mora EC**. Neurons in the inferior colliculus of the mustached bat are tuned both to echo-delay and sound duration. *Neuroreport* 24: 404–409, 2013.

Manser MB. The acoustic structure of suricates' alarm calls varies with predator type and the level of response urgency. *Proc R Soc London Ser B Biol Sci* 268: 2315–2324, 2001.

Mora EC, **Kössl M**. Ambiguities in Sound-Duration Selectivity by Neurons in the Inferior Colliculus of the Bat Molossus molossus From Cuba. *J Neurophysiol* 91: 2215–2226, 2004.

Mörchen A, **Rheinlaender J**, **Schwartzkopff J**. Latency shift in insect auditory nerve fibers. *Naturwissenschaften* 65: 656–657, 1978.

Narins P, **Capranica R**. Communicative significance of the two-note call of the treefrogEleutherodactylus coqui. *J Comp Physiol A* 127: 1–9, 1978.

Narins PM, **Capranica RR**. Neural adaptations for processing the two-note call of the Puerto Rican treefrog, Eleutherodactylus coqui. *Brain Behav Evol* 17: 48–66, 1980.

O'Neill WE, **Suga N**. Encoding of target range and its representation in the auditory cortex of the mustached bat. *J Neurosci* 2: 17–31, 1982.

Pérez-González D, **Malmierca MS**, **Moore JM**, **Hernández O**, **Covey E**. Duration

selective neurons in the inferior colliculus of the rat: topographic distribution and relation of duration sensitivity to other response properties. *J Neurophysiol* 95: 823–836, 2006.

Pinheiro AD, **Wu M**, **Jen PS**. Encoding repetition rate and duration in the inferior colliculus of the big brown bat, Eptesicus fuscus. *J Comp Physiol A* 169: 69–85, 1991.

Pollack GS, **Hoy RR**. Temporal pattern as a cue for species-specific calling song recognition in crickets. *Science* 204: 429 LP-432, 1979.

Potter HD. Patterns of Acoustically Evoked Discharges of Neurons in the Mesencephalon of the Bullfrog. *J Neurophysiol* 28: 1155–1184, 1965.

Rose JE, **Greenwood DD**, **Goldberg JM**, **Hind JE**. Some discharge characteristics of single neurons in the inferior colliculus of the cat. I. Tonotopical organization, relation of spike counts to tone intensity, and firing patterns of single elements. *J Neurophysiol* 26: 294–320, 1963.

Sayegh R, **Aubie B**, **Faure PA**. Duration tuning in the auditory midbrain of echolocating and non-echolocating vertebrates. *J Comp Physiol A* 197: 571–583, 2011.

Sayegh R, **Casseday JH**, **Covey E**, **Faure PA**. Monaural and binaural inhibition underlying duration-tuned neurons in the inferior colliculus. *J Neurosci* 34: 481–92, 2014.

Schnitzler H-U, **Kalko EK V**. Echolocation by insect-eating bats. *Bioscience* 51: 557–569, 2001.

Shannon R V, **Zeng FG**, **Kamath V**, **Wygonski J**, **Ekelid M**. Speech recognition with

primarily temporal cues. *Science* 270: 303–304, 1995.

Simmons JA. Echolocation in Bats: Signal Processing of Echoes for Target Range. *Science* 171: 925–928, 1971.

Suga N, **O'Neill WE**. Neural axis representing target range in the auditory cortex of the mustache bat. *Science* 206: 351–353, 1979.

Tan ML, **Borst JGG**. Comparison of Responses of Neurons in the Mouse Inferior Colliculus to Current Injections, Tones of Different Durations, and Sinusoidal Amplitude-Modulated Tones. *J Neurophysiol* 98: 454–466, 2007.

Tan X, **Wang X**, **Yang W**, **Xiao Z**. First spike latency and spike count as functions of tone amplitude and frequency in the inferior colliculus of mice. *Hear Res* 235: 90–104, 2008.

Valdizón-Rodríguez R, **Faure PA**. Frequency tuning of synaptic inhibition underlying duration-tuned neurons in the mammalian inferior colliculus. *J Neurophysiol* 117: 1636–1656, 2017.

Wang J, **van Wijhe R**, **Chen Z**, **Yin S**. Is duration tuning a transient process in the inferior colliculus of guinea pigs? *Brain Res* 1114: 63–74, 2006.

Xia YF, **Qi ZH**, **Shen JX**. Neural representation of sound duration in the inferior colliculus of the mouse. *Acta Otolaryngolica* 120: 638–643, 2000.

Yavuzoglu A, **Schofield BR**, **Wenstrup JJ**. Circuitry underlying spectrotemporal integration in the auditory midbrain. *J Neurosci* 31: 14424–14435, 2011.

Yin S, **Chen Z**, **Yu D**, **Feng Y**, **Wang J**. Local inhibition shapes duration tuning in the inferior colliculus of guinea pigs. *Hear Res* 237: 32–48, 2008.

Zhou X, **Jen PH-S**. The effect of sound intensity on duration-tuning characteristics of bat inferior collicular neurons. *J Comp Physiol A Sensory, Neural, Behav Physiol* 187: 63–73, 2001.

Zorović M. Temporal processing of vibratory communication signals at the level of ascending interneurons in Nezara viridula (Hemiptera: Pentatomidae). *PLoS One* 6: 1–8, 2011.